

CRANFIELD INSTITUTE OF TECHNOLOGY

**COLLEGE OF AERONAUTICS
IMPACT CENTRE**

PH.D. THESIS

Academic Year 1990-1

ALI HASHIM AL-HAKEEM

**STRUCTURAL ANALYSIS OF
TRUCK CHASSIS FRAMES
UNDER LONGITUDINAL LOADS
CONSIDERING BIMOMENT EFFECTS**

Supervisor

J C Brown

July 1991

بِسْمِ اللَّهِ الرَّحْمَنِ الرَّحِيمِ

وَمَا أُوتِيتُمْ مِنَ الْعِلْمِ إِلَّا قَلِيلًا

In the name of God, most Gracious Most Merciful

"Of Knowledge it is only a little that is
communicated to you, (O men!)"

Quran 17/85

**This thesis is dedicated to
my son Hashim, my daughter Haneen
and my little boy Hussein
to whom the future belongs.**

ACKNOWLEDGEMENTS

WITHOUT the help given by several benefactors this work could not have been done.

وَتَأْتِي عَلَى قَدْرِ الْكِرَامِ الْمَكَامُ

in other words "great gifts are from great men".

Words are not enough to express my deepest gratitude to;-

- Mr. J C Brown, my supervisor whose excellent tuition, valuable advice, continuous encouragement and productive guidance has a vital role for the accomplishment of this research.
- Mr. G H Tidbury, for his help, kind encouragement, timely suggestion and useful discussions.
- Cranfield impact centre staff, for their support and friendly relationship.
- My wife Muna, for her patience and support through the darkest hours of this work.

For those persons whose names are not mentioned, but in one way or another have assisted me, I am much obliged.

What merits this work may have, spring from the meticulous help from the people whom I have named. As for the demerits, responsibility for which rests on my shoulders, may I ask for the user's indulgence.

الْبِعْصَةُ لِلَّهِ وَحْدَهُ

- "perfection is exclusively a divine attribute'.

ABSTRACT

Thin walled beams warp under torsional and longitudinal loads. Warping restraint produces high longitudinal stresses.

This is an analysis of the stress distribution in the side members of commercial vehicle chassis frames under the effects of the previously little studied longitudinal loads which may act on a truck chassis through spring hanger brackets. The structure analysed is a model chassis frame consisting of channel section side members and four cross members with different joint connections.

The developed theories are incorporated into a special purpose finite element program which may be used in the preliminary stages of chassis frame design. Although the program is only used for the longitudinal load case in this thesis, it is generally applicable for other chassis load cases, including torsion, bending,...etc and combination of these.

The theoretical results obtained from the program and the finite element analysis on complete chassis frame models are validated against experiments performed on a strain-gauged chassis frame model constructed with the same dimensions and constructional details as the finite element models with the appropriate loading and boundary conditions.

Suggestions for the optimum design and attachment positions for components such as spring hanger bracket which may apply longitudinal loads to the side members of the chassis frame are discussed from the point of view of longitudinal loadings.

CONTENTS

CHAPTER.	PAGE
1. <u>INTRODUCTION</u>	
1.1 GENERAL	1
1.2 REVIEW OF PREVIOUS WORK	3
1.3 RESEARCH CONTRIBUTION AND PRESENTATION	13
2. <u>WARPING THEORY OF THIN-WALLED OPEN SECTION BEAMS</u>	
2.1 INTRODUCTION	18
2.2 WARPING	18
2.3 SAINT VENANT THEORY (FREE WARPING)	20
2.4 AXIAL CONSTRAINT EFFECTS (RESTRAINED WARPING)	20
2.5 TORSION BENDING THEORY	21
2.6 BIMOMENT AND FLEXURAL TWIST	22
2.7 THE DIFFERENTIAL EQUATION FOR RATE OF TWIST ALONG A THIN-WALLED BEAM	23
2.8 COMPLETE WARPING RESTRAINT	24
2.9 PARTIAL WARPING RESTRAINT	27
3. <u>STIFFNESS MATRIX OF THIN-WALLED OPEN SECTION BEAMS</u>	
3.1 GENERAL	37
3.2 FUNDAMENTAL CONSIDERATIONS	37
3.3 EQUILIBRIUM AND COMPATIBILITY	38
3.4 DERIVATION OF THE STIFFNESS MATRIX	39
3.5 TRANSFORMATION FOR STIFFNESS MATRIX	44
4. <u>THIN-WALLED CLOSED-SECTION BEAMS</u>	
4.1 GENERAL	52

4.2	WARPLESS CLOSED SECTIONS	52
4.3	COMPLETELY RESTRAINED WARPING	54
4.4	PARTIALLY RESTRAINED WARPING	57
4.5	THE STIFFNESS MATRIX	58
5.	<u>CHASSIS FRAME JOINTS</u>	
5.1	GENERAL	65
5.2.1	RIGID JOINTS ASSUMPTIONS	65
5.2.2	JOINT COMPATIBILITY	65
5.2.3	EQUILIBRIUM MATRIX	68
5.3.1	FLEXIBLE JOINT ASSUMPTIONS	70
5.3.2	RATE OF TWIST STIFFNESS	70
5.3.3	BENDING AND TORSION STIFFNESS COEFFICIENTS	71
5.3.4	THE JOINT ELEMENT	71
6.	<u>THEORETICAL INVESTIGATION OF THE EFFECT OF LONGITUDINAL LOADS</u>	
6.1	GENERAL	78
6.2	LONGITUDINAL LOADS APPLIED OUTSIDE SECTION PROFILE	78
6.3	TOTAL STRESSES DUE TO LONGITUDINAL LOAD	80
7.	<u>FINITE ELEMENT ANALYSIS</u>	
7.1	GENERAL	84
7.2	FINITE ELEMENT SYSTEM	84
7.3	STRUCTURAL IDEALISATION OF A JOINT	85
7.3.1	CROSS-MEMBER IDEALISATION	85
7.3.2	SIDE-MEMBER IDEALISATION	85
7.4	FINITE ELEMENT IDEALISATION OF THE JOINTS	86
7.5	RESULTS FROM JOINT FINITE ELEMENT ANALYSIS	88
7.6	FINITE ELEMENT IDEALISATION OF A COMPLETE CHASSIS FRAME	90

8.	<u>THE "A.SAFE PROGRAM"</u>	
8.1	GENERAL	112
8.2	A.SAFE PROGRAM	112
8.3	THEORETICAL CHASSIS FRAME MODEL UNDER LONGITUDINAL LOAD	115
9.	<u>EXPERMENTAL INVESTIGATIONS</u>	
9.1	GENERAL	124
9.2	MATERIAL PROPERTIES	124
9.3	CONSTRUCTION OF THE TEST MODEL	124
9.4	STRAIN MEASURMENT	125
9.5	SUPPORT AND LOADING CONDITIONS	126
9.6	TESTING PROCEDURE	127
10.	<u>CONCLUSION</u>	
10.1	GENERAL	145
10.2	SUMMARY	145
10.2.1	THEORETICAL INVESTIGATION	145
10.2.2	EXPERIMENTAL INVESTIGATION	146
10.3	DISCUSSION	147
10.3.1	THEORETICAL ANALYSIS	147
10.3.2	FINITE ELEMENT ANALYSIS	148
10.3.3	A.SAFE PROGRAM	149
10.3.4	GENERAL	149
10.3.5	THE GRAPHS SHAPE	149
10.4	PRACTICAL SUGGESTIONS	150
10.5	SUGGESTIONS FOR FURTHER RESEARCH	151
	<u>REFERENCES</u>	153
	<u>BIBLIOGRAPHY</u>	159
	<u>APPENDIX (A)</u>	

LIST OF FIGURES

FIGURE	PAGE
1.1 Typical commercial vehicle with a ladder chassis frame	16
1.2 A ladder chassis frame with variety of joint designs	17
2.1 Typical types of thin-walled open section beams	30
2.2 Channel section beam under pure torsion	31
2.3 Shear stress variation of an open section across the thickness under torsion	31
2.4 Distribution of sectorial area	32
2.5 Warping inhibition in open section beams	33
2.6 Boundary conditions for the chassis frame cross members	33
2.7 Loads that introduce a bimoment into a channel section	34
2.8 The distortion of an I-section due to torsion	35
3.1 Mode of load transfer	48
3.2 Moment and bimoment equilibrium at a joint	48
3.3 Force and displacement components in local coordinates	49
3.4 Sign convention for loads and displacements in a warped channel-section beam element	49
3.5 Stiffness matrix for beam element with bimoment terms	50
3.6 Coordinate system for a grillage	51
3.7 A generalised coordinate for 3D frame	51
4.1 Generation of warping displacement of closed section	61
4.2 Warping of rectangular box section	61
4.3 General coordinate system of thin-walled tube	62
4.4 Displacement function of a box beam	62
4.5 Displacement function in the plane of the cross section of a box beam	63
5.1 A joint defined by a (TSW) node with a horizontal web channel cross member	73
5.2 A joint with a vertical web channel cross member	73

5.3	Displacements of nodal points at the ends of beams meeting at a joint, used to build up the equilibrium matrix [H]	74
5.4	Loads corresponding to the displacement in fig. (5.3)	75
5.5	Distances of torsion axes and warping point from the centroid axis for various joint configuration, see fig. (5.3)	76
5.6	Warping lines and warping axis of a channel section beam	77
5.7	Example of a joint element	77
6.1	Bimoment created due to longitudinal load	81
6.2	Principal sectorial area (ω_s) of the model used	81
6.3	Bimoment created due to longitudinal load	82
6.4	Bimoment created due to longitudinal load	83
7.1	Finite element idealisation of joints type 1 & 2	91
7.2	Finite element idealisation of joints type 3 & 4	92
7.3	Displacements due to bending flexibility	93
7.4	Displacements due to rate of twist flexibility	93
7.5	Joint deformations	94
7.6	Joint deformations	95
7.7	Stress distribution due to partial warping inhibition at joint No.1	96
7.8	Stress distribution due to partial warping inhibition at joint No.2	97
7.9	Stress distribution due to partial warping inhibition at joint No.3	98
7.10	Stress distribution due to partial warping inhibition at joint No.4	99
7.11	Warping displacements for joint No.1	100
7.12	Warping displacements for joint No.2	101
7.13	Warping displacements for joint No.3	102
7.14	Warping displacements for joint No.4	103
7.15	Ladder chassis frame used for F.E. analysis and experimental tests	104
7.16	Finite element idealisation of model chassis frame under longitudinal loads, case -1-	105
7.17	Finite element idealisation of model chassis frame under longitudinal loads, case -2-	106
7.18	Finite element idealisation of model chassis frame under longitudinal loads, case -3-	107

7.19	Deformation and stress distribution for case (1), when the longitudinal loads are applied at position (2)	108
7.20	Deformation and stress distribution for case (2), when the longitudinal loads are applied at position (2)	109
7.21	Deformation and stress distribution for case (3), when the longitudinal loads are applied at position (2)	110
8.1	Flow chart of A.SAFE program	116
8.2	Flow charts of subroutines used in A.SAFE program	117
8.3	Flow charts shows the incorporation of A.SAFE program into chassis design programme	118
8.4	Cases and positions of loading	119
8.5	Bimoment distribution due to longitudinal load, (see fig. 8.5)	120
8.6	Moment case (1), (p) at position (2), (see fig. 8.4)	121
8.7	Moment case (2), (p) at position (2), (see fig. 8.4)	122
8.8	Moment case (3), (p) at position (2), (see fig. 8.4)	123
9.1	Stress-strain curves for a mild steel tensile test	130
9.2	Strain-gauge positions and stations	131
9.3	Stress distribution for load-case No.1, when the load (p) is applied at position (1)	132
9.4	Stress distribution for load-case No.1, when the load (p) is applied at position (2)	133
9.5	Stress distribution for load-case No.2, when the load (p) is applied at position (1)	134
9.6	Stress distribution for load-case No.2, when the load (p) is applied at position (2)	135
9.7	Stress distribution for load-case No.3, when the load (p) is applied at position (1)	136
9.8	Stress distribution for load-case No.3, when the load (p) is applied at position (2)	137
9.9	Total stresses around selected cross sections of the side member, see fig. (9.2), for loading-case No.1, when the load (p) is applied at position (2)	138

9.10	Total stresses around selected cross sections of the side member, see fig. (9.2), for loading-case No.2, when the load (p) is applied at position (2)	139
9.11	Total stresses around selected cross sections of the side member, see fig. (9.2), for loading-case No.3, when the load (p) is applied at position (2)	140
10.1	A variety of typical spring hanger brackets	152
10.2	Alternative design and attachment of a spring hanger bracket	152

LIST OF TABLES

TABLE		PAGE
2.1	Comparision of the sectorial properties	36
4.1	Summary of functions used in the analysis of open and closed section beams	64
4.2	Summary of constants used in stiffness matrices of open and closed section beams	64
7.1	Rate of twist stiffnesses of joints, obtained by F.E. analysis	111

LIST OF PLATES

PLATE		PAGE
9.1	General arrangement of chassis test rig	141
9.2	Loading-case No.1	142
9.3	Loading-case No.2	143
9.4	Loading-case No.3	144

NOTATION

b	cross section width
B	bimoment of a node in open section member
B_p	bimoment due to partial warping in open section member
B_r	bimoment due to complete warping inhibition in open section member
c	denotes closed section member
e	distance from the shear centre to web of the member
E	Young's modulus of member materials
G	shear modulus of member materials
h	half the web width of a channel section or the height of a box section
$[H]$	equilibrium matrix
J	torsion constant of an open section
J_p	torsion constant of an open section with partially warping restrained at one end
J_r	torsion constant of an open section with completely warping restrained at one end
K	warping restraint factor
$[K_w]$	stiffness sub-matrix for the warping terms of an open section member
L	length of a member
s	cross section profile
t	thickness
$[T]$	transformation matrix
T	total torque
T_v	St. venant (or pure) torque
T_r	torque due to bimoment (or flexural twist)
W	warping displacement of an open section member
W_p	warping displacement of an open section member partially warping restrained at one end
W_r	warping displacement of an open section member completely warping restrained at one end
x	distance along the member

θ_x	angle of twist of an open section member
θ_{TP}	angle of twist at the free end of an open section member partially restrained against warping at the other end
'	denotes differentiation w.r.t x
ϕ_x	angle of twist of a closed section member
ϕ_{TP}	angle of twist at the free end of a closed section member partially restrained against warping at the other end
ν	Poisson's ratio
τ	shear stress
ω_s	principal sectorial area of a point
μ	characteristic length of an open section, $\mu = \sqrt{GJ/E\Gamma}$
Γ	warping constant
σ_r	stress due to bimoment with complete warping inhibition at one end
σ_p	stress due to bimoment with partial warping inhibition at one end
σ_A	stress due to axial load
σ_y	stress due to moment (M_y)
σ_z	stress due to moment (M_z)
σ_s	stress due to bimoment
σ_T	total stress

CHAPTER ONE

INTRODUCTION

1.1 GENERAL

Thin walled beams are used for many types of structures such as a ship, a bridge, an aircraft, a space-ship, a motor-car and other structural design. They are popular with vehicle designers since the manufacturing and economic possibilities are greater. There is no clear distinction between thin and thick walled beams. It is generally accepted that thin walled beam theory may be applied with reasonable accuracy to sections for which the wall thickness is small compared with any cross section dimension (≤ 0.1), which is itself small compared with the length of the beam. The latter condition may not be as important as the first. The first condition is important and if it is not satisfied the theory of thin walled beams may lead to erroneous numerical results due to the break down of the approximating assumptions used.

Under torsional load thin walled beams can be divided into two types. The first are warpless sections (i.e. plane sections remain plane) such as squares, circles, triangles and other regular polygons will not warp if the material thickness is constant. The second type comprises warping sections (i.e. plane sections do not remain plane) such as rectangular, channel, and I-sections.

In members subject to torsion or longitudinal loads, warping effects are more significant in open sections than in closed sections. Thin walled beams with closed or open section are used in the construction of commercial vehicle chassis frames (see figure 1.1).

Commercial vehicles such as trucks, trailers and semi-trailers have chassis frames which are of the ladder type. These are so termed because of the configuration of their members. They generally consist of two side members arranged parallel to the longitudinal axis of the chassis and several cross members placed laterally between the side members. Thus, the axles, as well as the power plant, the driver's cab and platform or other superstructures, are easy to attach. Whilst it must be stated that the conventional ladder type frame is an inefficient structure for carrying bending and torsion loads it remains true that for historical and economic reasons virtually every commercial vehicle in the world is based on such a chassis. The demand for vehicles

with chassis frames continues to increase in the commercial vehicle industry where the modern trend is towards lorries and articulated vehicles carrying large loads.

The side members of ladder chassis frames are usually made from open channel or I-sections. An I-section is very efficient in providing bending stiffness but manufacturers prefer channel section side members because of cost and ease of construction. The cross members are often made from hollow rectangular, channel, tophat or I-sections. Hollow rectangular sections give efficient torsional and bending stiffness, but can lead to high overall frame torsional stiffness. The most flexible design of frame would have open section cross members attached through end plates to the side member webs. Cross members can have variable cross section, i.e, shaped members to act as engine supports, cab mounts, also members whose depths are reduced in centre span to miss transmission arrangements.

There is a great variety of design of joints between cross members and side members (see figure 1.2), both as to joint configuration and the method of attachment of cross member to side member. The joints can greatly affect the torsional stiffness of the frame and cause high stress concentrations to develop. It is necessary that the desired torsional stiffness of a frame should not produce very high stresses in the joints which could cause them to fail. Welded joints are more difficult and hence more expensive to fabricate. Bolts and rivets in joints, although being the easiest methods of fixation, can cause stress concentration in the region of holes through which they pass.

British chassis frames tend to be much more flexible in torsion than their continental counter-parts which employ closed section cross members or extensive use of gusseting to increase torsional stiffness. However, frames should be stiff enough to ensure good vehicle road holding as well as flexible enough to supplement the suspension system. thus ensuring that wheel to ground contact is maintained.

Chassis frames are an important structure that must resist various loads during operation; vertical as well as longitudinal and torsional static and dynamic loads. Although adequate durability under dynamic conditions is an important design

requirement, static loads can not be disregarded and should be analysed. It is necessary to forecast fatigue life of a frame already in the construction process as well as to maximize the value of the load-carrying capacity of the material used. This, in turn necessitates more accurate estimation of stresses in those elements of frames.

The conventional design of ladder chassis frames has hitherto been based on the provision of side members of sufficient strength and stiffness to support the bending load due to the payload carried by the vehicle. The cross members chosen are based on the designers experience, while the effects of warping restraint, which is the major factor for the cause of high stresses in the frame, are neglected completely or regarded as secondary. The bimoment due to horizontal braking forces can cause large stresses in the frame, which are not usually considered in the design of side members.

Analysis of the whole chassis frame by standard beam elements in finite element programs leads to unacceptable approximation especially where the beam element has uniform cross section. Thus, automatic structural programmes based on a hybrid method of analysis, which combines finite element idealization of the joint areas with analytically derived beam elements for the chassis frame members are required to obtain a more reliable estimation of overall stiffness and stress distribution in chassis frame members for various loading conditions.

1.2 REVIEW OF PREVIOUS WORK

The inhibition of the warping at joints by other elements in the frame, gives rise to large longitudinal stresses, which have been the cause of many failures in chassis frames. These effects have been analysed by many authors following the publication of the major work on thin walled beams by Vlasov (1) where he introduced the concept of the bimoment. His theory allows for the extreme cases of complete warping inhibition or free warping at the joint. An introduction to Vlasov's work is given by Zbirohowski-koscia (2).

Hanke (3) analysed a ladder frame joint consisting of a channel section cross member symmetrically bolted to the web or flanges of the channel section side

member. The rate of twist of all members ending in the joint was assumed to be equal and the condition of bimoment equilibrium at the joint was obtained. He developed a differential equation using this concept and solved for certain boundary conditions. Hanke was one of the first authors who suggested that joints do not behave in a rigid manner and introduced the term 'induction factor' to estimate the degree of warping restraint in them. If the side member completely restrains the warping of the cross member, the joint is perfectly inductive and the factor has a unity value. In the case of complete absence of an inductive connection, when the cross member is allowed to warp freely, the induction factor is zero. However, the true value for a real joint lies somewhere between the two. He carried out experiments on several types of joints to determine the value of the 'induction factor' by measuring rotation and stresses of the members for each constructed joint. He obtained a high 'induction factor' when the cross member was bolted to the flanges of the side member, while bolting to the web of the side member alone resulted in a low 'induction factor'.

Zaks (4-5) investigated the warping effects in cross members welded to channel section side members. The asymmetry of the connection of the cross member to the side member with the intersection of the neutral axes offset was considered. He used Vlasov (1) thin walled beam theory and introduced the term 'bonding factor' which is equivalent to Hanke's (3) 'induction factor' to estimate the degree of warping restraint by measuring stresses and rotations on members of individual joints. He used these values to estimate stresses and deflection in the chassis frame. He also introduced the concept of 'kinematic aspect' which implies that a rigid joint has perfect kinematic coupling between members meeting in the joint.

Zaks also included the length of the member in the derivation of the bimoment equation and pointed out that the 'bonding factor' could depend on the length of the member if the beams are very short (very short beams are rarely used in practice). Otherwise the 'bonding factor' is constant for any particular design. He compared results obtained from plate theory (6) with those obtained from Vlasov's theory (1) for an I-section cross member symmetrically attached to a channel section side member. Both predicted values compared well with measured values in the regions

away from the joint where there are no localised effects of the joint. Plate theory equations developed by Zaks have been used by Kobrin, Kilimnik and Titov (7) to investigate the stresses in the walls of the chassis frame side member and good agreement between the predicted and experimentally measured values were obtained.

Seitler (8) also carried out tests on a model of a welded chassis frame using tubular cross members. He obtained about 80% lower stresses at the joints and he found that the torsional stiffness of the whole frame was about three times greater by using circular tubes rather the channel sections as cross members.

Cooke (9) demonstrated an iterative method using the strain energy theorems of Castigliano to estimate chassis frame stiffness with uniform section members. He first considered the rectangular outerframe, consisting of the two end cross members as a basic outline frame and determined its torsional stiffness by strain energy methods. Then the torque required on each internal cross member so that it would cause no further displacements of the outline frame when placed in the deflected outline was calculated. This torque was then converted to an external torque on the frame. The new external torque was applied to the outline frame to find the new deflected shape, the iterative process being repeated until no significant difference in the two values of the torque was obtained. Cooke's method requires a careful prediction of the deflection mode and, especially for a large number of cross members, can become very laborious. It does not take into account the effect of actual warping restraint in the joints.

Tidbury/Marshall/Roach (10-12) dealt with the problem of determining theoretically the warping restraint factor for a chassis joint and the torsional stiffness of a ladder frame, and of verifying the theoretical results experimentally. The arrangement selected for the main analysis was a chassis/joint connecting channel section cross members. In the analysis of the warping restraint factor, only the web of the channel section side member was taken into consideration. This web was divided into independent strip beams which were taken to be simply supported at the flange/web corner. The strip beams were taken to resist the cross member warping forces by bending. Linear variations of these forces on a strip beam were

approximated by point load. Bending theory was applied to the strip beams and Wagner-Kappus torsion theory to the cross member.

It was assumed that the partial warping displacement of the cross member at its joint end was proportional to its free warping displacement and that the partial warping stress was proportional to its fully warping inhibited stresses. An average value of the warping restraint factor was found and used for the cross member cross section at its joint end. From the warping restraint factor the effective torsion constant of the cross member was found.

The effective torsion constant for the side member was found by taking only the web of the side member into consideration within a bay. The web was treated as rectangular plates under torsion and restrained at both ends by the cross members. The effective torsion constant of the cross member and the side member were used in a modified Erz (13) formula to get overall torsional stiffness of the chassis, which compared well with measured values. Also good agreement with experimentally measured values for stresses in the side member were obtained when the value of the partial warping restraint factor was smaller than (0.4). Similar work on the effect of warping inhibition in joints on the torsional stiffness of chassis frame has been reported by Awudu (14).

Megson/Alade/Nuttall (15-20) dealt with the theoretical determination of warping restraint factor for a chassis joint and from it the torsional stiffness of a chassis under torsion. Also they dealt with the theoretical determination of warping stresses and displacement of the cross member under torsion and the verification of the theoretical results by experimentally measured values.

The arrangement analysed was a chassis having channel or I-section members. The torsion load was applied as equal and opposite couples at the ends of the chassis. The couples were comprised of individual loads applied through the shear centres of the side members to prevent local twisting. Two methods of idealisation ,i.e, assumptions of infinite and finite stiffness in warping of all members of the chassis, were used in the determination of the torsional stiffness of the chassis. For the infinite

solution, the Erz (13) formula was used to find the torsional stiffness. For the finite stiffness solution the finite element method was used. Nodes were taken especially at the joint between the side member and the cross member and at the points where the member changes section. The beam elements were solved for bending, shear force and torsion and the results were super-imposed to get resultant terms. Stiffness method (displacement method) was used in an available computer program which solved for a chassis comprised of beam elements. The effective torsion constant used to find the torsional stiffness was found by considering the warping restraint factor of the cross member on the side member. The warping restraint factor used to find the effective torsion constant of the cross member, was found from the joint of a section of the chassis.

In the joint, the side member was treated as a plate (web only considered) simply supported at a channel or I-section cross member attached symmetrically. One end of the cross member was considered partially restrained and the other (mid-span) free to warp. Torque was applied at the free end. In the finite element solution the side member was considered using plate elements in bending, and for the cross member plate and membrane elements, in bending and stretching were used.

Wagner's torsion bending theory for axially constrained open sections was applied to the cross members and side members. The assumption made was that the partially restrained warping displacement of the cross member was directly proportional to its completely free warping displacement. The warping restraint factor for the cross member was obtained from the solution of Wagner's torsion theory and finite elements. The moment couple method was used in Wagner's torsion theory to include the effect of warping restraint of the cross member on the side member and from this the effective torsion constant for the side member was found.

Experimental values for a range of torque, loads, dimensions for the chassis member were obtained using strain gauges. The agreement between experimental and theoretical results was found to be good, so was the correlation between infinite and finite stiffness in warping assumption. Also the assumption that the partial warping displacement was linearly proportional to the completely free warping displacement

was validated. The limitation of this method is that it is applicable only for symmetrical attachment of the cross member to the side member. The assumption mentioned immediately above may not be true for unsymmetrical attachments. Also the local twisting of the side member is not considered.

Similar work but on the stress distribution in the vicinity of the connection of a joint of a ladder frame subjected to torsion has been reported by Dattoo (21). His finite element analyses indicate a redistribution of the axial constraint stresses in the vicinity of the connection which produces stress concentrations at the cross member flange tips. He carried out torsion tests on glued perspex and welded steel joints to verify those stresses. He produced guidance charts of stress concentration factors for selected joints, using the finite element method.

Alvi (22-23) dealt with the problem of determining theoretically the stress distribution in a chassis joint and of verifying the theoretical results by measured values. The arrangement selected by him was a cross member attached to the web of the side member. Two cases for the side member were taken. In the first, the side member was a plate and in the second a channel section. The cross member was a channel section. Free warping was taken for the side member ends and a torsion load was applied at the (free) end of the cross member. The ends of the channel section side member were taken to be simply supported and so were all the edges of the plate.

Alvi applied Wagner's torsion theory for thin walled open sections to the cross members and classical plate theory (6) to the side member. The channel section side member was treated as three plates joined together, i.e the two flanges and the web. Bending and stretching of the plates due to the warping and couple loads of the cross member acting on it were included in the solution. For the cross member which is under torsion, the partial warping stress developed at its joint end was taken to be proportional to the total warping inhibition stress and the partial warping displacement proportional to the free warping displacement. The proportionality was expressed in terms of the warping restraint factor. An average warping restraint factor for the cross member cross section at the joint was found using plate theory and Wagner's torsion

theory. From this thesis it is not clear what method was used to find the average stress. Stresses due to partial warping restraint at the cross member joint end was found from the warping restraint factor.

By using plate theory Alvi had overcome the problem of unsymmetrical attachment of the cross member to side member, and he solved for both symmetrical and unsymmetrical attachments. Fourier series form was used to express terms of displacement, stress and the external force acting on the web. By this method it was possible to find the stress and displacement at any point on the side member. Superposition of the bending and stretching solution gave the final distribution of the stress and displacement. The critical area where the shear stress attains its peak value was found to be in line with the zero warping line of the cross member flange and near the flange web corner of the side member. A warping restraint factor was calculated and it showed good agreement with those of the other two previous methods, i.e strip beam theory and finite element method.

A photo-elastic technique was used to measure the values of stress and verify the theoretical results. The theoretical results compared well with the experimentally measured values and was considered more accurate than the other two methods of joint analysis mentioned above. From Alvi's thesis it can be concluded that the region of the joint contains high localised stresses, due to the warping restraint of the cross member and can not be left out of an analysis of the side member.

Sharman (24) investigated the optimisation of ladder frames. A technique was presented to maximise the torsional stiffness with minimum weight of chassis frame having uniform closed or solid section with rigid joints. The members are analysed in terms of their stiffness-weight ratios and the weight parameter was calculated for families of peripheral and ladder frames. He developed a torsional stiffness theory which considered ladder frames of uniform spacing as an assembly of peripheral frames. He produced design charts for certain cases. Unfortunately the method did not ensure compatibility of bending deformations of the cross members leading to torsional stiffnesses which were in error by up to (5%) and more for cross members very stiff in bending.

Optimising techniques are generally multi-constraint problems most suited to computer analysis. Sharman in his paper considered just one aspect of the more complicated problem which includes various parameters such as different geometries, load, displacements, stress, warping restraints and other economic constraints which have to be considered. Similar work which chose maximum direct stress and minimum weight as their variable has been reported by Lasevich, Sholnikov and Podlegaeva (25).

Later Sharman (26-27) considered the torsional problems of chassis frames. He discussed the types of torsional load being applied to the chassis frame, and outlined four main cases, those cases are asymmetric loading, twist ground plane, lateral acceleration on the load during cornering and finally, severe manoeuvres. The chassis structure is then considered and observations made about the effects of the different types of loading on different types of frame. He considered the side members from the point of view of optimum cross sectional shape. Other weight saving features are then explored. Since his design is dependent on the allowable stresses in tension and compression, these values are derived from a series of experiments in which the dynamic strain in semi-trailer are recorded. Sharman (28) showed that closed members are generally more efficient but emphasised that careful design of joints is necessary to avoid high localised stresses. He carried out experiments on thin fabricated box members in a tee joint to investigate the effect of joint flexibility in torsion. The behaviour was also observed in finite element analyses of the joints. The application of classical beam and torsional theory gave a result which was ten times the experimental value, while his method which includes the joint flexibility as predicted by finite element model of the localized region at the joint, gave an improved result which was (26%) higher than the experimental value. He suggested that further investigations should be made to find ground rules for defining the extent of the joint area.

Sharman (29) has also investigated the problems of incorporating the effects of cross sectional warping, offset shear centre and orientation of an element for structures assembled from channel and I-sections. He incorporated the kinematics of a variety of joint intersections and stiffening schemes. A transformation matrix was given to

account for non-coincidence of the shear centre and centroid, which enabled a solution to be obtained for comparison with a number of experimental and analytical studies. He has shown that the inclusion of the torsion warping terms for thin walled open section beams into the standard stiffness for a uniform beam may be achieved by the addition of the twist rates at each end as a degree of freedom. He concluded that the torsional aspects of chassis frame design are complex and though approximate analytical methods can be used in the early stage of design, computer analysis appears to be necessary to ensure structural integrity under a variety of load conditions.

Tidbury (30-31) described matrix computer methods which may be applied to analysis vehicle structures. They are displacement methods and force methods. He used a force method to estimate the torsional stiffness of a rectangular frame and derived an expression similar to the one proposed by Cook (9). His method requires a careful selection of the unknown redundant forces in order to make the flexibility matrix manageable when solved by the computer. A determinate system capable of supporting the external load should be chosen and then calculating the loads induced in all members.

Marshall (32) extended Tidbury's matrix force method for simple frames to frames with five cross members. This demonstrated the disadvantage of the method which has to be reprogrammed for each new type of structure analysed. Automatic selection of redundancies in the force method has been developed by Robinson (33), which in turn adjusts the flexibility matrix for a particular problem.

The displacement method which is based on the formulation of a stiffness matrix is much easier. It is widely used in computer analysis by the finite element method.

Ali, Hedges and Mill (34) used a finite element method which is basically a displacement method to analyse a chassis frame. A stiffness matrix based on beam theory was used to predict the static deflection of the frame subject to torsion or bending loads. Hedges, Noville and Gurdogen (35) extended this analysis to determine the stress values in chassis frame members. The results compared well with the measured values for bending loads but not for torsional loads due to imperfectly

idealised torsional properties of the cross members and joints. The effects of warping restraint in the joint were not taken into consideration.

Triman (36) included the effects of warping torsion in a computer program which uses the stiffness matrix method. The bimoment and the rate of twist are added as an additional degree of freedom. His program was successfully tested by him to calculate the internal forces including bimoment as well as nodal displacement including the rate of twist in a cantilever beam, fixed-ended beam and continuous beam. The limitation of the program was that it was unable to calculate bimoment distribution in the grid structures such as frames.

Lee (37) developed Triman's (36) work to allow for the bimoment equilibrium at the joints. This was concerned with completely inhibited warping only.

Beermann (38-39) included the elasticity of nodal points in the finite element analysis. He defined the node by more than one point. The (TSW) node incorporating the torsion centre, the centroid and the warping point at the end of one of the beam elements meeting at the joint are used for this definition. This theory and further development by the present author will be shown in chapter (5). The effective lengths of the cross members were used in his analysis. He included the flexibility of the joints obtained from a finite element idealization together with the compatibility of their displacement.

A hybrid method of analysis is presented, which combines finite element idealization of the joint areas with analytically derived beam elements for the cross member and side member sections. The beam element includes warping/torsion force displacement relationships. The flexibility of the joints is included together with the compatibility of their displacements. He claimed that his method gives close agreement with experimental results.

The concepts of 'zero warping lines' and the 'zero warping axis' in a cross section have been introduced by Tidbury the editor of reference (39) for clarification of the author's argument.

Al-Hakeem (40) dealt with the problem of longitudinal or torsional loads acting on channel section side member through a spring hanger bracket and the longitudinal stresses developed in the side member. His study has shown that the bimoments due to the horizontal braking forces can cause large stresses in the frame which are not usually considered in the design of the side members.

The arrangement selected was a bracket attached to the flanges of the channel section side member equivalent to one bay of a chassis side member. Vlasov's (1) bimoment theory was applied to the side member. The boundary conditions taken for the side member were, total inhibition and free warping of the ends. The localised effects due to the bracket were not taken into consideration. He also applied bending theory to the side member to include and compare the stresses due to bending with those of bimoment.

Fixed-fixed and fixed-free end conditions for the side member were taken in bending. Direct stress was also included in the summing of the longitudinal stresses. He obtained close agreement between theoretical and experimental results with both loading cases. The conclusion was that the bimoment stresses due to longitudinal loads were quite large when compared with the sum of bending and direct stress, and added significantly to the accuracy of the results.

In view of the volume work, it has only been possible in this review to point out some emphasis on chassis frame researches. Similarly, no claim can be made that review is exhaustive and the reference list is in any way comprehensive or that even all the significant contribution have been included. Apologies are therefore offered to those individuals and organization whose work, although known to me, has only been included in the bibliography.

1.3 RESEARCH CONTRIBUTION AND PRESENTATION

This project deals with the problem of longitudinal loads acting on the side members of chassis frames through spring hanger brackets and the longitudinal stresses developed in the side members due to warping restraint effects.

The members of a ladder chassis frame are regarded as having thin walled sections. Hence, the established Vlasov theory for thin walled open section beams, when their cross sections are allowed to warp freely (St. venant torsion) or completely restrained from warping (torsion bending theory), are presented in chapter (2).

Also the theory of torsion of thin walled open section beams, having cross sections partially restrained from warping are presented in the same chapter. Investigators have made various assumptions for determining the torsional stiffness and eventually stresses in cross members. These analyses are now quite well understood and documented, with the work of various authors (see section 1.2).

In chapter (3), a general elastic stiffness matrix is derived including warping inhibition in thin walled open section beams. The rate of twist and bimoment are used to modify the conventional (6) degrees of freedom beam structural analysis to one which has (7) degrees of freedom for each node. The warping displacement at the joints for the derivation of this stiffness matrix is considered as being completely transferred to the other connected parts as far as the joints are concerned. Accordingly a general transformation from local to global axes was derived to account for the new load system.

The analysis of chassis frame members with closed section cross members is also considered. In chapter (4) formulae for analysing thin walled box section beams subjected to torsional loading and considering fully restrained warping is presented. The method is extended to take only partial restraint of warping into account but does not include the effects of cross sectional distortion. A stiffness matrix similar to the one presented in chapter (3), but for thin walled closed section beams was developed in this chapter.

Chapter (5) contains a developed equilibrium matrix for different types and orientation of cross members beams meeting at the joint. This equilibrium matrix is built on a rigid joint assumptions, but it allows for the axis offset of the members meeting at the joint. Flexible joint assumptions are also presented, and the rate of twist stiffness coefficient of a joint was defined.

A method developed for calculating the bimoment created due to the longitudinal load was presented in chapter (6).

In chapter (7), a description is given of the finite element system used for this research project and the structural and finite element idealisations of ladder chassis frame joints having channel and closed section cross members. A finite element idealisation of complete chassis frames under longitudinal loads were also presented. The same chapter contains the description and the results of the finite element analyses on ladder chassis frame joints.

In chapter (8) theories and methods, developed in previous chapters, were incorporated into a special purpose finite element program using the direct stiffness method. The program includes warping inhibition effects in thin walled beams. Both assumptions for either rigid or flexible joints are used in the analysis by this program. The program can be used as a design tool in the preliminary stages of chassis design. The distribution of bimoments and of moments along the side members of a chassis frame due to longitudinal loads for different loading cases is also presented in this chapter.

A description of the longitudinal load tests performed on a ladder chassis frame in the laboratory with different longitudinal load cases are presented in chapter (9). The experimental rig used together with the measurement techniques adopted to determine stresses in the side members are discussed in detail. The discussion of the measured and corresponding finite element values with the theoretical results of stresses obtained from the program developed in chapter (8) are also presented.

Finally, chapter (10) contains general conclusions, discussion and several suggestions for the optimum design and attachment positions for components such as spring hanger brackets to the side members of the chassis frame, from the point of view of longitudinal loadings. Lines of research are suggested which follow on from those presented in this thesis.

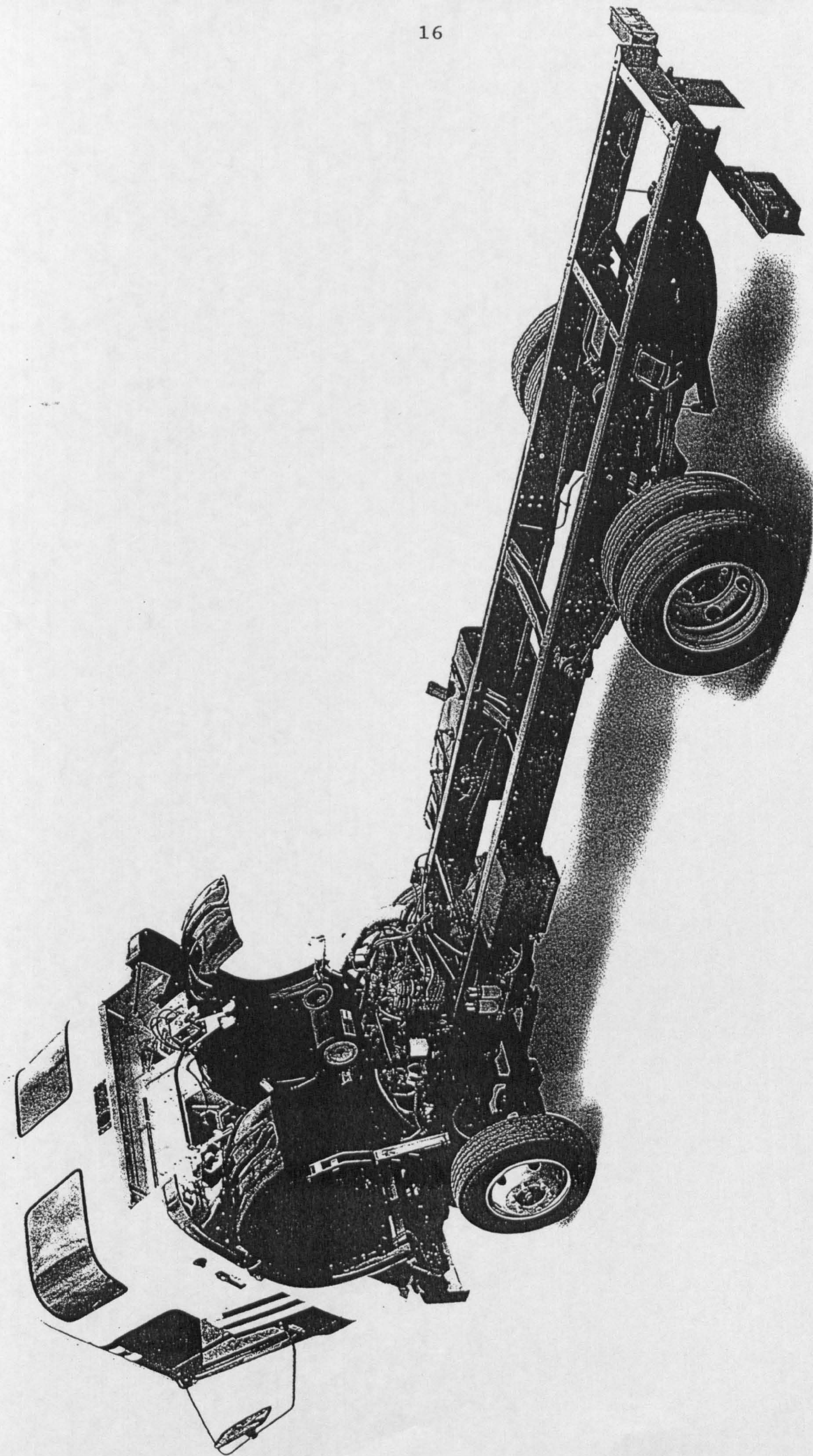
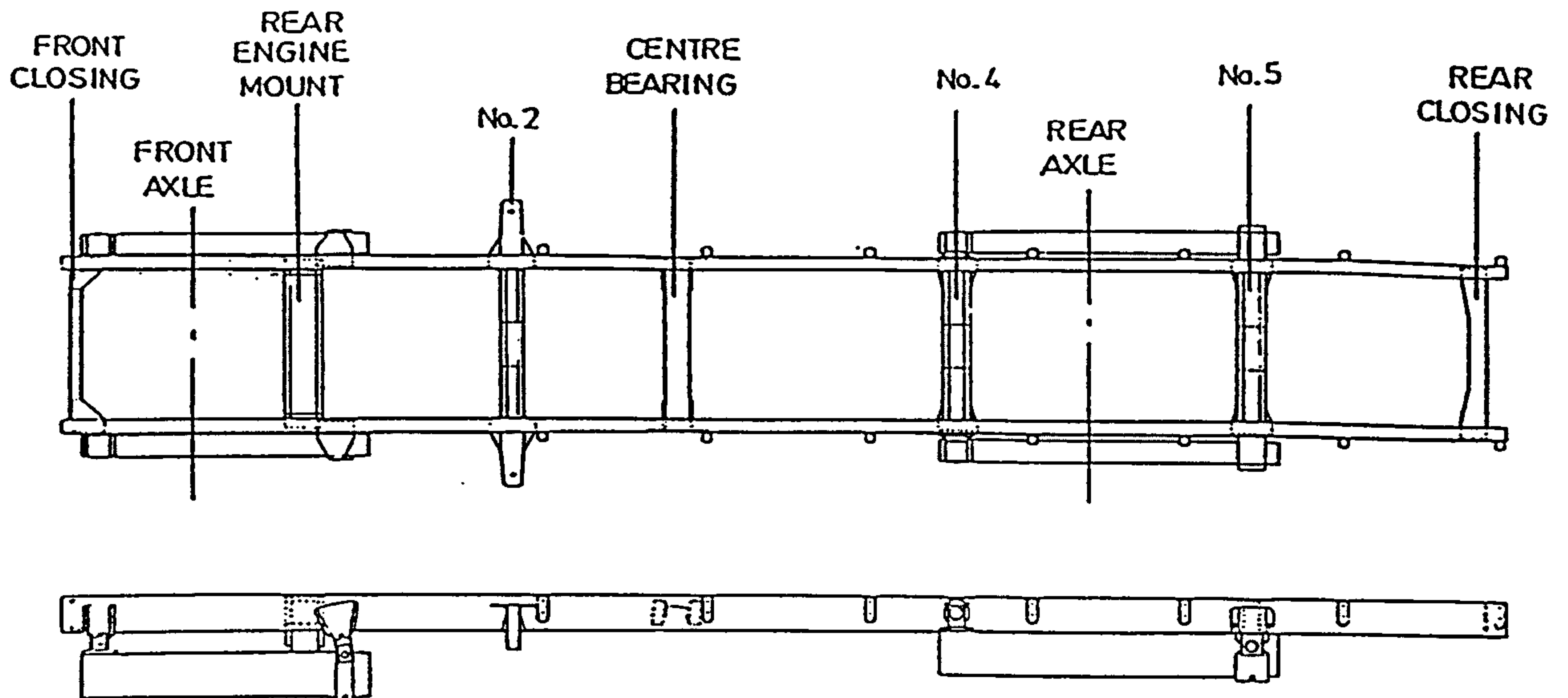
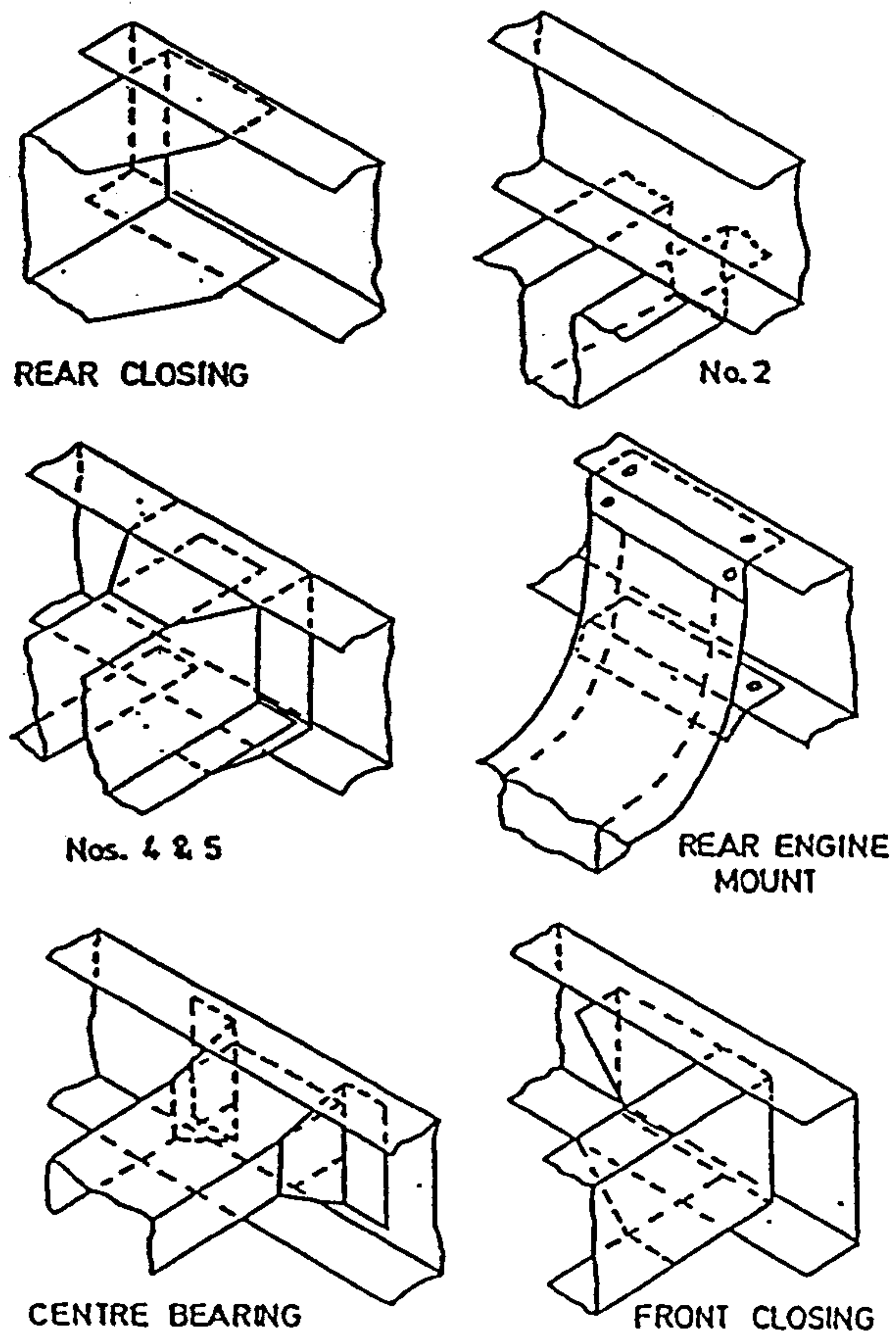


Fig.(1.1) Typical commercial vehicle with a ladder chassis frame



a) Truck chassis



b) Cross member joints

Fig.(1.2) A ladder chassis frame with variety of joint designs

CHAPTER TWO

**WARPIING THEORY OF
THIN-WALLED OPEN
SECTION BEAMS**

2.1 INTRODUCTION

Thin walled beams have been defined as structural elements whose three dimensions all have a different order of magnitude. The wall thickness being small compared with any cross section dimension which is itself small compared with the length. Such a definition can be applied to sheet metal cold formed or coiled strip to form various shapes such as a channel, I- or tophat sections as shown in figure (2.1). It is assumed that the shape of the cross section is maintained constant. Most of the beam structures may be classified as having either thick or thin walled sections. There is no clearly defined border between sections which may be regarded as thin and those which must be considered as thick. Some criterion is therefore required to distinguish between a thick and a thin sections, as assumptions of thin walled theory will decrease in validity the thicker a section becomes. It has been suggested by Vlasov (1) that thin walled theory may be applied with reasonable accuracy to sections for which the ratio:-

$$\frac{t_{\max}}{h} \leq 0.1$$

where (t_{\max}) is the maximum thickness in the section, and (h) is the typical cross sectional dimension.

Warping effects of thin walled beams can be as important as bending in determination of stresses and displacements of these structural elements. The torsional properties of thin walled beams can be markedly different from those calculated by elementary methods and an appreciation of the theory is of considerable importance in Automotive structural design. For this reason a summary of the theory is given in this chapter with an emphasis on the important relationships for chassis frame analysis.

2.2 WARPING

The cross section of a thin walled open section beam subject to pure torsion will not remain plane, the displacements of the cross section in the axial direction of the beam is called warping. Two types of warping displacement take place

simultaneously. The first type is the warping of the mid-plane of the cross section as shown in figure (2.2) which is assumed constant across the wall thickness and is known as primary warping. The second type is the warping of the section across its wall thickness and this is known as secondary warping. Secondary warping and the effects of restrained secondary warping are very much less than primary warping and the effects of restrained primary warping, therefore secondary warping effects are usually neglected. As far as this research is concerned, the primary warping will be considered as the main effect to be studied.

Although warping of the cross section of thin walled beams occurs mainly in torsion, it can also arise:-

- i) from longitudinal loads, except when they act through special points on the cross section and,
- ii) from bending moments caused by pairs of normal loads acting in planes which do not pass through the torsion centre as shown in figure (2.7).

Thus, the warping displacement of the mid-plane of the cross section of an open beam is shown by Vlasov (1) to be of form:-

$$W = - \omega_s \frac{d\theta}{dx} \quad \text{-----} \quad (2-1)$$

Where (ω_s) is called sectorial area (or sectorial co-ordinate). This is twice the area swept out by a generator rotating about the centre of twist (R) from the point of zero warping in the cross section to any point (s) as shown in figure (2.4).

With respect to the physical properties of thin walled beams, additional sectional properties based on the sectorial co-ordinate, which are called the sectorial properties should be introduced. In the same way as for the conventional beam theory, those sectorial properties are defined as shear centre, sectorial linear statical moment of a section, second moment of sectorial area and principal second moment of sectorial area from the principal sectorial co-ordinate. The relationship between the sectorial and conventional properties of thin walled open section are expressed in table (2.1).

2.3 SAINT VENANT THEORY (FREE WARPING)

The assumptions on which the theory is based are similar to those for the torsion of a closed section in that the cross section is assumed to remain undistorted in its own plane after loading. In this case the beam is under pure torsion and does not produce any longitudinal stresses even when there is an axial restraint (so long as this does not restrain warping). The rate of twist of the beam is constant. The axial displacement which is called warping displacement must not be prevented at any section and the warping distribution of the cross section is identical throughout the beam as shown in figure (2.2). Thus, the plane of the cross sections do not remain plane.

To obtain the value of the shear stress in a section subject to St. venant torsion, it is necessary to solve the Laplace equation. Shear stress varies across the thickness. The distribution of shear stress across the thickness is shown in figure (2.3). The expression for St. venant maximum shear stress distribution in thin walled open section beam subject to unrestrained torsion is given by Megson (17) to be:-

$$\tau_{\max} = \pm T_j \frac{t}{J} \quad \text{-----} \quad (2-2)$$

Where (J) is St. venant torsional constant

(t) is the thickness

(T_j) is the applied torque in the St. venant case

St. venant torsion (T_j) is given as:-

$$T_j = GJ \frac{d\theta}{dx} \quad \text{-----} \quad (2-3)$$

2.4 AXIAL CONSTRAINT EFFECTS (RESTRAINED WARPING)

As pointed out in section (2.3), the cross sections of thin walled open beams subjected to unrestrained (St. venant) torsion experience a free warping distribution.

In such a case the complete cross section suffers identical warping displacement distribution along the longitudinal generator of the beam surface. If one end of the beam is completely or partially prevented from warping as shown in figure (2.5), the longitudinal generators of the beam surface are strained, the rate of twist along the length of the beam is no longer constant.

2.5 TORSION BENDING THEORY

Consider a thin walled open section beam subjected to a torque at one end and rigidly restrained from warping at the other end as shown in figure (2.5). The total resistance is provided by a combination of the St. Venant shear stresses and the resistance of the web and flanges of a channel or an I-section which are no longer free to warp at the built-in end and this is responsible for the bending of the flanges in their own planes. Therefore, the total torque is a sum of St. Venant torque and an additional term called by Vlasov the flexural twist.

$$T = T_j + T_r \quad \text{-----} \quad (2-4)$$

Where (T_j) is St. Venant torque from the free end warping, but $(d\theta/dx)$ is no longer constant and (T_r) is the contribution from the warping restraint.

The validity of equation (2-4) has been shown in figure (2.8) for an I-section beam where the first deformation is due to St. Venant torque while, the second due to flexural twist. The relevant equations are shown by Vlasov (1) to be:-

$$\begin{aligned} T_j &= GJ \frac{d\theta}{dx} \\ T_r &= - E\Gamma \frac{d^3\theta}{dx^3} \end{aligned} \quad \text{-----} \quad (2-5)$$

Where (Γ) is the warping constant or principal sectorial moment of inertia and:-

$$\Gamma = \int_{\text{section}} \omega_s^2 t \, ds$$

2.6 BIMOMENT AND FLEXURAL TWIST

Vlasov (1), introduces the concept of a bimoment, (B), as shown in figure (2.7), which is defined as the product of a pair of equal and opposite moments and the distance between them. He defines the flexural twist (T_r) as the derivative of the bimoment. The relevant equations are quoted from Vlasov (1).

$$\begin{aligned}
 W_{(x)} &= -\omega_s \frac{d\theta}{dx} \\
 B_{(x)} &= -E\Gamma \frac{d^2\theta}{dx^2} \\
 T_{r(x)} &= \frac{dB}{dx} = -E\Gamma \frac{d^3\theta}{dx^3} \\
 \sigma_{r(x)} &= \frac{B\omega_s}{\Gamma}
 \end{aligned}
 \tag{2-6}$$

From figure (2.8) it can be concluded that the flexural twist causes a bimoment representing the warping forces acting at a sectorial area, and resembling of two mutually balancing equal but opposite bending moments acting in two parallel planes. Substituting equations (2-5) into equation (2-4):-

$$T = GJ \frac{d\theta}{dx} - E\Gamma \frac{d^3\theta}{dx^3}
 \tag{2-7}$$

Where (GJ) is defined as torsional rigidity and,
(EΓ) sectorial rigidity

If the applied torsion load is distributed along the member, this becomes a fourth order differential equation. The fourth order differential disappears if external torsion is applied at the ends only.

For thin walled beams it should be noted that the sectorial rigidity is much greater than the torsional rigidity.

2.7 THE DIFFERENTIAL EQUATION FOR RATE OF TWIST ALONG A THIN-WALLED BEAM

In actual structures, the geometrical restraint along the longitudinal direction of the member, such as that at the joints of a chassis frame, will cause additional flexural twist, so the rate of twist ($d\theta/dx$) is not constant.

Rearranging equation (2-7) using $\mu^2 = \frac{GJ}{EI}$

Thus:-

$$\frac{d^2}{dx^2} \left(\frac{d\theta}{dx} \right) - \mu^2 \frac{d\theta}{dx} = - \mu^2 \frac{T}{GJ} \quad \text{-----} \quad (2-8)$$

To find the general solution for the rate of twist ($d\theta/dx$) in equation (2-8) we apply:-

i) Complementary function to solve L.H.S with auxiliary equation.

$$m^2 - \mu^2 = 0$$

$$m = \pm \mu$$

$$\text{Accordingly, } \left(\frac{d\theta}{dx} \right)_{CF} = Ce^{\mu x} + De^{-\mu x}$$

$$\left(\frac{d\theta}{dx} \right)_{CF} = (C+D) \cosh \mu x + (C-D) \sinh \mu x$$

$$\text{Let } (C+D) = C_1, \text{ and } (C-D) = C_2$$

$$\left(\frac{d\theta}{dx} \right)_{CF} = C_1 \cosh \mu x + C_2 \sinh \mu x \quad \text{-----} \quad (2-9)$$

ii) Particular Integral to solve R.H.S

$$\frac{d\theta}{dx} = K$$

$$\frac{d^2\theta}{dx^2} = \frac{d}{dx} \left(\frac{d\theta}{dx} \right) = 0$$

and,

$$\frac{d^3\theta}{dx^3} = \frac{d^2}{dx^2} \left(\frac{d\theta}{dx} \right) = 0$$

substitute in equation (2-8) becomes:-

$$0 - \mu^2 (K) = - \mu^2 \frac{T}{GJ}$$

$$K = \frac{T}{GJ}$$

$$\left(\frac{d\theta}{dx} \right)_{P.I} = \frac{T}{GJ}$$

So the general solution for the rate of twist is:-

$$\frac{d\theta}{dx} = C_1 \cosh \mu x + C_2 \sinh \mu x + \frac{T}{GJ} \quad \text{-----} \quad (2-10)$$

Where (x) is measured from the built-in end (see figure 2.6), and (C₁) and (C₂) are constants determined from the boundary conditions.

As far as warping is concerned with the chassis frame subjected to any type of loading such as, torsional or longitudinal load, equation (2-10) is the basic equation to be executed with the appropriate boundary conditions for free and completely inhibited warping conditions at the ends of the members, and also in the case of partially inhibited warping.

2.8 COMPLETE WARPING RESTRAINT

For a uniform member with complete warping inhibition at both ends it can be shown that, using symmetry, the correct result for torsional stiffness can be obtained by considering it as two torsional cantilevers half of the length as shown in figure (2.6).

Therefore, for an open section cantilever, the arbitrary constants (C_1) and (C_2) in equation (2-10) can be obtained using the following boundary conditions.

i) at the warping inhibited end where $x=0$, $W=0$

$$\text{Thus:- } \frac{d\theta}{dx} = 0$$

$$C_1 = - \frac{T}{GJ}$$

ii) at free end where $x=L$, $\sigma_r = 0$

$$\text{Thus:- } \frac{d^2\theta}{dx^2} = 0$$

$$C_2 = \frac{T}{GJ} \tanh \mu L$$

Substituting these constants for (C_1) and (C_2) in equation (2-10) becomes:-

$$\frac{d\theta}{dx} = \frac{T}{GJ} \left(1 - \frac{\cosh \mu(L-x)}{\cosh \mu L} \right) \quad \text{-----} \quad (2-11)$$

in which (L) is the beam span.

The first term of equation (2-11) corresponds to the rate of twist in the unconstrained (free warping) open section beam. The second term represents the reduction in the rate of twist due to axial restraint.

After integrating equation (2-11) with the appropriate boundary condition (i.e $\theta=0$ at the warping inhibited end, where $x=0$). The angle of twist (θ) thus can be obtained as:-

$$\theta_x = \frac{T}{GJ} \left(x + \frac{\sinh \mu(x-L) - \sinh \mu L}{\mu \cosh \mu L} \right) \quad \text{-----} \quad (2-12)$$

At the free end where $x=L$, the angle of twist is:-

$$\theta_{TP} = \frac{TL}{GJ} \left(\frac{\mu L - \tanh \mu L}{\mu L} \right) \quad \text{-----} \quad (2-13)$$

Thus, defining an effective torsion constant (J_T) for the member where warping is completely inhibited at the end as:-

$$J_T = \frac{TL}{G\theta_{TP}} \quad \text{-----} \quad (2-14)$$

and substituting for (θ_{TP}) from equation (2-13) get:-

$$J_T = J \left(\frac{\mu L}{\mu L - \tanh \mu L} \right) \quad \text{-----} \quad (2-15)$$

Substituting equation (2-11) in equations (2-6) for a beam completely restrained from warping at one end and subjected to a torque at the another, the bimoment (B), the warping displacement (W) and the longitudinal normal stress variation along the axial direction of the beam (x) can be written as:-

$$\begin{aligned} W_{r(x)} &= - \frac{T\omega_s}{GJ} \left(1 - \frac{\cosh \mu(L-x)}{\cosh \mu L} \right) \\ B_{r(x)} &= - \frac{T}{GJ} \frac{\sinh \mu(L-x)}{\cosh \mu L} \\ \sigma_{r(x)} &= - \frac{T\omega_s}{\mu \Gamma} \frac{\sinh \mu(L-x)}{\cosh \mu L} \end{aligned} \quad \text{-----} \quad (2-16)$$

2.9 PARTIAL WARPING RESTRAINT

So far, the boundary conditions are taken to be simplified extreme cases of warping behaviour for the end conditions in a bay of open section chassis frame. The boundary conditions discussed so far are:-

- i) free warping behaviour of the beam cross section in the case of unrestrained torsion (St. venant).
- ii) completely restrained warping at some section of the beam in case of restrained torsion.

In a real chassis frame the cross members are restrained at the joint by the side members. Therefore, the boundary conditions in the joints are partially restrained from warping and the connection is partially built-in as shown in figure (2.5b). The degree of partially restrained warping can be assumed to be directly proportional to that of free warping in the joint obtained by equation (2-1), e.g see reference (23) of the bibliography. The constant of proportionality, (K), which is called the warping restraint factor, is determined by the degree of restraint provided by the side members.

Thus:-

$$W_p = K * W_f = -K \omega_s \frac{d\theta}{dx} \quad \text{-----} \quad (2-17)$$

Where (W_p) is partial warping displacement of the cross section,

(W_f) is free warping displacement of the cross section.

When $K=1$, the cross sections of the cross members of the chassis frame are completely free to warp and, when $K=0$ the cross section is completely restrained from warping in the joint.

The warping restraint factor, (K), can be obtained by dividing the area under the partial warping curve round the cross member section (which can be obtained from a finite element analysis of the detailed joint or from experiments) by the area

under the free warping curve round the same section. This is similar to the approach used by Lee (37). The method was chosen in preference to taking simple ratios at single points. The justification for this may be seen from comparisons made in chapter (7) for every joint examined.

Comparing equation (2-17) with equation (2-1) we get:-

$$\frac{d\theta}{dx} = K \frac{T}{GJ} \quad \text{-----} \quad (2-18)$$

This gives a new boundary condition for equation (2-10) in solving for $(d\theta/dx)$, and the modified rate of twist of the beam is shown by Alade (19) to be:-

$$\frac{d\theta}{dx} = \frac{T}{GJ} \left(1 - (1-K) \frac{\cosh \mu(L-x)}{\cosh \mu L} \right) \quad \text{-----} \quad (2-19)$$

As in the case of free warping, the angle of twist is given with the proper boundary condition being $\theta=0$ at $x=0$.

Hence:-

$$\theta_x = \frac{T}{GJ} \left(x - \frac{(1-K)(\sinh \mu(x-L) - \sinh \mu L)}{\mu \cosh \mu L} \right) \quad \text{-----} \quad (2-20)$$

and the total angle of twist (θ_{TP}) at $x=L$ would be:-

$$\theta_{TP} = \frac{TL}{GJ} \left(\frac{\mu L - (1-K)\tanh \mu L}{\mu L} \right) \quad \text{-----} \quad (2-21)$$

Hence, the effective torsion constant for the cross member is then given by either:-

$$J_p = \frac{TL}{G\theta_{TP}} \quad \text{-----} \quad (2-22)$$

or;

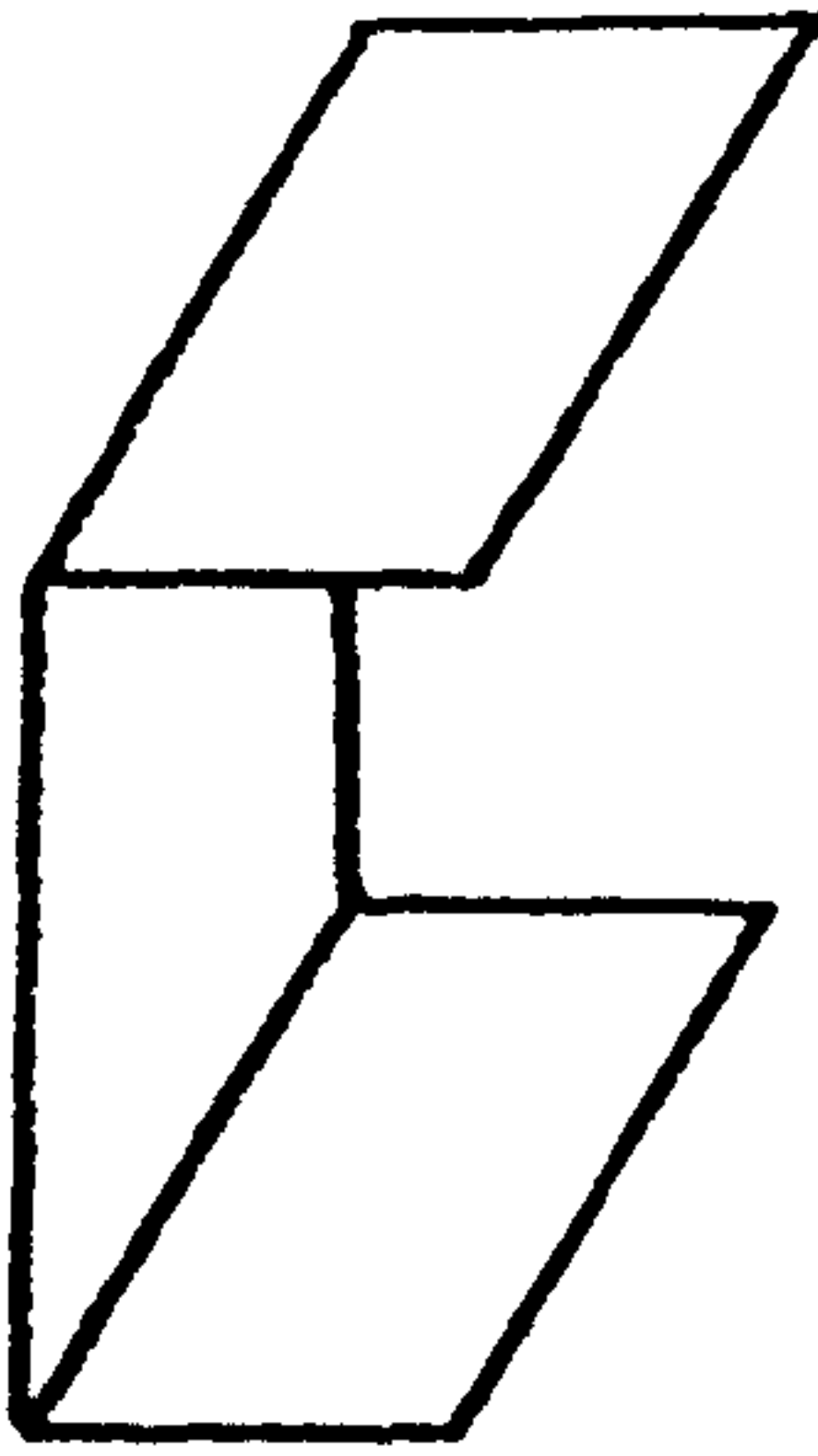
$$J_p = J \left(\frac{\mu L}{\mu L - (1-K) \tanh \mu L} \right) \quad \text{-----} \quad (2-23)$$

Therefore, equations (2-16) for partially restrained warping can be written as:-

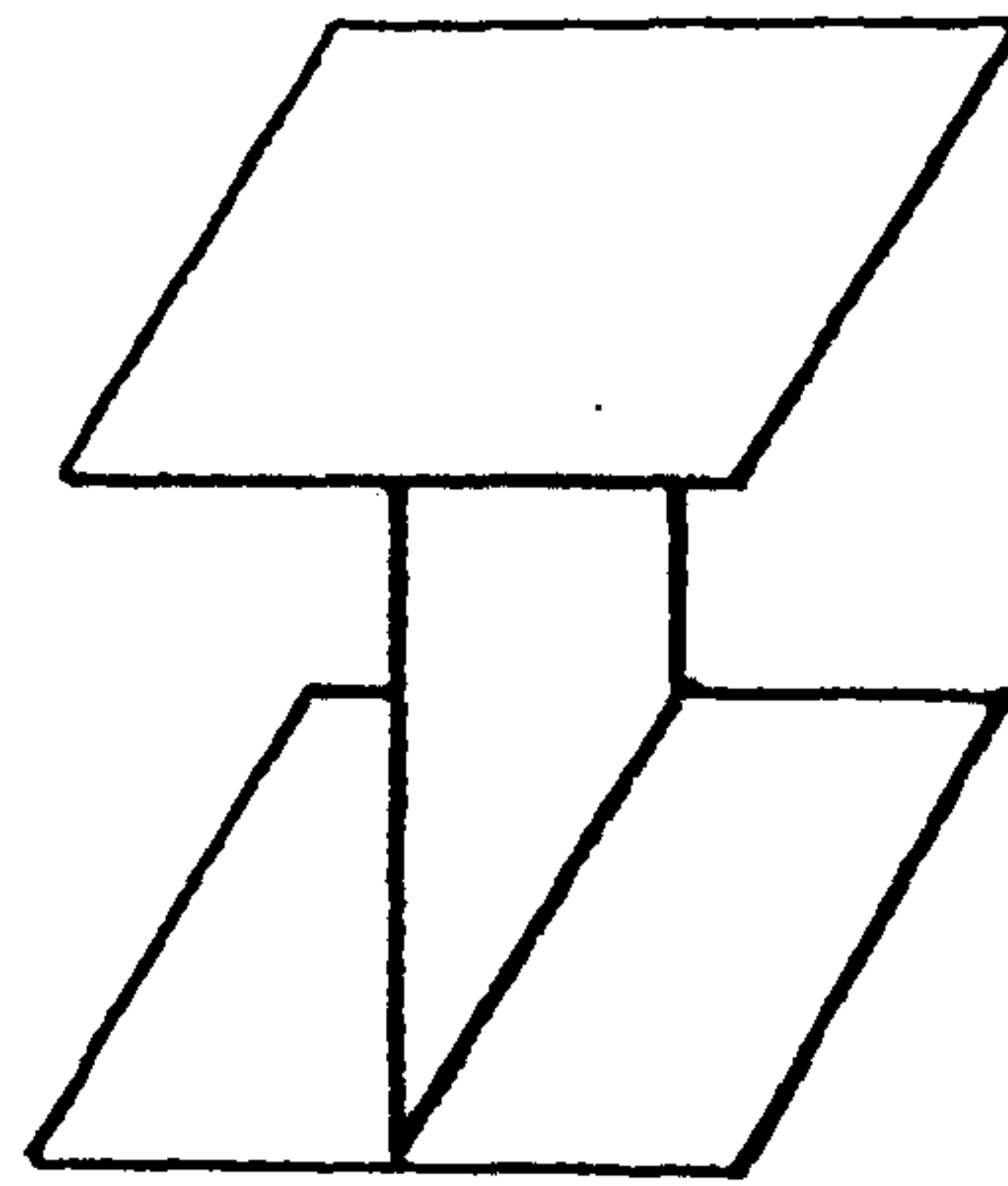
$$B_{P(x)} = (1-K) B_{\Gamma(x)} \quad \text{-----} \quad (2-24)$$

$$\sigma_{P(x)} = (1-K) \sigma_{\Gamma(x)}$$

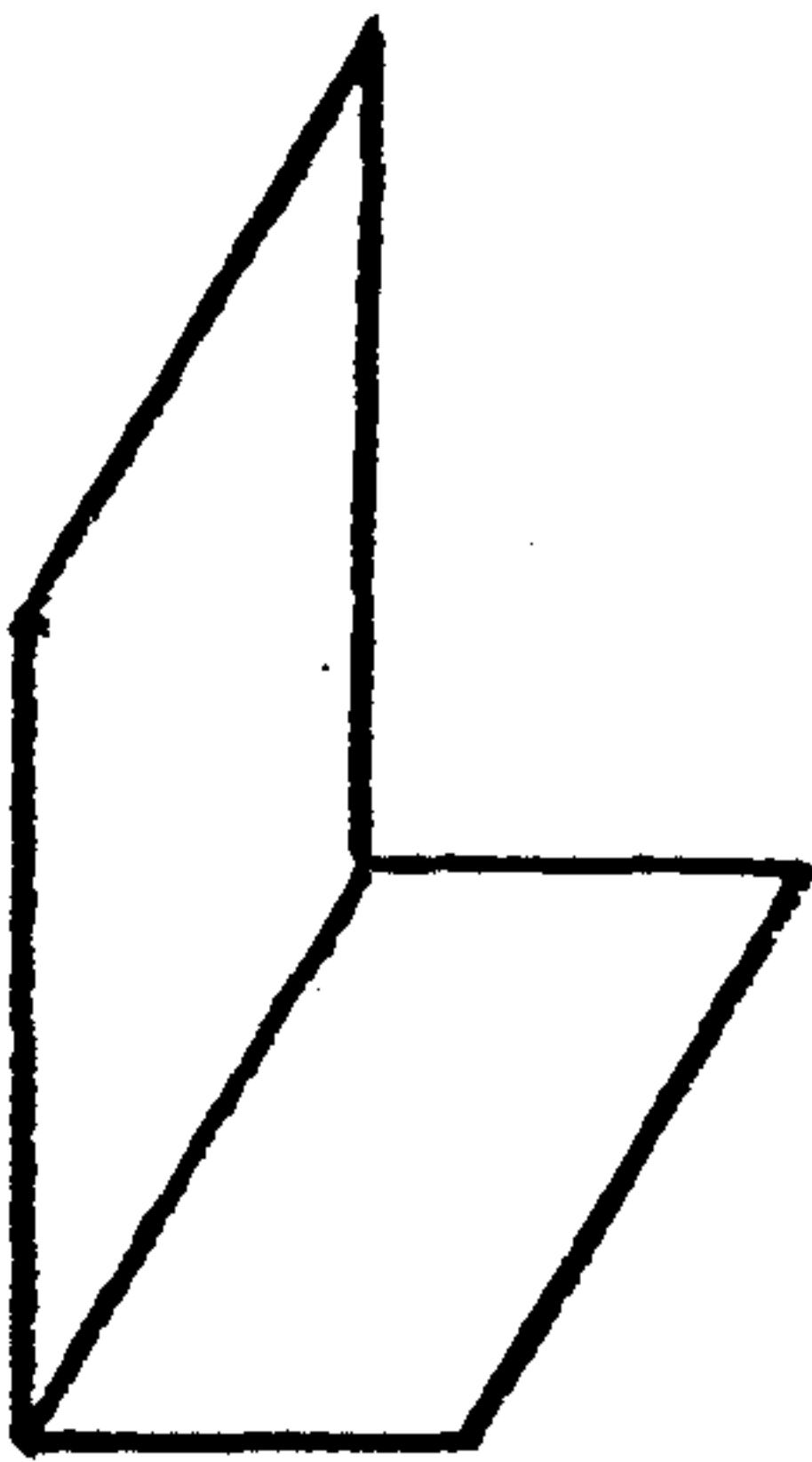
Measured values by Alade (19) for open section cross members in isolated joints agreed closely with the predicted values using the above expressions.



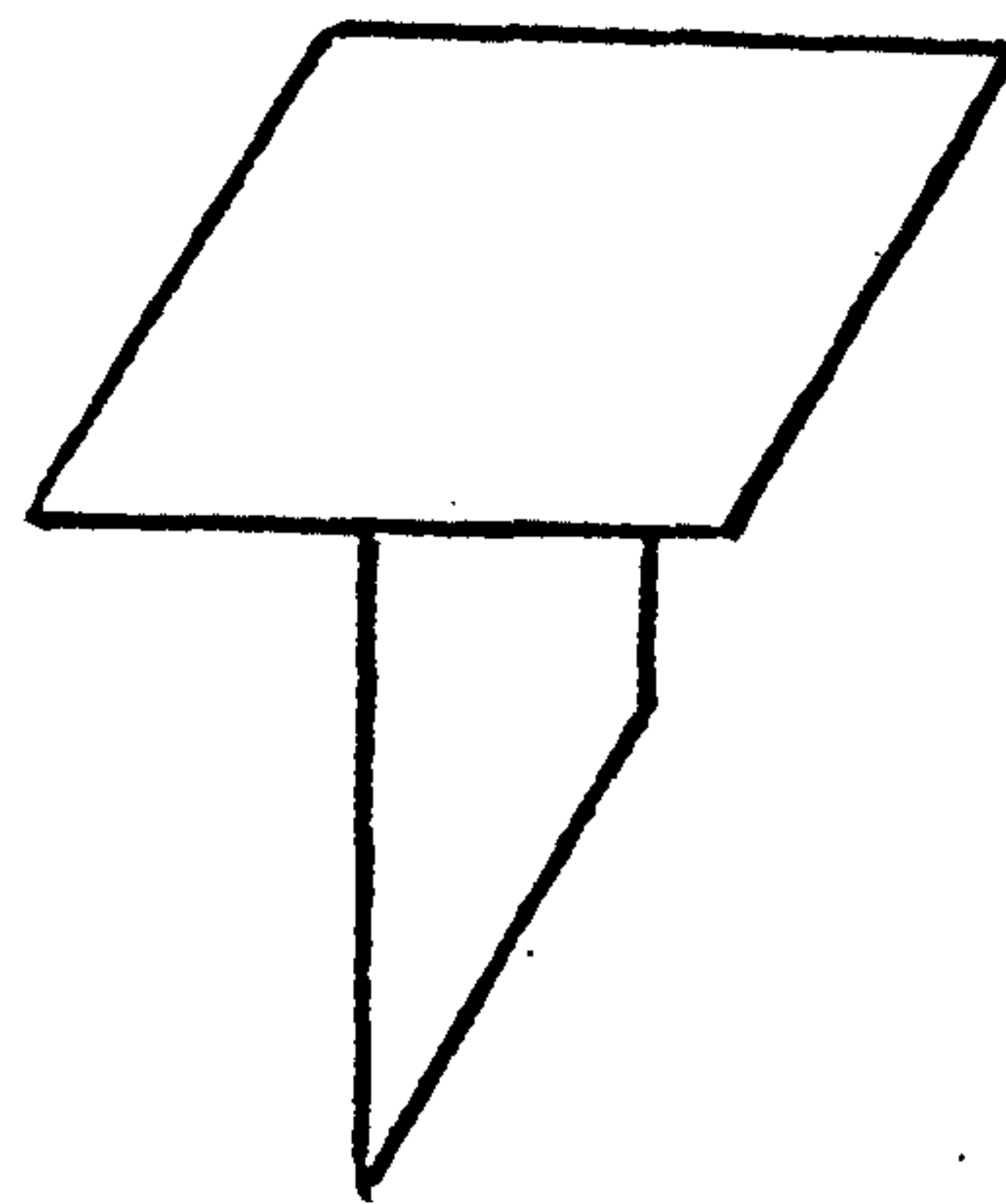
a) Channel section



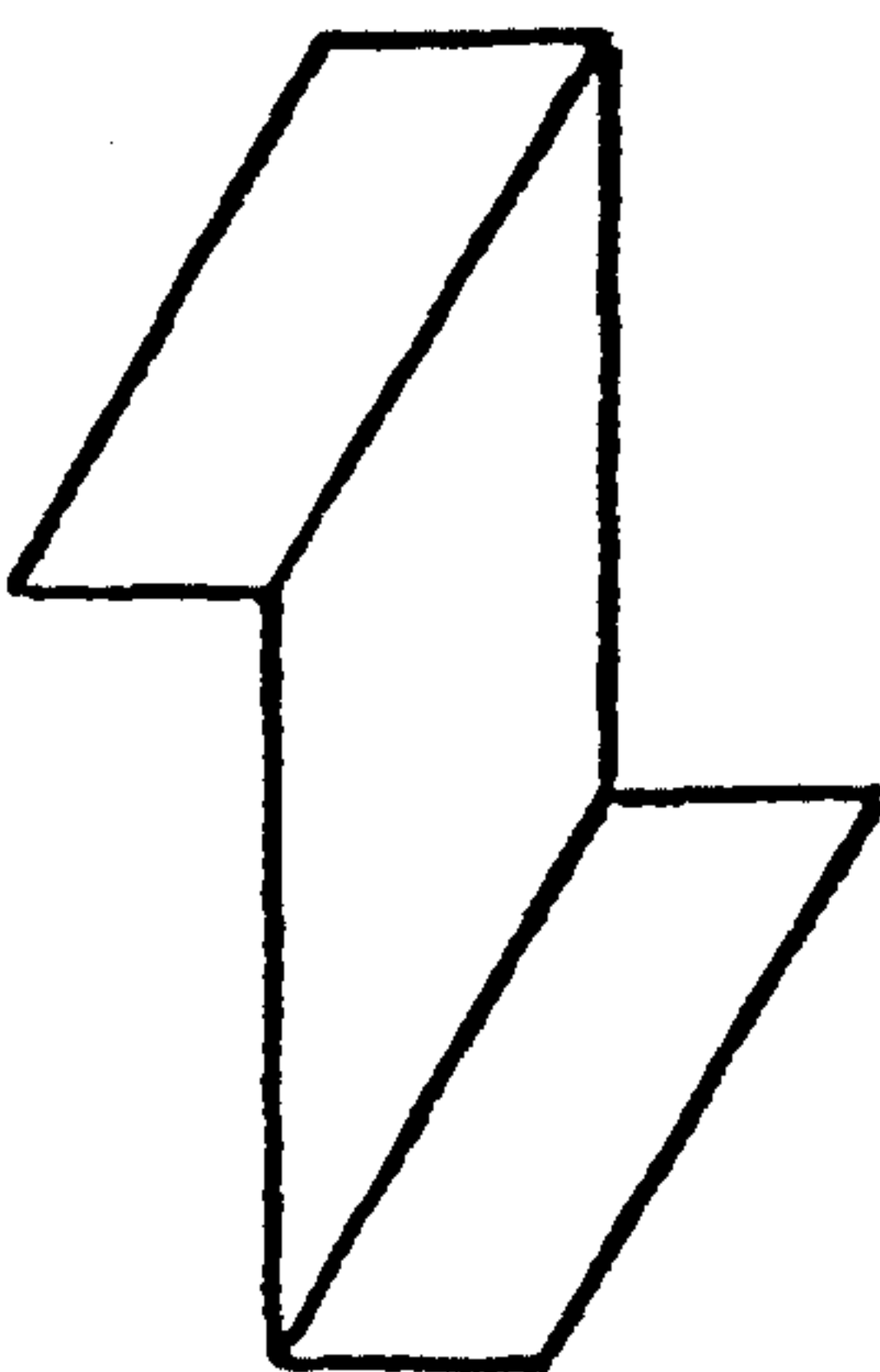
b) I-section



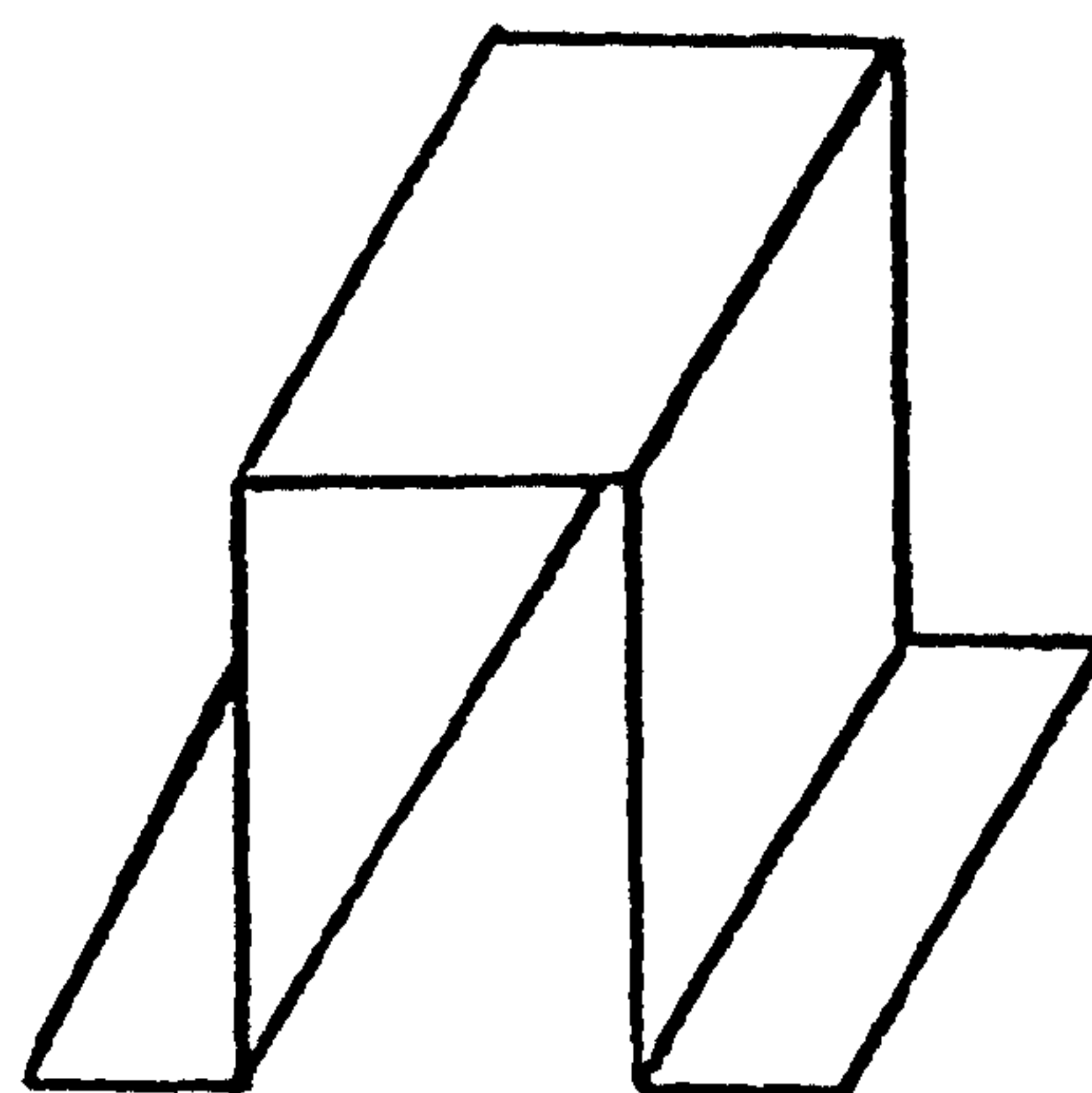
c) L-section



d) T-section

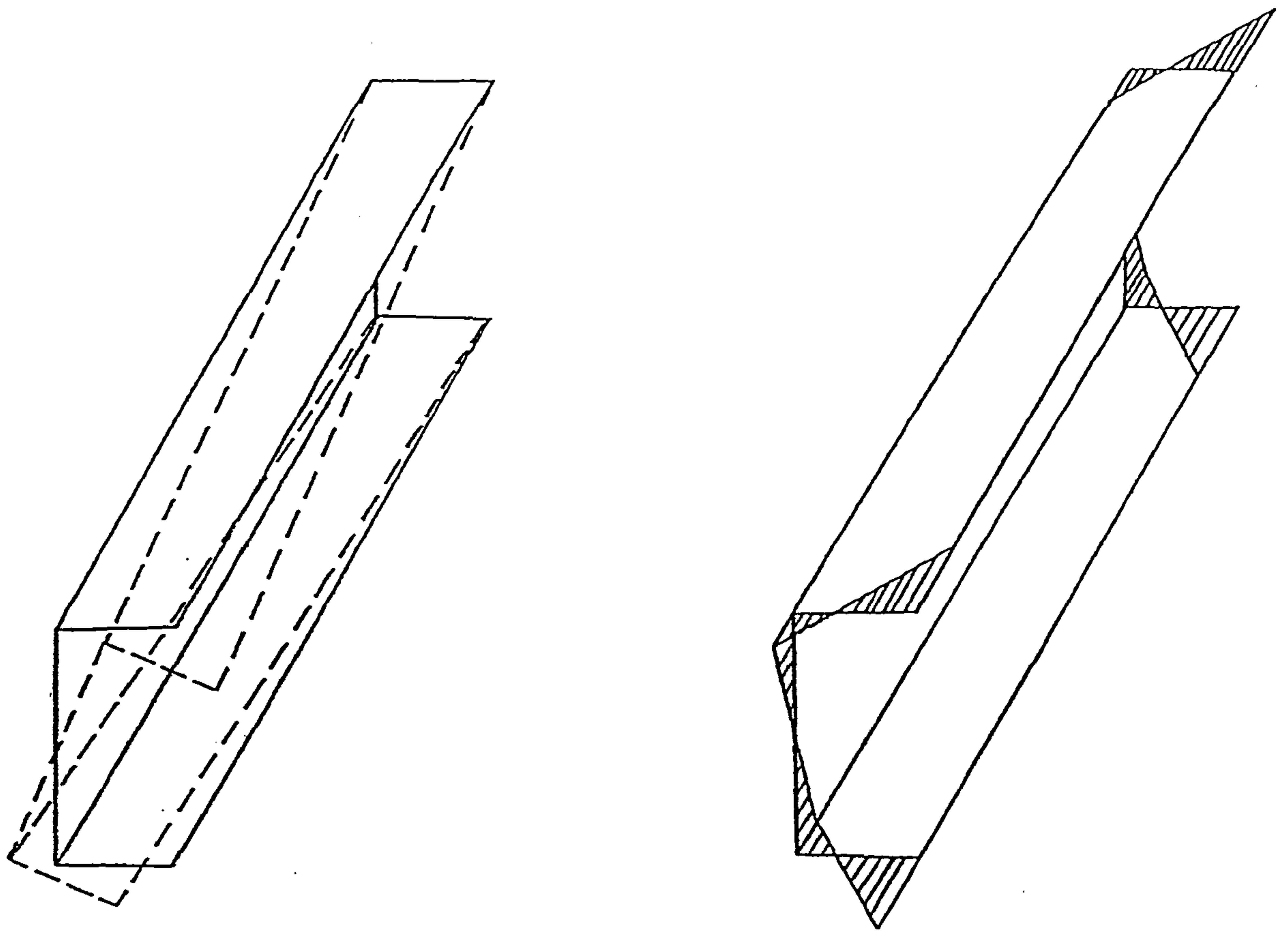


e) Z-section



f) Top-hat section

Fig.(2.1) Typical types of thin-walled open section beams



a) Unrestrained torsion

b) Free warping displacement

Fig.(2.2) Channel section beam under pure torsion

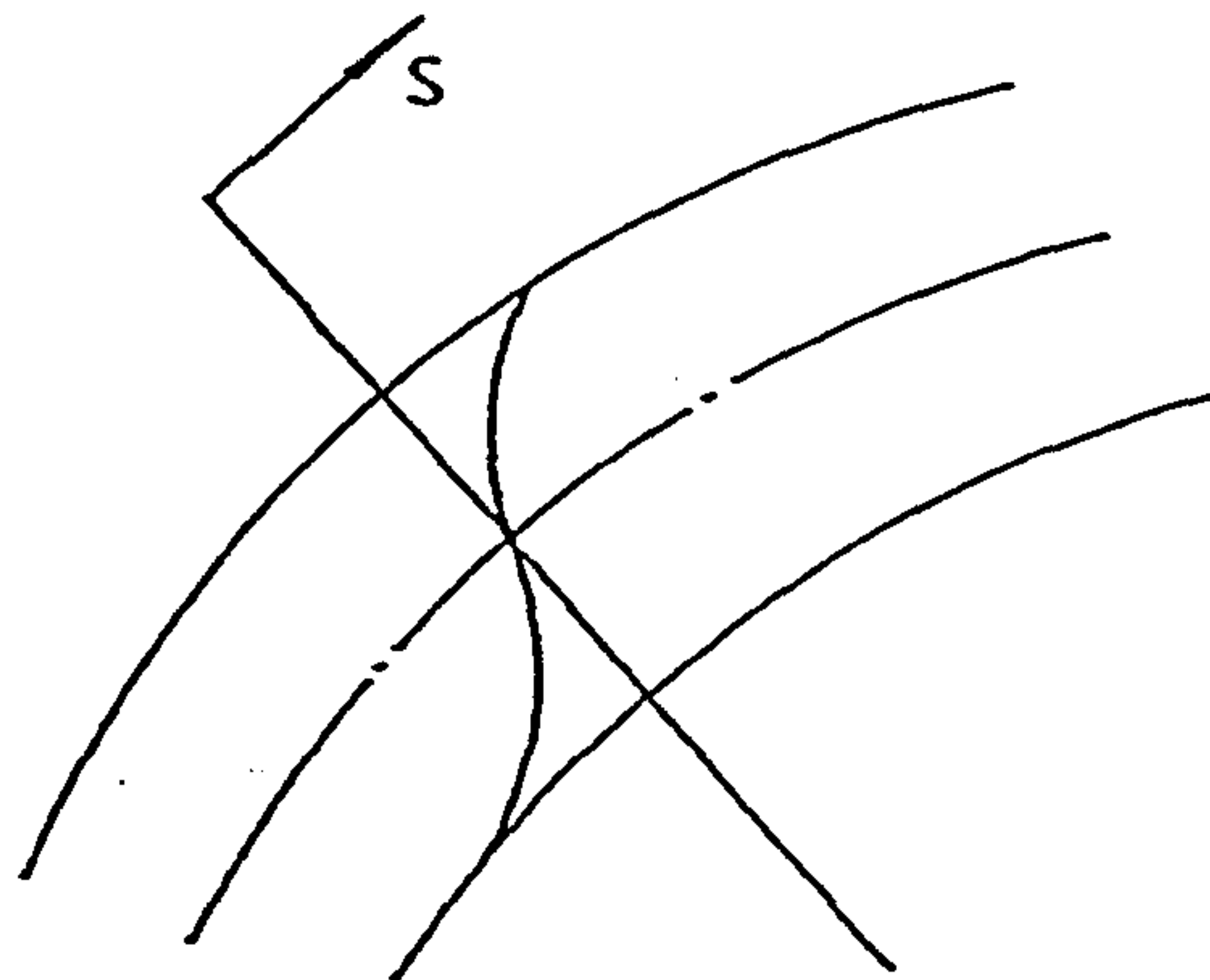
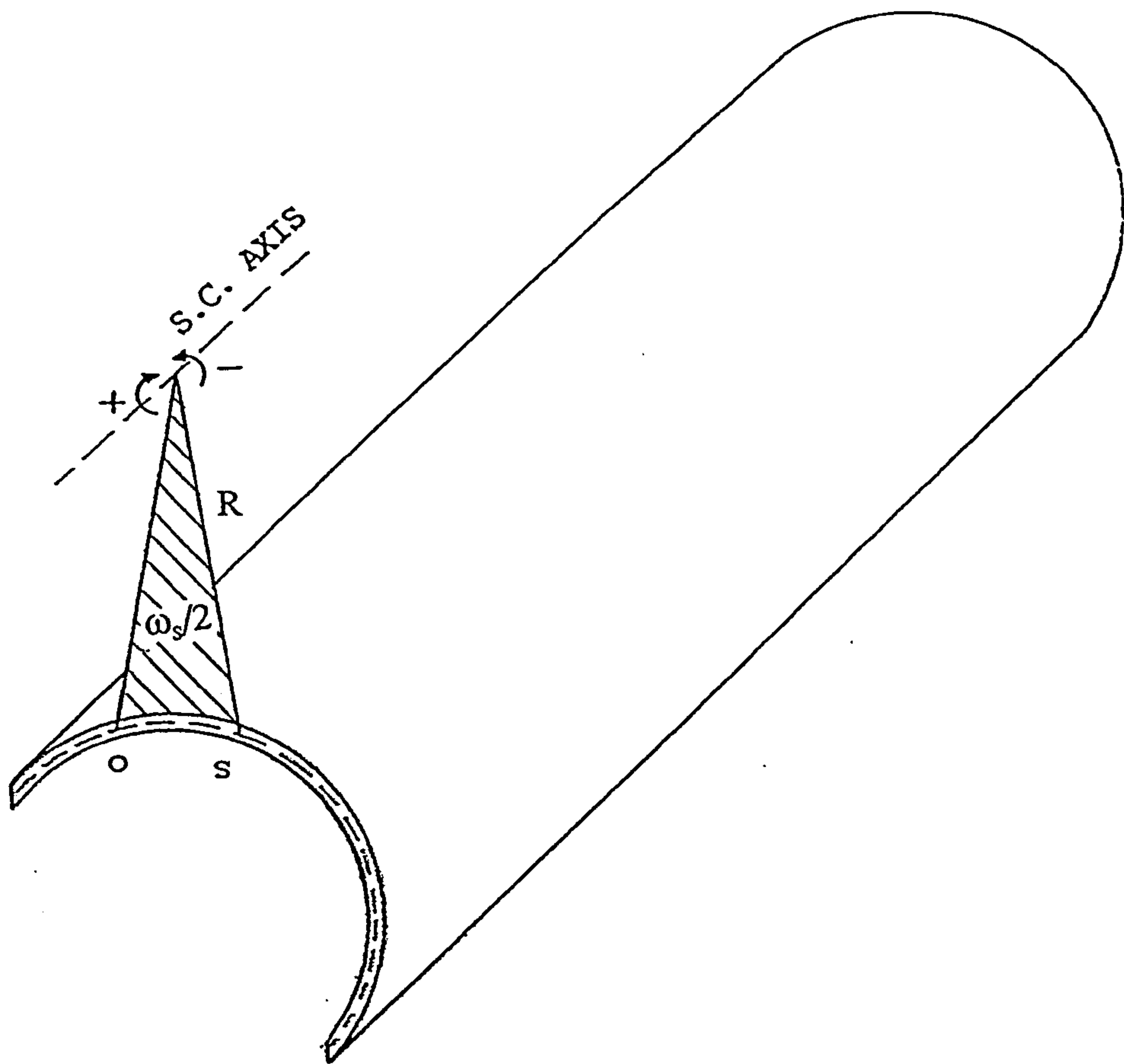
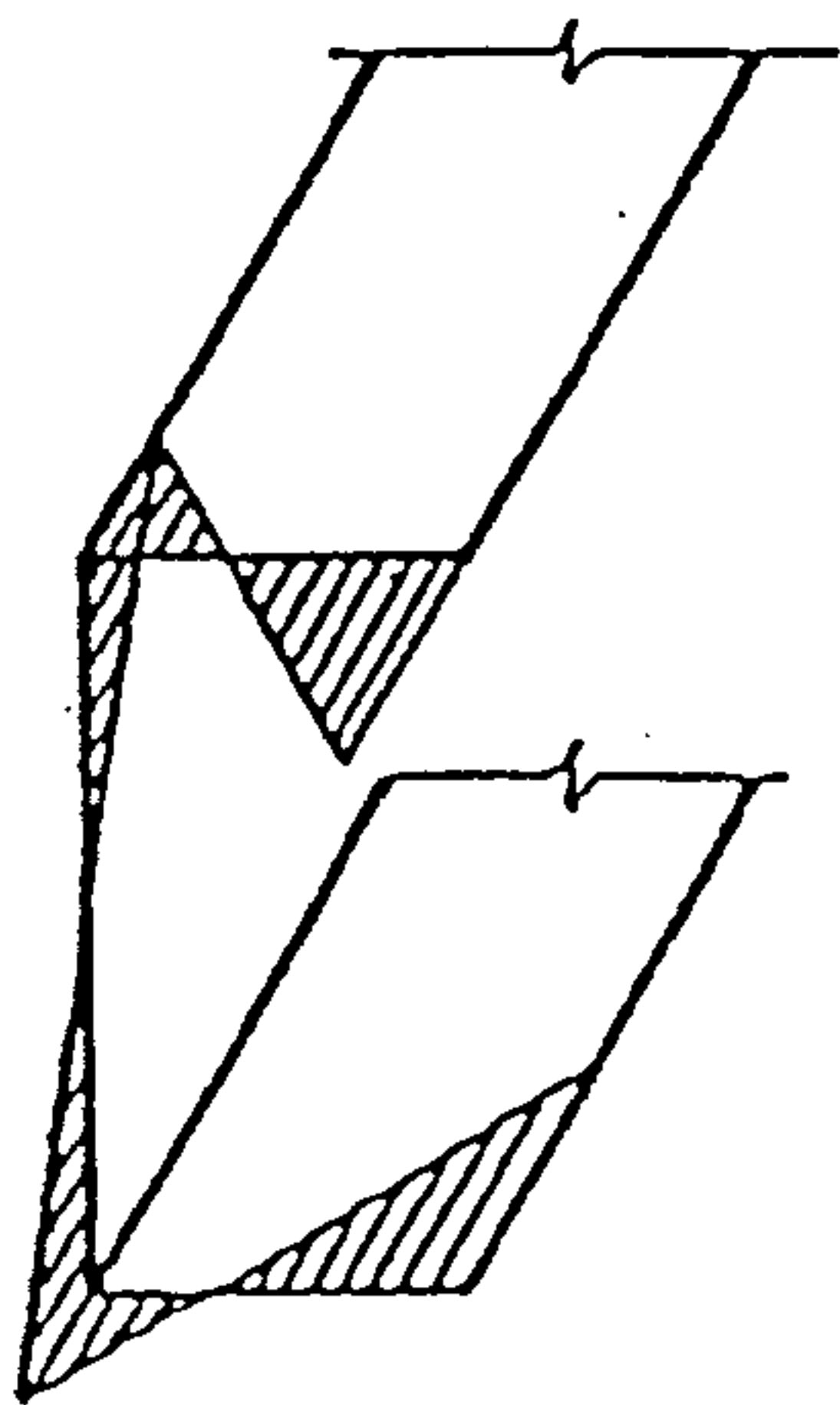


Fig.(2.3) Shear stress variation of an open section across the thickness under torsion

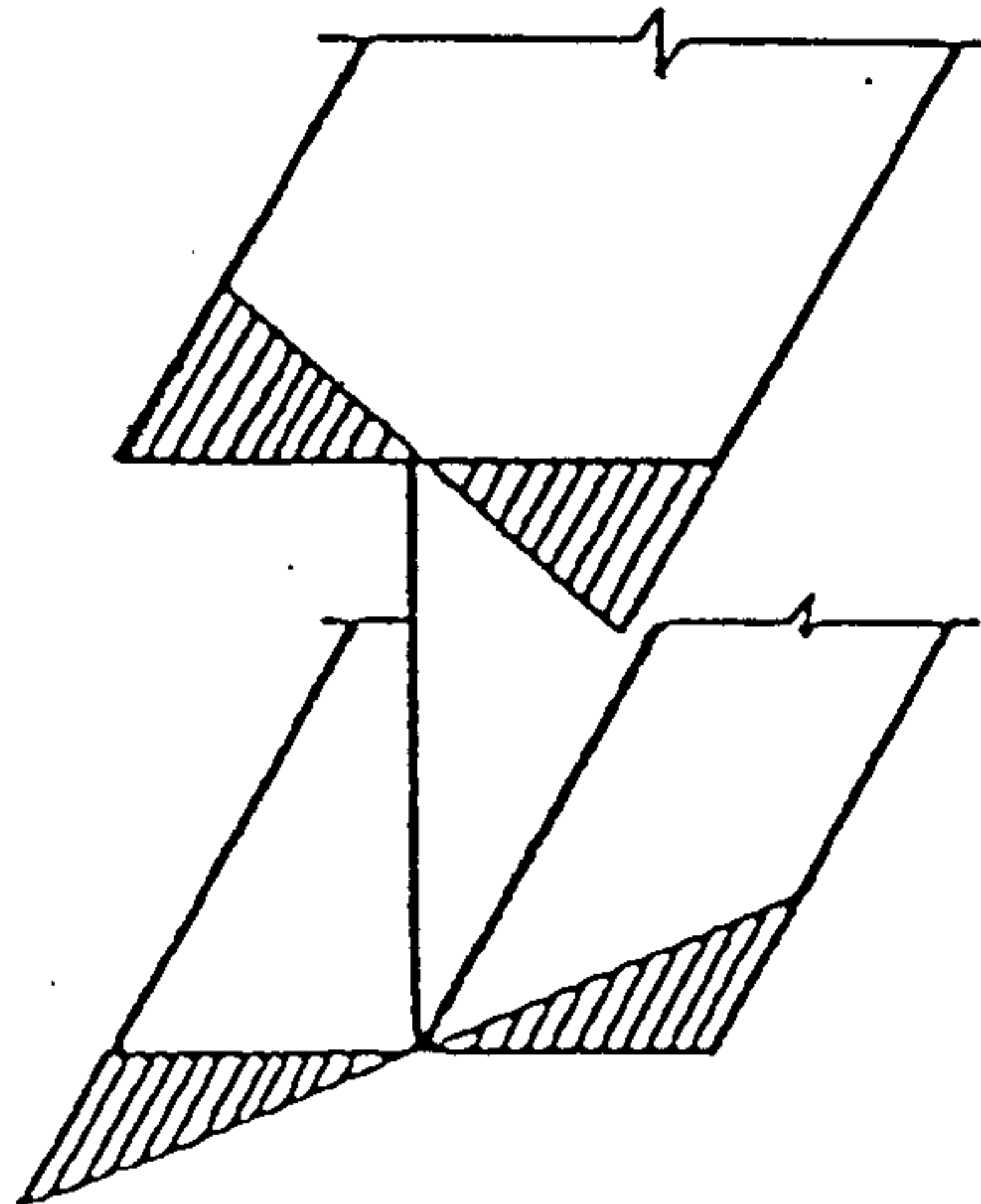
[St. Venant theory assumes a linear variation of shear stress through the thickness]



a) Generation of sectorial area of an open section beam

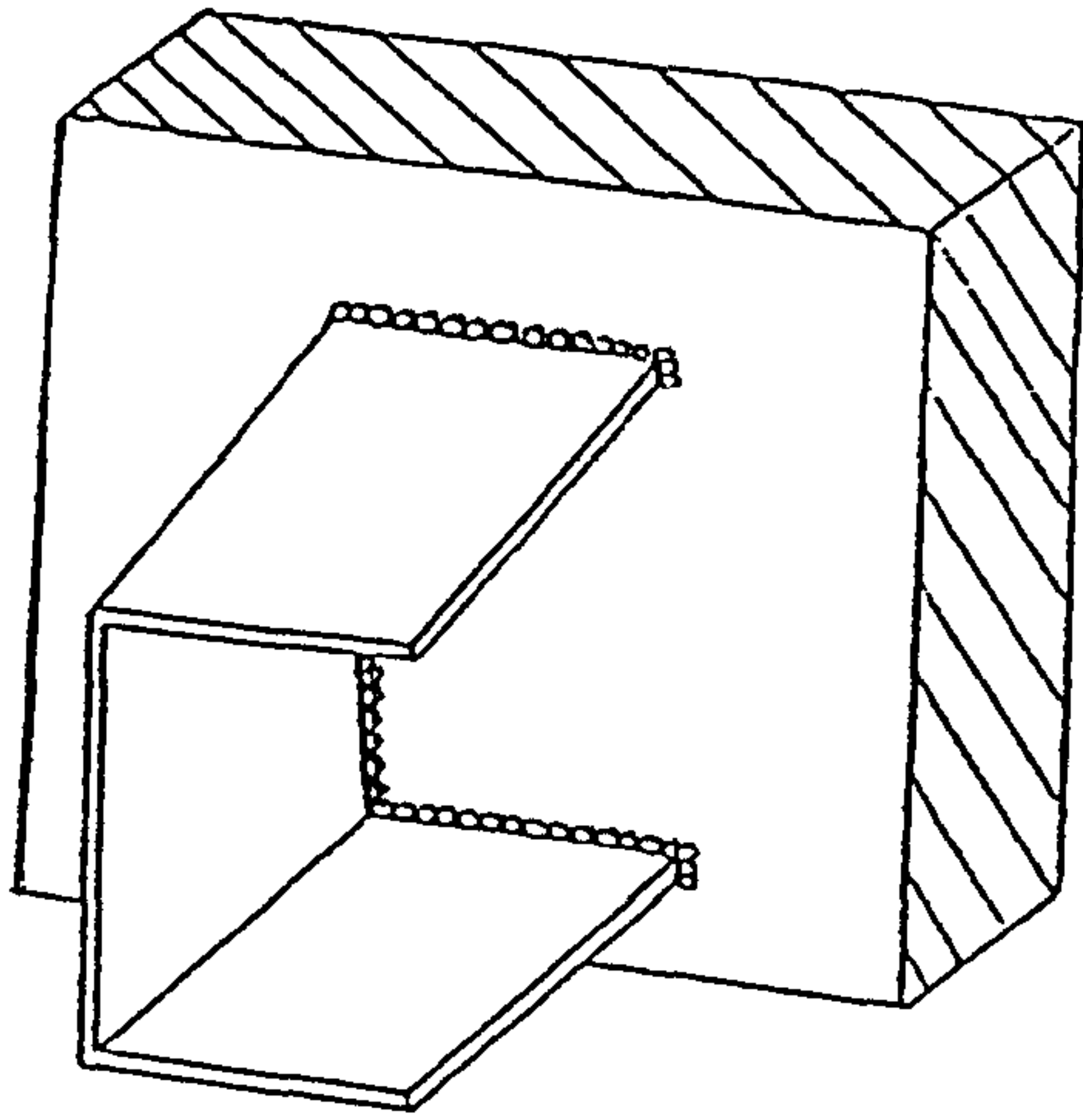


b) Channel section

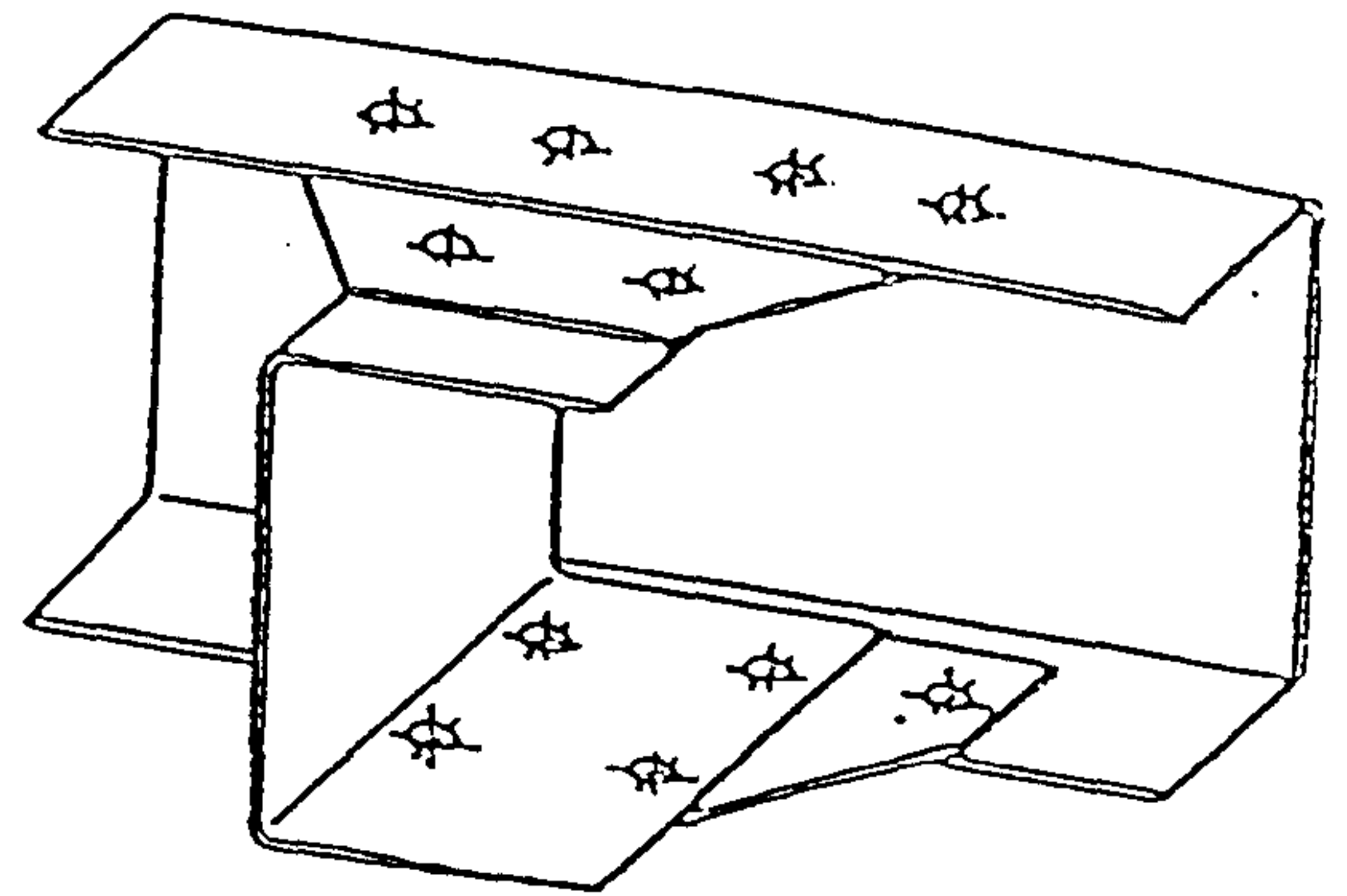


c) I-section

Fig.(2.4) Distribution of sectorial area



a) Completely inhibited warping



b) Partially inhibited warping

Fig.(2.5) Warping inhibition in open section beams

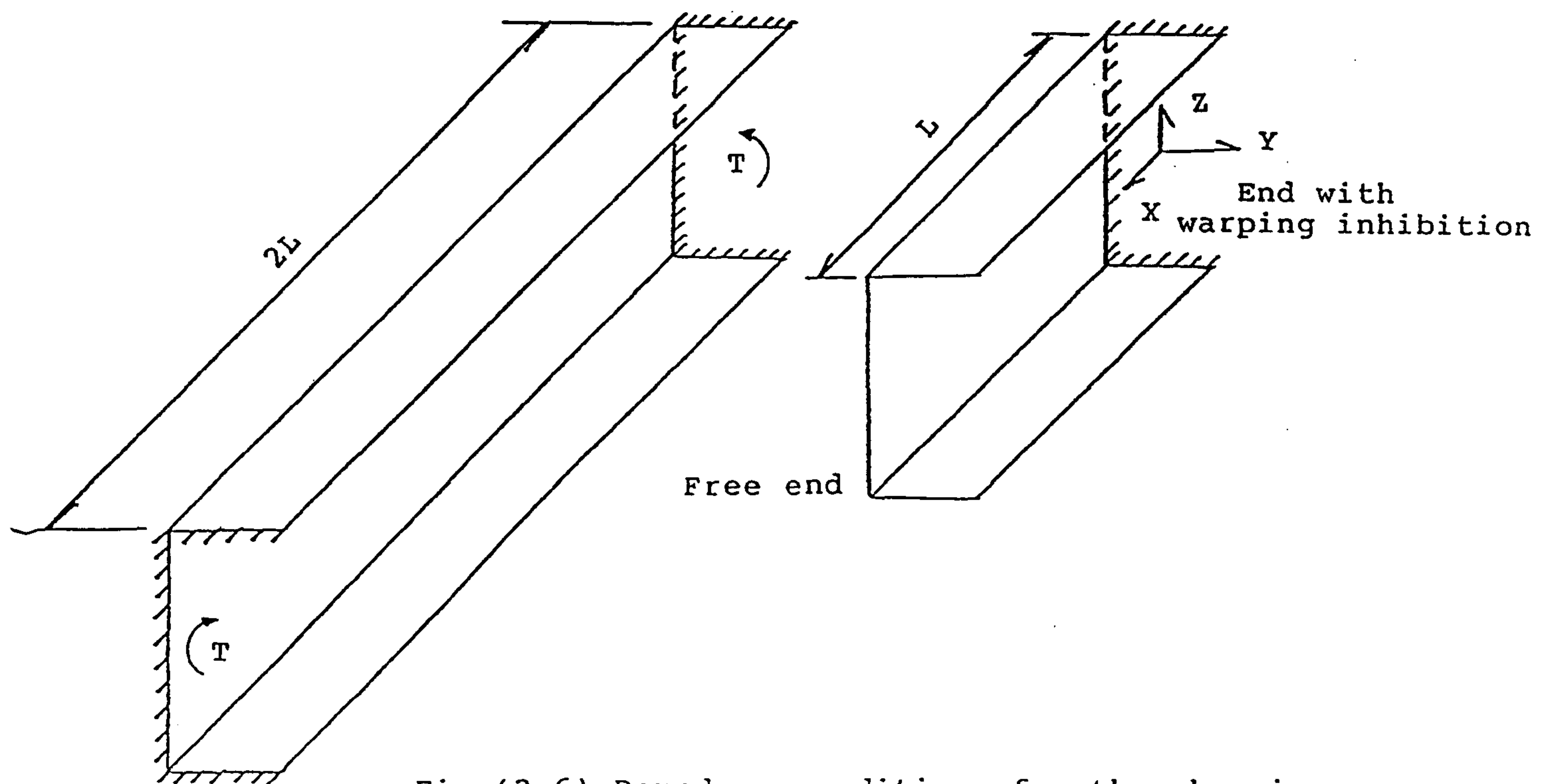
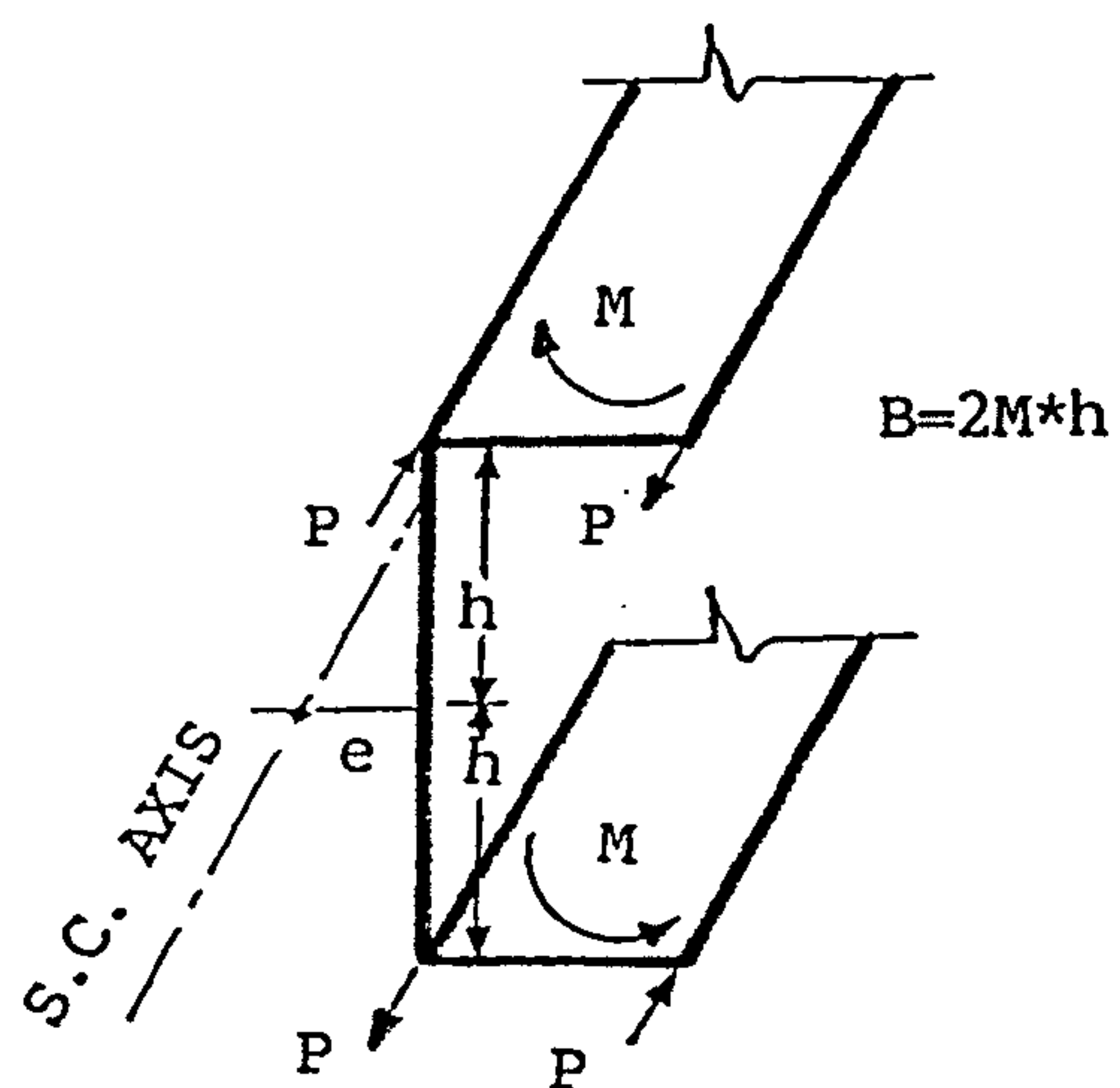
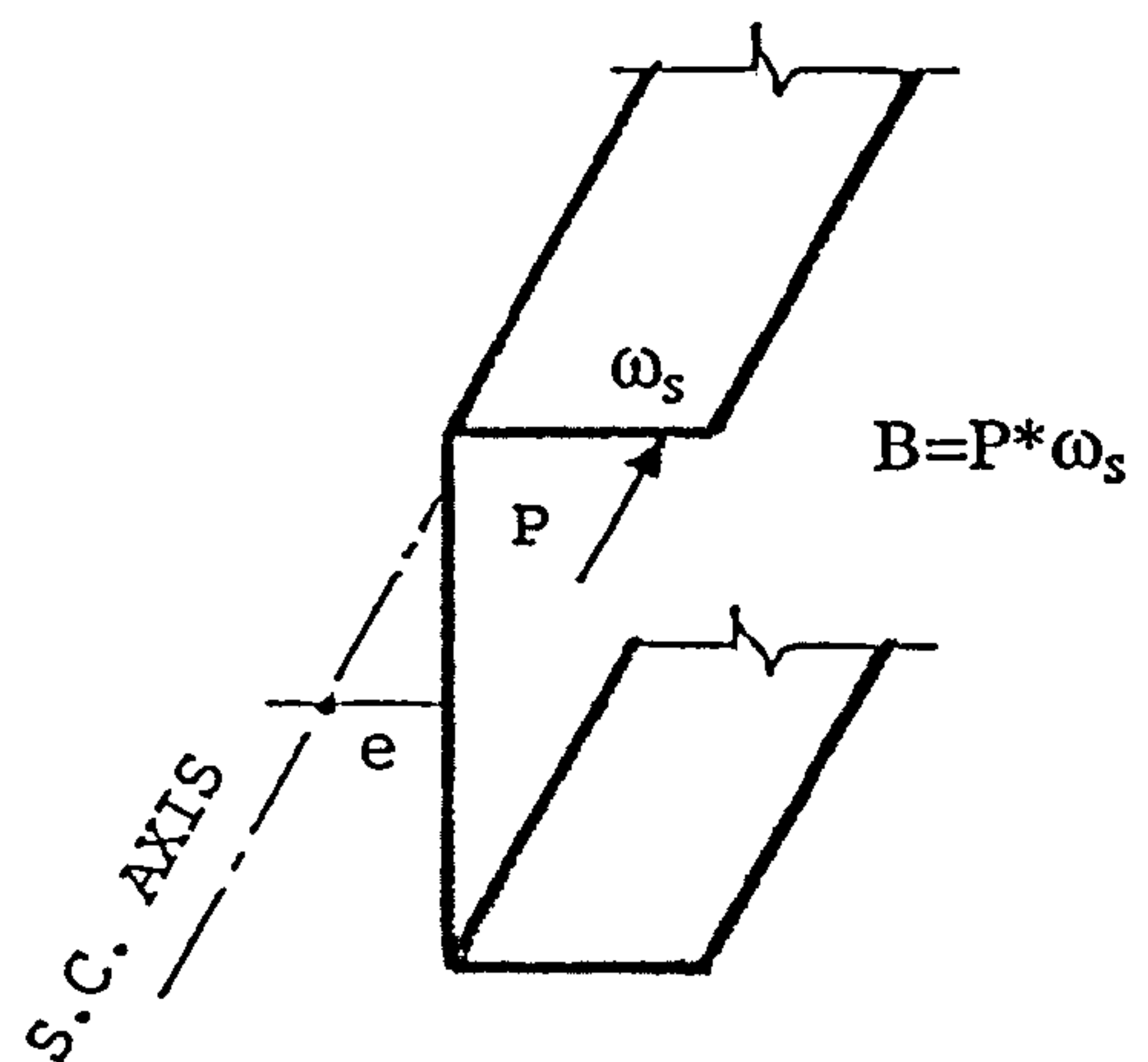


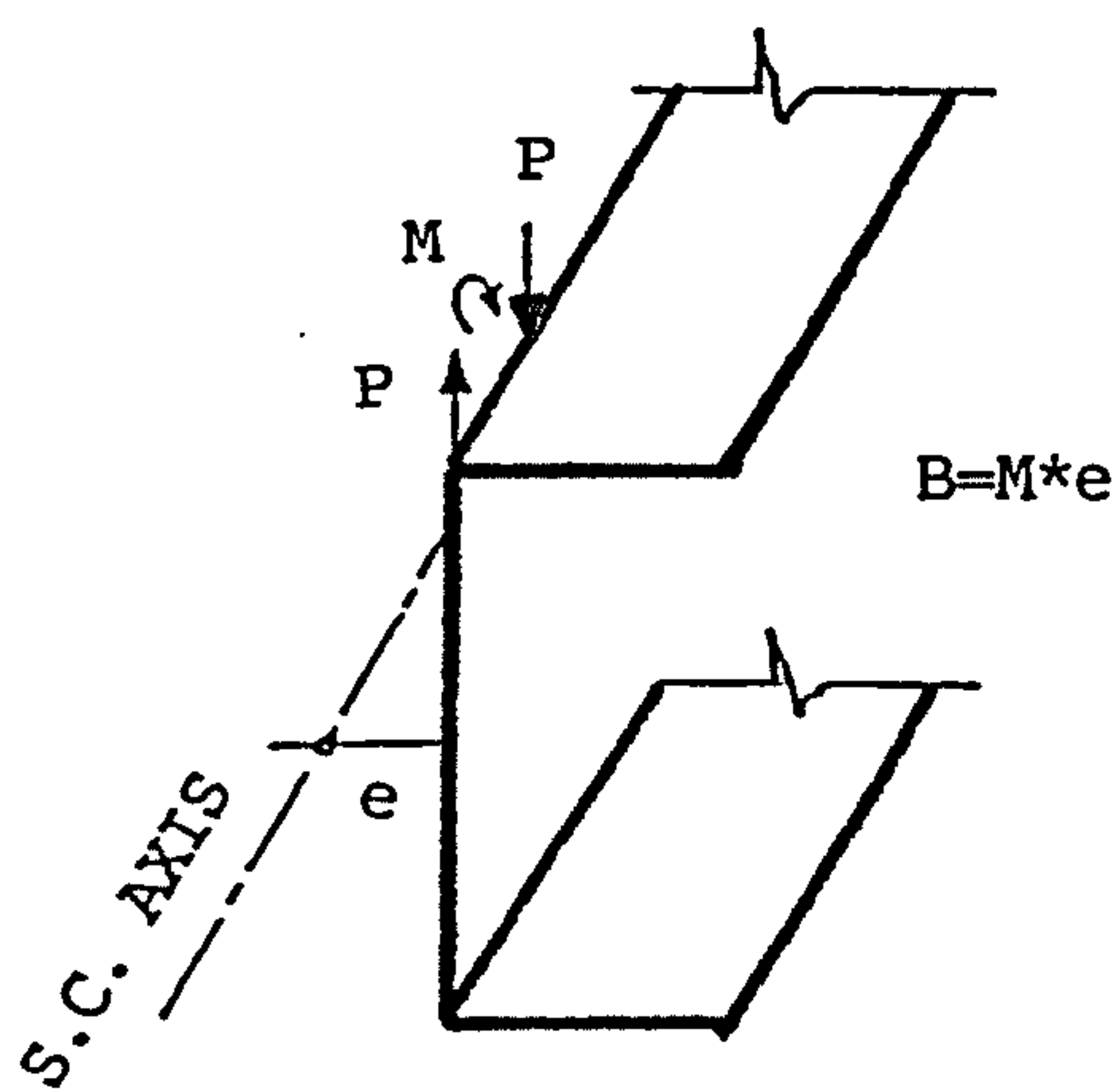
Fig.(2.6) Boundary conditions for the chassis frame cross members



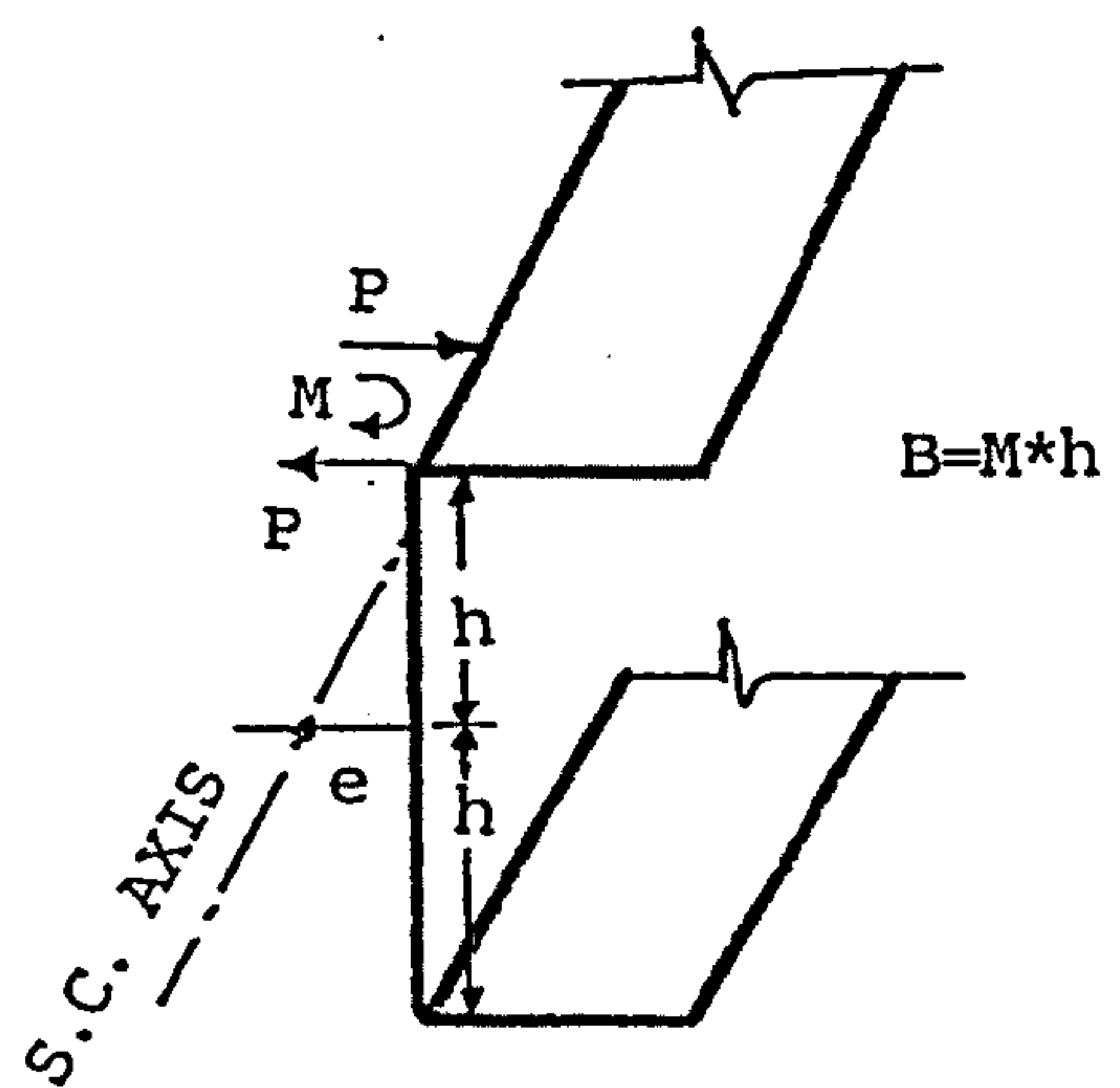
a) Two opposite bending moments



b) Longitudinal load

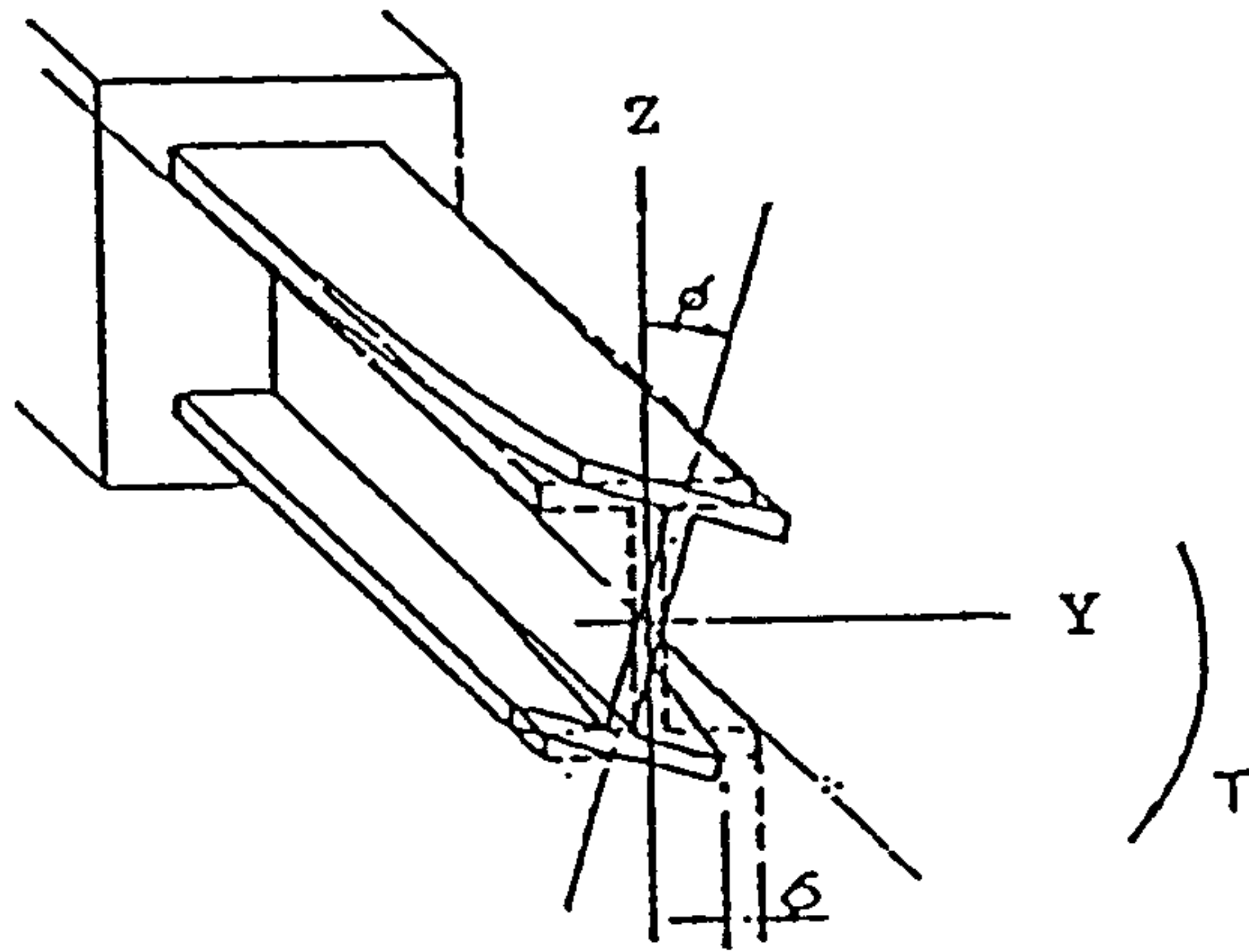


c) Pair of normal loads



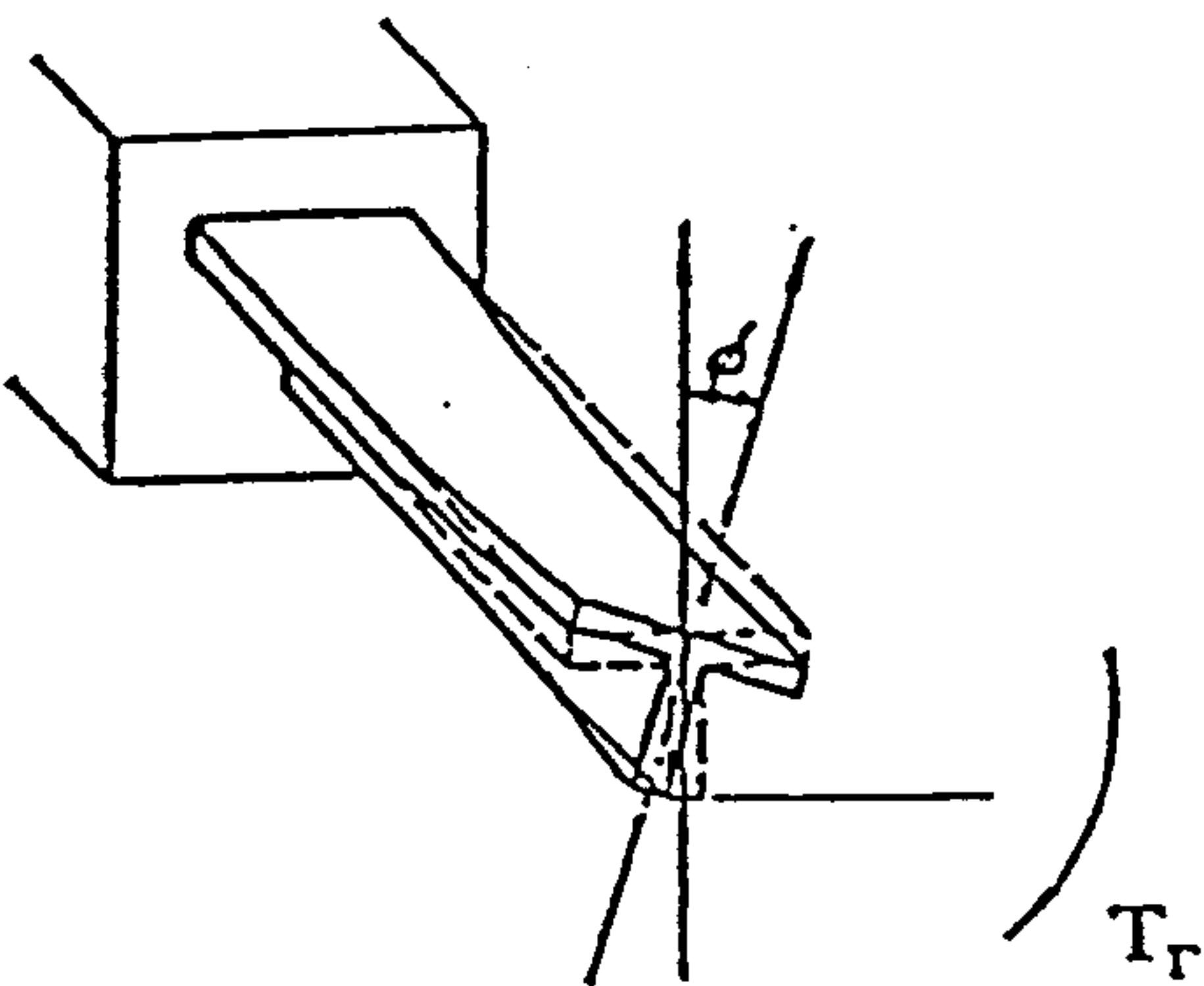
d) Pair of lateral loads

Fig.(2.7) Loads that introduce a bimoment into a channel section



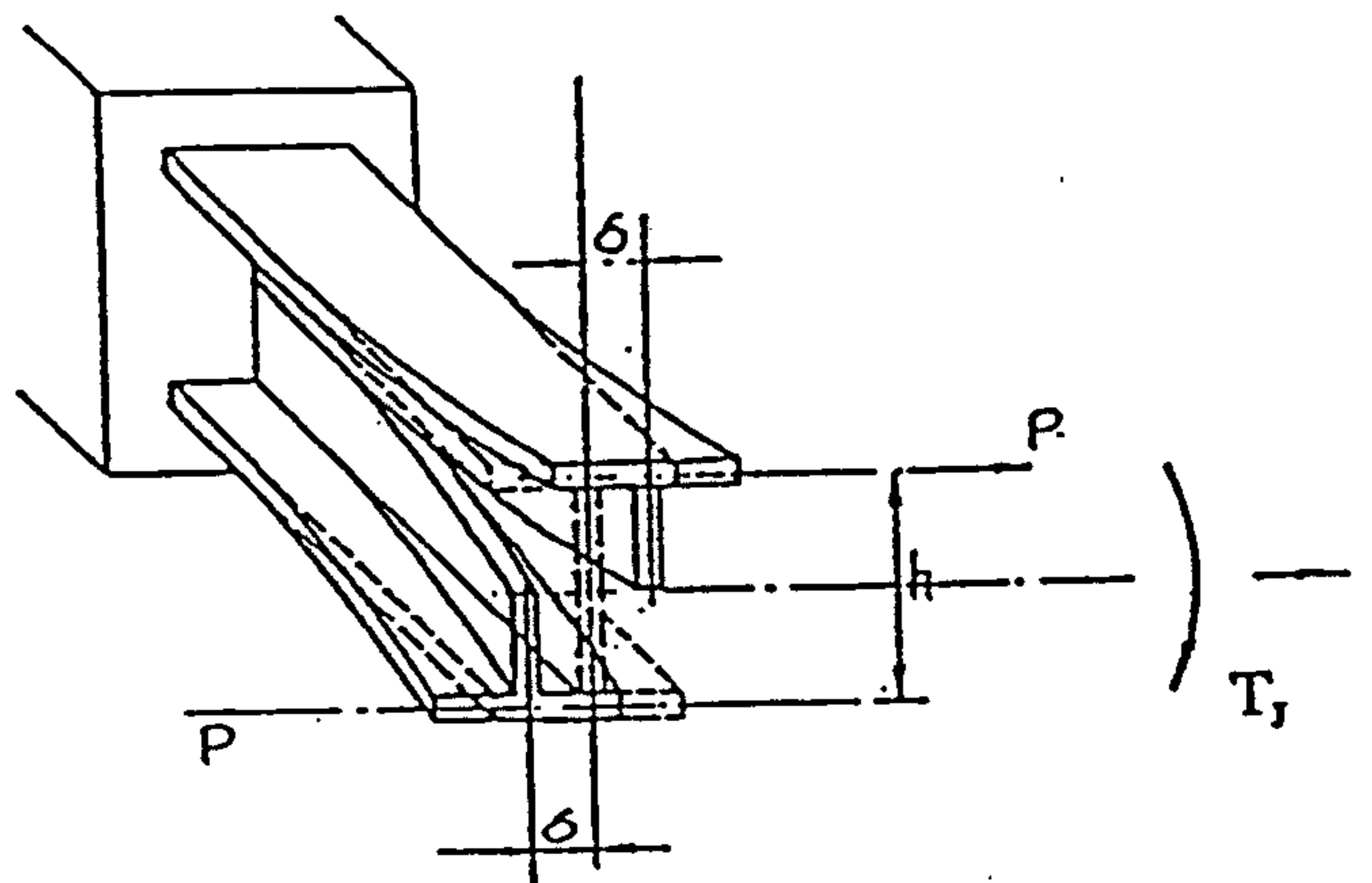
a) Total torque

||



c) St. Venant torque

+

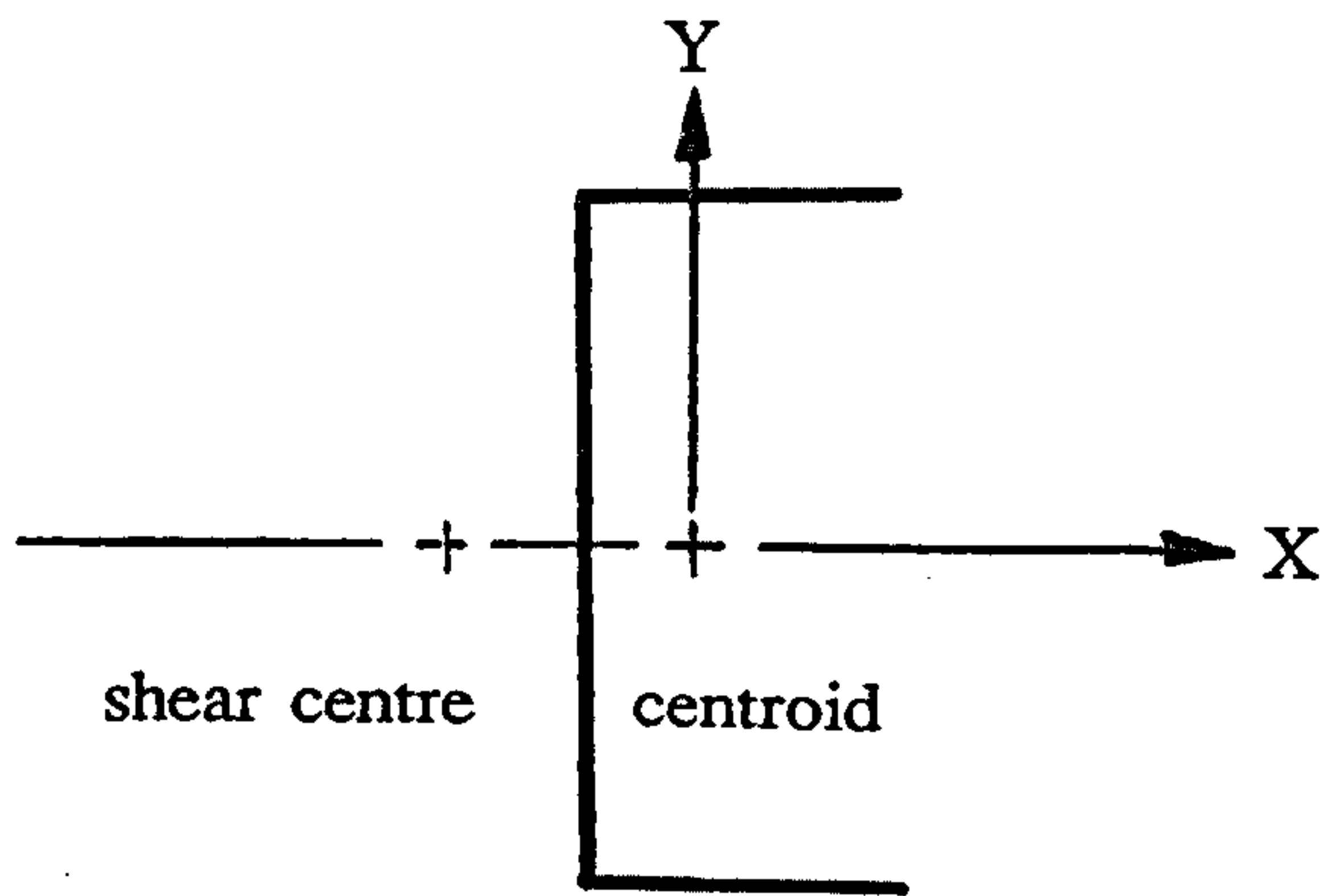


b) Torque due to bimoment

Fig.(2.8) The distortion of an I-section due to torsion

Table (2.1) Comparision of the sectional properties

Items	Sectorial properties	Conventional properties
center of properties	shear centre	centroid
co-ordinate required	sectorial co-ordiate X,Y co-ordinate	X,Y co-ordinate
principal sectorial area	$\int \omega \, dA$	$\int xy \, dA$
statical moment	$\int x \omega \, dA, \int y \omega \, dA$	$\int x \, dA, \int y \, dA$
2nd moment of sectorial area	$\int \omega^2 \, dA$	$\int x^2 \, dA, \int y^2 \, dA$



CHAPTER THREE

STIFFNESS MATRIX OF THIN-WALLED OPEN SECTION BEAMS

3.1 GENERAL

Mainly there are two matrix computer methods which may be applied to analyse vehicle structures. The first is called the force (flexibility) method, while the second is called the displacement (stiffness) method.

An excellent comprehensive bibliography together with an account of the historical developments of these methods may be found in a paper by Argyris (41).

Stiffness method is the primary method used in computer analysis of structures. One of its advantages over the flexibility method is that it is conducive to computer programming. Once the analytical model of the structure has been defined, no further engineering decisions are required in the stiffness method in order to carry out the analysis. In this respect it differs from the flexibility method, although the two approaches have similar mathematical forms.

In the flexibility method the unknown quantities are redundant actions that must be arbitrarily chosen, but in the stiffness method the unknowns are the joint displacements in the structure, which are automatically specified. Thus, in the stiffness method the number of unknowns to be calculated is the same as the degree of kinematic indeterminacy of the structure.

In this chapter the stiffness method is developed on the basis of writing joint equilibrium equations in terms of stiffness coefficients and unknown joint displacements. The method is formalized into a procedure for assembling the overall stiffness matrix of the structure from individual member stiffness matrices.

3.2 FUNDAMENTAL CONSIDERATIONS

In chassis frame structures, the axial warping displacements due to plane deformations will influence considerably the structure with respect to the strength and torsional stiffness. When designing a chassis frame, very often warping at the joints has been regarded as rigidly restrained, as shown in equation (2-15) of the previous chapter.

In this chapter, however, the warping displacement at the joints is considered as being completely transferred to the other connected parts as far as the joints are concerned.

When warping inhibition is included in the matrix stiffness method, the stiffness matrix must be increased in size. The rate of twist is added to the displacements, and the bimoment is added to the loads. Hence, all the mathematically relevant quantities such as St. Venant torsion, flexural twist and bimoment are derived and used to modify the conventional (6) degrees of freedom beam structural analysis to the newly developed one which has (7) degrees of freedom for each node. Accordingly, the condition of bimoment equilibrium at the joints is introduced for the derivation of this stiffness matrix.

3.3 EQUILIBRIUM AND COMPATIBILITY

As far as the chassis frame consisting of open section members is concerned, warping in the structure tends to cause a significant gap between the theoretical approach and experimental results. This is attributed to the difference of the conventional concepts, regarding the transmission of the load between the open section members, and those generally accepted.

Generally, it is considered that the torsional moment along a cross member will cause only bending moment on the side member, as shown in figure (3.1b), without causing warping. However, the actual behaviour shown in figure (3.1a) occurs such that both the cross member and the side member experience torsional moment as well as bending moment. This phenomenon can be regarded as a result of transmission of warping produced in the cross member to the side member.

The aim of a static analysis is to determine the internal loads and displacements of a structure when subjected to external loads. The basis for this analysis is that the equilibrium of forces and the compatibility of displacements shall be maintained at all points in the structure. Therefore, in order to interpret the joint behaviour shown in figure (3.1b), the condition of bimoment equilibrium at the joint must be

introduced, ($\sum B_i=0$) in addition to that of torsional and bending moment equilibrium ($\sum M_i=0$) at the joint, as shown in figure (3.2).

Consequently, the relationship between bimoment and the rate of twist, i.e, plane deformation, which is mathematically based on Vlasov's theory of thin walled elastic beams, will be added to the conventional (12x12) beam stiffness matrix, giving a (14x14) stiffness matrix for each element as will be shown later.

3.4 DERIVATION OF THE STIFFNESS MATRIX

There are four basic design quantities for thin walled beams. Two of them are kinematical terms; these are the angle of twist (θ) and the warping which is related to the rate of twist (θ'). The other two are statical items; they are the bimoment (B) and the total torsional moment (M_x).

It is required mathematically to derive the relationship between these four quantities. It shown in chapter two that the latter two items (B&T) can be expressed in terms of the former kinematical quantities (θ & θ') as the follows:-

$$B = - E\Gamma\theta'' \quad \text{-----} \quad (3-1)$$

$$T_r = - E\Gamma\theta''' \quad \text{-----} \quad (3-2)$$

$$T_t = GJ\theta' \quad \text{-----} \quad (3-3)$$

As shown in equation (2-4), the total torsional moment (M_x) consists of the sum of the flextural twist (T_r) due to the axial stresses and of the St. venant torsional moment due to the non-uniform distribution of the tangential stresses over the thickness of the wall.

Thus:-

$$M_x = T_r + T_l = - E \Gamma \theta''' + GJ \theta' \quad \text{-----} \quad (3-4)$$

Where (θ') is $(d\theta/dx)$, and by differentiating w.r.t (x) we get:-

$$E \Gamma \theta''' - GJ \theta' = 0$$

$$\theta''' - \mu^2 \theta' = 0 \quad \text{-----} \quad (3-5)$$

Where; (μ) is dimension constant, $\mu^2 = \frac{GJ}{E\Gamma}$

The solution can be written in the form:-

$$\theta_{(x)} = C_1 + C_2 x + C_3 \sinh \mu x + C_4 \cosh \mu x \quad \text{-----}$$

and, by differentiating this we obtain:-

$$\theta'_{(x)} = C_2 + \mu C_3 \cosh \mu x + \mu C_4 \sinh \mu x \quad \text{-----} \quad (3-6)$$

Hence by further differentiation of $\theta'_{(x)}$ equation (3-1), and equation (3-4) become:-

$$B_{(x)} = - GJ (C_3 \sinh \mu x + C_4 \cosh \mu x) \quad \text{-----}$$

$$M_{x_{(x)}} = GJ C_2 \quad \text{-----}$$

Having found the relationship between four basic design quantities $(\theta_x, \theta'_x, B_x, M_x)$ in the above equations. The four unknown constants (C_1, C_2, C_3, C_4) can be obtained

by applying the following boundary conditions at both ends of each beam element as shown in figure (3.3).

$$\text{Where at } x=0, \theta=\theta_1, \theta'=\theta'_1, B=B_1, Mx=-Mx_1 \quad \text{-----} \quad (3-7)$$

$$\text{and; at } x=L, \theta=\theta_2, \theta'=\theta'_2, B=B_2, Mx=Mx_2 \quad \text{-----} \quad (3-8)$$

Applying the first boundary conditions as in equation (3-7) to equations (3-6) get:-

$$\begin{array}{l} \theta_1 = C_1 + C_4 \\ \theta'_1 = C_2 + \mu C_3 \\ B_1 = -C_4 GJ \\ Mx_1 = -C_2 GJ \end{array} \quad \begin{array}{c} \text{solving} \\ \text{yields} \\ \text{the} \\ \text{values} \\ \text{of the} \\ \text{constants} \end{array} \quad \begin{array}{l} C_1 = \theta_1 + \frac{B_1}{GJ} \\ C_2 = -\frac{Mx_1}{GJ} \\ C_3 = \frac{1}{\mu} \left(\theta'_1 + \frac{Mx_1}{GJ} \right) \\ C_4 = -\frac{B_1}{GJ} \end{array} \quad \text{-----} \quad (3-9)$$

Substituting the constants obtained in (3-9) into equation (3-6) get:-

$$\theta_{(x)} = \theta_1 + \frac{B_1}{GJ} - \frac{Mx_1}{GJ} x + \frac{1}{\mu} \left(\theta'_1 + \frac{Mx_1}{GJ} \right) \sinh \mu x - \frac{B_1}{GJ} \cosh \mu x$$

$$\theta'_{(x)} = -\frac{Mx_1}{GJ} + \left(\theta'_1 + \frac{Mx_1}{GJ} \right) \cosh \mu x - \frac{\mu B_1}{GJ} \sinh \mu x$$

$$B_{(x)} = -\frac{GJ}{\mu} \left(\theta'_1 + \frac{Mx_1}{GJ} \right) \sinh \mu x + B_1 \cosh \mu x$$

$$Mx_{(x)} = -Mx_1$$

Rearranging all the above equations in terms of (θ, θ', B, Mx) ,

$$\begin{aligned}
\theta_{(x)} &= \theta_1 + \left(\frac{1}{\mu} \sinh \mu x \right) \theta'_1 + \frac{1}{GJ} (1 - \cosh \mu x) B_1 - \frac{1}{GJ} \left(x - \frac{\sinh \mu x}{\mu} \right) M_{x_1} \\
\theta'_{(x)} &= (\cosh \mu x) \theta'_1 - \frac{1}{GJ} (\mu \sinh \mu x) B_1 - \frac{1}{GJ} (1 - \cosh \mu x) M_{x_1} \\
B_{(x)} &= -\frac{GJ}{\mu} (\sinh \mu x) \theta'_1 + (\cosh \mu x) B_1 - \frac{1}{\mu} (\sinh \mu x) M_{x_1} \\
M_{x_{(x)}} &= - (1) M_{x_1}
\end{aligned} \tag{3-10}$$

The above equations give the load-displacement relations at the ends of the beam. Now by applying the second boundary conditions as in equation (3-8) to equations (3-10) we get the following:-

$$\theta_2 = \theta_1 + \left(\frac{1}{\mu} \sinh \mu L \right) \theta'_1 + \frac{1}{GJ} (1 - \cosh \mu L) B_1 - \frac{1}{GJ} \left(L - \frac{\sinh \mu L}{\mu} \right) M_{x_1} \tag{3-11}$$

$$\theta'_2 = (\cosh \mu L) \theta'_1 - \frac{1}{GJ} (\mu \sinh \mu L) B_1 - \frac{1}{GJ} (1 - \cosh \mu L) M_{x_1} \tag{3-12}$$

$$B_2 = -\frac{GJ}{\mu} (\sinh \mu L) \theta'_1 + (\cosh \mu L) B_1 - \frac{1}{\mu} (\sinh \mu L) M_{x_1} \tag{3-13}$$

$$M_{x_2} = - (1) M_{x_1} \tag{3-14}$$

As far as the stiffness matrix is concerned, all of the member forces have to be arranged in terms of the node displacements, i.e., $(\theta_1, \theta'_1, \theta_2, \theta'_2)$.

From equation (3-11) and equation (3-12), the following expressions can be obtained:-

$$M_{x_1} = K_1 \theta_1 - K_2 \theta'_1 - K_1 \theta_2 - K_2 \theta'_2 \tag{3-15}$$

$$B_1 = -K_2 \theta_1 + K_3 \theta'_1 - K_2 \theta_2 + K_4 \theta'_2 \tag{3-16}$$

Where;

$$K_1 = \frac{GJ\mu \sinh\mu L}{D} \quad \text{-----} \quad (a)$$

$$K_2 = \frac{GJ(1 - \cosh\mu L)}{D} \quad \text{-----} \quad (b)$$

$$K_3 = \frac{GJ(\mu L \cosh\mu L - \sinh\mu L)}{\mu D} \quad \text{-----} \quad (c)$$

$$K_4 = \frac{GJ(\sinh\mu L - \mu L)}{\mu D} \quad \text{-----} \quad (d)$$

$$D = 2(1 - \cosh\mu L) + \mu L(\sinh\mu L)$$

Since there is no external torque applied along the beam element, the internal torque is the same at all points along its length, therefore:-

$$M_x = M_{x_2} = -M_{x_1}$$

Hence, equation (3-15) becomes:-

$$M_{x_2} = -K_1\theta_1 + K_2\theta'_1 + K_1\theta_2 + K_2\theta'_2 \quad \text{-----} \quad (3-17)$$

Finally, from equation (3-13), the expression for (B_2) can be obtained as:-

$$B_2 = -K_2\theta_1 + K_4\theta'_1 + K_2\theta_2 + K_3\theta'_2 \quad \text{-----} \quad (3-18)$$

Consequently, the above equations can be combined in the matrix equation as follows:-

$$\begin{bmatrix} M_{x_1} \\ B_1 \\ M_{x_2} \\ B_2 \end{bmatrix} = \begin{bmatrix} K_1 & -K_2 & -K_1 & -K_2 \\ -K_2 & K_3 & K_2 & K_4 \\ -K_1 & K_2 & K_1 & K_2 \\ -K_2 & K_4 & K_2 & K_3 \end{bmatrix} \begin{bmatrix} \theta_1 \\ \theta'_1 \\ \theta_2 \\ \theta'_2 \end{bmatrix} \quad \text{-----} \quad (3-19)$$

Where (K_1, K_2, K_3, K_4) are given in equations (a), (b), (c), and (d) respectively.

The load-displacement equation for warping can be expressed as:-

$$(M_{x_1} \ B_1 \ M_{x_2} \ B_2)^T = K_w (\theta_1 \ \theta'_1 \ \theta_2 \ \theta'_2)^T$$

Where (K_w) is the stiffness sub-matrix for the warping terms.

Therefore, the additional 7th degree of freedom due to the bimoment effects and the rate of twist are incorporated with those due to torsional moment along the axial direction of the beam.

Consequently, the beam stiffness matrix has been written using the direct stiffness method, as shown in figure (3.5). The positive load and displacement direction are shown in figure (3.4) with four discrete forces used to indicate the bimoment. The sign convention is chosen in order that a positive twisting angle (θ_1) will be associated with a positive twisting moment (M_{x_1}) , where the other three degrees of freedom $(\theta'_1, \theta_2, \theta'_2)$ have a value of zero and positive twisting angle (θ_2) , will be associated with a positive twisting moment (M_{x_2}) , where $(\theta_1, \theta'_1, \theta'_2)$ are zero. The same rule will be used for the warping mode and the bimoment, i.e, a positive warping mode (θ'_1) , will be associated with a positive bimoment (B_1) , where $(\theta_1, \theta_2, \theta'_2)$ are zero, and the same for (θ'_2) and (B_2) .

3.5 TRANSFORMATION FOR STIFFNESS MATRIX

Compatibility and equilibrium are the basis for assembling the global stiffness

matrix. So far the element stiffness matrix is established with reference to the local co-ordinates. It must be transformed into the global co-ordinates. Therefore, it is required to derive the transformation matrix associated with (7) degrees of freedom. Through the transformation matrix, all the quantities such as displacements and forces pertaining to the local co-ordinates can be related to the global co-ordinates by taking into account the geometrical relationship between the two co-ordinate systems.

Many chassis frames consist of plane grillages. For this case, the procedure to get the transformation matrix is such that Y-axes of the global and local co-ordinates are parallel, i.e, when a grillage structure is analysed.

$$\check{g} = [T_i] g \quad \text{-----} \quad (3-20)$$

Where;

\check{g} ; denotes the quantities with reference to global co-ordinates.

g ; denotes the quantities with reference to local co-ordinates.

$[T_i]$; is the transformation matrix.

Referring to figure (3.6), the following relation can be written as follows:-

$$\begin{array}{l} P_y = P_y \\ M_x = M_x \cos \phi - M_z \sin \phi \\ M_z = M_x \sin \phi - M_z \cos \phi \\ B = B \end{array} \quad \left. \begin{array}{l} \text{-----} \\ \text{-----} \\ \text{-----} \\ \text{-----} \end{array} \right\} \quad \text{-----} \quad (3-21)$$

The direction Cosines of the local X-axis may be written in terms of the projections as follows:-

$$\begin{aligned} \cos\phi &= \frac{X_j - X_i}{L} \\ \sin\phi &= \frac{Z_j - Z_i}{L} \end{aligned} \quad \begin{array}{c} \text{-----} \\ | \\ \text{-----} \end{array} \quad \text{-----} \quad (3-22)$$

Where;

$$L = \sqrt{(X_j - X_i)^2 + (Z_j - Z_i)^2}$$

Hence, the transformation matrix for a grillage member can be expressed as:-

$$[T_i] = \begin{bmatrix} 1 & 0 & 0 & 0 \\ 0 & \cos\phi & -\sin\phi & 0 \\ 0 & \sin\phi & \cos\phi & 0 \\ 0 & 0 & 0 & 1 \end{bmatrix} \quad \text{-----} \quad (3-23)$$

A more general approach for the (3) dimensional case is shown in figure (3.7). If the components of a vector quantity (V) are (x,y,z) in the local axis system, and (x',y',z') in the global axis system. Then the relationship between (x,y,z) and (x',y',z') is:-

$$\begin{bmatrix} x' \\ y' \\ z' \end{bmatrix} = \begin{bmatrix} l_1 & m_1 & n_1 \\ l_2 & m_2 & n_2 \\ l_3 & m_3 & n_3 \end{bmatrix} \begin{bmatrix} x \\ y \\ z \end{bmatrix}$$

Where (l₁,m₁,n₁) are the direction Cosines of the local (x,y,z) axes w.r.t the global x-axis.

(l₂,m₂,n₂) are the direction Cosines of the local (x,y,z) axes w.r.t the global y-axis.

(l₃,m₃,n₃) are the direction Cosines of the local (x,y,z) axes w.r.t the global z-axis.

(V) must be (or approximate to) a vector quantity for this transformation to be valid. Forces, moments, small rotations satisfy this requirement.

Or, expressing grillage transformation matrix in equation (3-23) in more generalised form for node (i), which has (7) degrees of freedom we have:-

$$[T_i] = \begin{bmatrix} l_1 & m_1 & 0 & & & & \\ l_2 & m_2 & 0 & & & & \\ 0 & 0 & 1 & & & & \\ & & & l_1 & m_1 & 0 & \\ & & & l_2 & m_2 & 0 & \\ & & & 0 & 0 & 1 & \\ & & & & & & 1 \end{bmatrix} \quad \text{-----} \quad (3-25)$$

A transformation matrix for the beam element (i-j) will be:-

$$[T_{ij}] = \begin{bmatrix} [T_i] & 0 \\ 0 & [T_j] \end{bmatrix} \quad \text{-----} \quad (3-26)$$

Consequently, the transformation from local to global axes for the (14x14) element stiffness matrix will be:-

$$[K_{ij}]_G = [T_{ij}][K_{ij}]_L[T_{ij}]^T \quad \text{-----} \quad (3-27)$$

Where;

$[K_{ij}]_G$ is Global element stiffness matrix. and,

$[K_{ij}]_L$ is Local element stiffness matrix.

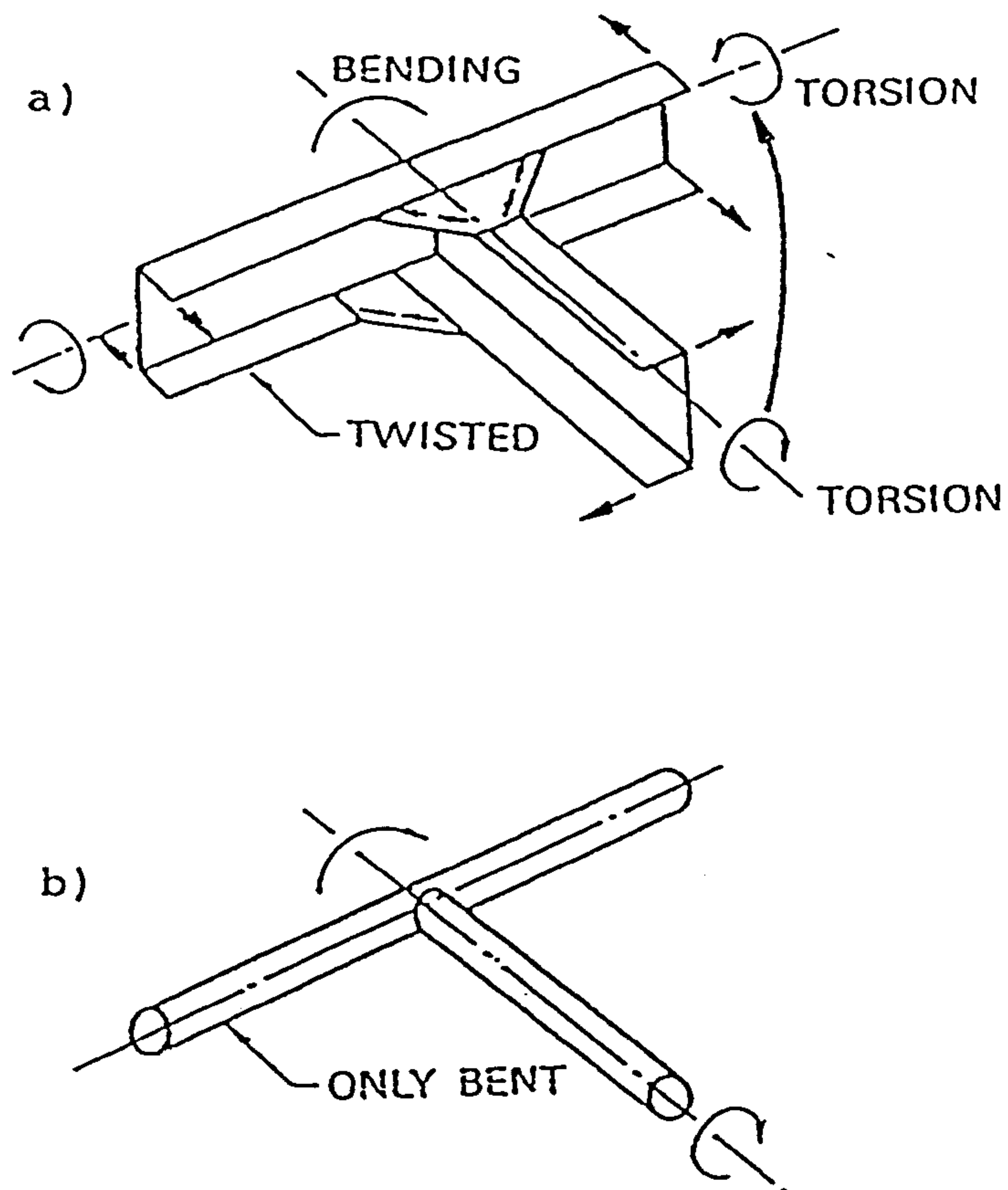


Fig.(3.1) Mode of load transfer

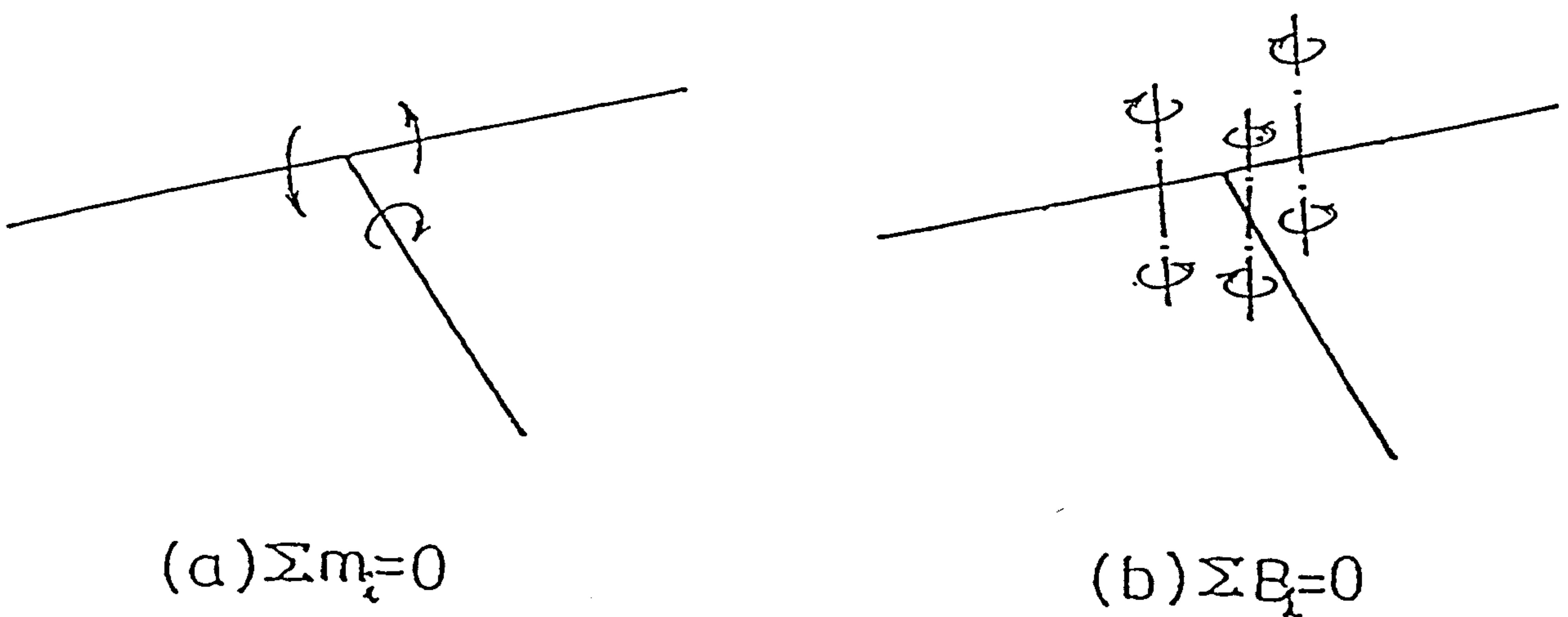


Fig.(3.2) Moment and bimoment equilibrium at a joint

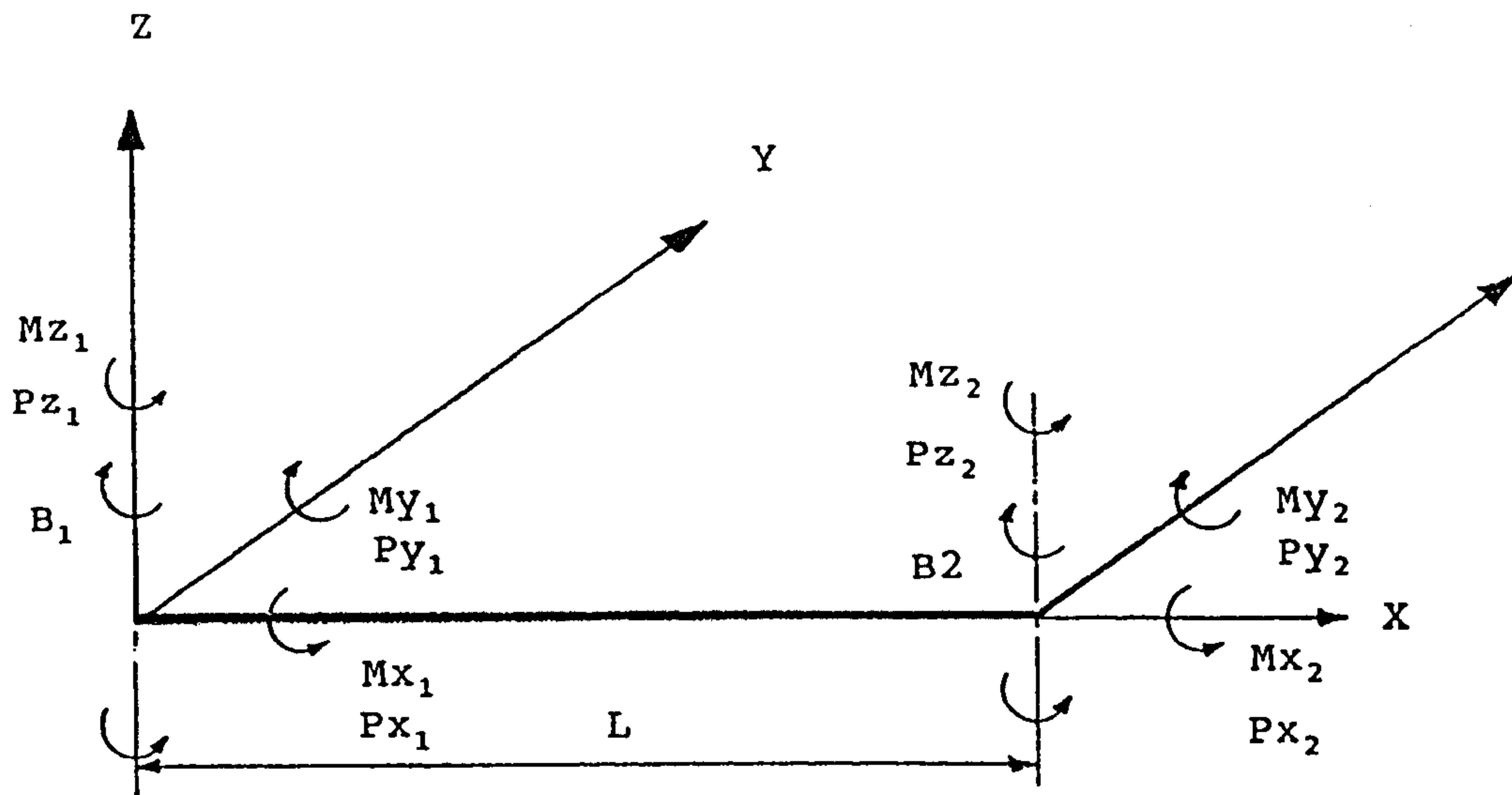


Fig.(3.3) Force and displacement components in local coordinates

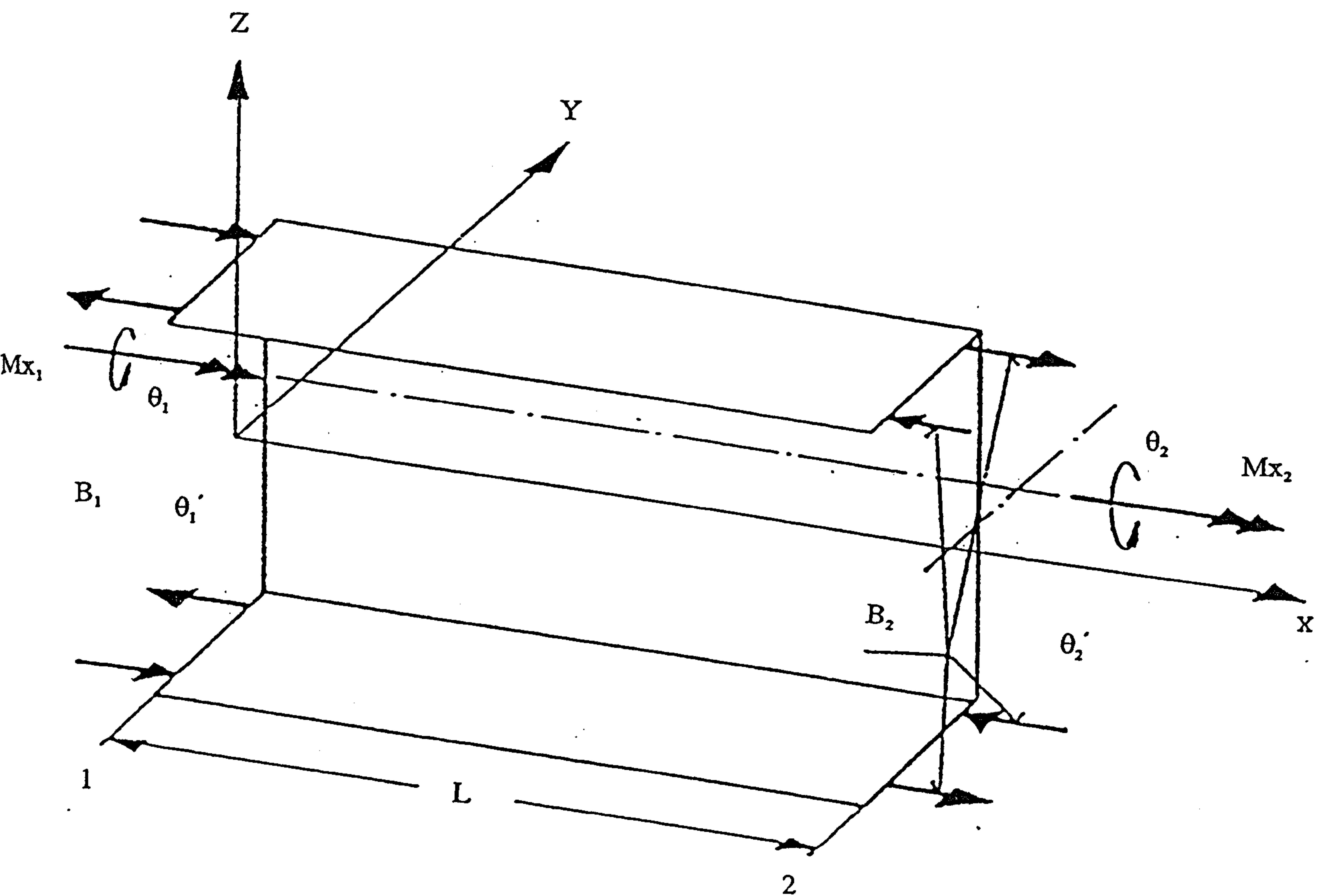


Fig.(3.4) Sign convention for loads and displacements in a warped channel-section beam element

$$\begin{bmatrix} P_{x_1} \\ P_{y_1} \\ P_{z_1} \\ M_{x_1} \\ M_{y_1} \\ M_{z_1} \\ B_1 \\ P_{x_2} \\ P_{y_2} \\ P_{z_2} \\ M_{x_2} \\ M_{y_2} \\ M_{z_2} \\ B_2 \end{bmatrix} = \begin{bmatrix} \bar{C}_1 & 0 & 0 & 0 & 0 & 0 & 0 & -C_1 & 0 & 0 & 0 & 0 & 0 & 0 \\ & C_2 & 0 & 0 & 0 & C_6 & 0 & 0 & -C_2 & 0 & 0 & 0 & C_6 & 0 \\ & & C_3 & 0 & -C_7 & 0 & 0 & 0 & 0 & -C_3 & 0 & -C_7 & 0 & 0 \\ & & & K_1 & 0 & 0 & -K_2 & 0 & 0 & 0 & -K_1 & 0 & 0 & -K_2 \\ & & & & C_4 & 0 & 0 & 0 & 0 & C_7 & 0 & C_8 & 0 & 0 \\ & & & & & C_5 & 0 & 0 & -C_6 & 0 & 0 & 0 & C_9 & 0 \\ & & & & & & K_3 & 0 & 0 & 0 & K_2 & 0 & 0 & K_4 \\ & & & & & & & C_1 & 0 & 0 & 0 & 0 & 0 & 0 \\ & & & & & & & & C_2 & 0 & 0 & 0 & -C_6 & 0 \\ & & & & & & & & & C_3 & 0 & C_7 & 0 & 0 \\ & & & & & & & & & & K_1 & 0 & 0 & K_2 \\ & & & & & & & & & & & C_4 & 0 & 0 \\ & & & & & & & & & & & & C_5 & 0 \\ & & & & & & & & & & & & & K_3 \end{bmatrix} \begin{bmatrix} \delta x_1 \\ \delta y_1 \\ \delta z_1 \\ \theta_{x1} \\ \theta_{y1} \\ \theta_{z1} \\ \theta_1' \\ \delta x_2 \\ \delta y_2 \\ \delta z_2 \\ \theta_{x2} \\ \theta_{y2} \\ \theta_{z2} \\ \theta_2' \end{bmatrix}$$

SYMMETRIC

Where, the following are the convectional stiffness co-efficients

$$\begin{aligned}
 C_1 &= E \cdot A / L & C_6 &= 6 \cdot E \cdot Z_i / L^2 \\
 C_2 &= 12 \cdot E \cdot Z_i / L^3 & C_7 &= 6 \cdot E \cdot Y_i / L^2 \\
 C_3 &= 12 \cdot E \cdot Y_i / L^3 & C_8 &= C_4 / 2 \\
 C_4 &= 4 \cdot E \cdot Y_i / L & C_9 &= C_5 / 2 \\
 C_5 &= 4 \cdot E \cdot Z_i / L
 \end{aligned}$$

And, K_1, K_2, K_3, K_4 are the co-efficients concerned with bimoment as given in equations (a), (b), (c) and (d) respectively.

Fig.(3.5) Stiffness matrix for beam element with bimoment terms

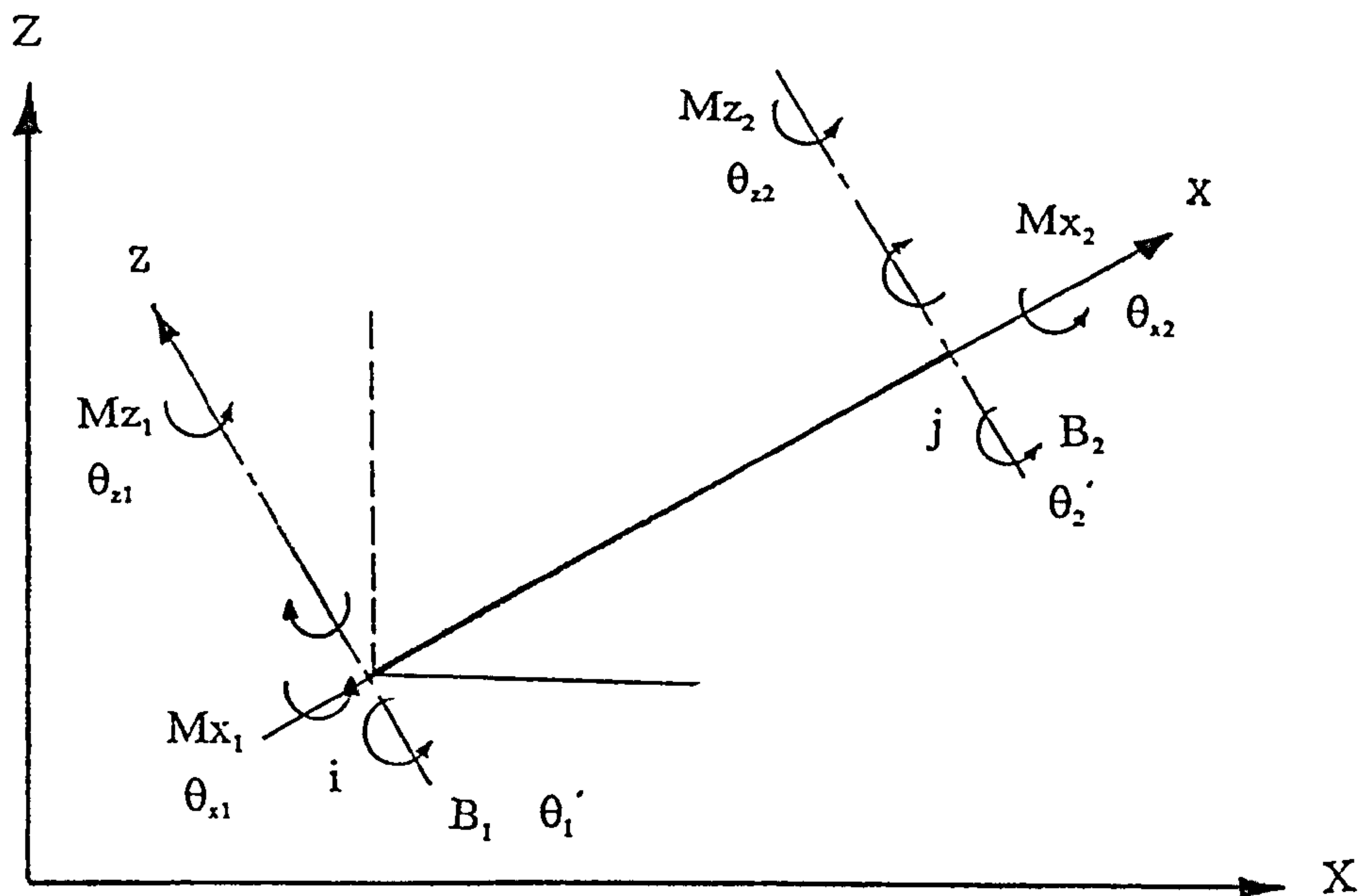


Fig.(3.6) Coordinate system for a grillage

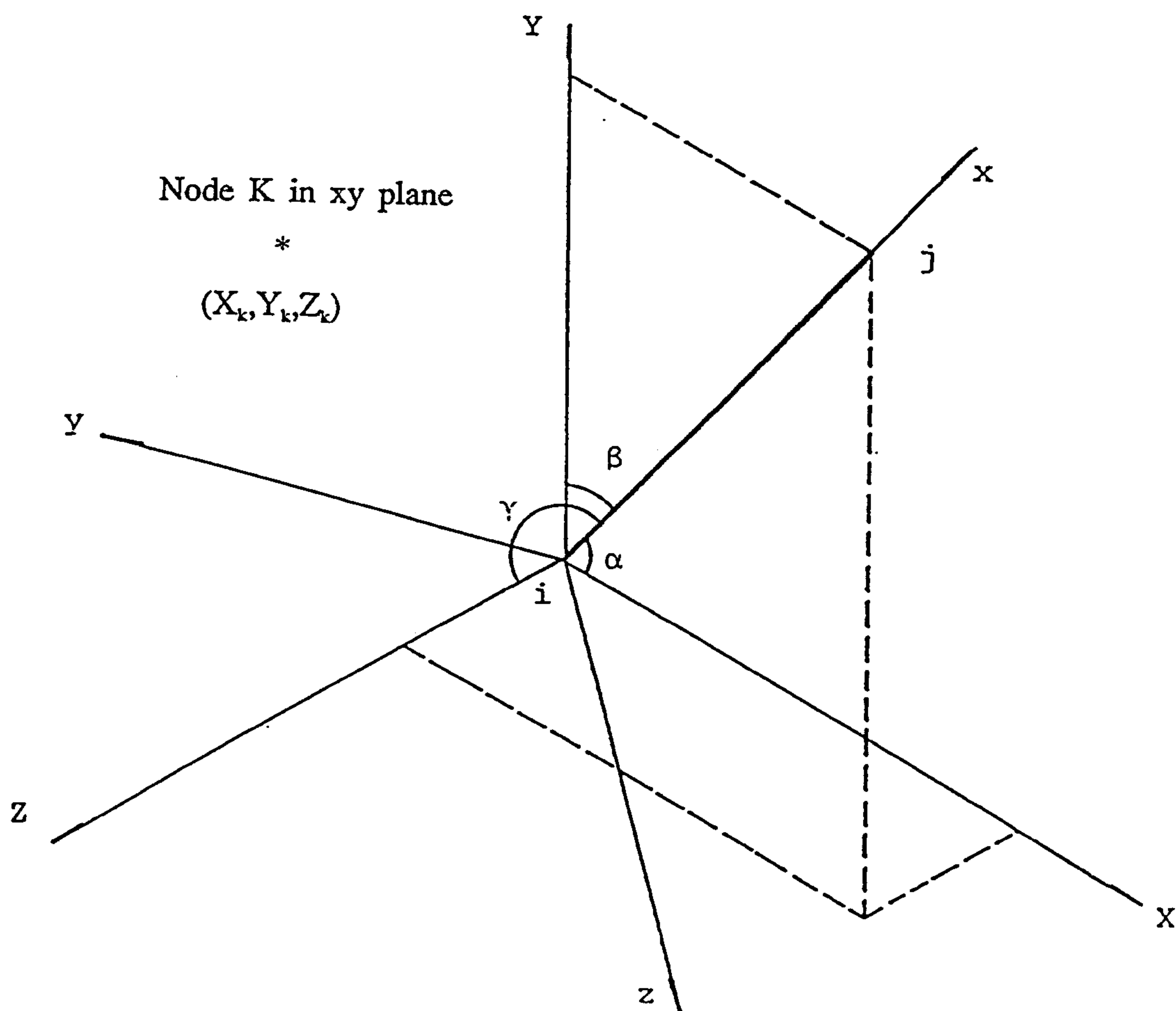


Fig.(3.7) A generalised coordinate for 3D frame

CHAPTER FOUR

THIN-WALLED

CLOSED-SECTION BEAMS

4.1 GENERAL

Warping effects in thin walled closed section beams are less important than those in open sections. If closed section cross members are used in chassis frame, the problem of torsional stiffness due to warping inhibition would disappear since there is no significant difference in the torsional stiffness of a closed section beam which is fully restrained against warping and one which is totally free to warp, unless the beam is very short, which it would not be in this application.

However, the compatibility of any warping displacement in the cross member and the rate of twist in the side member has to be ensured at the joints, even when warpleless sections, such as circular or square sections, are used.

The assumptions used in thin-walled open section beams such that the cross section shape remains constant after deformations and that there is negligible shear deformation, do not hold for thin walled closed section beams as they lead to kinematically impossible deformation.

The additional displacements arising from the deformation of the cross section can be added to the displacements assumed for open sections beams, while the corresponding so-called lateral bimoment can be added to the internal loads. These relations are more complex than those developed for open section beams.

In this chapter the load-displacement relations for torsion in closed sections will be derived for rectangular box beams, as they are the most common sections used in practice.

4.2 WARPLESS CLOSED SECTIONS

The free warping of a closed section subjected to torsion is well known and documented by various authors (17,37). The formula for the warping displacement of an arbitrary closed section is;-

$$W_c = \int \frac{\partial W_c}{\partial s} ds + W_\infty = \frac{T}{2AG} \left(\int \frac{ds}{t} - \frac{\int (1/t) ds}{2A} \int p ds \right) + W_\infty \quad \text{---} \quad (4-1)$$

where (p) is the perpendicular distance of the tangent at a point on the perimeter (S) to the shear centre as shown in figure (4.1) and, (W_∞) is the value of warping displacement (W_c) where ($S=0$), and (A) is the area enclosed by the mid-line of the tube wall.

Since $\{\int (1/t) ds\}$ is a constant for any given section of a tube, the warping displacements will be a function of the values of (t) and (p) at the point considered and at all the points from some arbitrary datum on the section to this point. If (pt) is constant, ($t \partial W/\partial s$) must be constant, but (t) is always positive, while (W_c) is a continuous function having opposite signs for different values of (s). Therefore, in order for ($\partial W/\partial s$) to be constant it must be zero.

Hence, the condition for zero warping is that (pt = constant) round the perimeter. This means that thin walled beams whose sections are circles, squares, triangles and other regular polygons will not warp if the material thickness (t) is constant since all these cases the distance of the tangent from the shear centre is constant.

If it is particularly important that no warping effects are present and the shape of the beam is not regular the thickness can be varied (in steps if necessary) to keep (pt) constant.

The free warping of rectangular box subjected to torsion is shown in figure (4.2). The variation of warping a round the section profile is linear and the axial displacement of the corners of the box section is;-

$$W_{CF} = \pm \frac{T}{8hbG} \left(\frac{b}{t_2} - \frac{h}{t_1} \right) \quad \text{-----} \quad (4-2)$$

4.3 COMPLETELY RESTRAINED WARPING

The theory for estimating variation in warping along the length of a uniform rectangular section thin walled beam subject to a constant torque is well known (e.g see Megson (17)). It is derived using the more general coordinate system shown in figure (4.3), and can be summarised as follows;-

$$\frac{d^2 W_c}{dx^2} - \mu_c^2 W_c = - \frac{T}{hbB_1 E} \left(\frac{bt_1 - ht_2}{bt_1 + ht_2} \right) \quad \text{-----} \quad (4-3)$$

Where;

$$\mu_c^2 = \frac{8Gt_1 t_2}{BE(bt_1 + ht_2)}$$

$$B_1 = \frac{1}{6} (ht_1 + bt_2)$$

The general solution for equation (4-3) can be written as;-

$$W_c = C_1 \cosh \mu_c x + C_2 \sinh \mu_c x + \frac{T}{8hbG} \left(\frac{b}{t_2} - \frac{h}{t_1} \right) \quad \text{-----} \quad (4-4)$$

where (x) is measured from the built-in end and C_1 and C_2 are constants determined from the boundary conditions.

The last term of equation (4-4) may be recognised as the free warping of the corners of the beam as shown before in equation (4-2). Other important results such as $(d\phi/dx)$ are derived as a matter of course in the development of the theory for the variation of (W_c) along the length of the box section as;-

$$\frac{d\phi}{dx} = \frac{4W_c(bt_1 - ht_2)}{hb(bt_1 + ht_2)} + \frac{T}{hbG(bt_1 + ht_2)} \quad \text{-----} \quad (4-5)$$

For a uniform beam with complete warping inhibition at the built-in end. Thus;-

$$W_c = 0 \quad \text{at} \quad x = 0$$

Also at the free end the direct stress is zero since a pure torque is applied.

Therefore;-

$$\sigma_{\Gamma(x=L)} = E \frac{\partial W_c}{\partial x} = 0$$

Substituting these boundary conditions in equation (4-4) gives;-

$$W_{cr} = W_{cf} \left(1 - \frac{\cosh \mu_c(L-x)}{\cosh \mu_c L} \right) \quad \text{-----} \quad (4-6)$$

The variation of direct stress is given by;-

$$\sigma_r = E \frac{\partial W_c}{\partial x}$$

Differentiating equation (4-6) and substituting gives;-

$$\sigma_r = \mu_c E W_{cf} \frac{\sinh \mu_c(L-x)}{\cosh \mu_c L} \quad \text{-----} \quad (4-7)$$

Substituting equation (4-6) into equation (4-5) get;-

$$\frac{d\phi}{dx} = \frac{T}{2h^2b^2G} \left[\frac{b}{t_2} + \frac{h}{t_1} \right] - \frac{T(bt_1 + ht_2)^2}{2h^2b^2Gt_1t_2(bt_1 + ht_2)} \frac{\cosh \mu_c(L-x)}{\cosh \mu_c} \quad \text{--} \quad (4-8)$$

The first term of this equation corresponds to the rate of twist in the unconstrained rectangular section tube as predicted by the Bredt-Batho theory. The second term represents the reduction in the rate of twist due to axial constraint.

Rearranging equation (4-8) and integrating with the appropriate boundary conditions over the length (L), the angle of twist (ϕ_T) at the free end where ($x=L$), thus can be obtained as;-

$$\phi_T = \frac{TL}{GJ_c} \left\{ \frac{\mu_c L - [(bt_1 - ht_2)^2 / (bt_1 + ht_2)^2] \tanh \mu_c L}{\mu_c L} \right\} \quad \text{-----} \quad (4-9)$$

where (J_c) is the torsion constant, which is given for a thin walled closed tube by the Bredt-Batho theory as;-

$$J_c = \frac{4A^2}{\delta}$$

where (A) is the area enclosed by the mid-line of the tube wall and,

$$\delta = \int \frac{ds}{t}$$

Hence, for a tube of length (L), which is constrained against warping at one end, the effective torsion constant (J_r) would be;-

$$J_r = \frac{TL}{G\phi_T} \quad \text{-----} \quad (4-10)$$

and substituting for (ϕ_T) from equation (4-9) get;-

$$J_{cr} = J_c \left\{ \frac{\mu_c L}{\mu_c L - [(bt_1 - ht_2)^2 / (bt_1 + ht_2)^2] \tanh \mu_c L} \right\} \quad \text{-----} \quad (4-11)$$

4.4 PARTIALLY RESTRAINED WARPING

In chapter (2), section (9), it was seen that for open section thin walled cross members the assumption that partial warping was directly proportional to free warping was valid for the sections analysed. The same assumption is made in the case of closed rectangular section cross members.

Thus;

$$W_{CP} = K * W_{CF} \quad \text{-----} \quad (4-12)$$

Where (K) is the warping restraint factor, (W_{CP}) partially restrained warping displacement and (W_{CF}) the free warping displacements.

This gives a new boundary condition for equation (4-4) in solving for (W_C). Hence, the modified expression is;-

$$W_{CP} = W_{CF} \left[1 - \frac{(1-K)\text{Cosh}\mu_c(L-x)}{\text{Cosh}\mu_c L} \right] \quad \text{-----} \quad (4-13)$$

From this result, the direct stress expression can be given as;-

$$\sigma_p = \mu_c E W_{CF} (1-K) \frac{\text{Sinh}\mu_c(L-x)}{\text{Cosh}\mu_c L} \quad \text{-----} \quad (4-14)$$

substituting the result of equation (4-13) into equation (4-5), then substituting for (W_{CF}) from equation (4-2) and rearranging gives;-

$$\frac{d\phi}{dx} = \frac{T}{GJ_c} \left[1 - \frac{(1-K)(bt_1 - ht_2)^2 \text{Cosh}\mu_c(L-x)}{(bt_1 + ht_2)^2 \text{Cosh}\mu_c L} \right] \quad \text{-----} \quad (4-15)$$

The angle of twist, (ϕ_{TP}), of the beam at ($x=L$), relative to the partially restrained end may be found by integrating equation (4-15);-

$$\phi_{TP} = \frac{TL}{GJ_c} \left[\frac{\mu_c L - (1-K)(bt_1 - ht_2)^2 / (bt_1 + ht_2)^2 \tanh \mu_c L}{\mu_c L} \right] \text{-----} \quad (4-16)$$

Hence, the effective torsion constant for the cross member is then given by either;

$$J_{CP} = \frac{TL}{G\phi_{TP}} \text{-----} \quad (4-17)$$

or;

$$J_{CP} = J_c \left[\frac{\mu_c L}{\mu_c L - (1-K)(bt_1 - ht_2)^2 / (bt_1 + ht_2)^2 \tanh \mu_c L} \right] \text{-----} \quad (4-18)$$

4.5 THE STIFFNESS MATRIX

In this section a stiffness matrix including warping effects as a seventh degree of freedom is developed for the closed section member. The total deformation of thin walled closed section beams can be separated into three parts, as shown in figure (4.4). Each can again be divided into two parts, the shape function depending on (s), and the magnitude depending on (x), the distance along the beam.

Therefore, the warping displacement (u), of any point can be written as the product of the two functions;-

$$u = \chi(s) W(x) \text{-----} \quad (4-19)$$

The terms which depend only on the dimensions of the cross section, as shown in figure (4.5), can be integrated in turn to give the following coefficients;-

$$\begin{aligned}
 a_1 &= \int_A \chi^2 dA = \frac{1}{24} b^2 h^2 (f_1 + f_2) \\
 a_2 &= \int_A \left(\frac{\partial \chi}{\partial s} \right) dA = \frac{1}{2} (b^2 f_1 + h^2 f_2) \\
 a_3 &= \int_A \zeta_1 \frac{\partial \chi}{\partial s} dA = \frac{1}{2} (b^2 f_1 - h^2 f_2)
 \end{aligned}
 \tag{4-20}$$

where; $f_1 = ht_1$, $f_2 = bt_2$

Table (4.1), summarizes the cross section constants and the load-displacement relations for closed section and compares them with those already derived for open section thin walled beams.

The load-deformation relations for closed section beams are considerably simplified if the lozenging and the lateral bimoment are neglected as in reference (39).

Therefore, using the same procedures as in chapter (3), section (4), the four basic expressions can be derived as;-

$$\begin{aligned}
 \varphi_{(x)} &= \varphi_1 + a_4 \left(\frac{1}{\mu_c} \sinh \mu_c x \right) W_1 + \frac{a_4}{a_1 E \mu_c^2} (1 - \cosh \mu_c x) B_1 - \frac{1}{a_1 E \mu_c^3} (\mu_c x - a_4^2 \sinh \mu_c x) M x_1 \\
 W_{c(x)} &= (\cosh \mu_c x) W_1 - \frac{1}{a_1 E \mu_c} (\sinh \mu_c x) B_1 - \frac{a_4}{a_1 E \mu_c^2} (1 - \cosh \mu_c x) M x_1 \\
 B_{c(x)} &= -E a_1 \mu_c (\sinh \mu_c x) W_1 + (\cosh \mu_c x) B_1 - \frac{a_4}{\mu_c} (\sinh \mu_c x) M x_1 \\
 M x_{(x)} &= (1) M x_1
 \end{aligned}
 \tag{4-21}$$

where ;-

$$\mu_c^2 = \frac{48G}{E} \frac{t_1 t_2}{(ht_2 + bt_1)(f_1 + f_2)}$$

$$a_4 = \frac{a_3}{a_2}$$

The constants a_1 , a_2 and a_3 are given in equation (4-20).

The load-displacement equation for warping in closed section beams can be expressed as;-

$$\{Mx_1 \ B_1 \ Mx_2 \ B_2\}^T = K_{wc} \{\varphi_1 \ W_1 \ \varphi_2 \ W_2\}^T \quad \text{-----} \quad (4-21)$$

where (K_{wc}) is the stiffness sub-matrix of the warping terms, and can be obtained from equation (4-20) as;-

$$K_{wc} = \begin{bmatrix} K_1 & -K_2 & -K_1 & -K_2 \\ -K_2 & K_3 & K_2 & K_4 \\ -K_1 & K_2 & K_1 & K_2 \\ -K_2 & K_4 & K_2 & K_3 \end{bmatrix} \quad \text{-----} \quad (4-22)$$

where K_1 , K_2 , K_3 and K_4 are given in table (4.2) with a comparison with those already derived for open section beams.

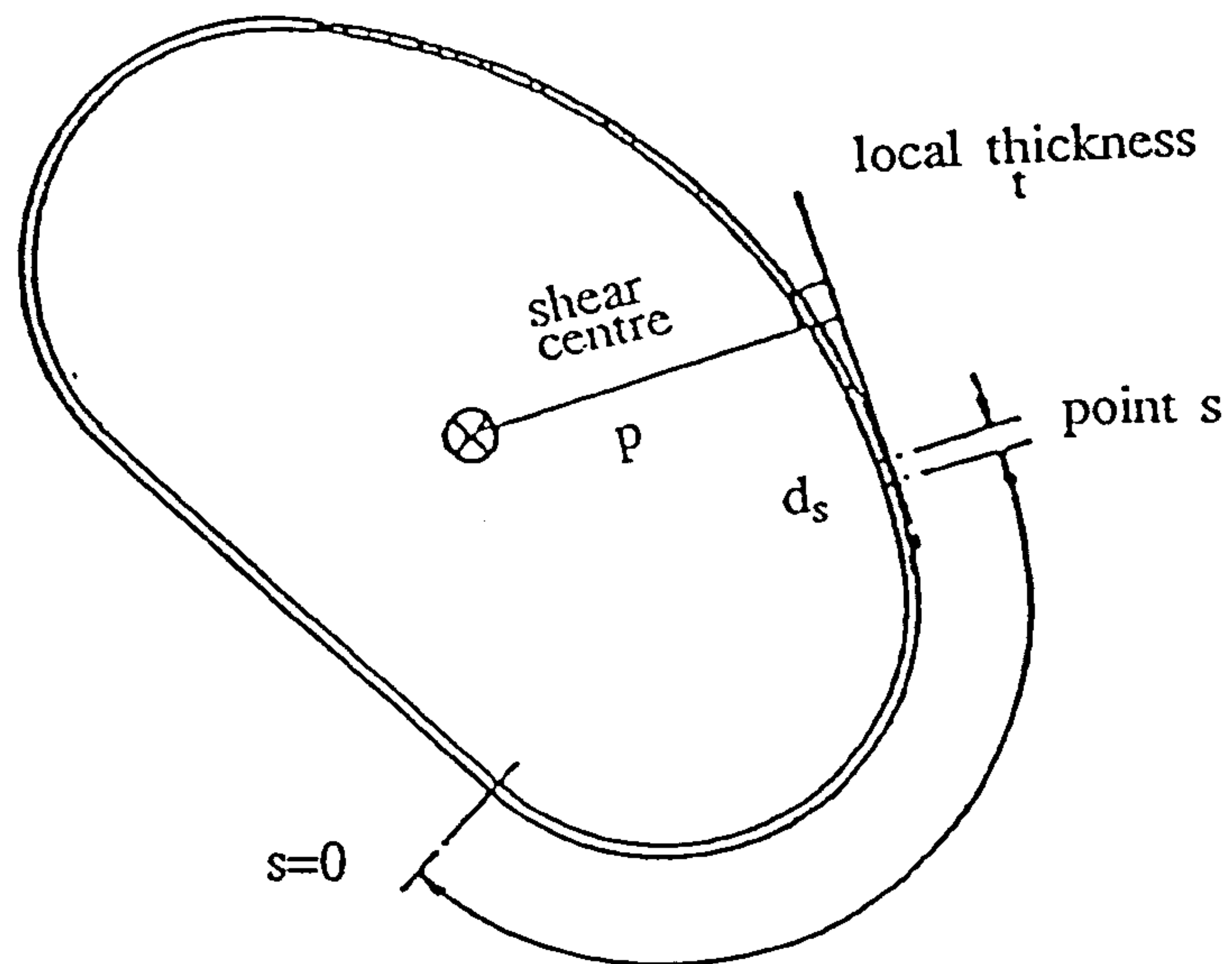


Fig.(4.1) Generation of warping displacement of closed section

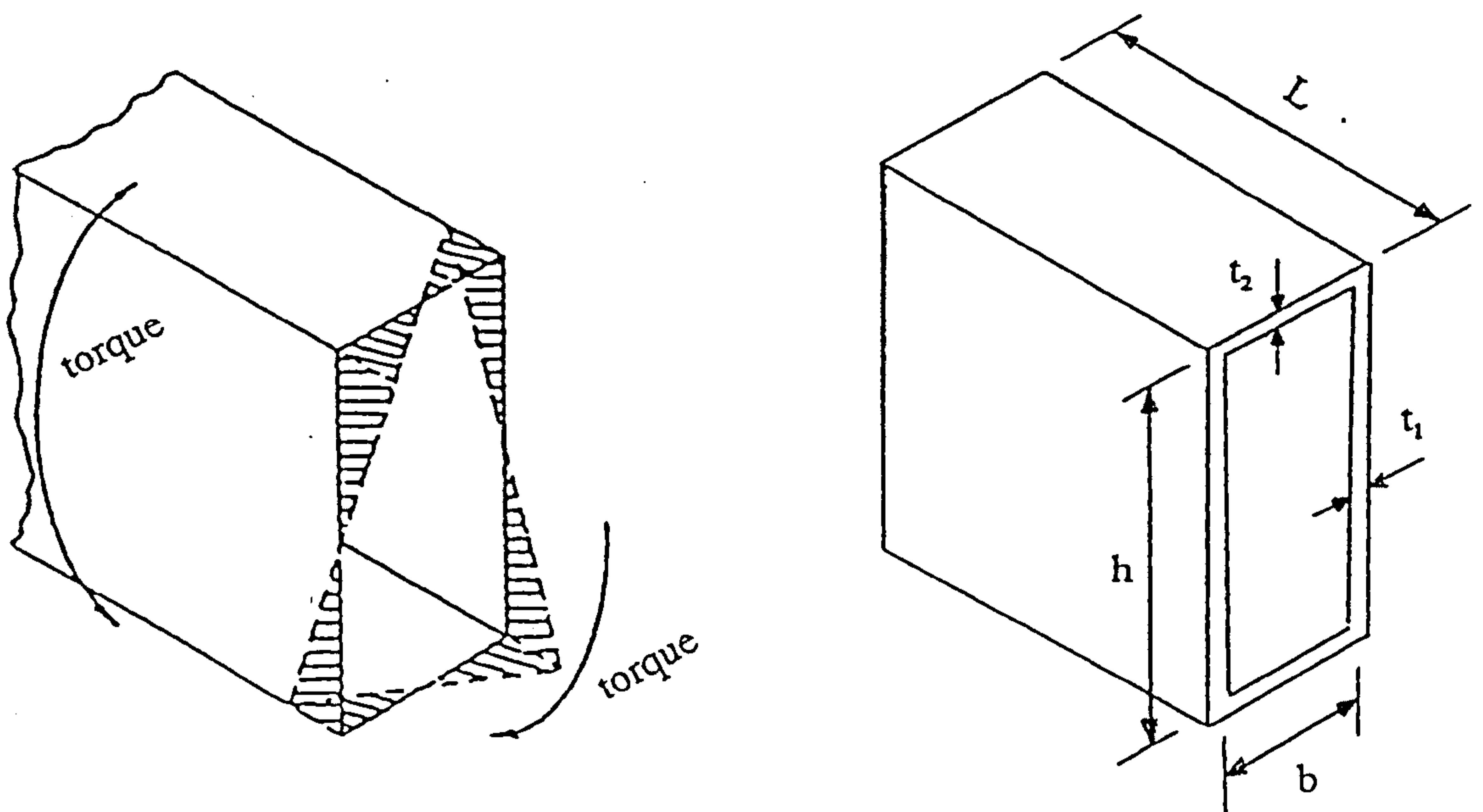


Fig.(4.2) Warping of rectangular box section

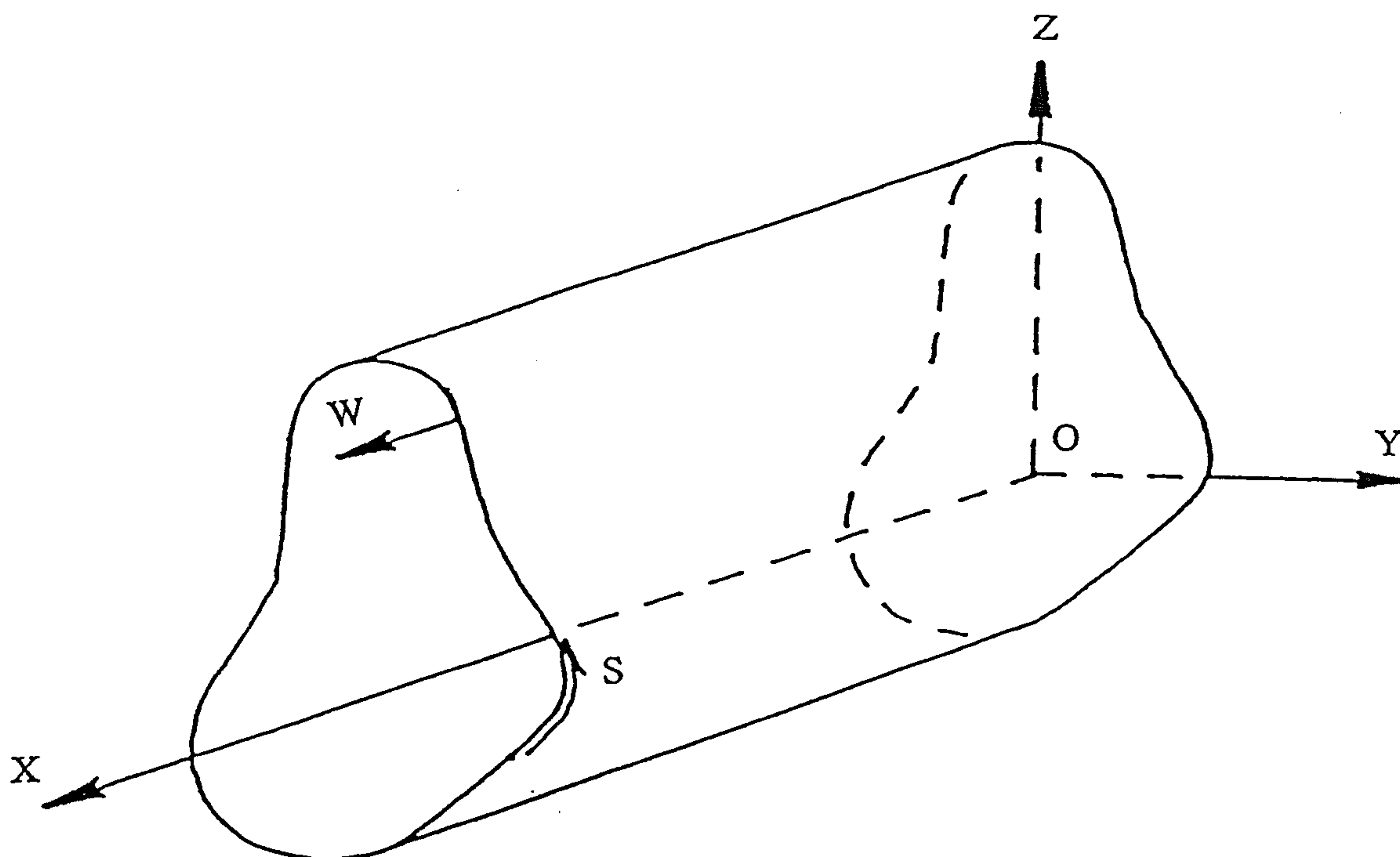


Fig.(4.3) General coordinate system of thin-walled tube

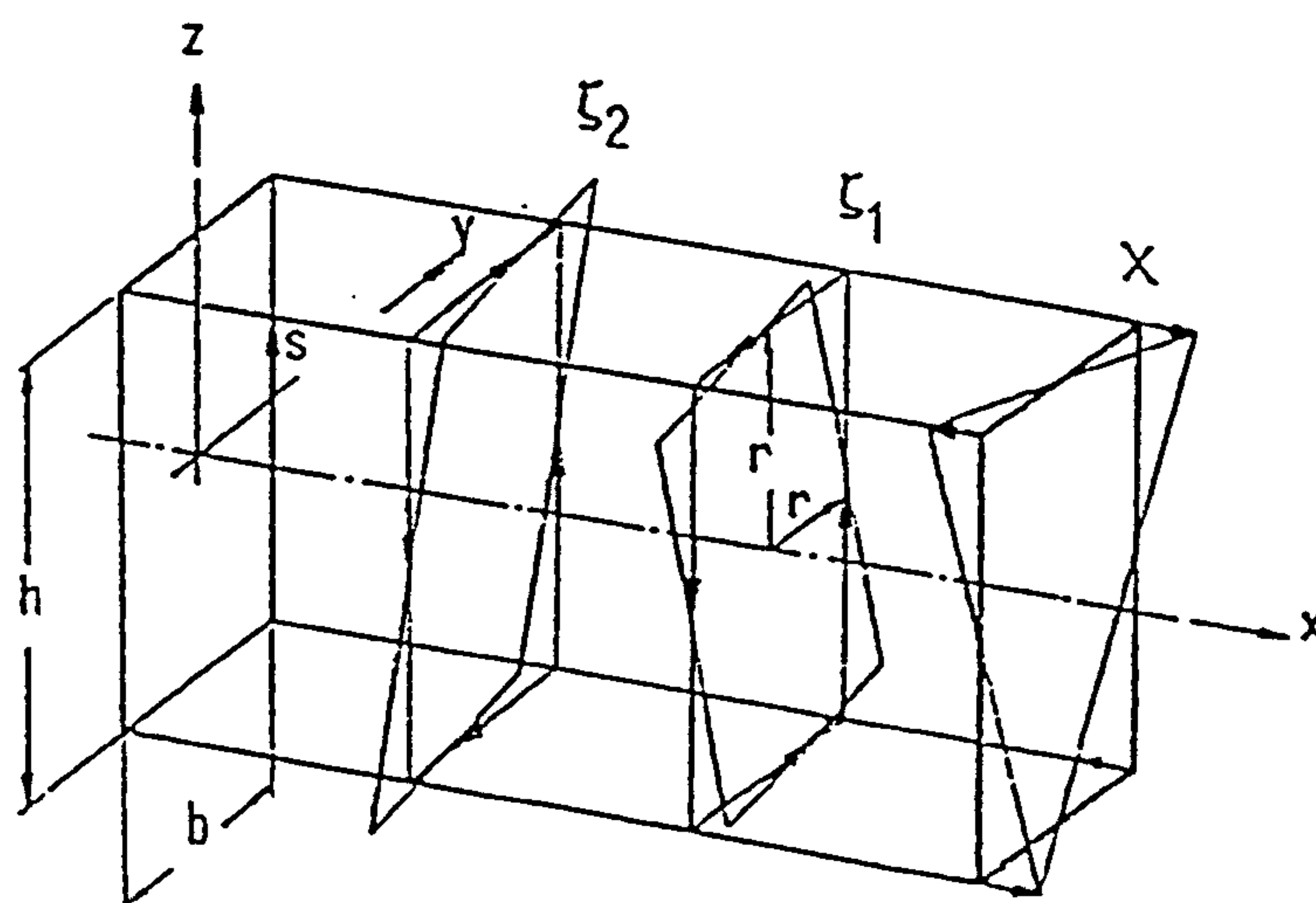


Fig.(4.4) Displacement function of a box beam

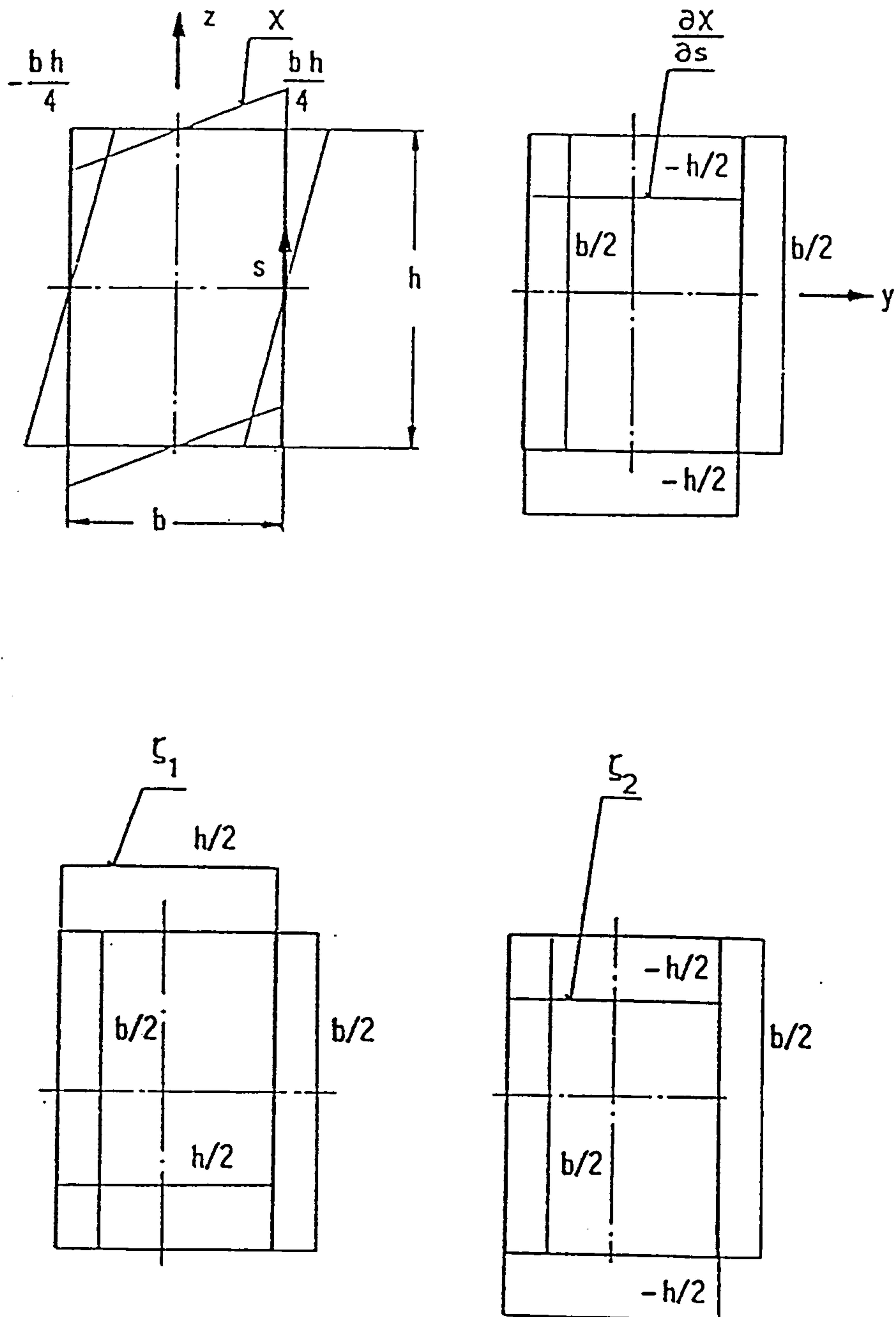


Fig.(4.5) Displacement function in the plane of the cross section of a box beam

Open cross section	Closed cross section
$u = \omega \theta'$	$u = \chi W$
$\omega_s = \int r \, ds$	$\chi = yz$
$\Gamma = \int_A \omega_s^2 \, dA$	$a_1 = \int_A \chi^2 \, dA$
$B = E \Gamma \theta'$	$B_c = E a_1 W'$
$B = \int_A \sigma_s \, dA$	$B_c = \int_A \sigma_{cs} \, dA$
$\sigma_s = (B/\sigma_s)\omega_s$	$\sigma_{cs} = (B/a_1)\chi$

Table (4.1) Summary of functions used in the analysis of open and closed section beams

	Open cross section	Closed cross section
K_1	$\frac{GJ\mu\text{Sinh}\mu L}{\{2(1-\text{Cosh}\mu L)+\mu L\text{Sinh}\mu L\}}$	$\frac{Ea_1\mu_c^2\text{Sinh}\mu_c L}{\{2a_4^2(1-\text{Cosh}\mu_c L)+\mu_c L\text{Sinh}\mu_c L\}}$
K_2	$\frac{GJ(1-\text{Cosh}\mu L)}{\{2(1-\text{Cosh}\mu L)+\mu L\text{Sinh}\mu L\}}$	$\frac{Ea_1a_4\mu_c^2(1-\text{Cosh}\mu_c L)}{\{2a_4^2(1-\text{Cosh}\mu_c L)+\mu_c L\text{Sinh}\mu_c L\}}$
K_3	$\frac{GJ(\mu L\text{Cosh}\mu L-\text{Sinh}\mu L)}{\mu\{2(1-\text{Cosh}\mu L)+\mu L\text{Sinh}\mu L\}}$	$\frac{Ea_1\mu_c(\mu_c L\text{Cosh}\mu_c L-\text{Sinh}\mu_c L)}{\{2a_4^2(1-\text{Cosh}\mu_c L)+\mu_c L\text{Sinh}\mu_c L\}}$
K_4	$\frac{GJ(\text{Sinh}\mu L-\mu L)}{\mu\{2(1-\text{Cosh}\mu L)+\mu L\text{Sinh}\mu L\}}$	$\frac{Ea_1\mu_c(a_4^2\text{Sinh}\mu_c L-\mu_c L)}{\{2a_4^2(1-\text{Cosh}\mu_c L)+\mu_c L\text{Sinh}\mu_c L\}}$

Table (4-2) Summary of constants used in stiffness matrices of open and closed section beams

CHAPTER FIVE

CHASSIS FRAME JOINTS

5.1 GENERAL

The stiffness of joints in a chassis frame can have a significant effect on bimoment distribution in it. Joints can be classified as rigid or flexible. In rigid joints all the member displacements are fully transferred to the other members, but in flexible joints the displacement transfer at the joint has to be interpreted with respect to the joint flexibility.

It is well known that direct load which does not act along the axis of the centroid of the cross section causes bending moment. Similarly, normal loads which do not act through the shear centre cause torque, and as shown in chapter (2-6), direct loads which do not act through the points of zero warping may cause bimoment. Finally, it is also shown in the same chapter, that couples made up of normal or lateral loads whose plane does not pass through the shear centre produce bimoments. Therefore, it is shown in this chapter that there are different beam axes for the various generalized forces and displacements, and these have to be taken into account in order to avoid serious errors when considering joints.

5.2.1 RIGID JOINTS ASSUMPTIONS

In chassis frames structures, the elastic properties of the joints are as important as those of the beams. As shown in the previous section, it is not correct to use the intersections of the centroid axes as a node without noting the effect of the intersections of the torsion centre axes and the zero warping lines along the beams. The zero warping lines are lines parallel to the axis of the beam passing through the points of zero warping in the cross section as shown in figure (5.6). Taking rigid joint assumptions into account when assembling the total stiffness matrix, the effect of different axes must be included. This can be done by transforming the non-coincident load and displacement components into the axes defined for the node.

5.2.2 JOINT COMPATIBILITY

The ends of beam elements at the joint can be defined by the intersections of the centroid axes. The intersections of the torsion axes and the zero warping axes will not be at the ends of the beam elements defined in this way. The zero warping

axis is defined as the axis formed by the intersection of the plane containing the zero warping lines in the flanges and the plane containing the centroid and the torsion axes as shown in figure (5.6).

Therefore, the node must be defined by three points (as introduced in reference 39), these points are the torsion centre (T), the centroid (S) and the warping point (W). Such a node is called (TSW) node. The warping point (W) is the point where the zero warping axes meet the end plane of the beam as shown in figure (5.6). The lack of coincidence of the axes between a channel section cross member with horizontal web and a channel section side member with vertical web are shown in figure (5.1), where the centroids of the two channels (S) and (S_c) are separated vertically by the distance (h_s).

When assembling the total stiffness matrix, the stiffness matrix [K_c] relating to the (T_c S_c W_c) node must be transformed to the matrix [K] relating to the (TSW) node. The relationship between the loads and the displacements is well known and can be written as;-

$$[P]=[K][d] \quad \text{-----} \quad (5-1)$$

or;-

$$[P_c]=[K_c][d_c] \quad \text{-----} \quad (5-2)$$

where the subscript (c) is denoted to (T_c S_c W_c) node, i.e, the node at the end of the cross member.

But;-

$$[P]=[H][P_c] \quad \text{-----} \quad (5-3)$$

or;-

$$[d_e]=[H]^T[d] \quad \text{-----} \quad (5-4)$$

where $[H]$ is the equilibrium matrix to allow for the (TSW) node.

Substituting equation (5-2) into equation (5-3) get;-

$$[P]=[H][K_e][d_e] \quad \text{-----} \quad (5-5)$$

From equation (5-5) and equation (5-4), the following expression can be obtained;-

$$[P]=[H][K_e][H]^T[d] \quad \text{-----} \quad (5-6)$$

Comparing equation (5-6) with equation (5-1), the following obtained;-

$$[K]=[H][K_e][H]^T \quad \text{-----} \quad (5-7)$$

Equation (5-7), gives the necessary relationship between the stiffness matrix relating to the (TSW) node and that relating to (T_e, S_e, W_e) node.

Combining equation (3-32) and equation (5-7), a comprehensive stiffness matrix for cross members in globalised system can be written as;-

$$[K_{ij}]_G=[T_{ij}][H_{ij}][K_{ij}]_L[H_{ij}]^T[T_{ij}]^T$$

Where;

$[T_{ij}]$ is the standard transformation matrix between local and global axes

$[H_{ij}]$ is equilibrium matrix for beam (ij) including (TSW) nodes.

This is a clarification of the approach in reference (39), where the 'equilibrium and the standard transformation matrices were combined in a single so called "transformation matrix". In reference (39) the transpose of this matrix is incorrectly referred to as the 'Transform' of the matrix.

5.2.3 EQUILIBRIUM MATRIX

The equilibrium matrix of the (TSW) node depends on both the profile of the cross sections and the orientation of the beams meeting at the joint. For commercial vehicle chassis frames where the beam elements meet at right angles, the equilibrium matrix can be straightforward enough for practical use.

The side member is taken as a channel section with vertical web and the flanges pointing towards the centre of the vehicle. The cross members are taken as a channel sections and may have;-

- i) Vertical web with the flanges pointing either to the left or right.
- ii) Horizontal web with the flanges pointing either up or down.

The derivation of the equilibrium matrix for each of these cases will be dealt with separately.

For the system shown in figure (5.2), with a vertical web channel cross member with the flanges pointing to the left, i.e, case (i) above, the equilibrium matrix may be written as;-

$$[H] = \begin{bmatrix} 1 & 0 & 0 & 0 & 0 & 0 & 0 \\ 0 & 1 & 0 & 0 & 0 & 0 & 0 \\ 0 & 0 & 1 & 0 & 0 & 0 & 0 \\ 0 & -h_s & -R_T & 1 & 0 & 0 & 0 \\ h_s & 0 & S_T & 0 & 1 & 0 & 0 \\ 0 & 0 & 0 & 0 & 0 & 1 & 0 \\ 0 & h_s S_w & 0 & -S_w & R_w & -h_s & 1 \end{bmatrix} \quad \text{-----} \quad (5-8)$$

where the constants (h_s , R_T , S_T , R_w and S_w) are given in figure (5-5).

When the corresponding axes at the two beam ends do not coincide, the rotation about one of the axes will make a contribution to the translation of the nodal point.

For instance, from figure (5.3c), the displacement (δy_c) is at a distance (h_s) from the centroid axis through (S) where the rotation is (θ_y) about the y-axis of the side member. Therefore, this gives a displacement of ($-h_s\theta_y$) in the y-direction of the cross member (y_c).

It is clear that when a direct load has an offset, it will produce a moment. For example, the force ($P y_c$) in figure (5.4c) gives a moment of ($-h_s P y_c$) to be added to the moment ($M y$) in figure (5.4a) as shown in equation (5-9).

The effects on bimoment behaviour of couples made up of normal or lateral loads as well as moment whose plane does not pass through the shear centre are also included in equation (5-8). For the system shown in figure (5.2), with a horizontal web channel cross member with flanges pointing down, i.e, case (ii), the equilibrium matrix can be written as;-

$$[H] = \begin{bmatrix} 1 & 0 & 0 & 0 & 0 & 0 & 0 \\ 0 & 1 & 0 & 0 & 0 & 0 & 0 \\ 0 & 0 & 1 & 0 & 0 & 0 & 0 \\ 0 & -(h_s+r_T) & 0 & 1 & 0 & 0 & 0 \\ h_s & 0 & S_T & 0 & 1 & 0 & 0 \\ 0 & 0 & 0 & 0 & 0 & 1 & 0 \\ 0 & (h_s+r_T)S_w & 0 & S_w & 0 & -(h_s+r_w) & -1 \end{bmatrix} \quad \text{-----} \quad (5-9)$$

A general equilibrium matrix can be obtained by combining equation (5-8) with equation (5-9) as follows;-

$$[H] = \begin{bmatrix} 1 & 0 & 0 & 0 & 0 & 0 & 0 \\ 0 & 1 & 0 & 0 & 0 & 0 & 0 \\ 0 & 0 & 1 & 0 & 0 & 0 & 0 \\ 0 & -(h_s+r_T) & -R_T & 1 & 0 & 0 & 0 \\ h_s & 0 & S_T & 0 & 1 & 0 & 0 \\ 0 & 0 & 0 & 0 & 0 & 1 & 0 \\ 0 & (h_s+r_T)S_w & 0 & \mp S_w & R_w & -(h_s+r_w) & \pm 1 \end{bmatrix} \quad \text{-----} \quad (5-10)$$

where in all cases the dimension (h_s) is positive when the centroid (S_c) is above the centroid (S).

The equilibrium matrix given in equation (5-10) can be applied to all situations if the sign of the terms in row (7) of columns (4) and (7), is taken to be the upper sign for cross members with vertical webs and the lower sign for those with horizontal webs. The displacements of the nodal points at the end of the beam element are shown in figure (5.3), while corresponding components of the loads are shown in figure (5.4). The distances from the centroid axes and their sign convention for the joints used in the general equilibrium matrix are given in figure (5.5).

5.3.1 FLEXIBLE JOINT ASSUMPTIONS

In the previous section, the joints are taken as rigid. In fact the joints deform under load as well as the beams. Therefore, the displacement transfer at the joints has to be interpreted with respect to the joint flexibility.

In short beams, joint deformation is more important than in long beams. Joints of chassis frames where the length of the beam elements is of the same order as the cross section dimension of the beam can be regarded as short beams. There are flexibilities associated with the various member end-forces, but the rate of twist flexibility is a major interest of this research.

5.3.2 RATE OF TWIST STIFFNESS

The rate of twist stiffness of the joints has considerable influence on the torsional stiffness of the whole chassis frame as well as the stress distribution in its members. The rate of twist of a joint can be included in the analysis of chassis frames by the matrix stiffness method by a rate of twist stiffness coefficient as will be shown later in the chapter on joint elements, section (5.3.4). This coefficient can be defined as the bimoment transmitted through the boundaries of a node between a side member and a cross member divided by the change in the rate of twist between those boundaries. Therefore, the rate of twist stiffness coefficient of a joint can be represented by the following expression;-

$$K_{\theta} = \frac{B}{\Delta\theta'} \quad \text{-----} \quad (5-11)$$

The stiffness of various joints can easily be compared using this simple quantity, and it is also used to introduce the joint element stiffness matrix as will be shown later. This is the reciprocal of the "rate of twist flexibility" introduced by reference (39).

5.3.3 BENDING AND TORSION STIFFNESS COEFFICIENTS

Bending and torsion stiffness of a joint can also each be represented by a single coefficient. This coefficient can be defined as the moment transmitted through the node boundaries between a side member and a cross member divided by the difference between the twist of the side member and the slope at the end of the cross member or the slope of the side member and the twist at the end of the cross member meeting at the joint.

These stiffness coefficients can be directly inserted into the stiffness matrix of the joint element, as will be shown in the next section. Reference (45) gives a definition of a stiffness constant for a joint with bending flexibility and shows how it is included in the beam element stiffness matrix.

As far as this research concerned, joints are regarded to behave rigidly except for the rate of twist where they regarded to behave in a flexible manner.

5.3.4 THE JOINT ELEMENT

In order to introduce the rate of twist stiffness of a joint into the matrix displacement (stiffness) method of analysis, the definition of the (TSW) node, considered in section (5.2.2), must be completed by including a node boundary at the end of the cross member. Since beams are represented by their centroid axes, the end of the cross member lies at the centroid of the side member as shown in figure (5.7).

It is necessary to introduce the joint elements to take into account the effect of the whole joint. The stiffness matrix for such a joint element can be obtained from a finite element analysis of the joint area (see chapter 6). Reference (39) suggested on the basis of experience that the length of the side member included in the analysis should exceed the width of the cross member by around 70 percent of the side member height as shown in figure (5.7).

To find the internal loads in the joint element, the displacements at one boundary are fixed and unit displacements made at the nodes of the other boundary. The unit displacements are ;-

$$\{\delta x \ \delta y \ \delta z \ \theta_x \ \theta_y \ \theta_z \ \theta'\}^T$$

while the internal loads at both boundaries are found by finite element analysis to be;-

$$\{P_x \ P_y \ P_z \ M_x \ M_y \ M_z \ B\}^T$$

Assuming the node has zero length, the joint element stiffness matrix can be written as;-

$$[K_J] = \begin{bmatrix} K_{\Delta x} & & & & & 0 \\ & K_{\Delta y} & & & & \\ & & K_{\Delta z} & & & \\ & & & K_{\theta x} & & \\ & & & & K_{\theta y} & \\ 0 & & & & & K_{\theta z} \\ & & & & & & K_{\theta'} \end{bmatrix} \quad \text{-----} \quad (5-12)$$

Note: (Cross coupling terms may be present, but these have been neglected in the above equation)

The equilibrium matrices defined in section (5.2.3) do not apply when a joint element is used because the axes offset is automatically included in the joint element.

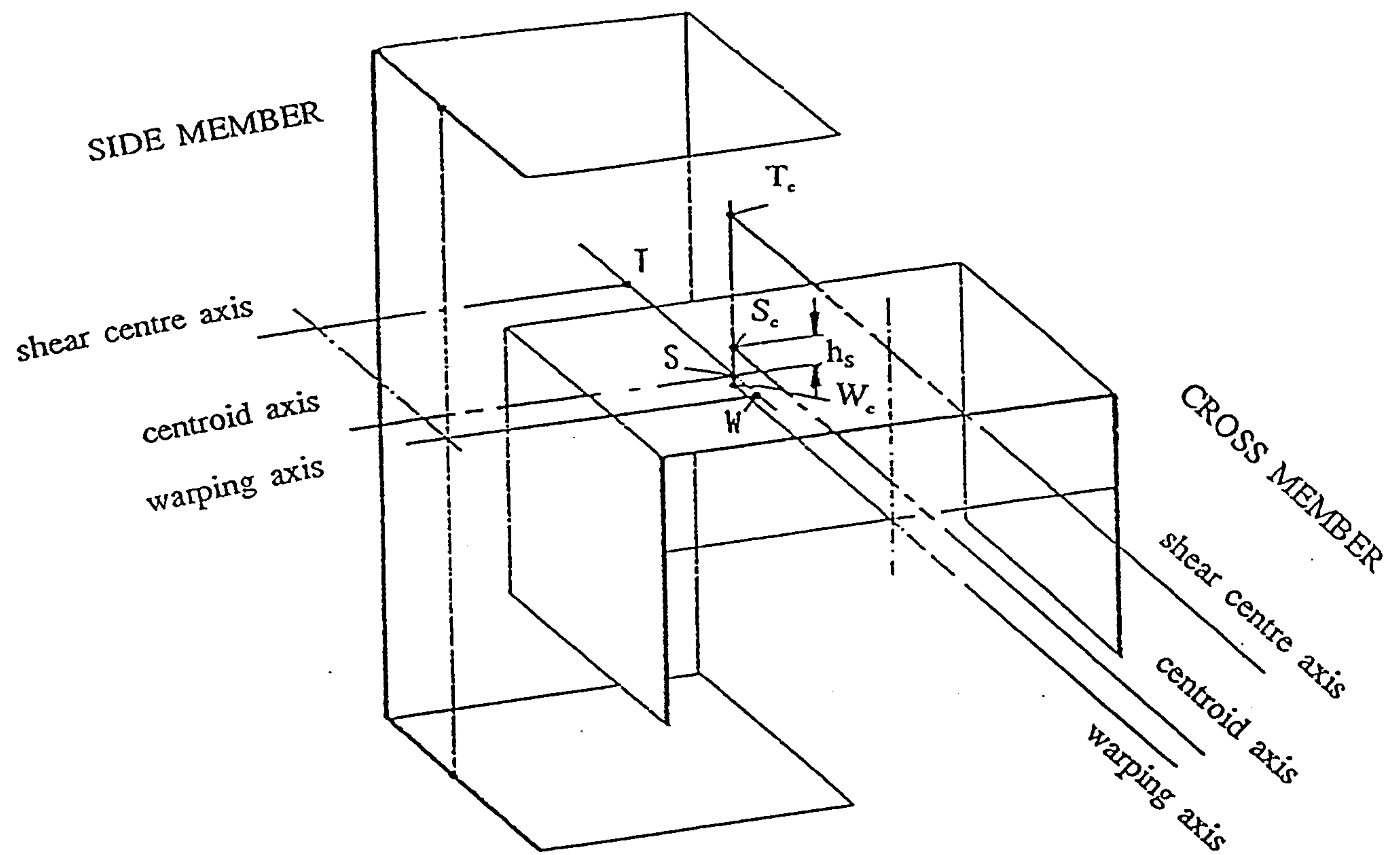


Fig.(5.1) A joint defined by a (TSW) node with a horizontal web channel cross member

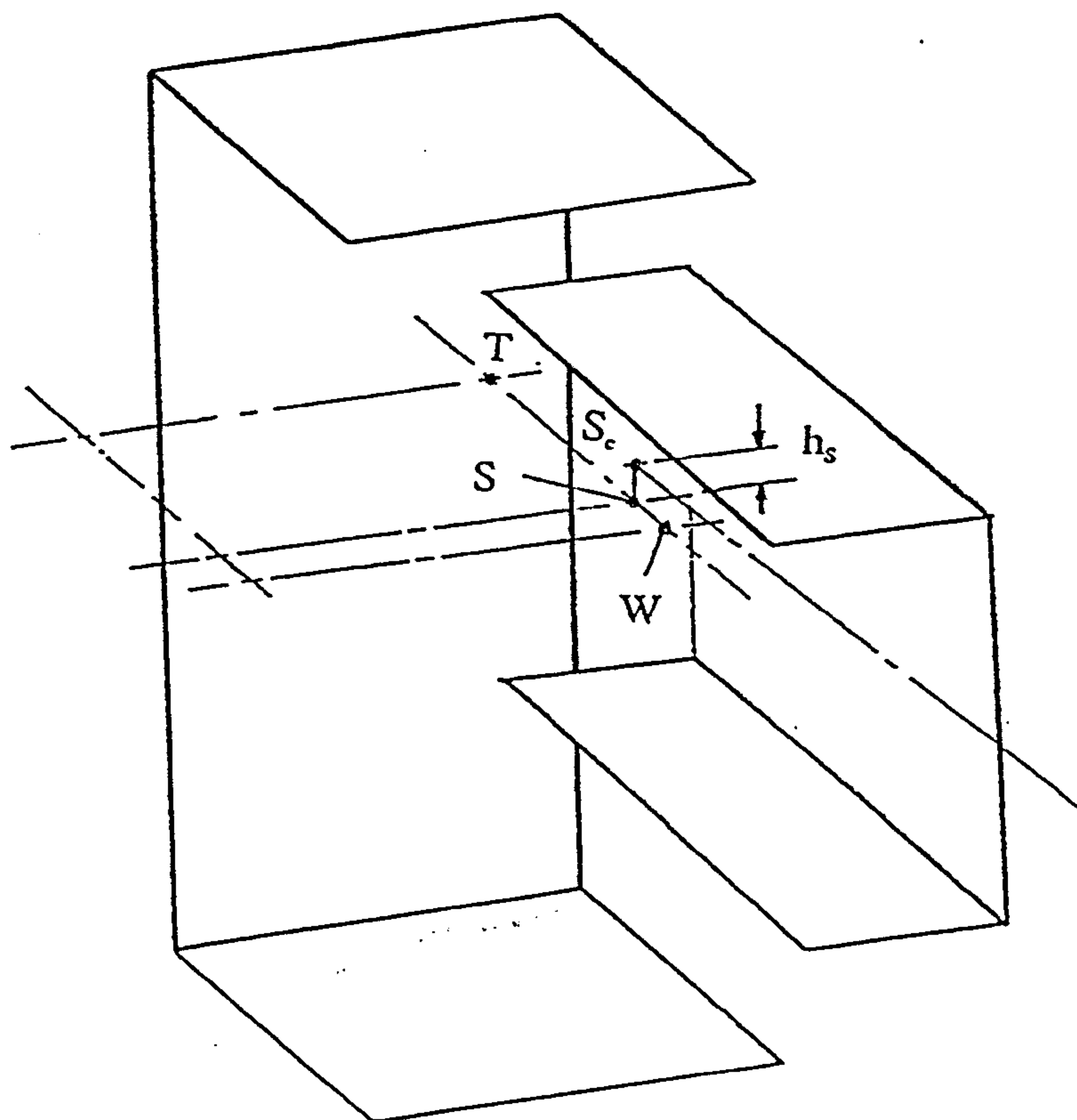
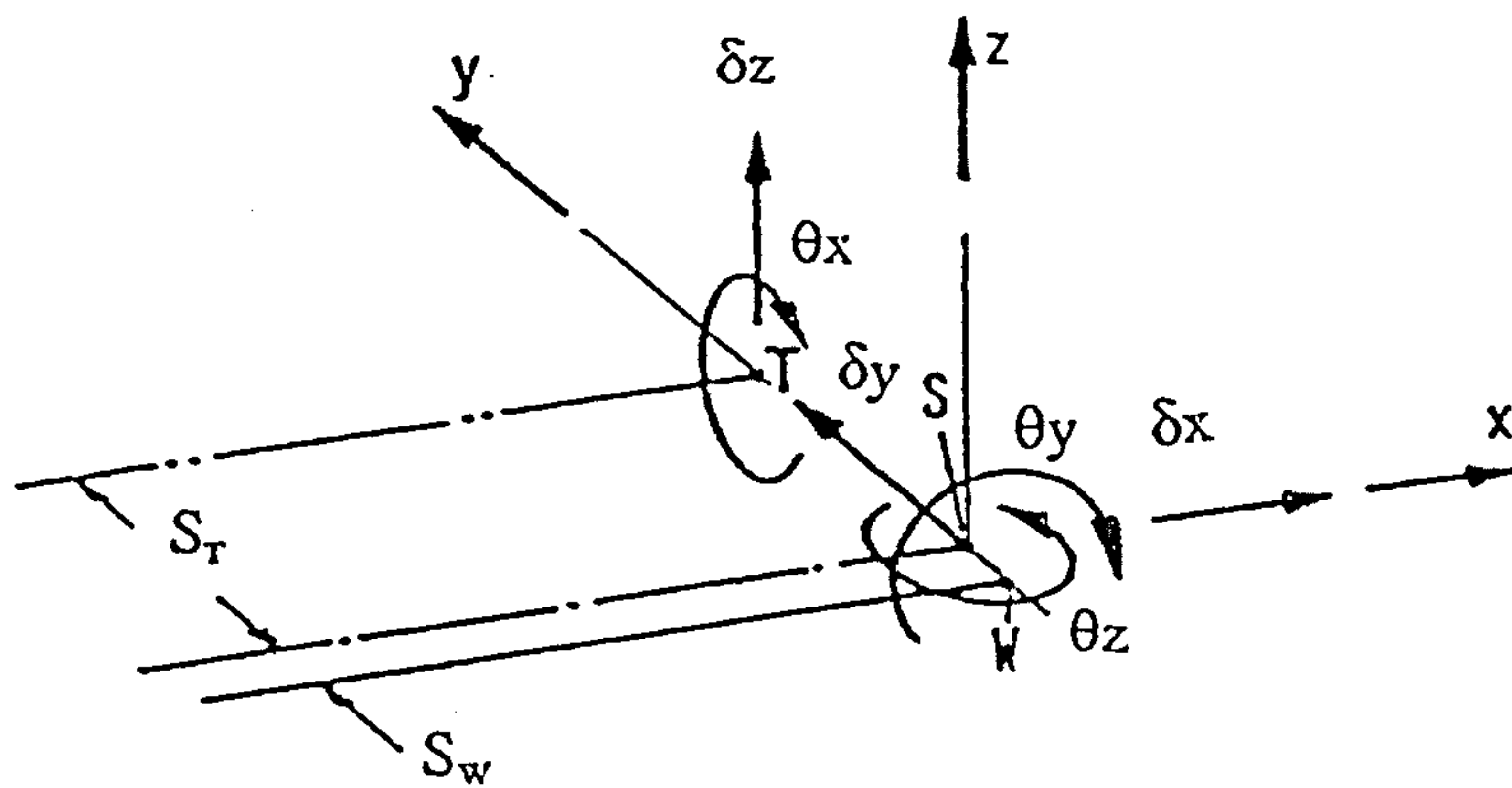
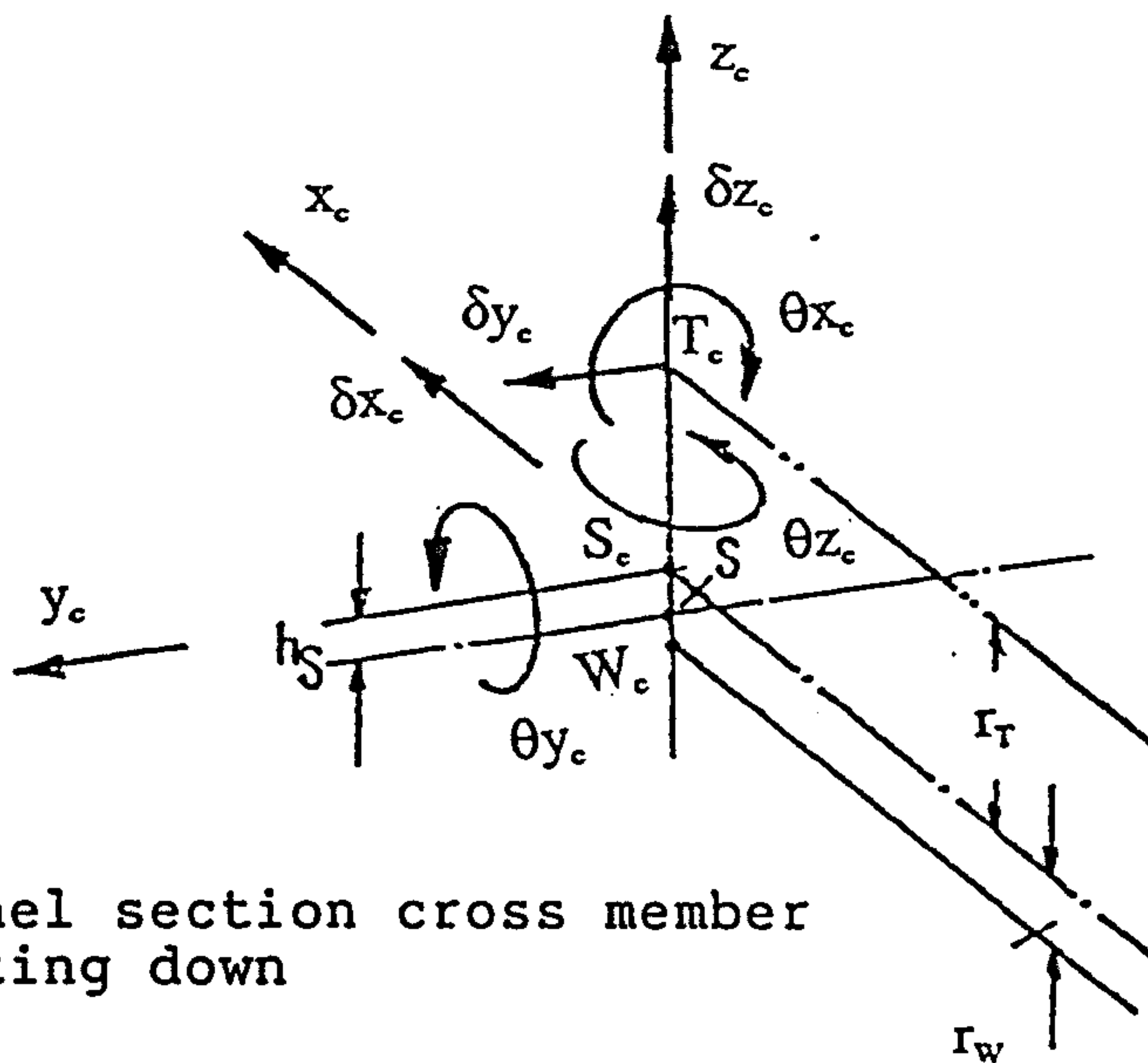


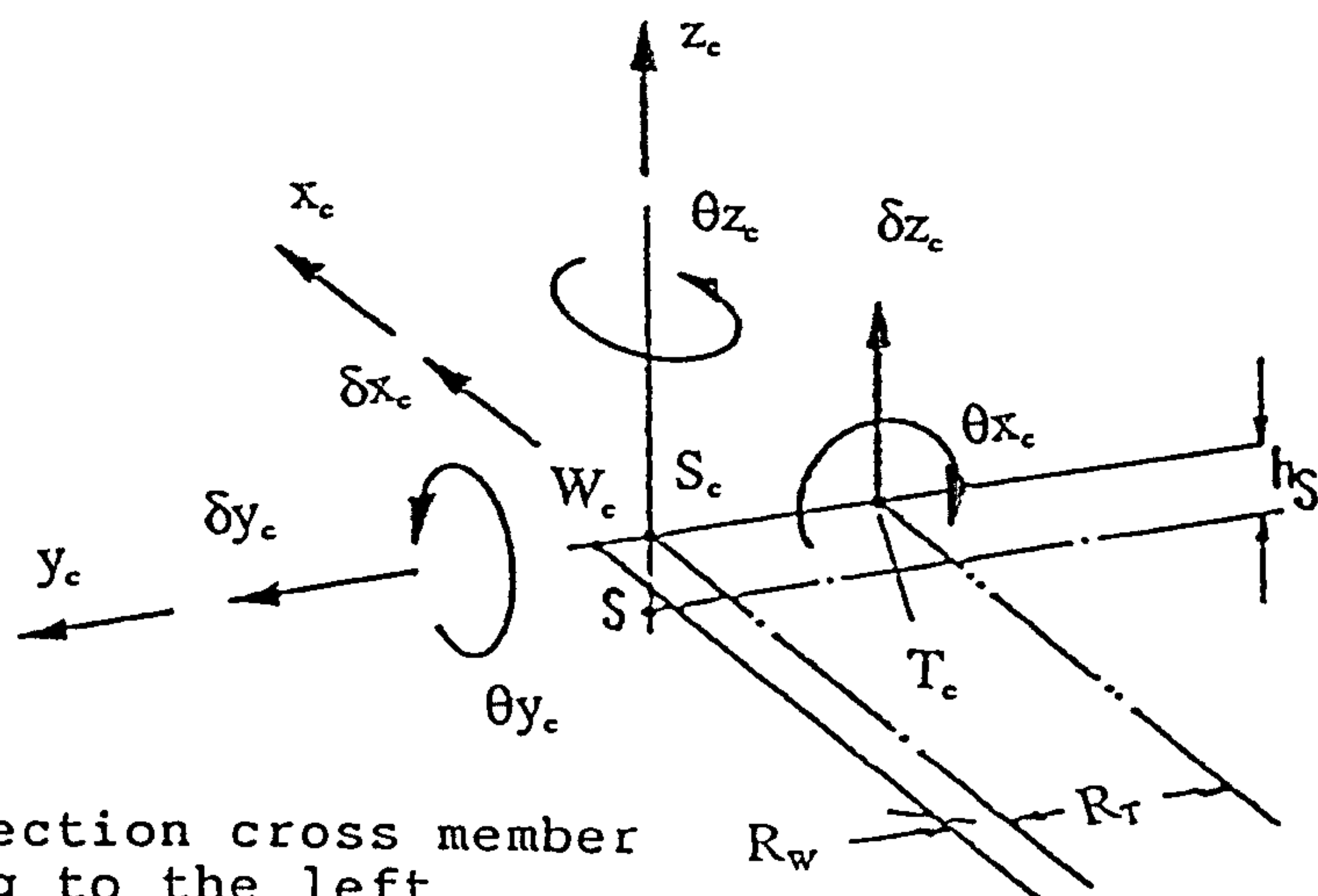
Fig.(5.2) A joint with a vertical web channel cross member



a) A vertical channel section side member with flanges pointing towards the centre



b) A horizontal channel section cross member with flanges pointing down



c) A vertical channel section cross member with flanges pointing to the left

Fig.(5.3) Displacements of nodal points at the ends of beams meeting at a joint, used to build up the equilibrium matrix [H]

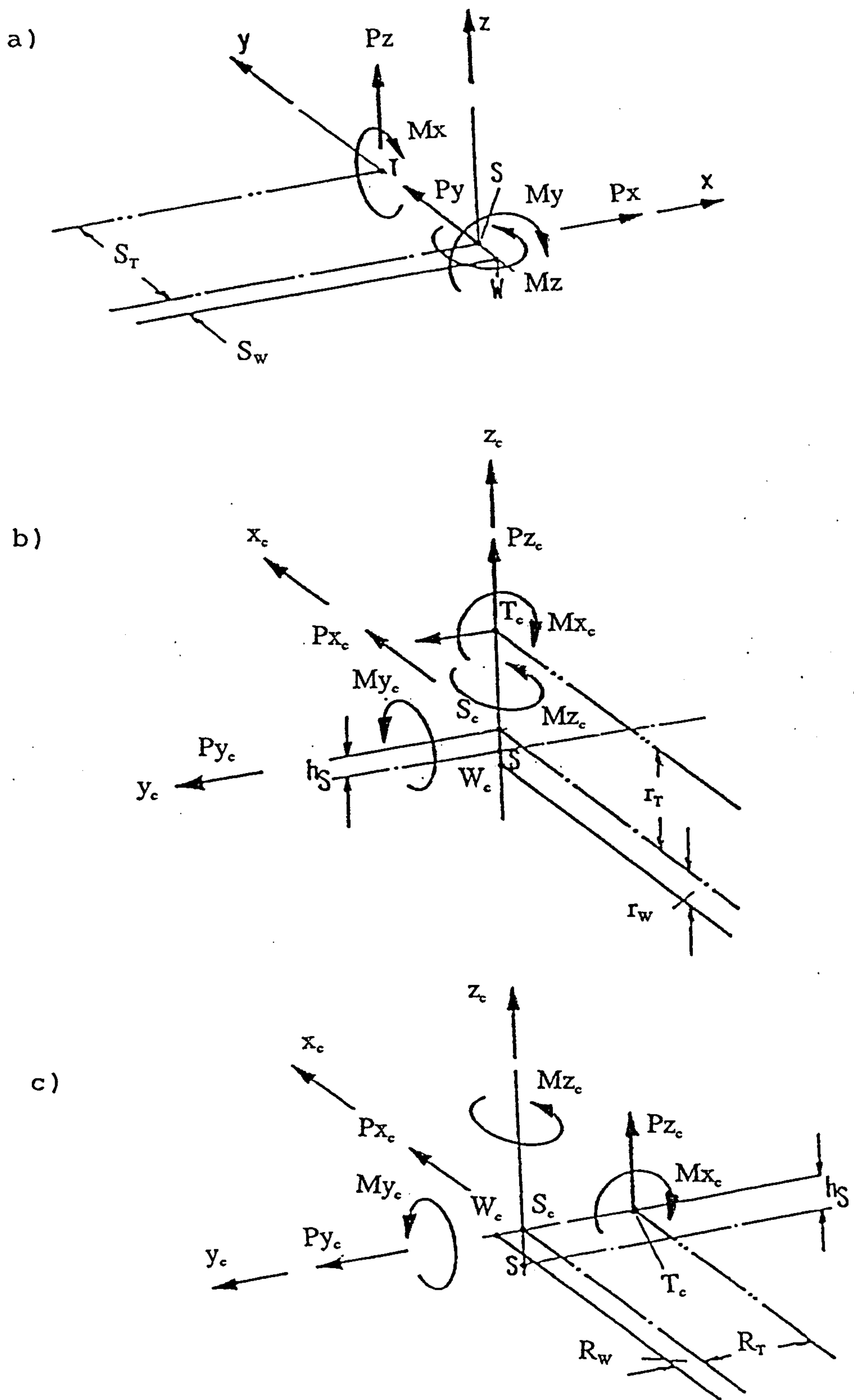


Fig.(5.4) Loads corresponding to the displacement in fig.(5.3)

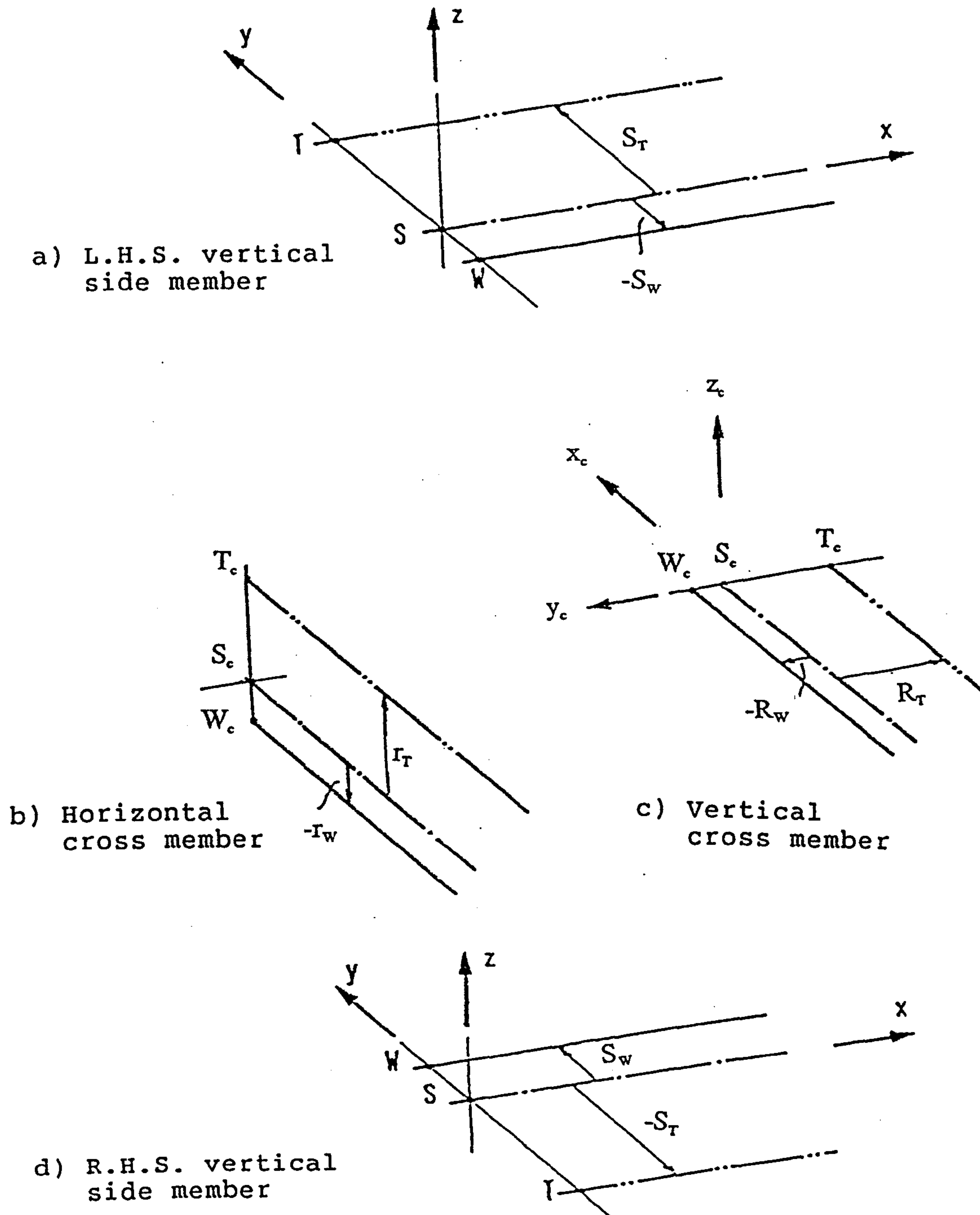


Fig.(5.5) Distances of torsion axes and warping point from the centroid axis for various joint configuration, see fig.(5.3)

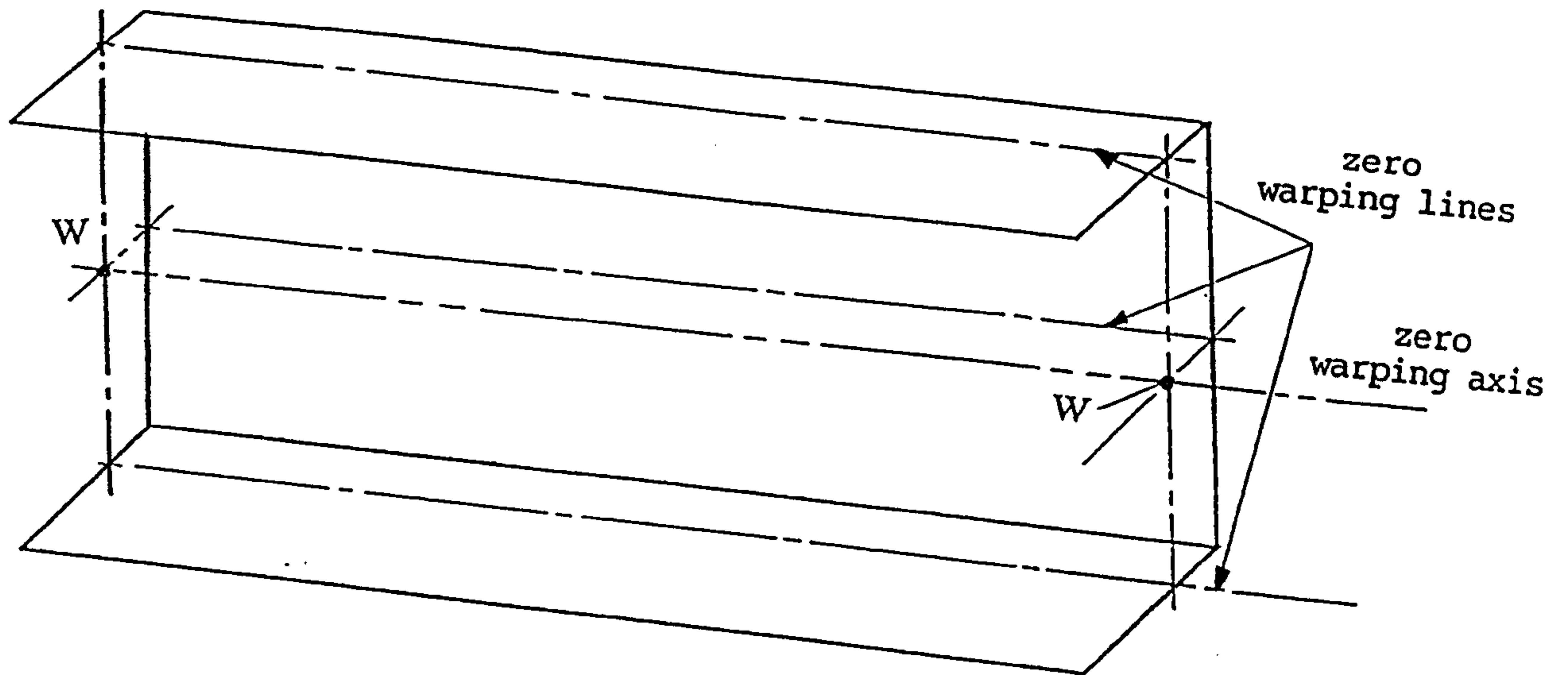


Fig.(5.6) Warping lines and warping axis of a channel section beams

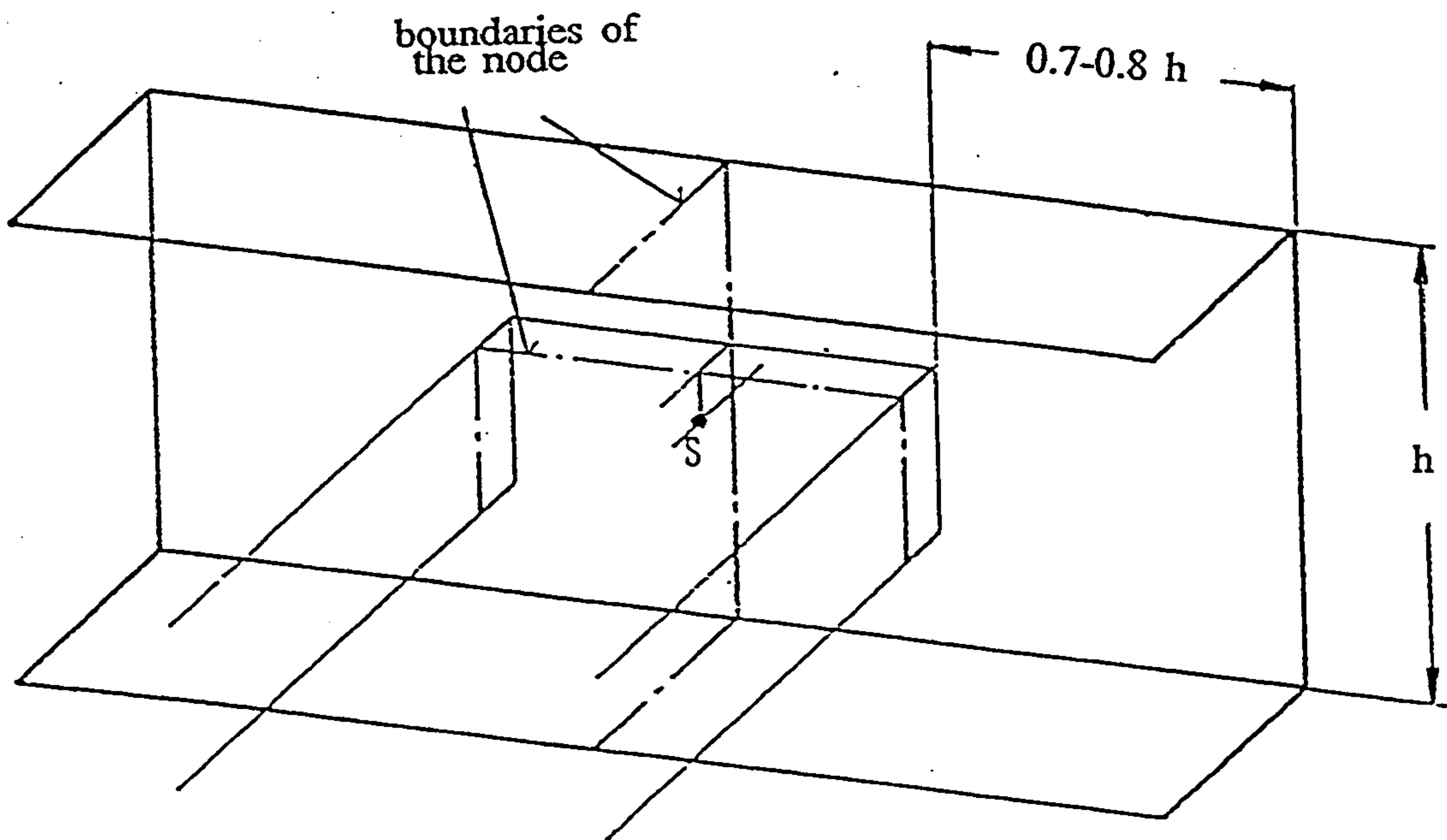


Fig.(5.7) Example of a joint element

CHAPTER SIX

THEORETICAL INVESTIGATION OF THE EFFECT OF LONGITUDINAL LOADS

6.1 GENERAL

This project investigates the stress distribution in the side members of a ladder chassis frame subject to longitudinal load. Hence, in this chapter the bimoment created due to the longitudinal load and some basic terms and concepts related to bimoment are discussed briefly.

6.2 LONGITUDINAL LOADS APPLIED OUTSIDE SECTION PROFILE

If the longitudinal load is not applied on the profile of the cross section, then the value of the bimoment produced depends on both the load position and the geometry of the connection of the loading point to the section.

If a force (p) is applied at point (A), parallel to an open section beam away from the shear centre as shown in figure (6.1). If the force is transmitted to the section through a rigid arm fixed at the contour (D), and if this force lies in a cross-sectional plane, the force will cause a bimoment equal to the product of the force (P) and twice the area (TMDA). This rule may be demonstrated as follows;-

$$B = p \omega_D + M h \quad (\text{from figure 2.7})$$

$$B = p e h + p z h$$

Where;

ω_D = principal sectorial area of point (D)

$$M = p z$$

$$\omega_D = e h$$

Hence;-

$$B = p\{(e + z) h\} \quad \text{-----} \quad (6-1)$$

but;

$$\{(e + z) h\} = 2 \text{ Area (TMDA)} = \omega_A \quad \text{-----} \quad (6-2)$$

Where;

ω_A = principal sectorial area of point (A) in which the longitudinal load (p) is applied

Therefore;-

$$B = p \omega_A \quad \text{-----} \quad (6-3)$$

From the above equations, it is clear that the value of the bimoment produced due to the longitudinal loads depends on the position in which the rigid arm carrying the force is connected to the member cross section.

To demonstrate this effect, two finite element models were created (see figures 6.3/6.4). In both of these, a longitudinal load was applied to a channel section side member at the same offset position profile via rigid arms, thus applying similar bending moments and axial load. However, the rigid arms were connected to different positions on the channel section profile.

The different bimoment effects may be seen in those figures is due to different area of (TMDA), i.e different principal sectorial area (ω_A) of the point outside the cross section profile as shown in equation (6-2).

The principal sectorial area (ω_s) distribution of a channel section is shown in figure (6.2), while the relevant constant such as warping constant (Γ), and torsion constant (J) for a channel section are quoted from reference (40) as follows;-

$$\Gamma = t \int \omega_s^2 ds = \frac{h^2 b^3 t (4h + 3b)}{6(h + 3b)}$$

(6-4)

$$J = \frac{2 (b + h) t^3}{3}$$

(6-5)

6.3 TOTAL STRESSES DUE TO LONGITUDINAL LOAD

The formula for total stresses at any point along the side members of chassis frame when a longitudinal loads applied can be defined as;-

$$\sigma_T = \sigma_A + \sigma_y + \sigma_z + \sigma_s$$

(6-6)

Where;

$$\sigma_A = \frac{P}{A}$$
$$\sigma_y = \frac{M_y z}{I_{yy}}$$
$$\sigma_z = \frac{M_z y}{I_{zz}}$$
$$\sigma_s = \frac{B \omega_s}{\Gamma}$$

(direct stress)

(moment stress)

(moment stress)

(warping stress)

(6-7)

Where; (y & z) are the coordinates of the point in which the stresses were calculated.

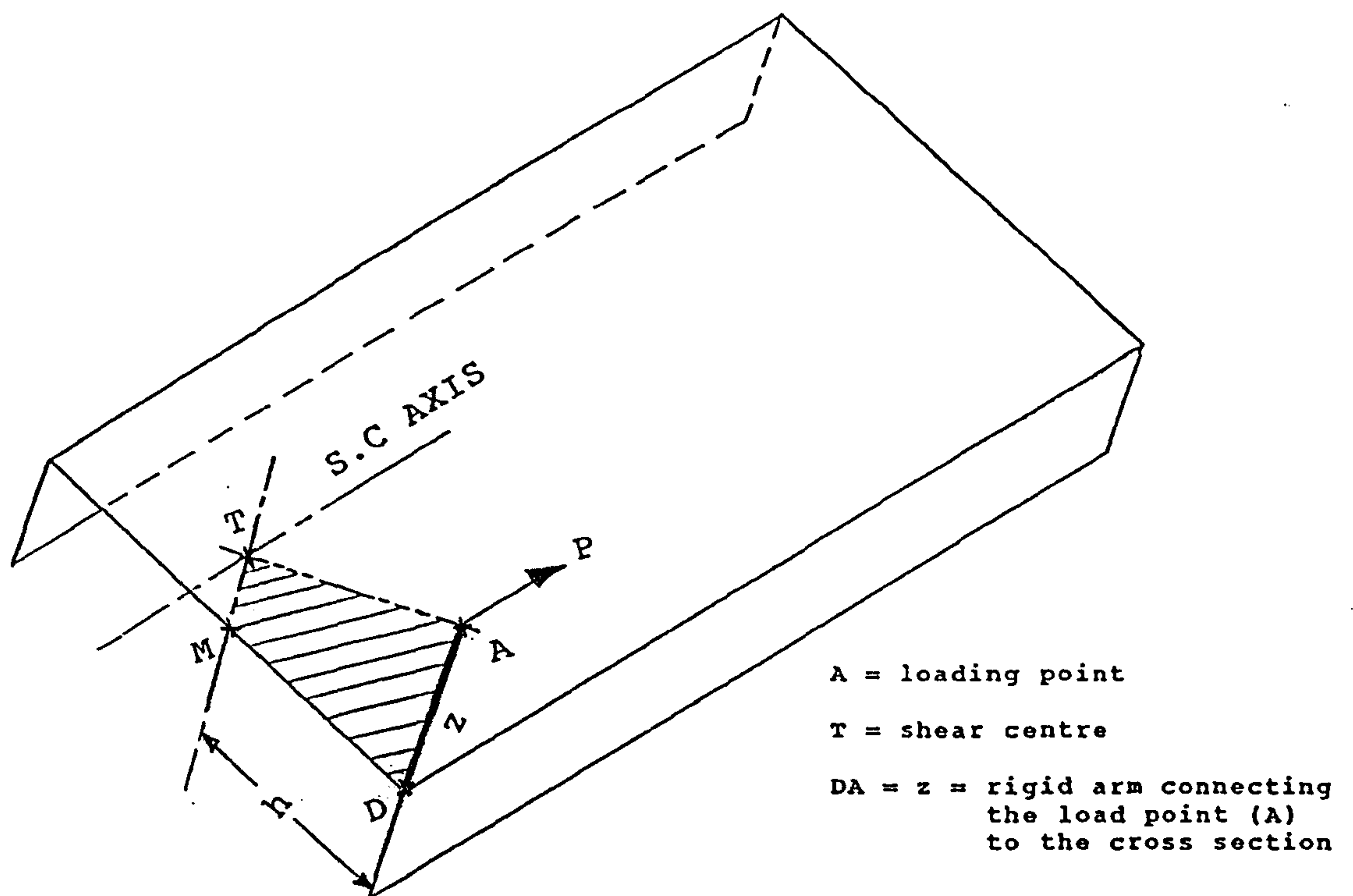
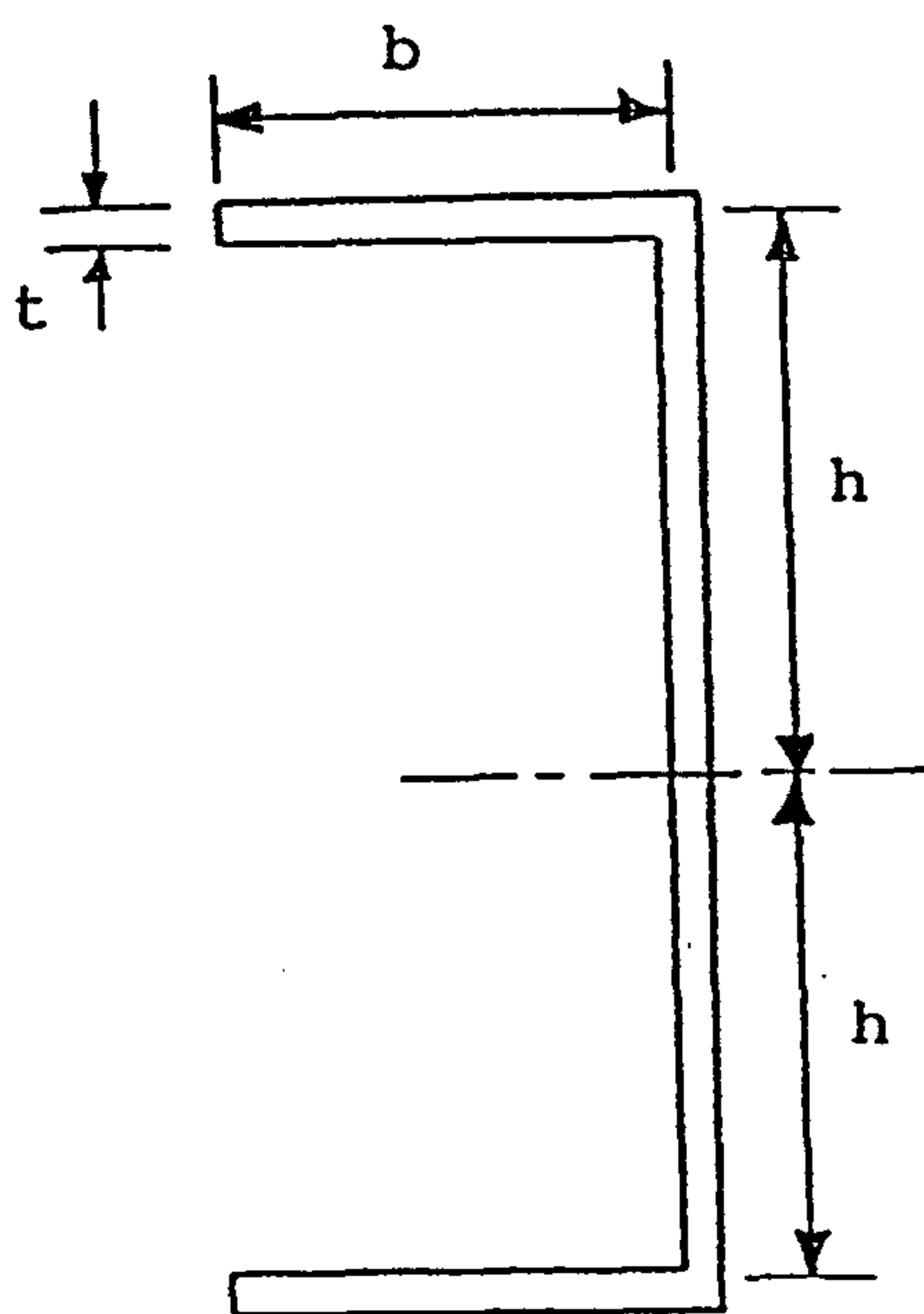
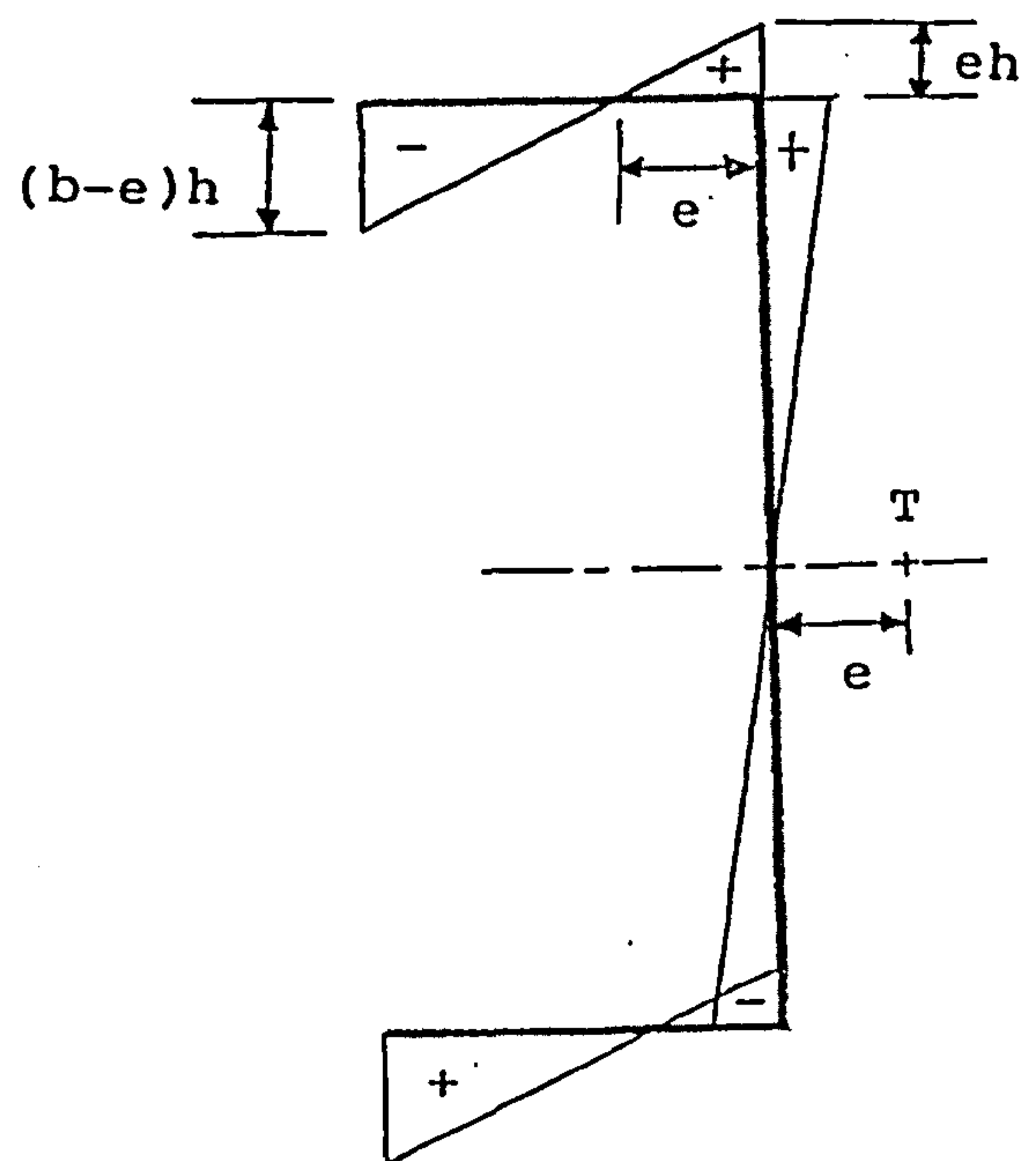


Fig.(6.1) Bimoment created due to longitudinal load



a) cross section dimensions of a channel section



b) principal sectorial area of a channel section

Fig.(6.2) Principal sectorial area (ω_s) of the model used

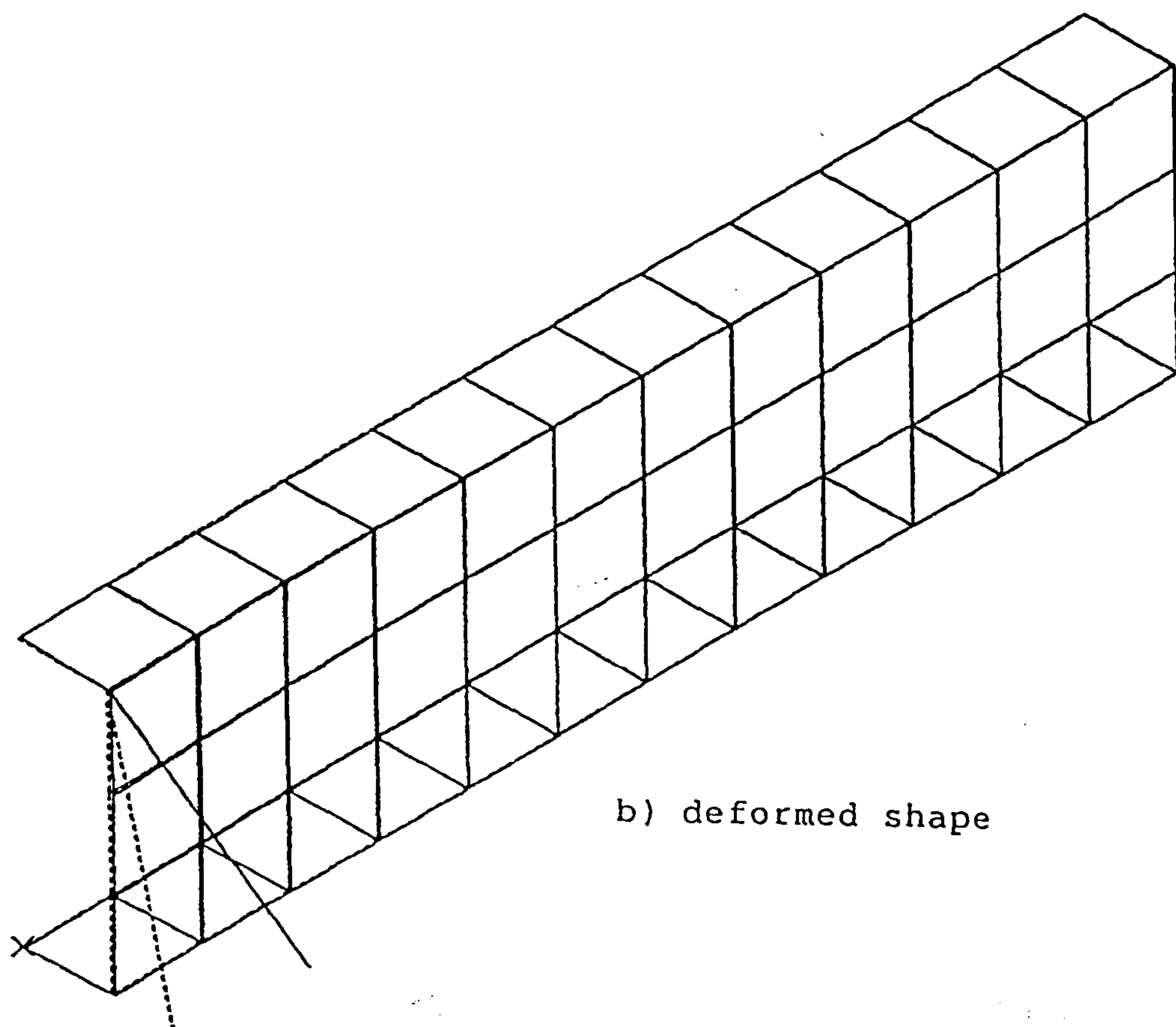
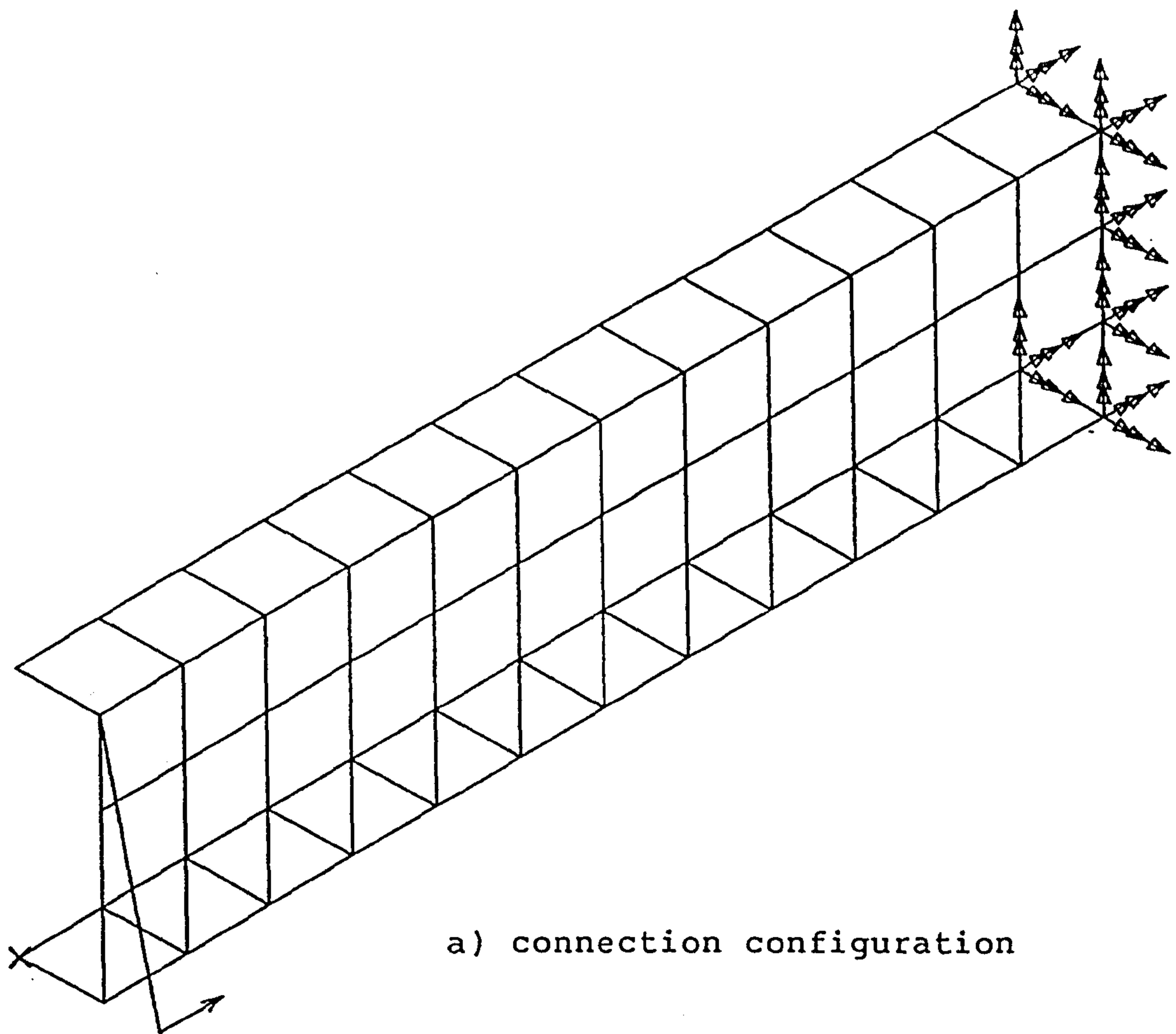


Fig.(6.3) Bimoment created due to longitudinal load

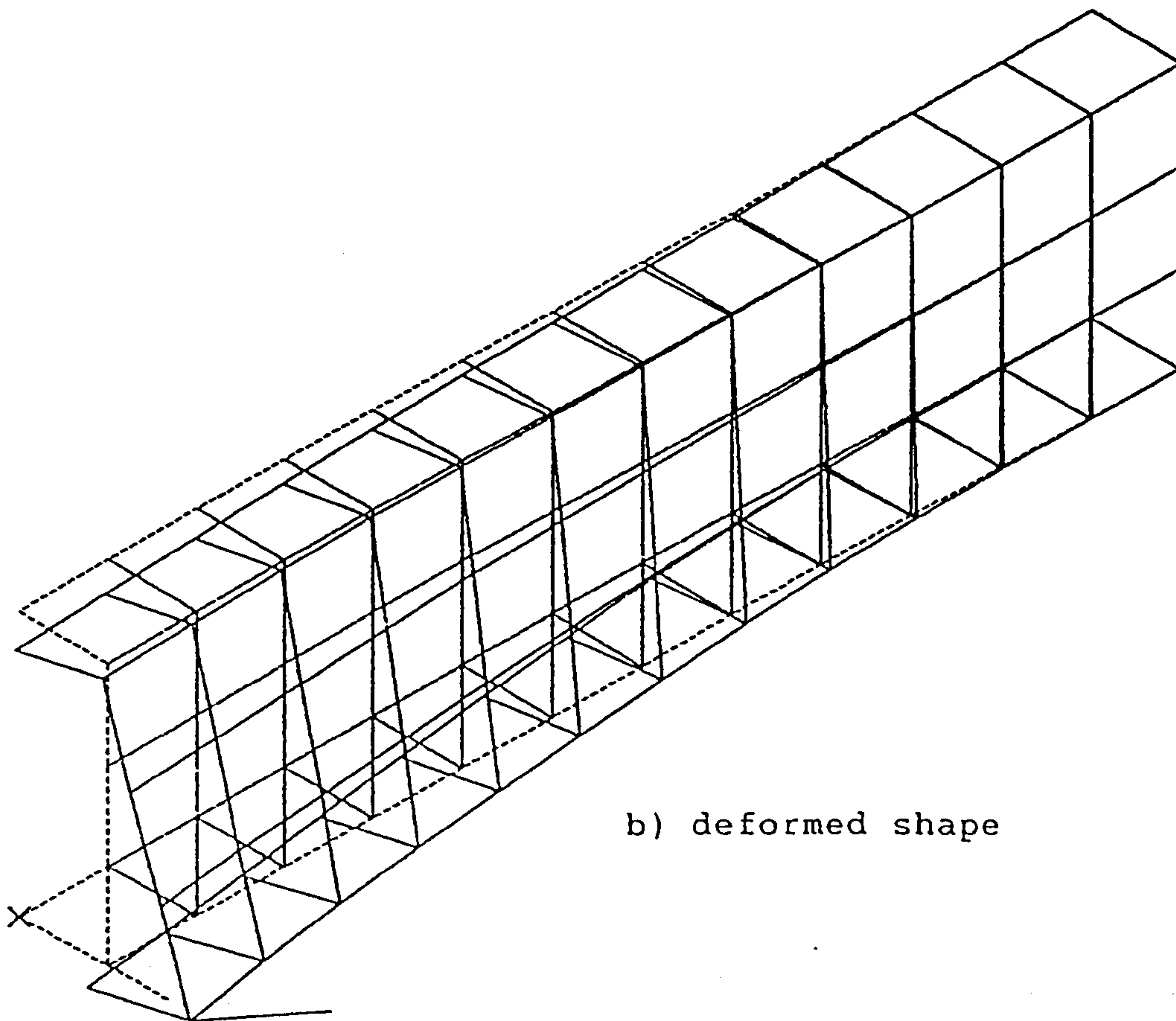
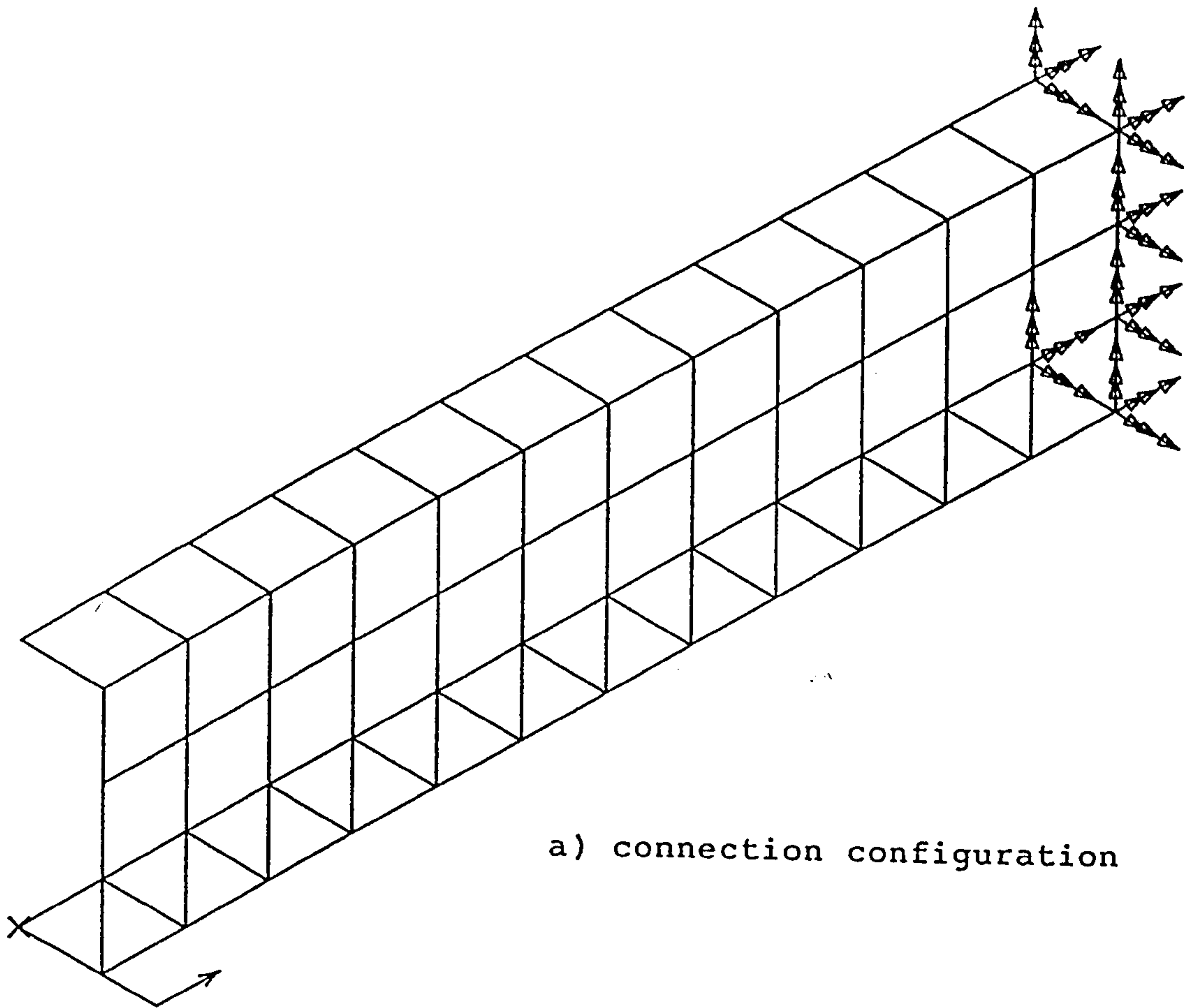


Fig.(6.4) Bimoment created due to longitudinal load

CHAPTER SEVEN

FINITE ELEMENT ANALYSIS

7.1 GENERAL

Modern engineering projects have become extremely complex, costly and subject to severe reliability and safety constraints. For a proper understanding analysts need mathematical models that can be used to simulate the design of the projects.

The finite element method has become one of the most popular of these methods. The method has successfully been applied to the solution of problems in linear and non-linear regions for one, two and three dimensional domains. It can easily handle discontinuous geometrical shapes as well as material discontinuities.

Finite element analysis is used to predict the effectiveness of design concepts of automotive chassis frames and body structures, and to evaluate the time and cost feasibility in early design stage, and to reduce and eliminate the development period and cost in accordance with the current trend of short life cycle of an automobile.

The finite element system used for this research work is known as I-DEAS supertab. This commercial software package is presently available on the Cranfield institute of Technology Computer Centre.

In this chapter a descriptions of the structural and finite element idealisation of isolated joints of a ladder frame subjected to pure torque are presented. Also presented is a finite element idealisation of complete laboratory chassis frame under longitudinal loads. The incorporation by the author of the theory described in the previous chapters, into a special finite element program which may be used in the preliminary stages of chassis design will be discussed in the next chapter.

7.2 FINITE ELEMENT SYSTEM

For this project, a static finite element analysis has been performed using the SDRC "Model solution" program to get the warping displacements and stresses at the joints and a complete chassis frame. The main characteristic of supertab is to use a wavefront solution algorithm and dynamic core allocation technique to minimise processing time and computer memory storage requirements. It was important, with

this project, that the elements were numbered so that the difference in number between adjacent element is as small as to enable the models produced to be run with the core storage available. More in depth information and theory of the I-DEAS system are given in references (42-43).

7.3 STRUCTURAL IDEALISATION OF A JOINT

A ladder chassis frame subjected to torsional or longitudinal loads exhibits an anti-symmetrical behaviour. This can be used to idealise an isolated joint of ladder frame and reduce the computing cost and time. In this section, a description of such an idealisation is given.

7.3.1 CROSS-MEMBER IDEALISATION

The cross member in a ladder chassis frame subjected to torsional or longitudinal loads may be treated as a beam whose ends are each partially restrained from warping by the side members. Half the cross member span can be considered since the warping is symmetrical about its mid-span and reaches its maximum value at mid-span. Therefore, half the cross member can be analysed, and its boundary conditions become;-

- i) one end of the cross member partially restrained from warping by the side member, and
- ii) the other end is free to warp (since the bimoment is zero at the mid point of the cross member).

7.3.2 SIDE-MEMBER IDEALISATION

It has been shown by Nuttall (20), that the bending in the side members is zero at mid-span approximately of each bay of a ladder chassis frame. This corresponds to a point of inflexion which can be modelled as a simple support. Therefore, the side member in a joint can be considered as a beam whose ends are free to warp, and which is simply supported.

7.4 FINITE ELEMENT IDEALISATION OF THE JOINTS

A finite element analysis of an isolated ladder chassis frame joint is performed to obtain the stiffness matrix of the joint elements described in chapter(5.3.4).

Figures (7.1/7.2) show the finite element idealisations of four joints whose dimensions were chosen such that they correspond to those being used to build the finite element chassis model shown in figure (7.15). As far as the joints were concerned, the following geometric characteristics were introduced.

- i) Joint No.(1), has a rectangular section cross member welded to the web of a channel section side member.
- ii) Joint No.(2), has a channel section cross member rivetted (with a plate used to reinforce the joint), using Huck bolts to the zero warping points in the flanges of a channel section side member.
- iii) Joint No.(3), has a channel section cross member rivetted using Huck bolts at the zero warping points in the flange of a channel section side member.
- iv) Joint No.(4), has a channel section cross member welded to the web of a channel section side member.

For the typical length of side members, (315-345)mm was chosen in such a way that it would not cause any undesirable effects to the joint (see figure 5.7). For the same reason, the side member was supported at the zero sectorial area, i.e zero warping points, of both flanges with a strong pin jointed bars which were mounted at the shear centre of the side member. Again the cross member was mounted at its shear centre by pin jointed bars connected to the zero warping points.

The main concern for the joint element stiffness is the warping displacements,

i.e, those along the longitudinal direction of the cross member. Therefore, to determine the joint element stiffness matrix by finite element calculation, the side member section passing through the centroid of the cross member section has to be fixed, as shown in figures (7.3/7.4).

For an accurate joint analysis, the ends of the beam elements and the boundaries of the joint element should be straight lines after deformation, as they represent the warped ends of the cross sections, and the shape of these cross sections should be undeformed.

The main characteristics of thin shell elements in I-DEAS supertab are that the linear thin shell four node element is formulated using classical thin shell equations and does not include shear deformation effects through the thickness. The formulation of parabolic and higher order thin shell elements includes bending and membrane behaviour as well as the effects of shear deformation.

Usually, for a straight-sided structure with a flat surface and constant thickness such as a channel section, a linear four node element can be an efficient choice (see reference 43). Therefore, the finite elements chosen for the joint analyses were thin shell four node quadrilateral linear elements for all of the members.

Beam elements could be attached normal to thin shell elements because, with respect to the nodal degrees of freedom, both elements were compatible with each other. Therefore, beam elements were used for the idealisation of Huck bolts between side members and cross members for joint(2) and joint(3).

Rod elements were connected to zero warping points of both ends of the side member and the free end of the cross member. These rod elements were mounted on the nodes lying on the shear centre line of each member. These elements were used rather than beam elements so as not to cause any other bending or torsional effects.

To fix the joints, the nodes which are at the shear centre lines of each member should be restrained corresponding to the three translational degrees of freedom.

The application of a tip torque to the free end of the idealised cross member can be introduced by applying shear forces along the flanges in opposite directions, i.e, to the nodes which coincided with the zero warping lines; so as not to cause any other force incorporation. The common value for the pure torque was $(300)N \times$ the height of the cross member section.

7.5 RESULTS FROM JOINT FINITE ELEMENT ANALYSIS

A finite element analysis was carried out on four typical isolated ladder chassis frame joints, three having a channel section cross-member, the other a closed section cross member. The material properties and dimensions of the members and their cross sections are given in table (7.1).

The deformed shape of the joints are shown in figures (7.5/7.6). The stress distributions due to partial warping inhibition at the connections along the longitudinal axes of the cross member and the side member are shown in figures (7.7/7.8/7.9/7.10). It is clear from these figures that the stress build-up in the cross member towards the connection is due to the bimoment created according to warping inhibition.

Once all the warping displacements and the transmitted bimoments at the node boundaries were obtained by finite element analysis, the change in the rate of twist at the node boundaries of the joint element of each joint can be calculated. The transferred bimoment can be obtained either from the reaction forces on the restrained plane in the side member (see figure 7.4), or from the ratio of the partial warping displacement to the free warping displacement (W_p/W_f) at the attached end of the side member. Values obtained from both these methods agreed closely. Hence the joint element stiffness matrix of each joint can be obtained as will be shown in later.

In the process of this project, as far as the joint element stiffness is concerned, the most important item was how to get a proper distribution of warping displacements, and obtaining the transferred bimoments which are reacted at the joint element boundaries. Values of mid-plane warping displacements round the cross member section at the partially built-in end ($x=0$) were determined for each joint.

The results are presented in figure (7.11) for the joints having a closed section cross member. The corresponding values for the joints having channel section cross members are presented in figures (7.12/7.13/7.14).

As mentioned in the previous chapters, the warping restraint factor (K) is defined as the ratio of area enclosed by the profile of partial warping displacements to that of free warping displacements.

Therefore, using equation (2-17), the warping restraint factor (K), can be obtained as follows;-

$$K = \frac{W_p}{W_f} \quad \text{-----} \quad (7-1)$$

Where (W_p) is partial warping displacement of the cross section,
 (W_f) is free warping displacement of the cross section.

It has been shown that the finite element values of warping factors at the partially built-in end are in close agreement with the theoretical values and the measured values have been shown in references (20,22).

Again from the same equation (2-17), by knowing the sectorial area (ω_s) of any point on the cross section and its partial warping displacements, the rate of twist at one joint element boundary can be calculated as follows;-

$$\theta' = \frac{W_p}{K \omega_s} \quad \text{-----} \quad (7-2)$$

The other boundary of the joint element is fixed along the longitudinal axis of the side member, i.e, the rate of twist at that boundary is zero. The transferred bimoments can be obtained at the boundary from the reaction forces around the cross section.

Hence, equation (7-2) can be combined with equation (5-11), to obtain the joint element stiffness coefficient due to the rate of twist stiffness as follows;-

$$K_{\theta} = - \frac{B W_p}{K \omega_s} \quad \text{-----} \quad (7-3)$$

The warping restraint factor (K), as well as the rate of twist joint element stiffness of each joint are also given in table (7.1).

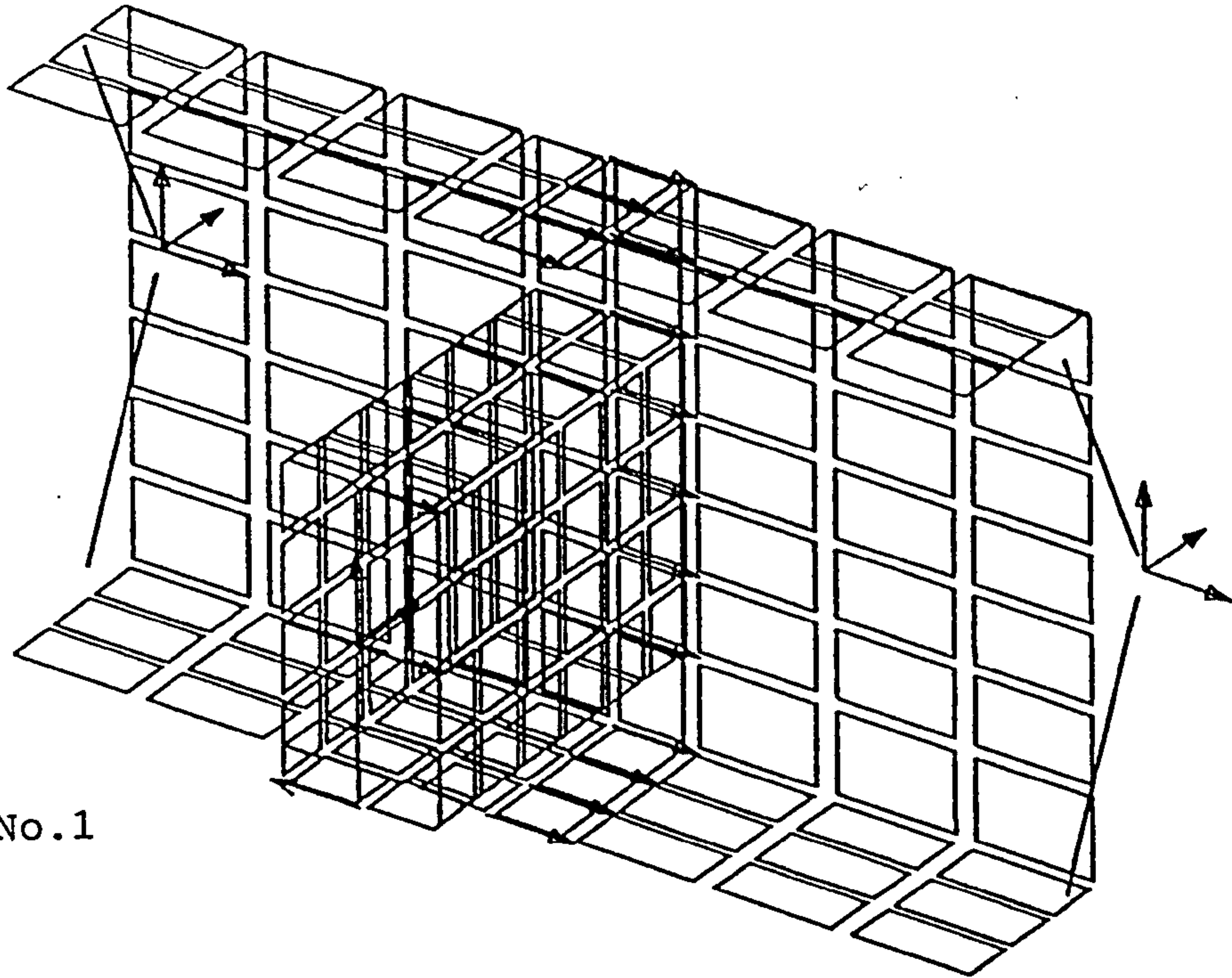
7.6 FINITE ELEMENT IDEALISATION OF A COMPLETE CHASSIS FRAME

A finite element analysis of a complete ladder chassis frame was performed. The dimensions of the model chassis frame, shown in figure (7.15), were chosen such that they correspond to those being used for experimental chassis frame shown in plate (9.1). Consequently, the same finite element types, and beam elements used to idealise the joints (discussed in section 7.4), are used in this idealisation.

The model chassis frame was supported with four supports, and appropriate restraints and boundary conditions were used. These were chosen to match an experimental validation discussed later. Three load-cases with the longitudinal load in different positions relative to the shear centre, and hence applying different bimoment, are considered as shown in figures (7.16/7.17/7.18). The load cases and loading positions are described in detail in section (9.6) of chapter (9), page (127), and they are shown in figure (8.4), page (119).

The common value for the longitudinal load applied was (10) KN. The deformed shapes of all cases, and the longitudinal stress distribution along the side members of the chassis frame due to the longitudinal loads applied in position (2), i.e, position where the longitudinal loads produces bimoment are shown in figures (7.19/7.20/7.21). The results of the complete chassis finite element analysis are discussed and compared with other results in chapter (9).

a) Joint No.1



→ = applied force
 → = translational restraint

b) Joint No.2

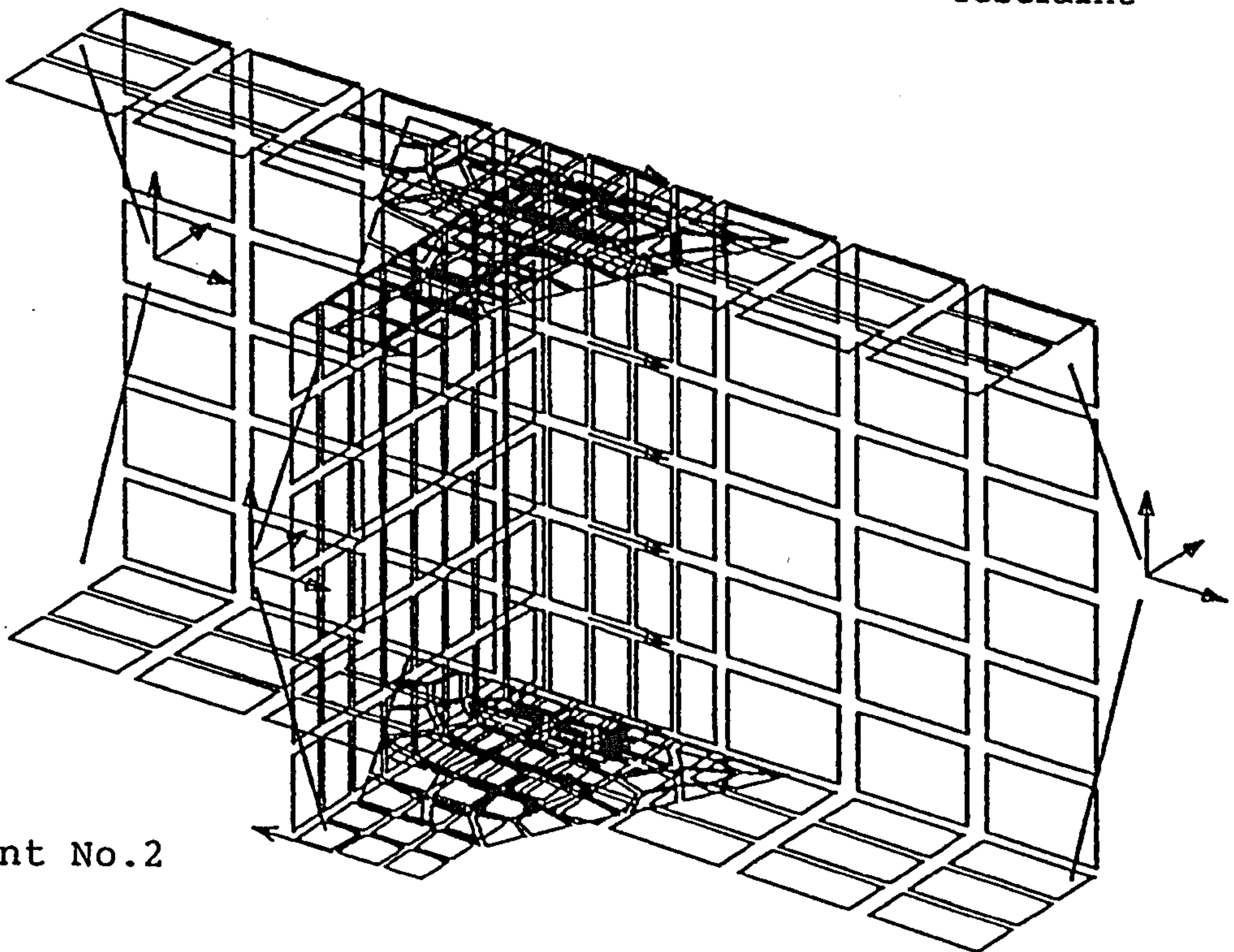
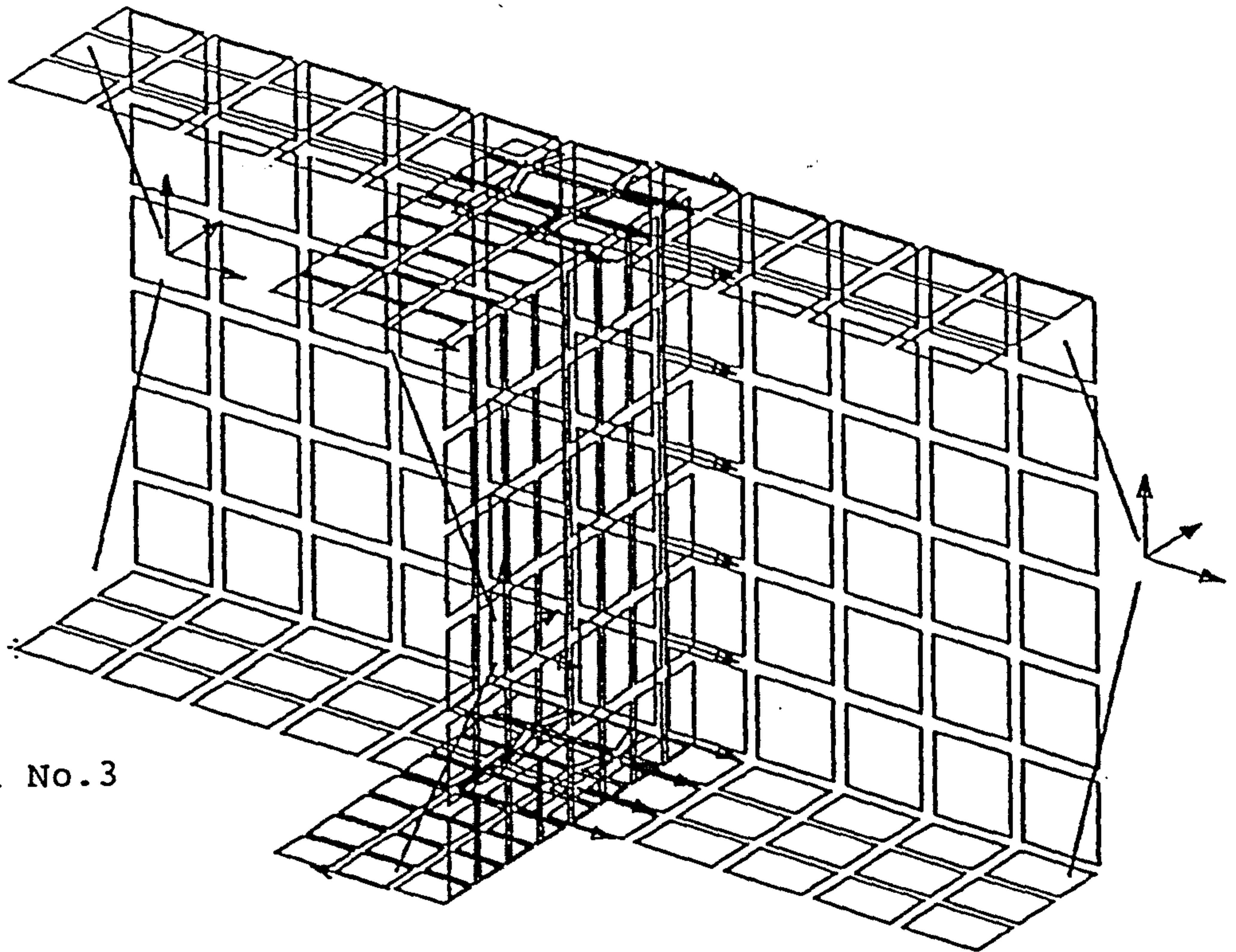


Fig.(7.1) Finite element idealisation of joints type 1 & 2

a) Joint No.3



→ = applied force
→ = translational restraint

b) Joint No.4

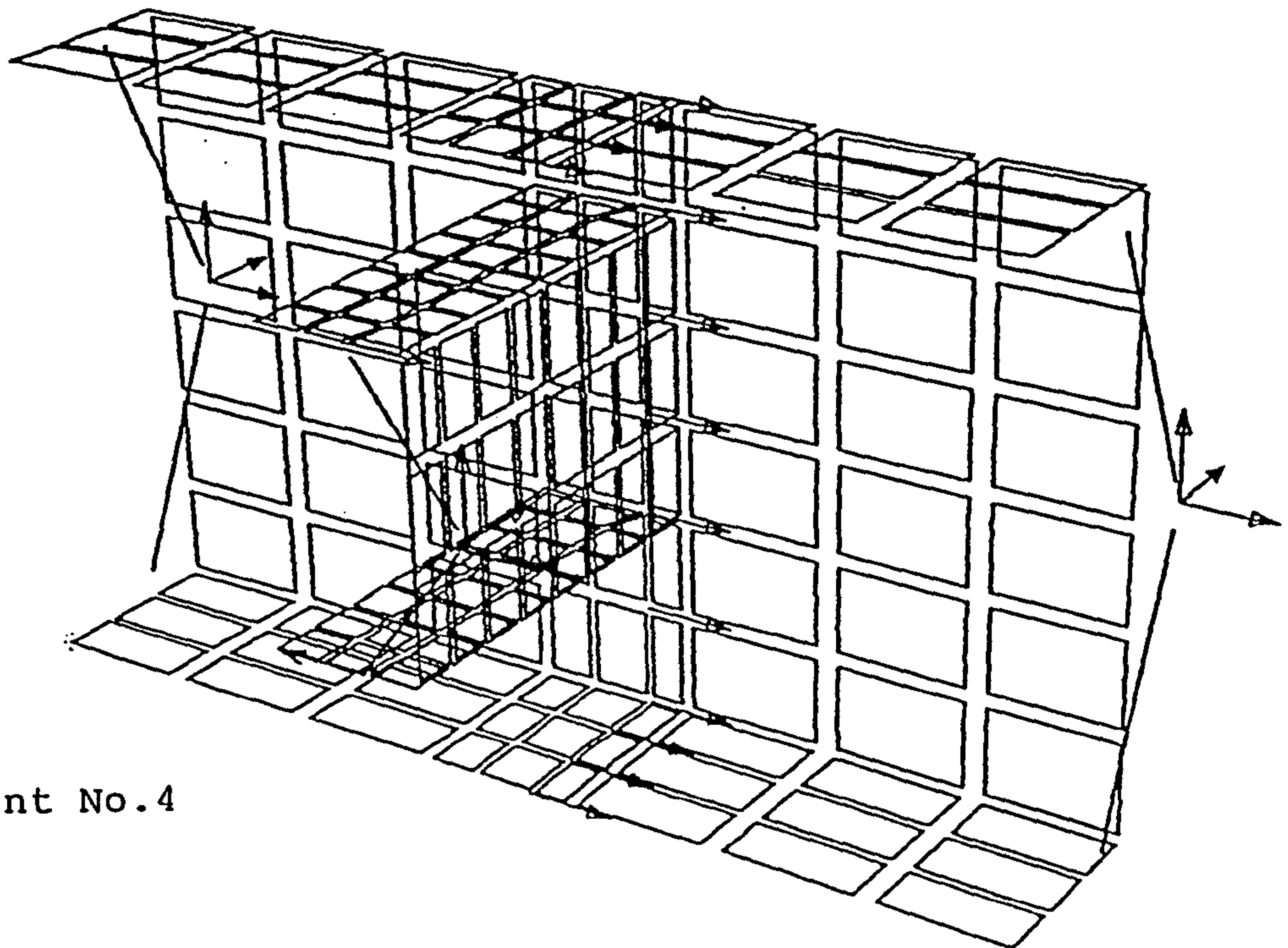


Fig.(7.2) Finite element idealisation of joints type 3 & 4

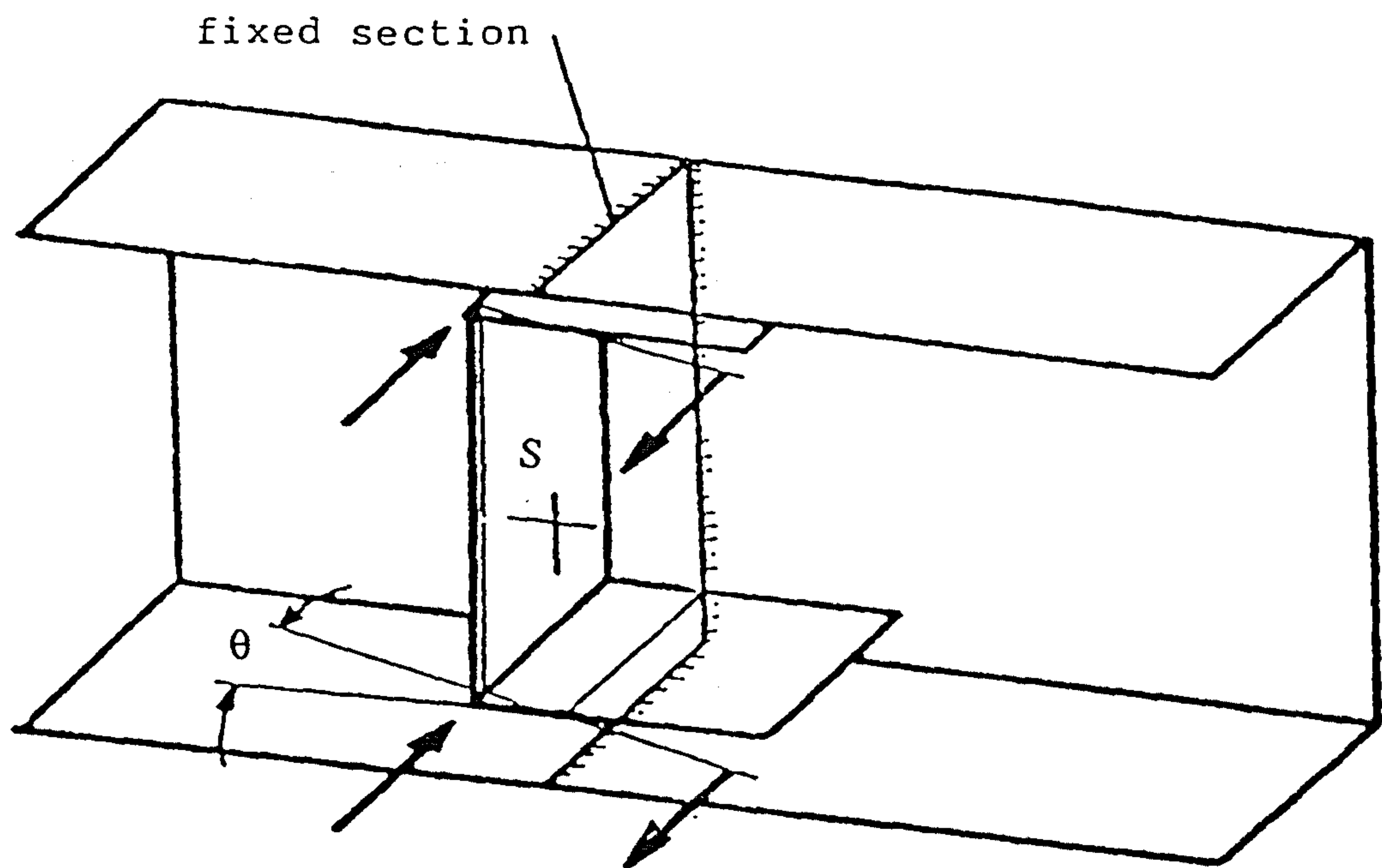


Fig.(7.3) Displacements due to bending flexibility

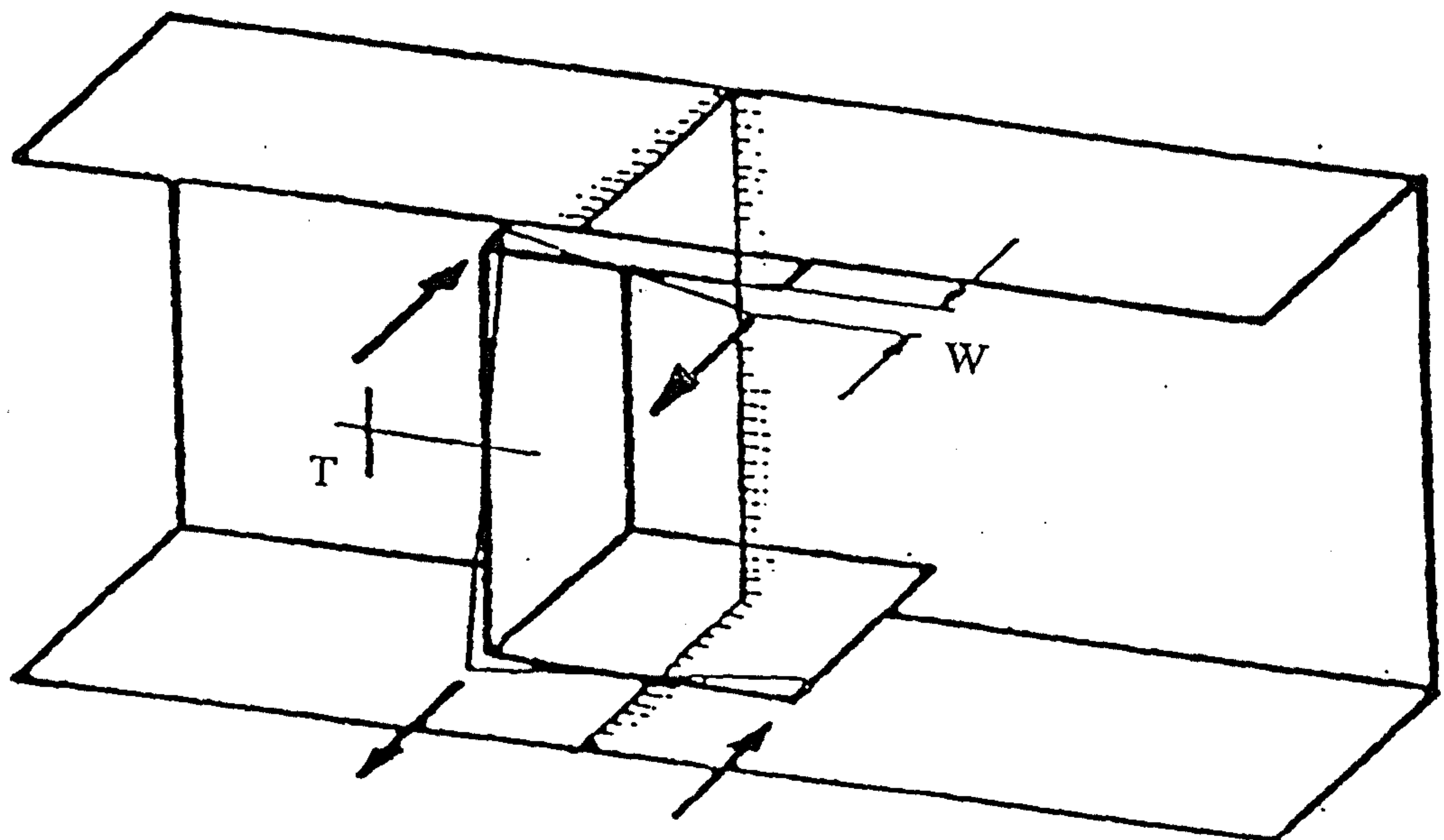
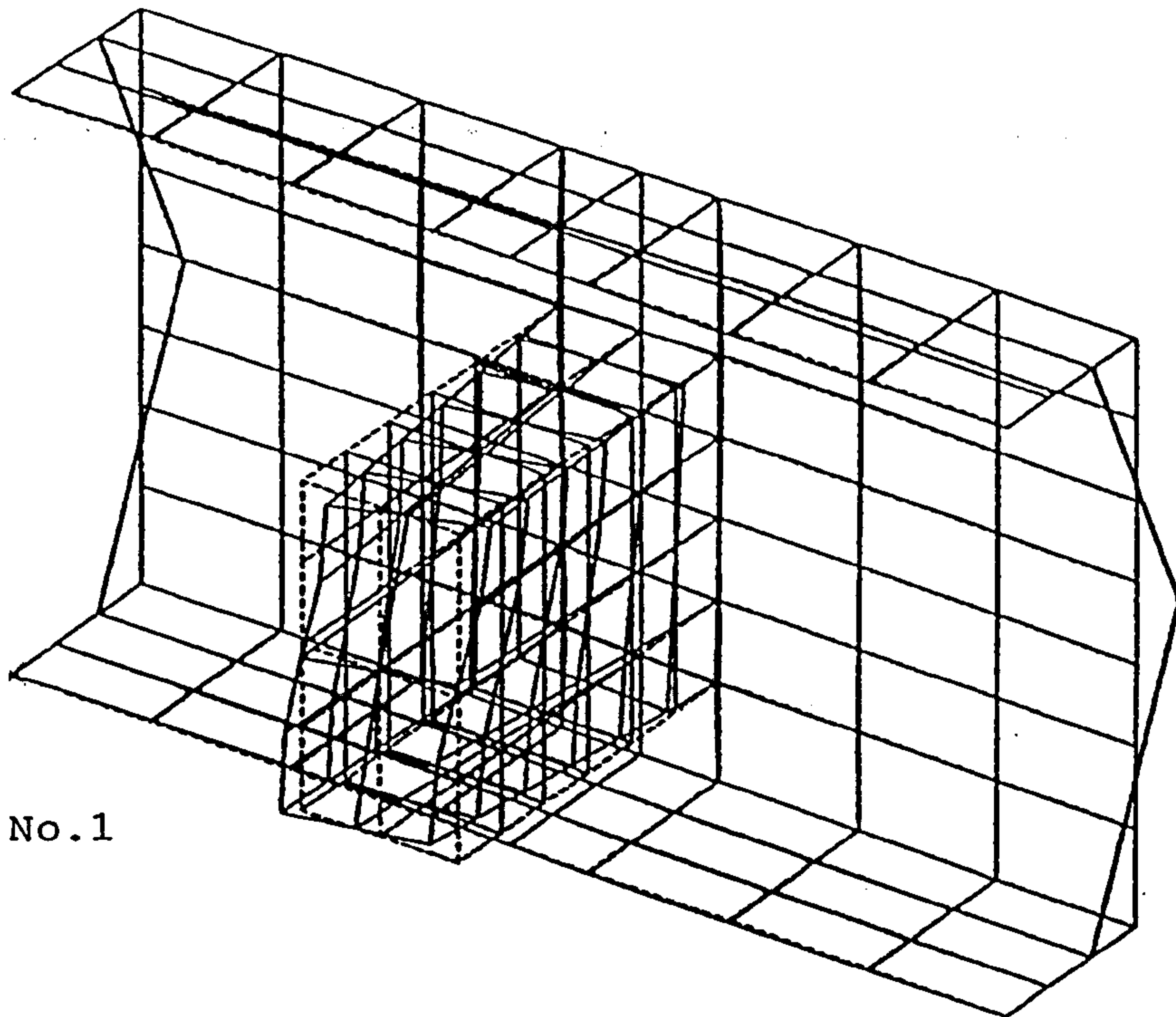


Fig.(7.4) Displacements due to rate of twist flexibility

a) Joint No.1



b) Joint No.2

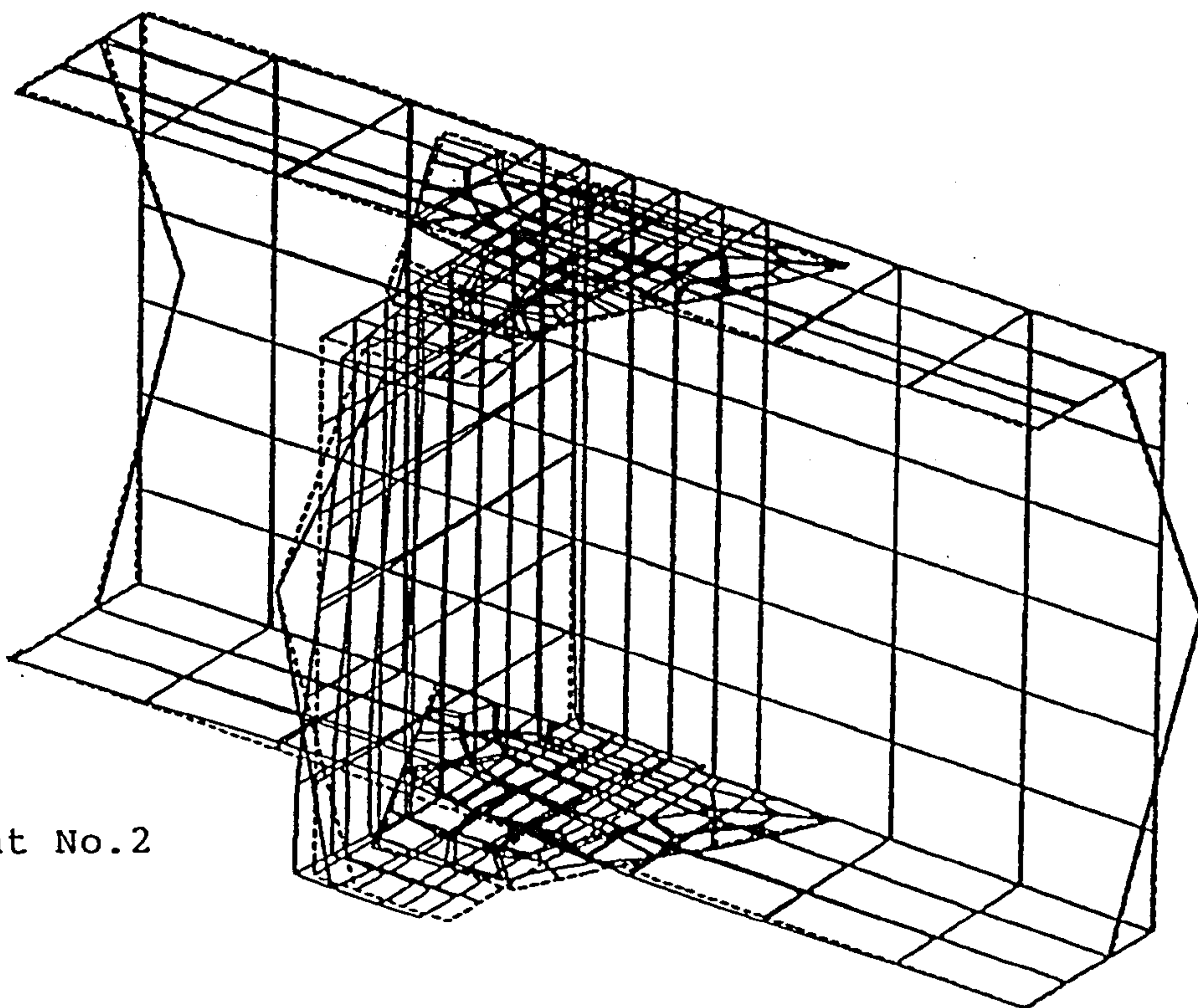
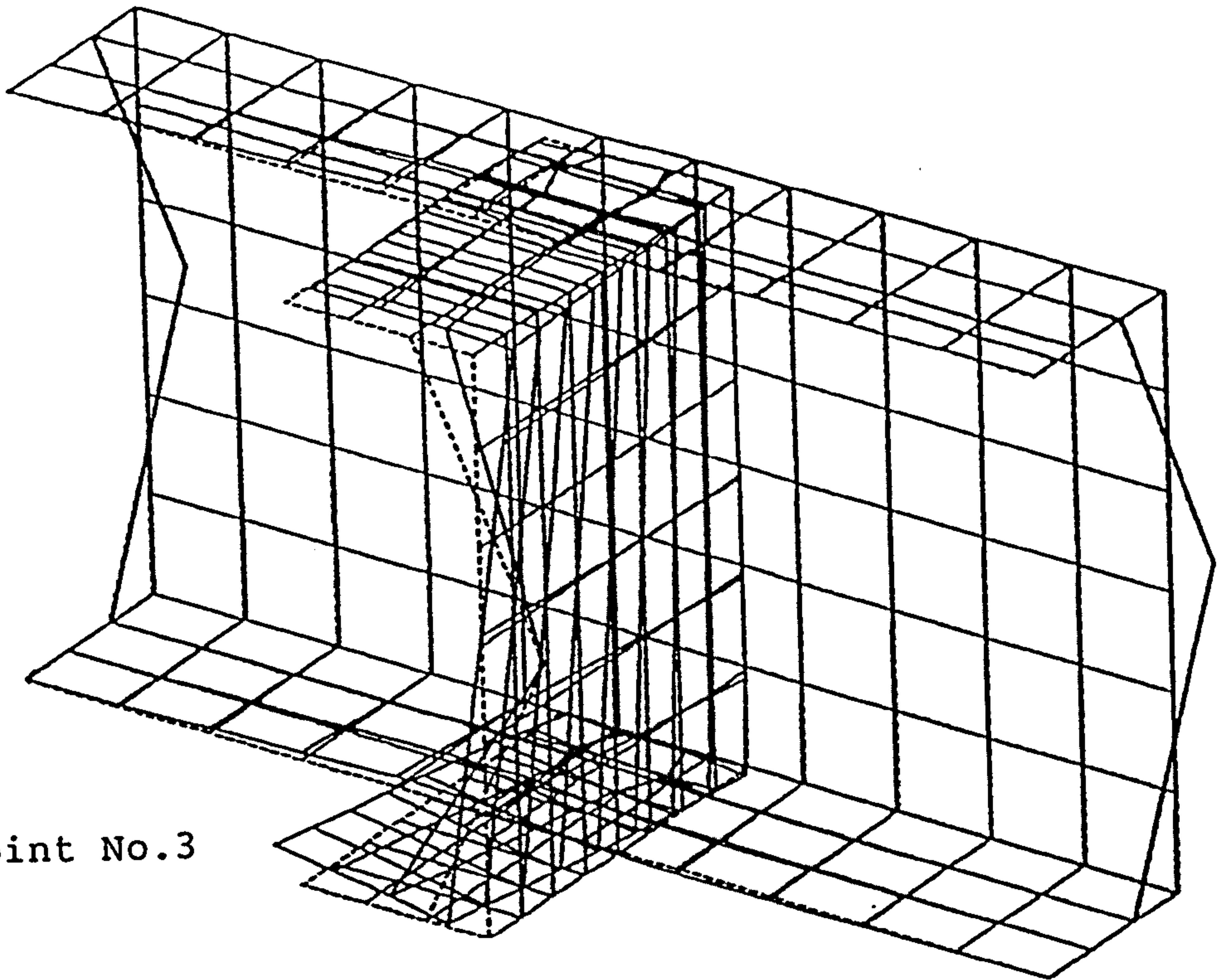


Fig.(7.5) Joint deformations

a) Joint No.3



b) Joint No.4

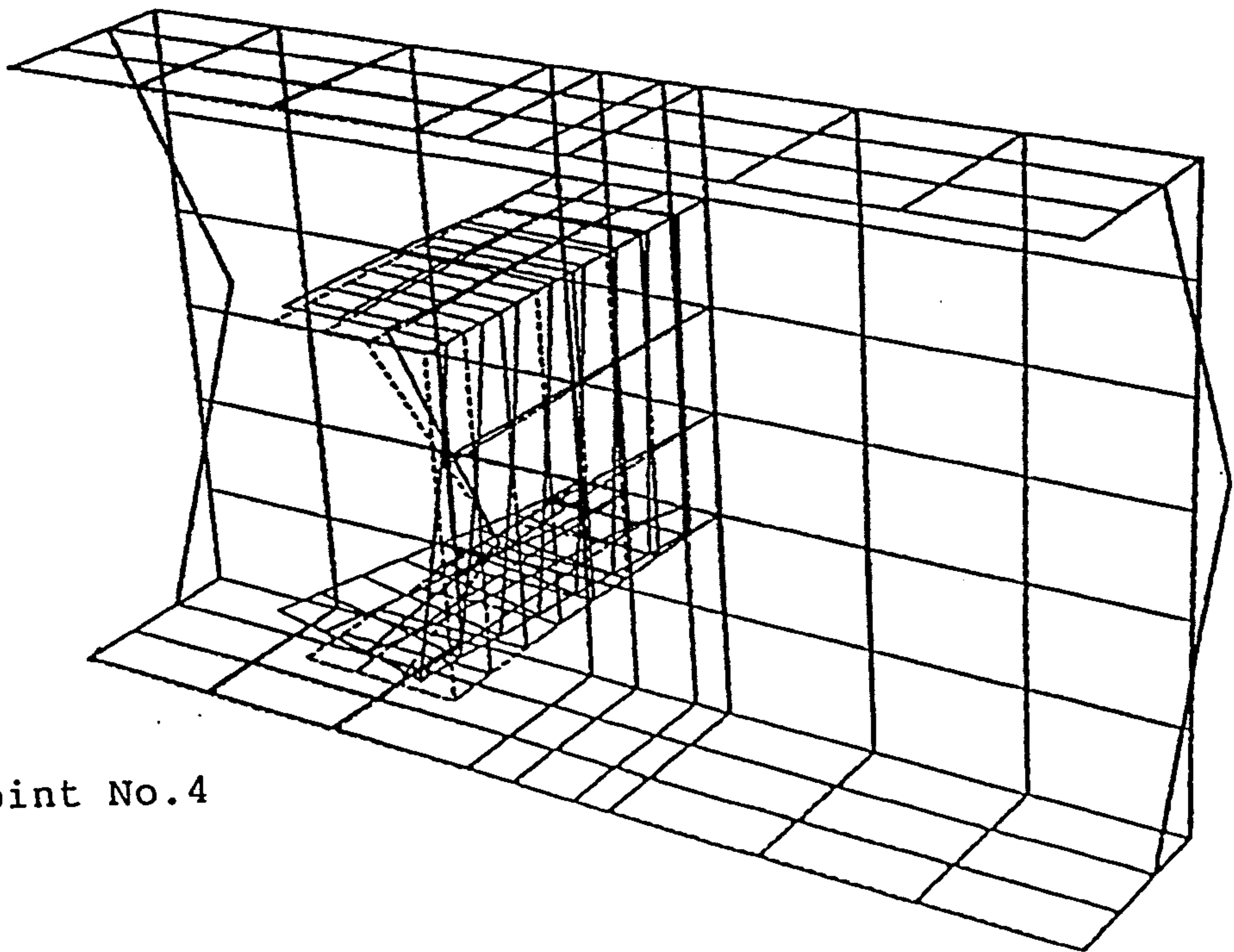


Fig.(7.6) Joint deformations

JOINT1

side member

STRESS - X MIN:-19999.98 MAX: 19999.97

19999.97

16923.05

13846.13

10769.22

7692.30

4615.38

1538.46

-1538.46

-4615.38

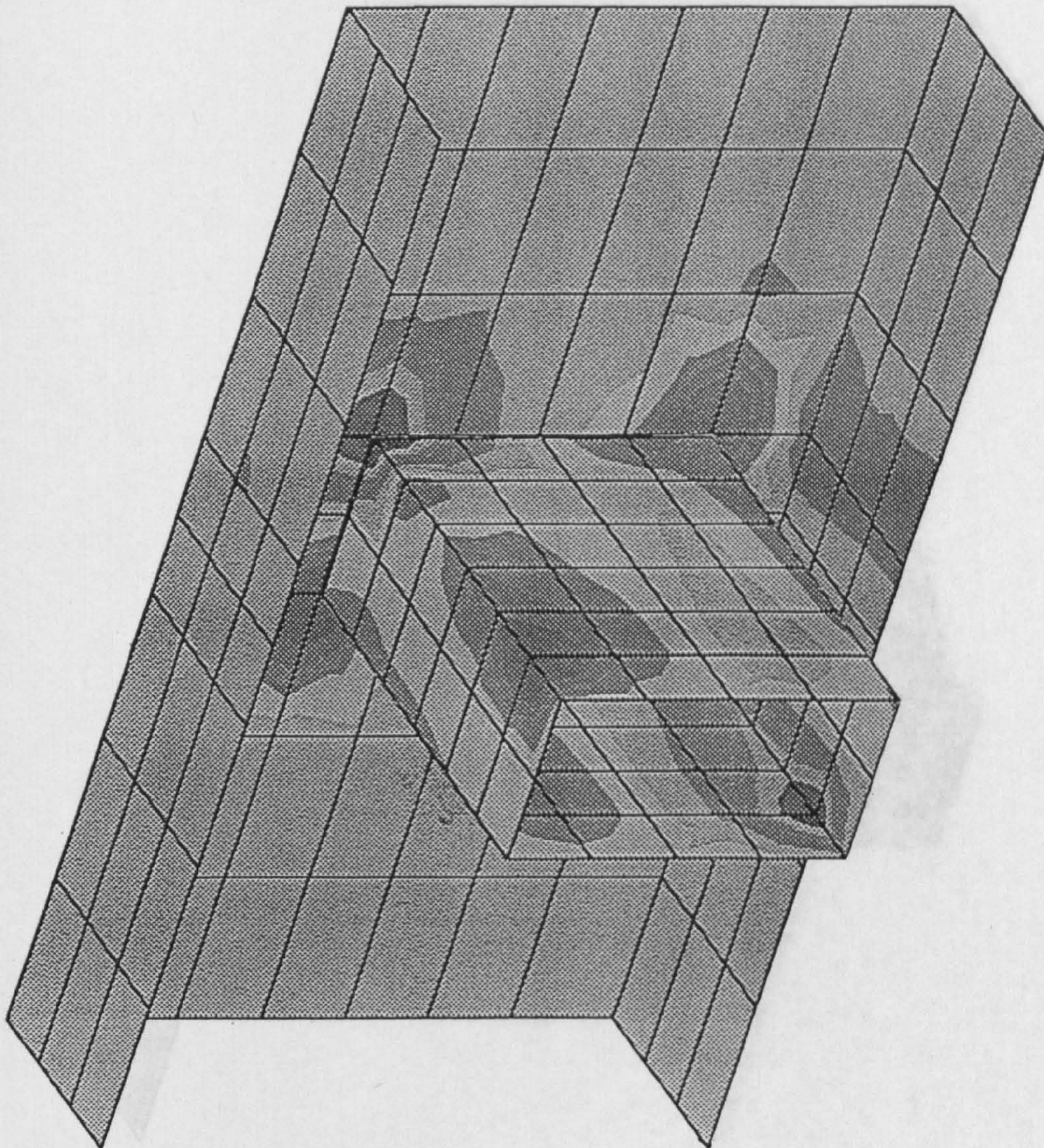
-7692.30

-10769.22

-13846.14

-16923.06

-19999.98



cross member

STRESS - Y MIN:-18565.81 MAX: 14568.55

14568.55

12019.76

9470.96

6922.16

4373.36

1824.57

-724.23

-3273.03

-5821.83

-8370.62

-10919.42

-13468.22

-16017.02

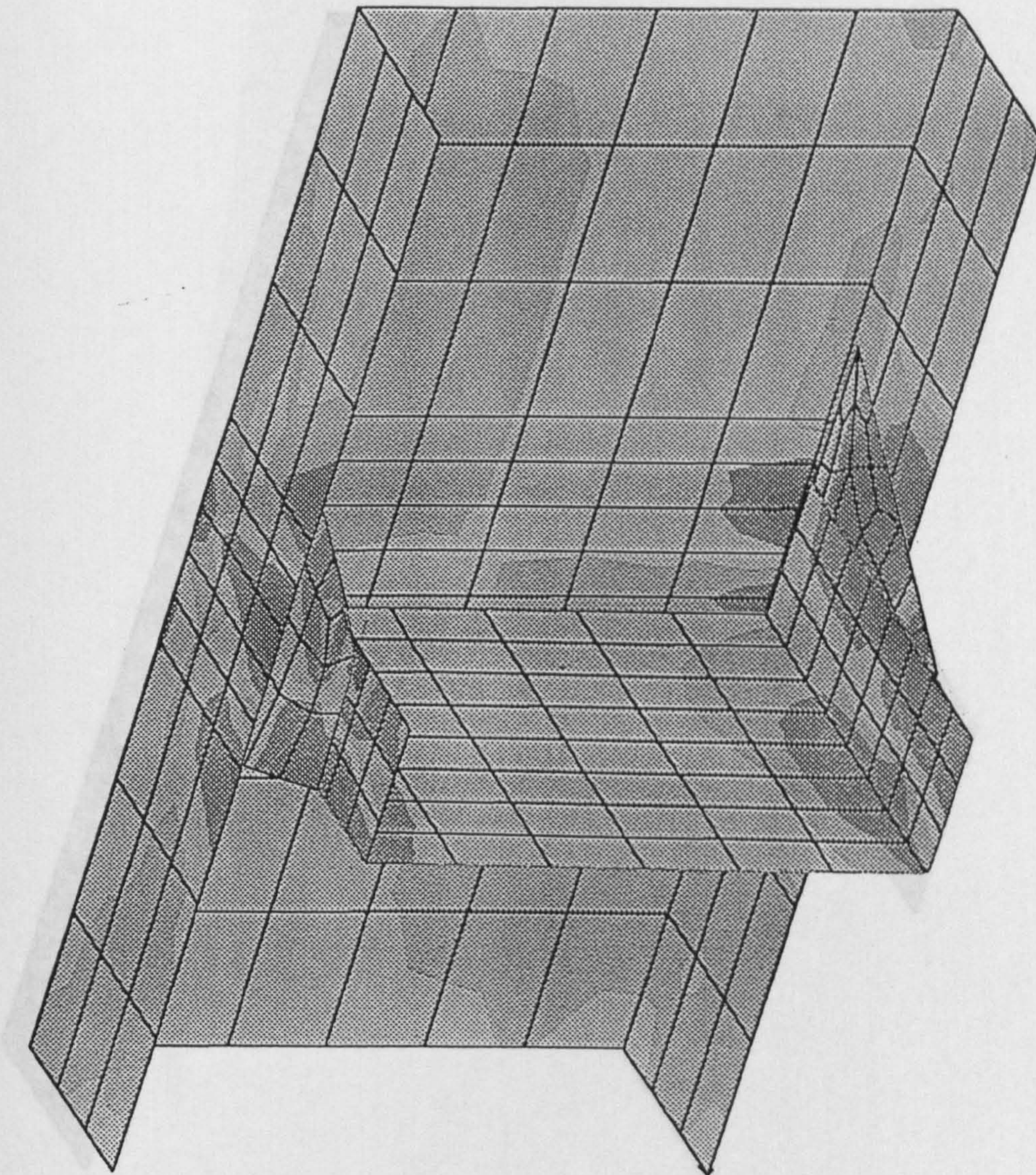
-18565.81

Fig.(7.7) Stress distribution due to partial warping inhibition at joint No.1

side member

STRESS - X MIN:-5461.92 MAX: 4646.26

4646.26
3868.71
3091.15
2313.60
1536.05
758.50
-19.06
-796.61
-1574.16
-2351.71
-3129.27
-3906.82
-4684.37
-5461.92



JONT2

cross member

STRESS - Y MIN:-16110.40 MAX: 12561.85

12561.85
10356.30
8150.74
5945.18
3739.62
1534.07
-671.49
-2877.05
-5082.61
-7288.16
-9493.72
-11699.28
-13904.84
-16110.40

Fig.(7.8) Stress distribution due to partial warping inhibition at joint No.2

JONT3

side member

STRESS - Y MIN:-20222.41 MAX: 20981.01

20981.01

17811.51

14642.02

11472.53

8303.03

5133.54

1964.05

-1205.45

-4374.94

-7544.43

-10713.93

-13883.42

-17052.91

-20222.41

STRESS - X MIN:-8294.38 MAX: 11668.57

11668.57

10132.95

8597.34

7061.73

5526.12

3990.51

2454.90

919.29

-616.32

-2151.94

-3687.55

-5223.16

-6758.77

-8294.38

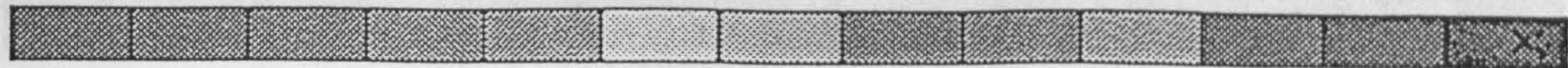
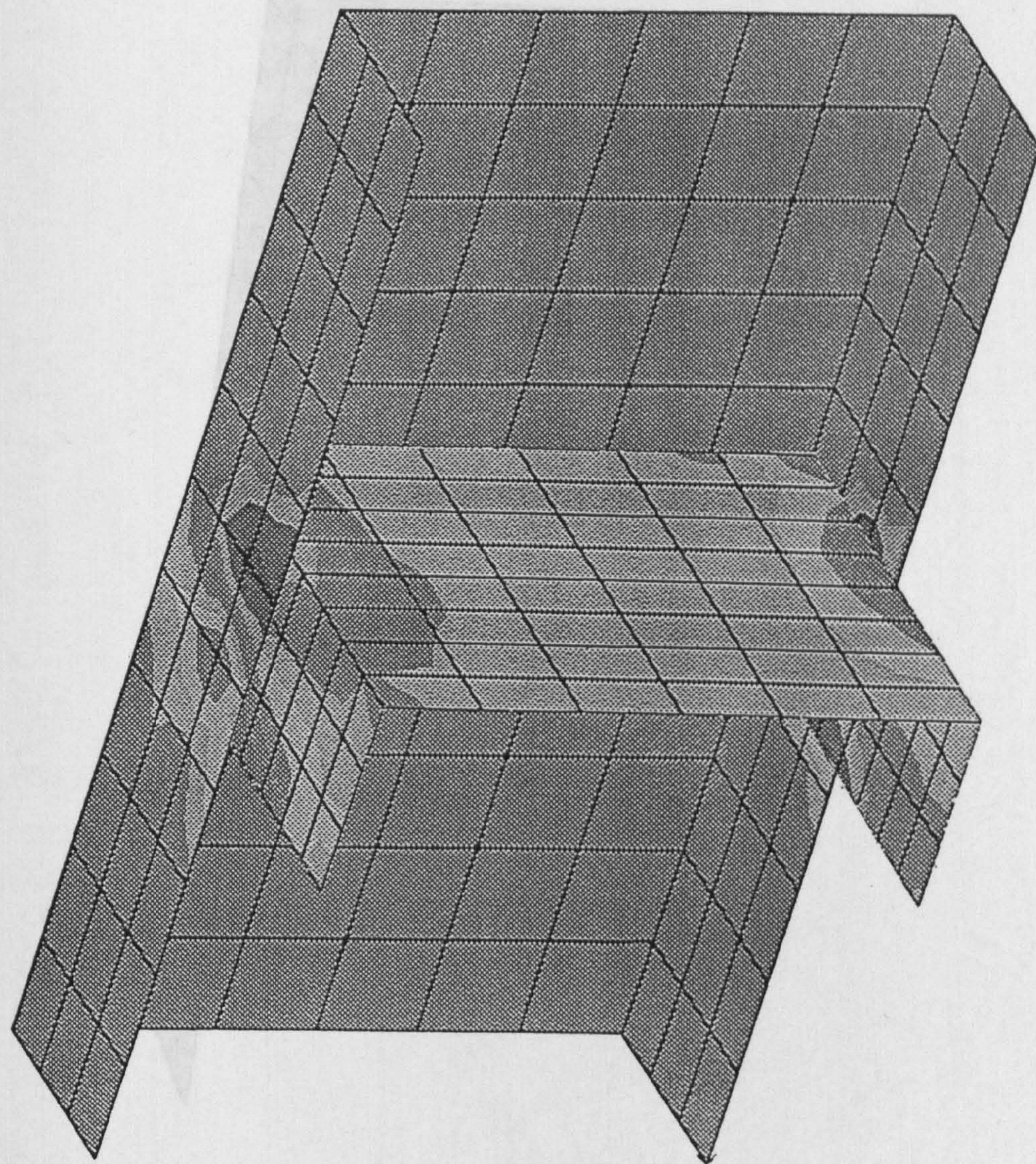


Fig.(7.9) Stress distribution due to partial warping inhibition at joint No.3

side member

STRESS - X MIN:-95323.69 MAX: 99741.30

99741.30

84736.30

69731.30

54726.31

39721.31

24716.31

9711.30

-5293.70

-20298.69

-35303.69

-50308.69

-65313.69

-80318.69

-95323.69

JONT4

cross member

STRESS - Y MIN:-126E+05 MAX: 66583.89

66583.89

51736.19

36888.49

22040.78

7193.07

-7654.63

-22502.34

-37350.04

-52197.75

-67045.46

-81893.16

-96740.87

-112E+05

-126E+05

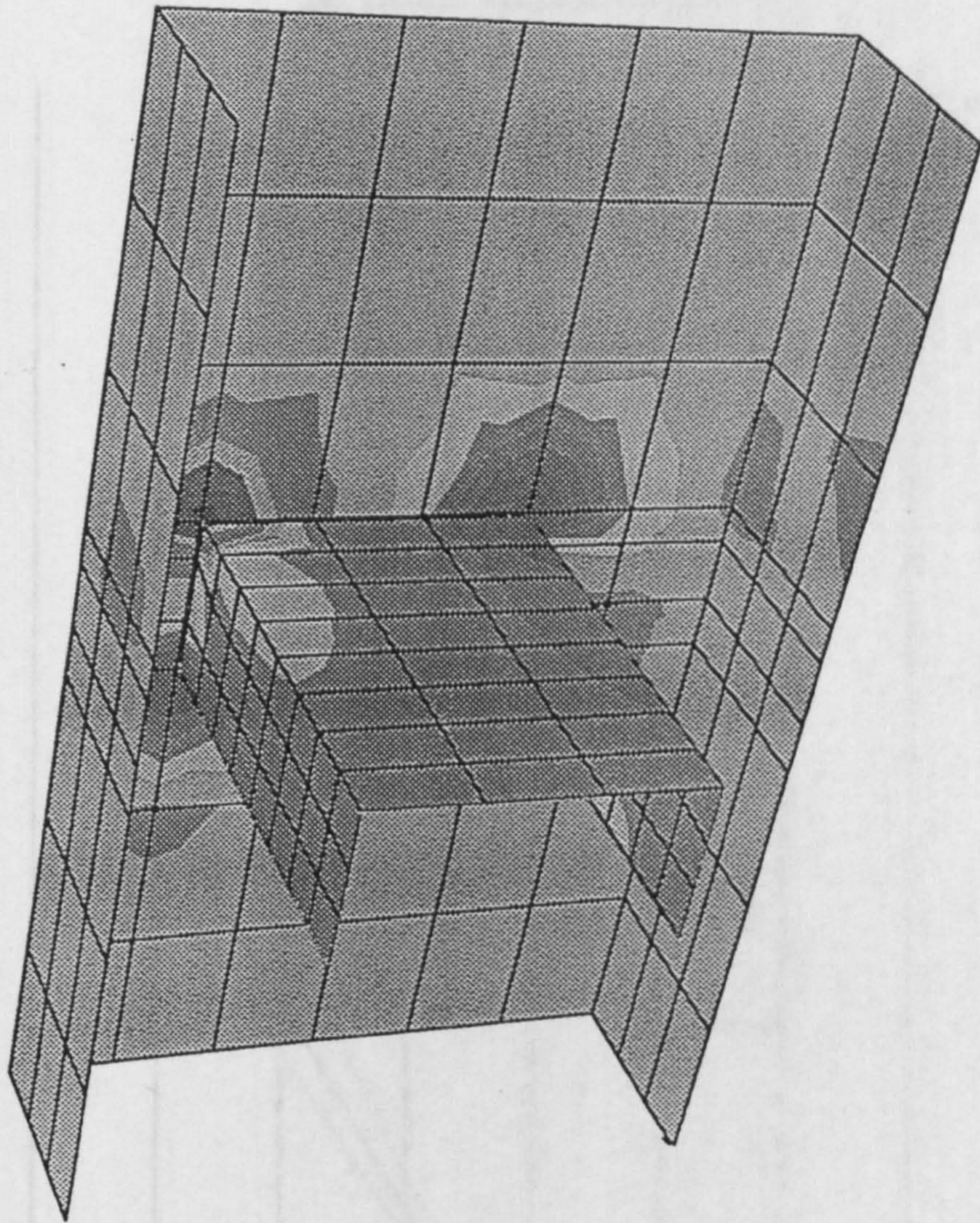


Fig.(7.10) Stress distribution due to partial warping inhibition at joint No.4

Z

Fig.(7.11) Warping displacements for joint No.1

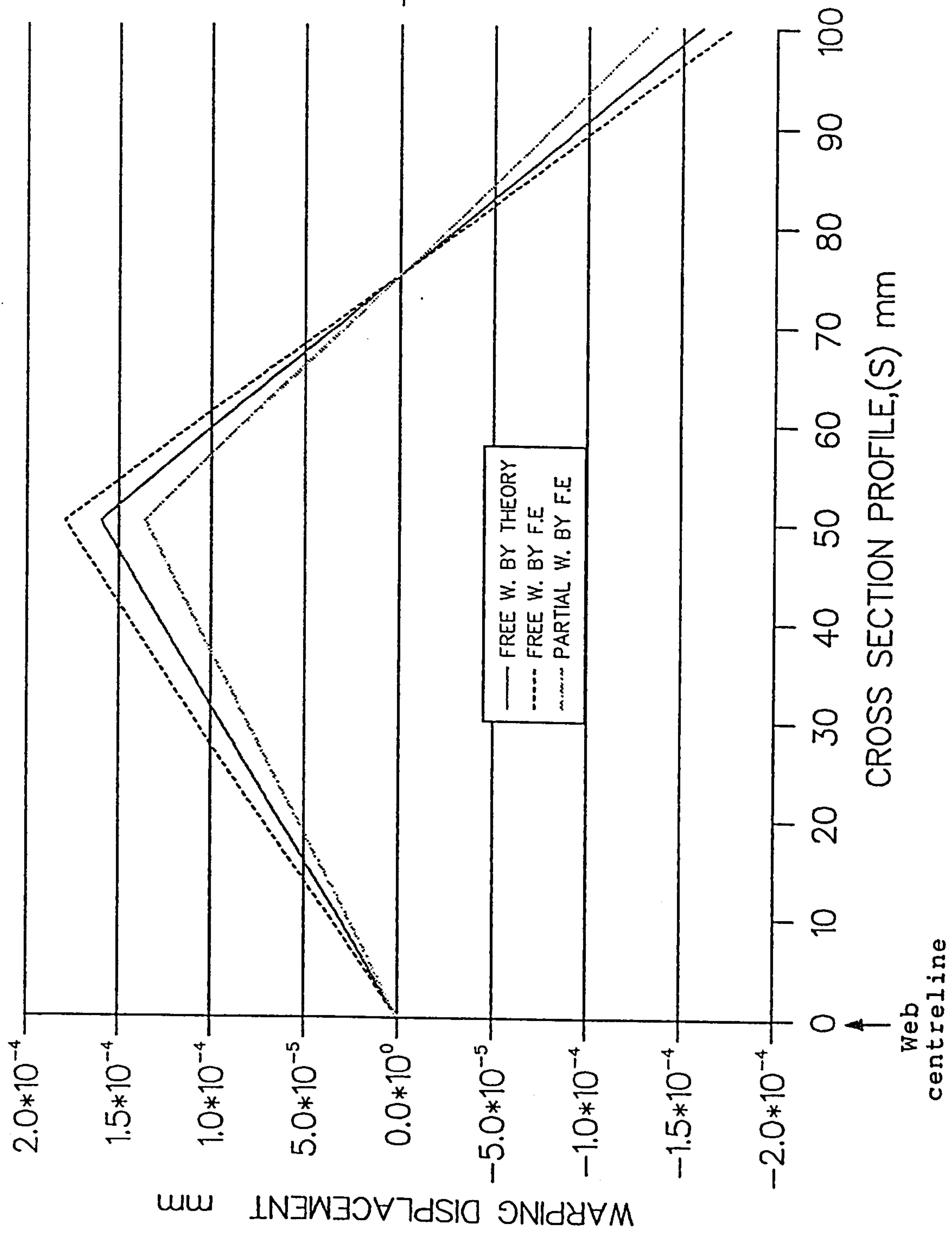


Fig.(7.12) Warping displacements for joint No.2

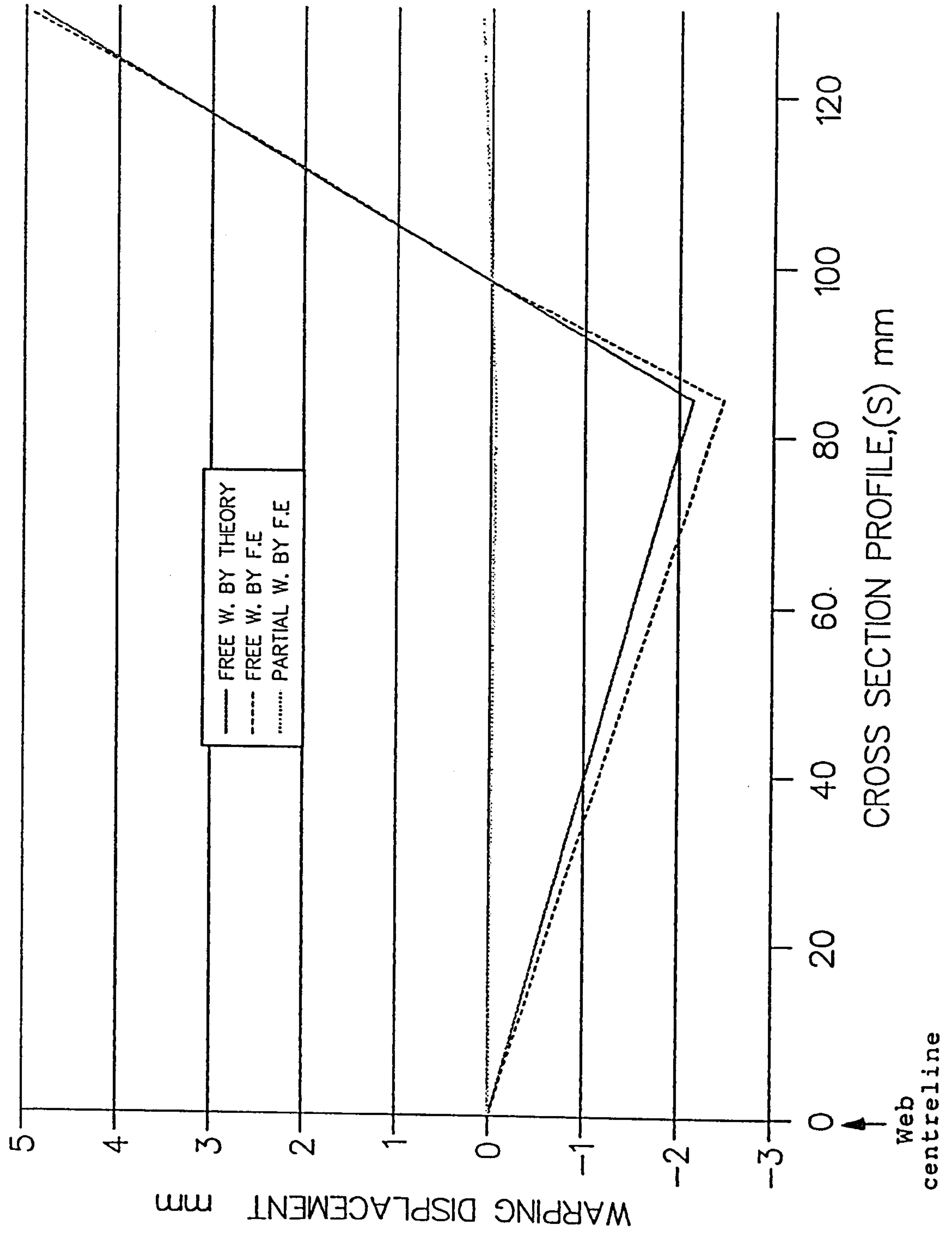


Fig. (7.13) Warping displacements for joint No.3

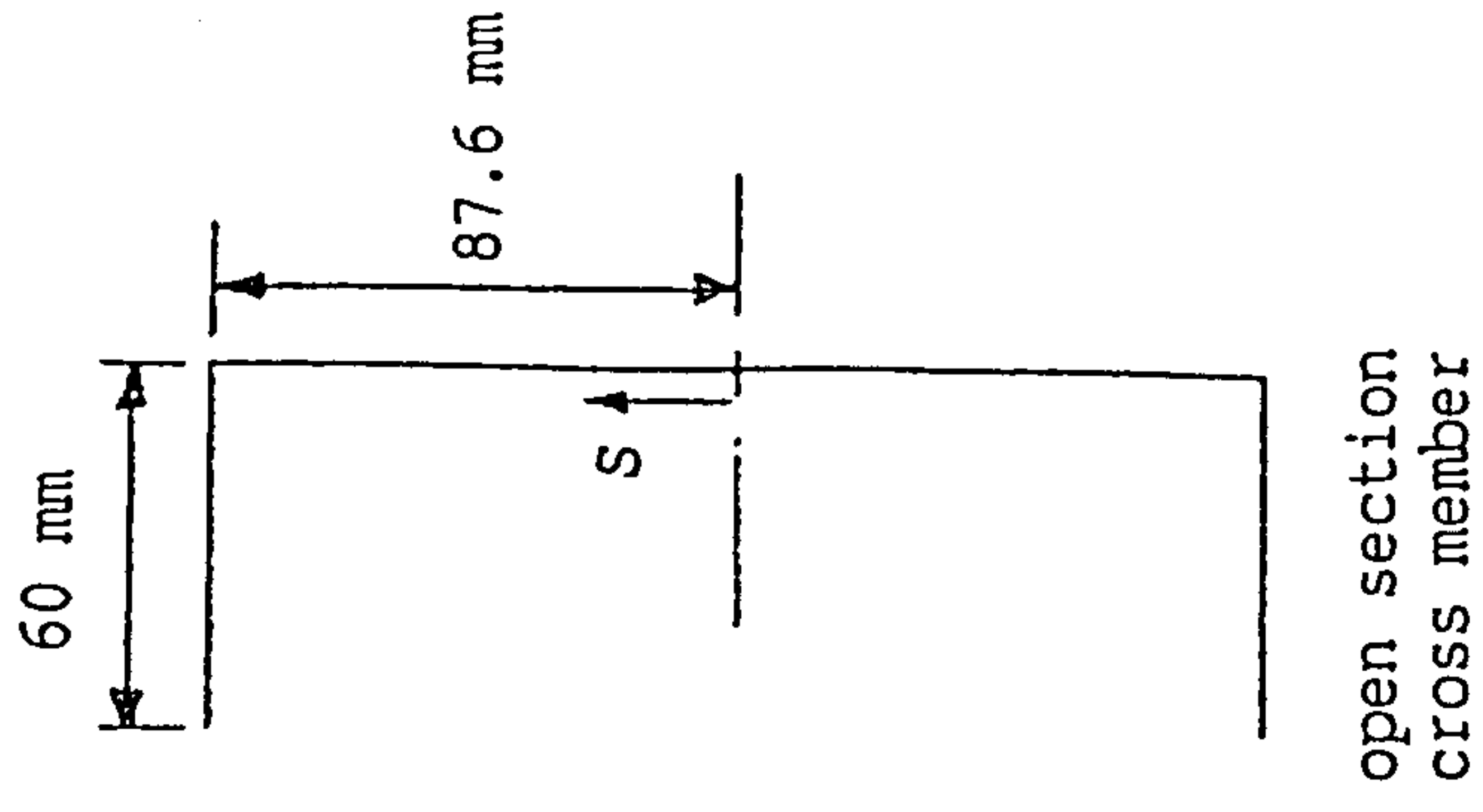
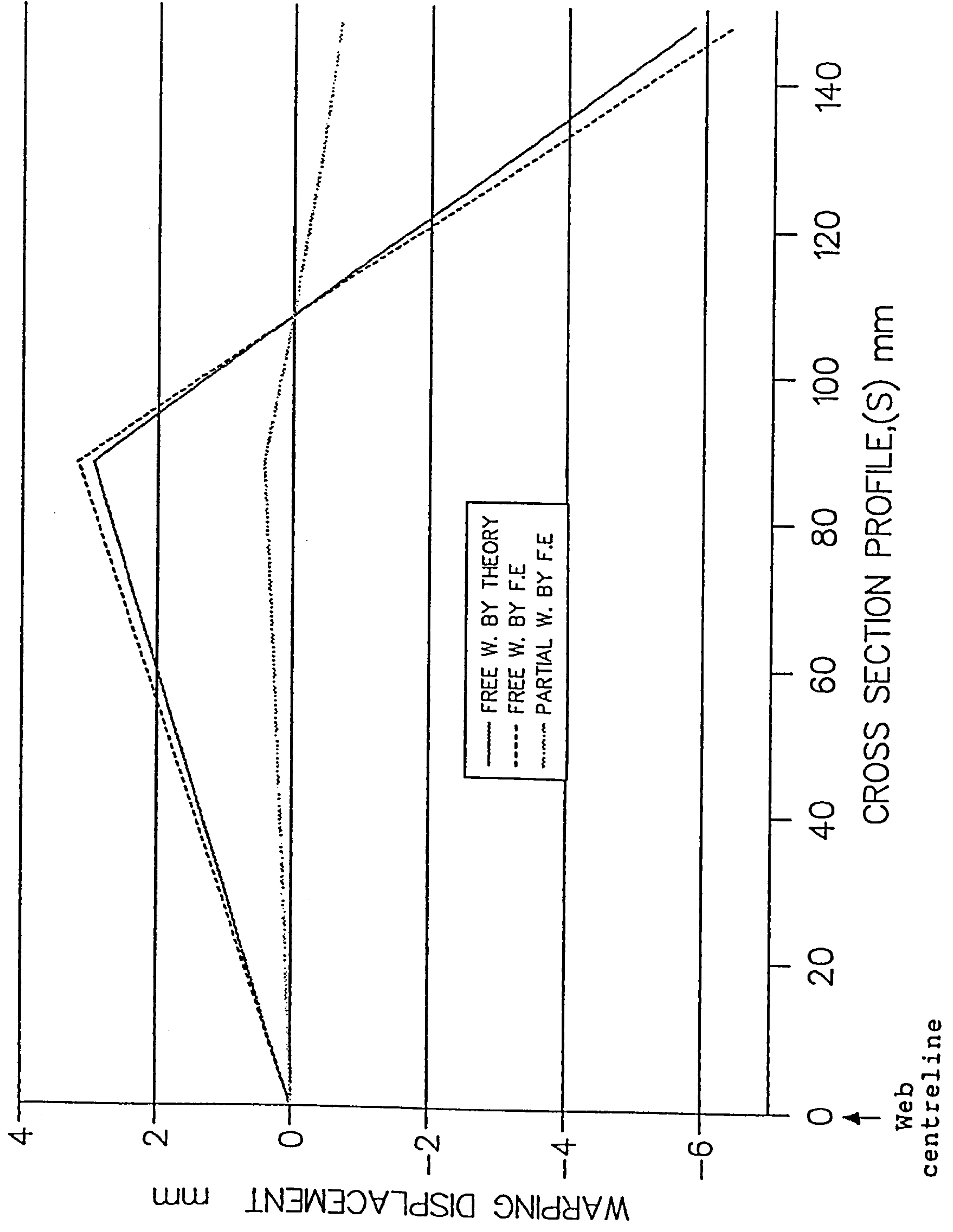
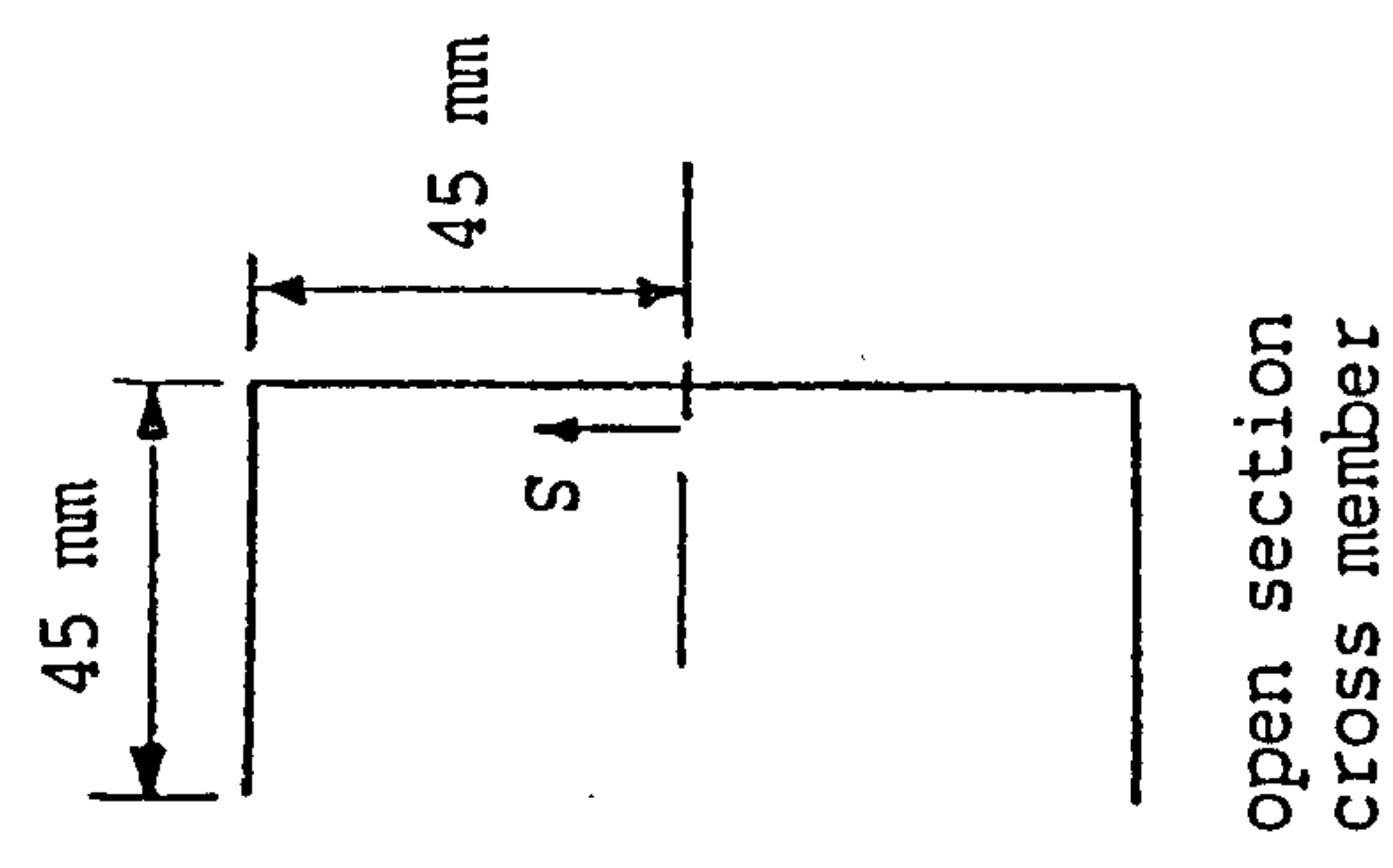
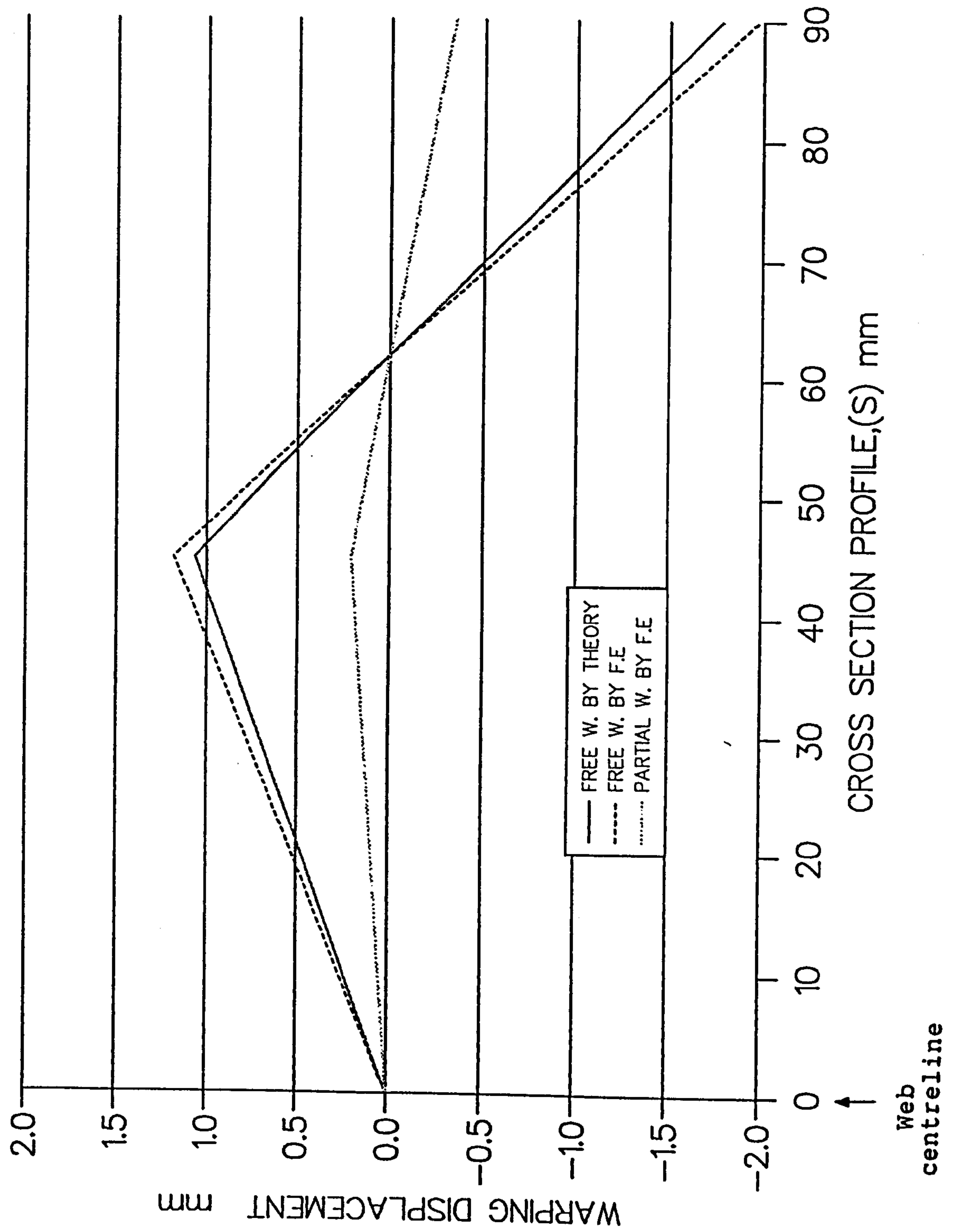
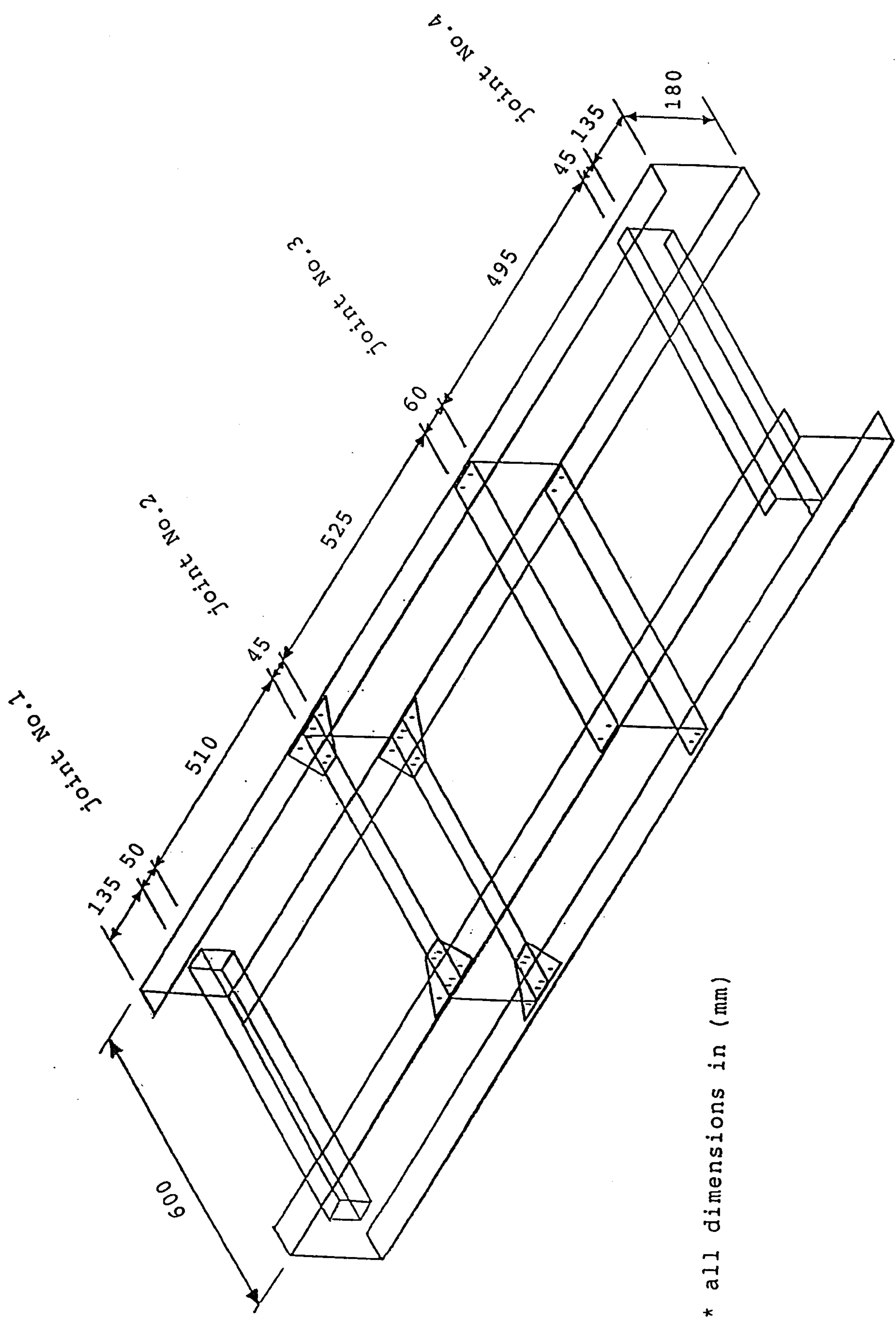


Fig.(7.14) Warping displacements for joint No.4





* all dimensions in (mm)

Fig.(7.15) Ladder chassis frame used for F.E. analysis and experimental tests

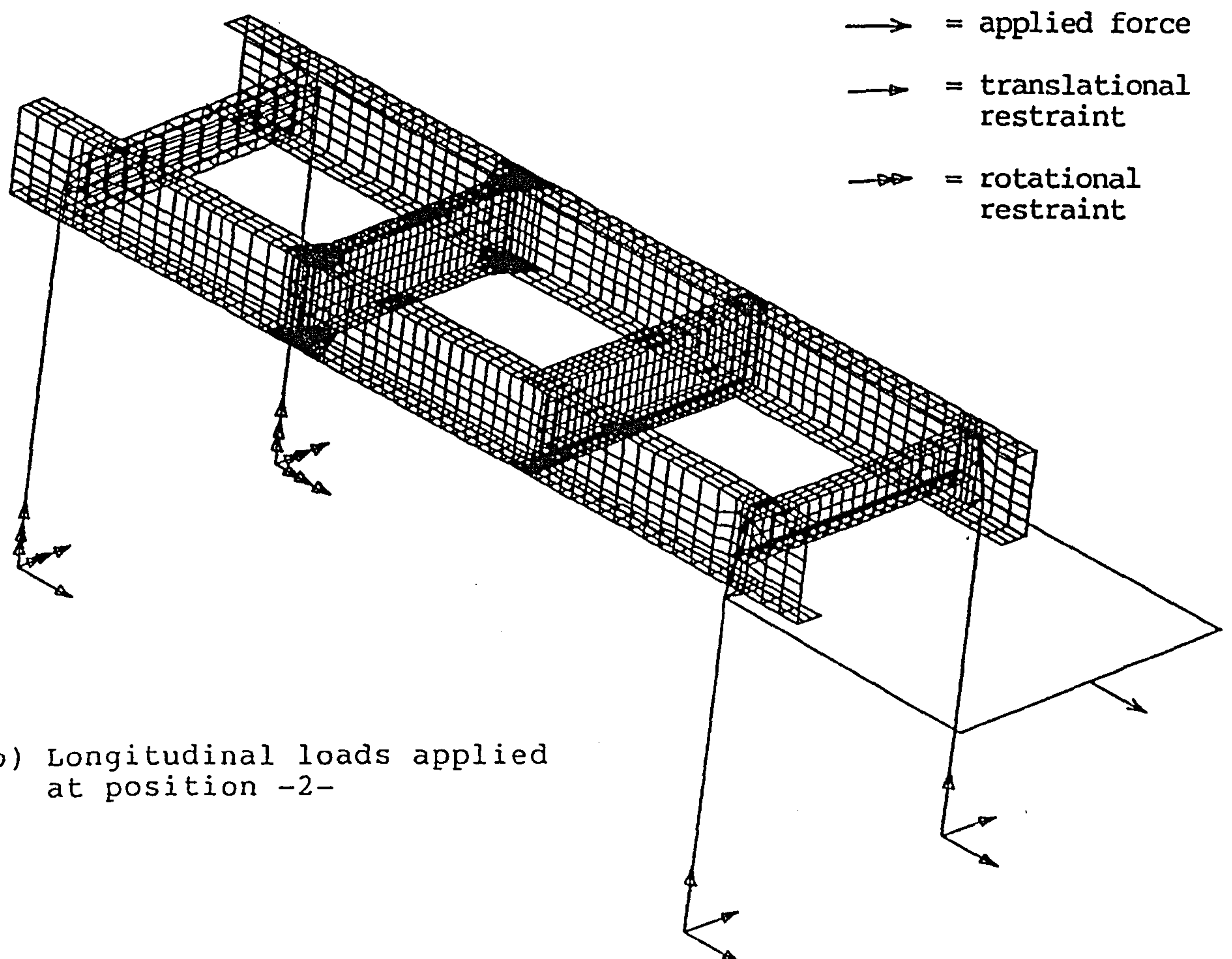
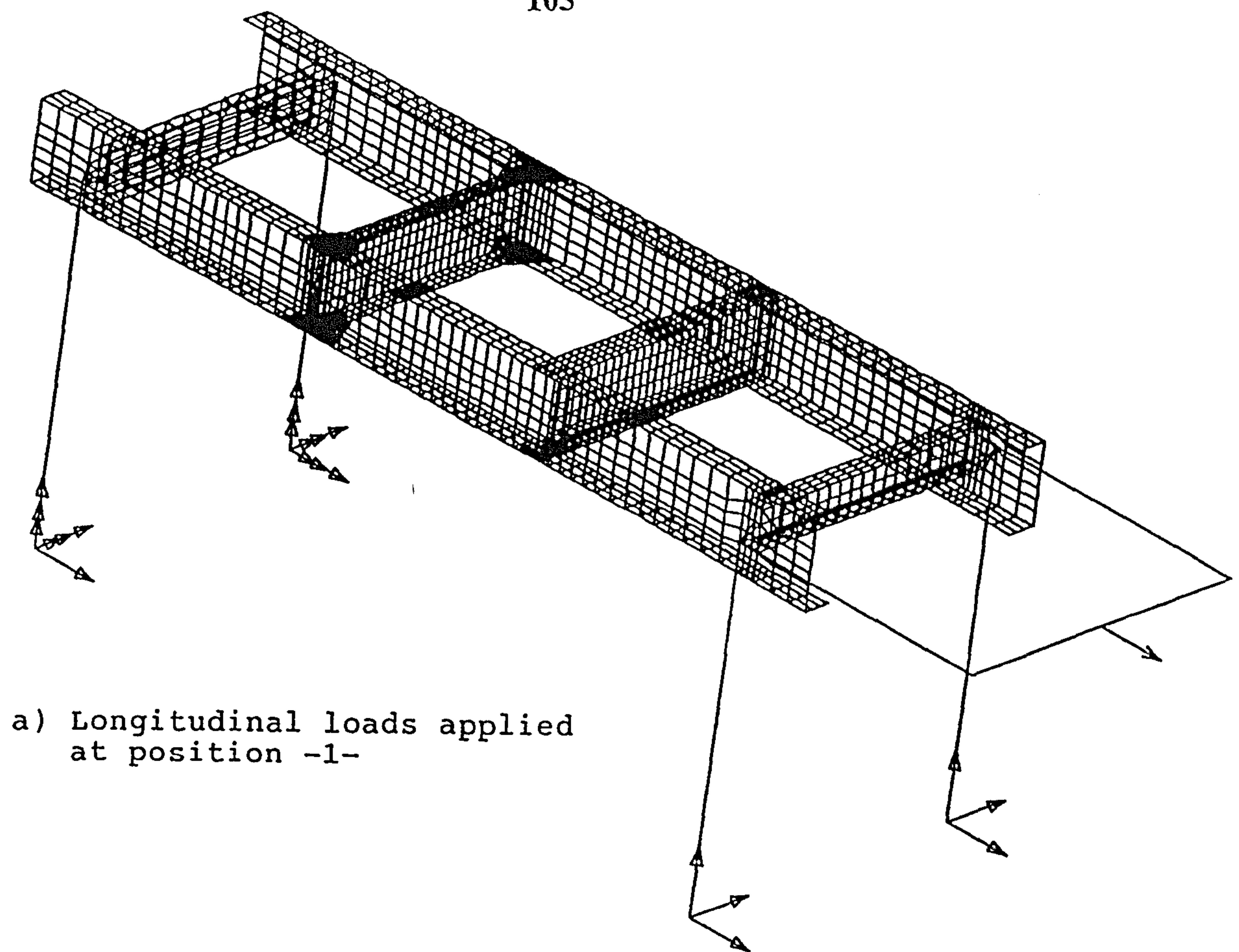
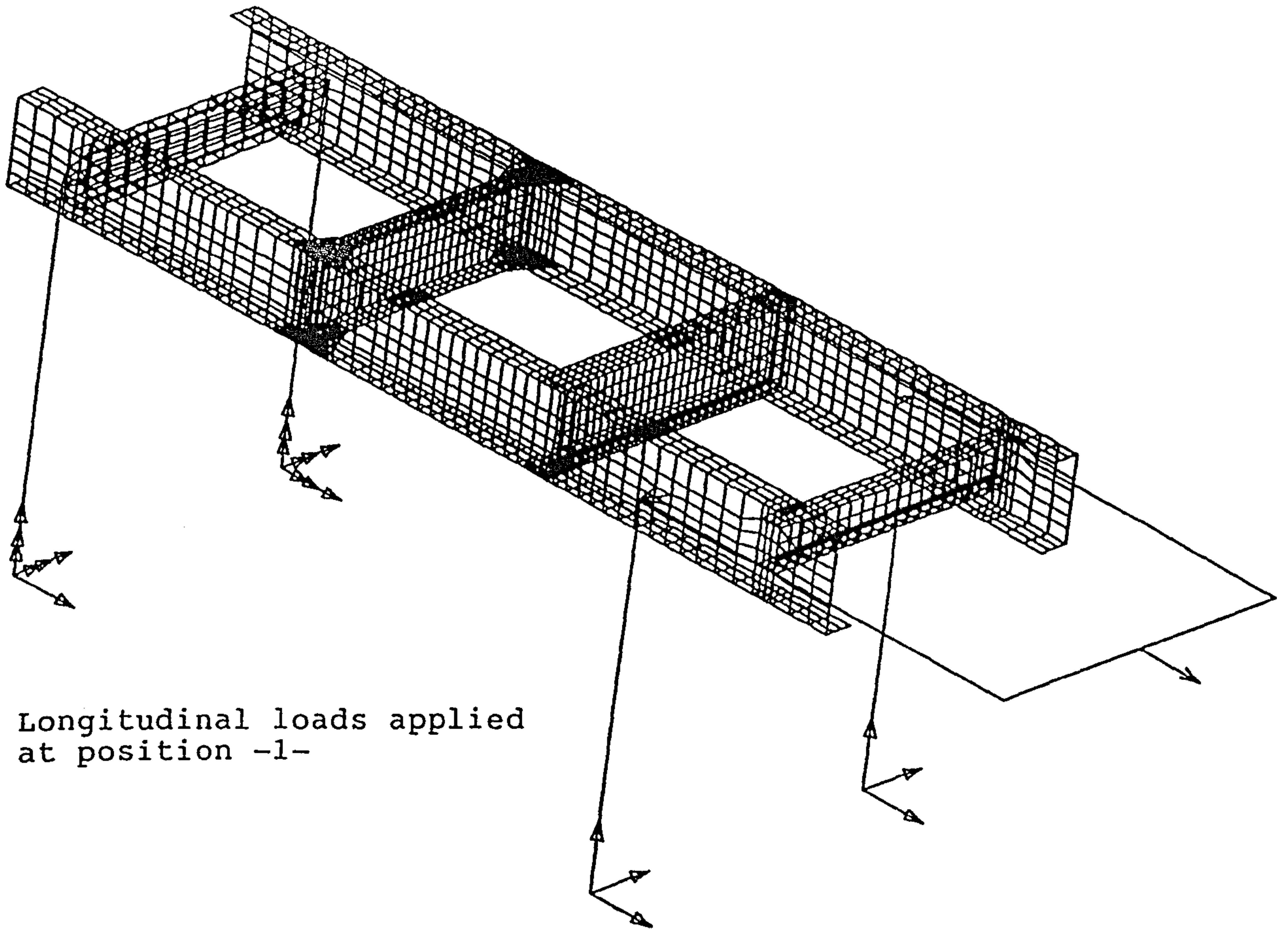


Fig.(7.16) Finite element idealisation of model chassis frame under longitudinal loads, case -1-

a) Longitudinal loads applied at position -1-



→ = applied force
 → = translational restraint
 → = rotational restraint

b) Longitudinal loads applied at position -2-

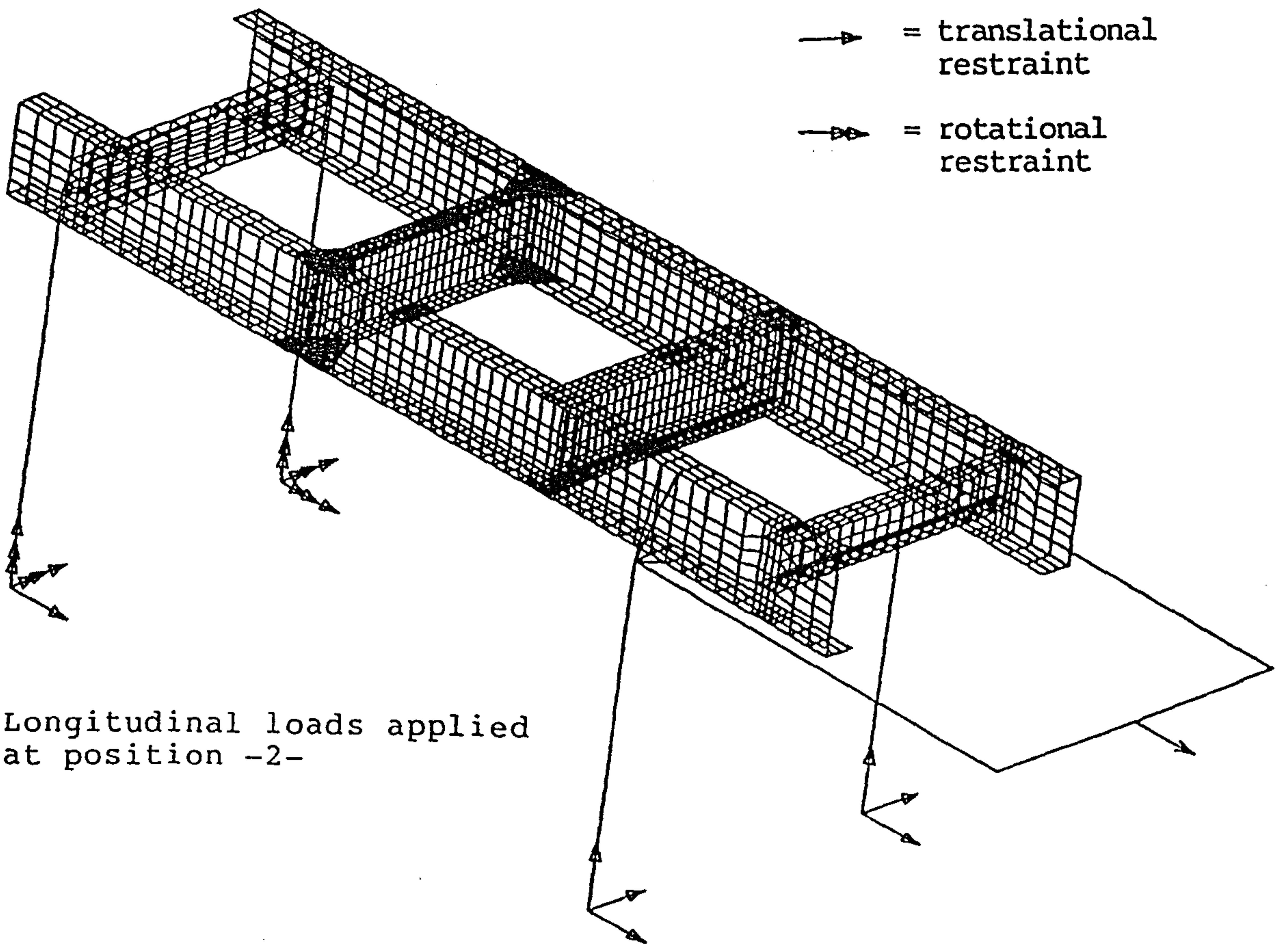


Fig.(7.17) Finite element idealisation of model chassis frame under longitudinal loads, case -2-

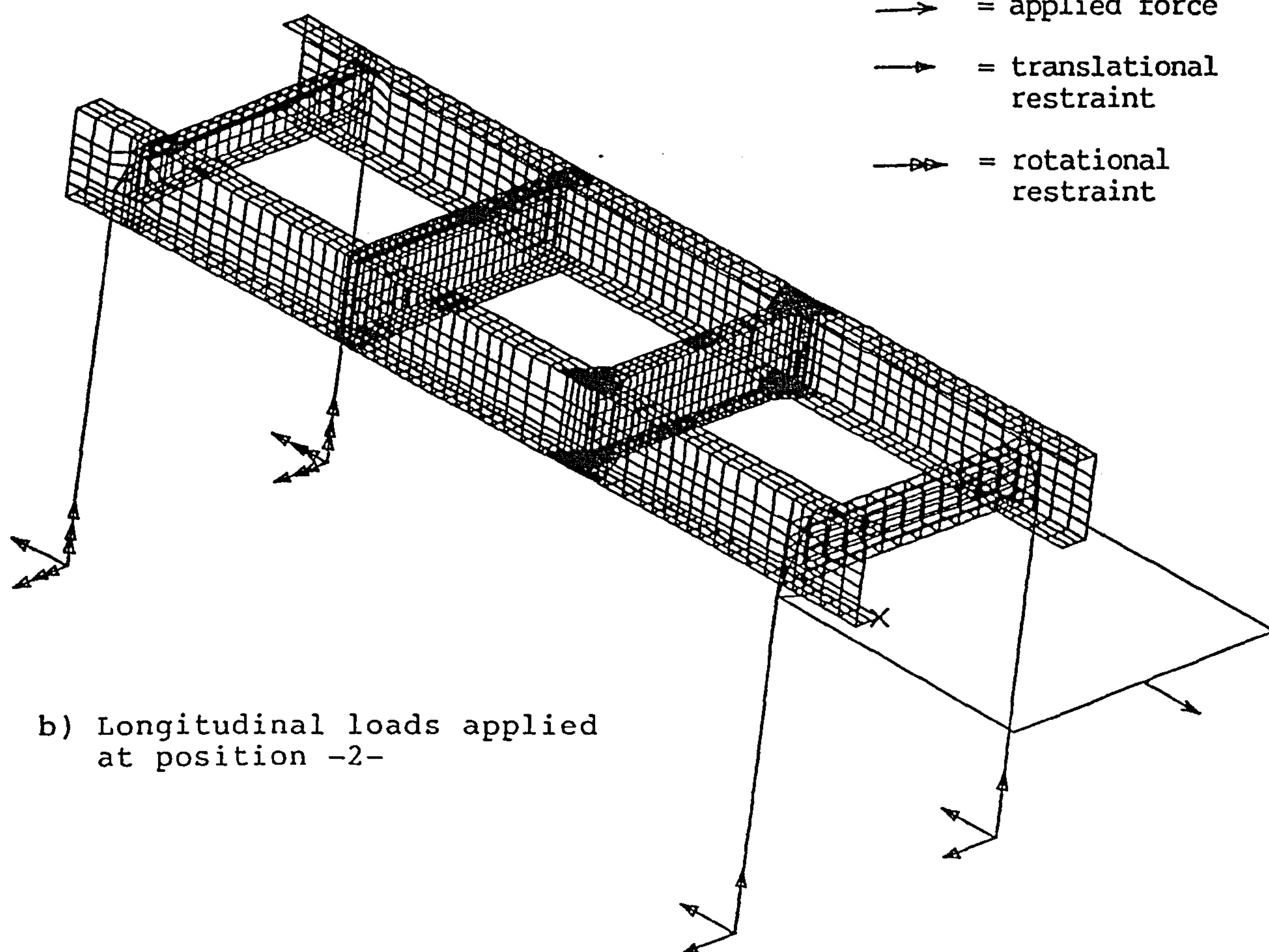
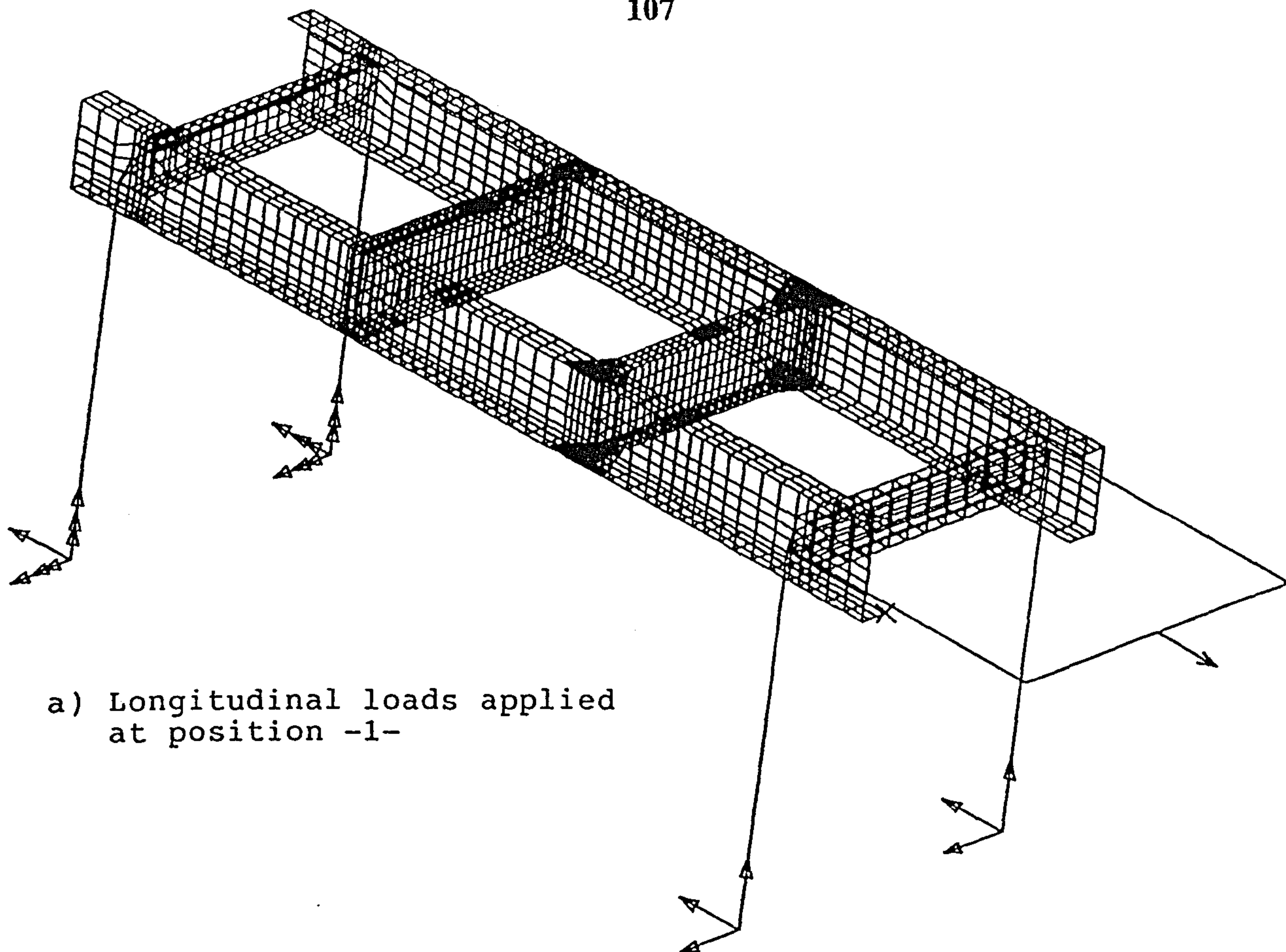
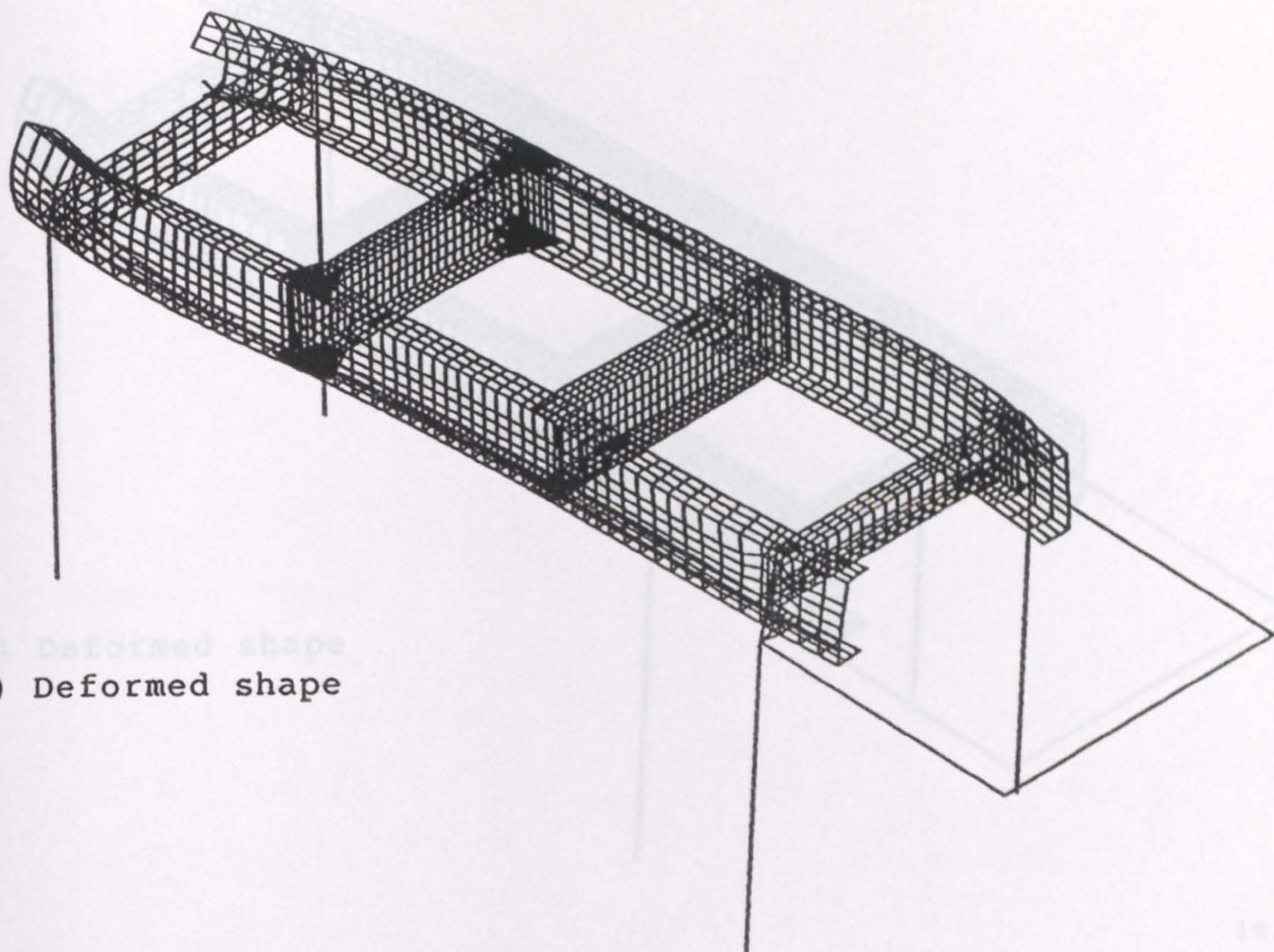


Fig.(7.18) Finite element idealisation of model chassis frame under longitudinal loads, case -3-

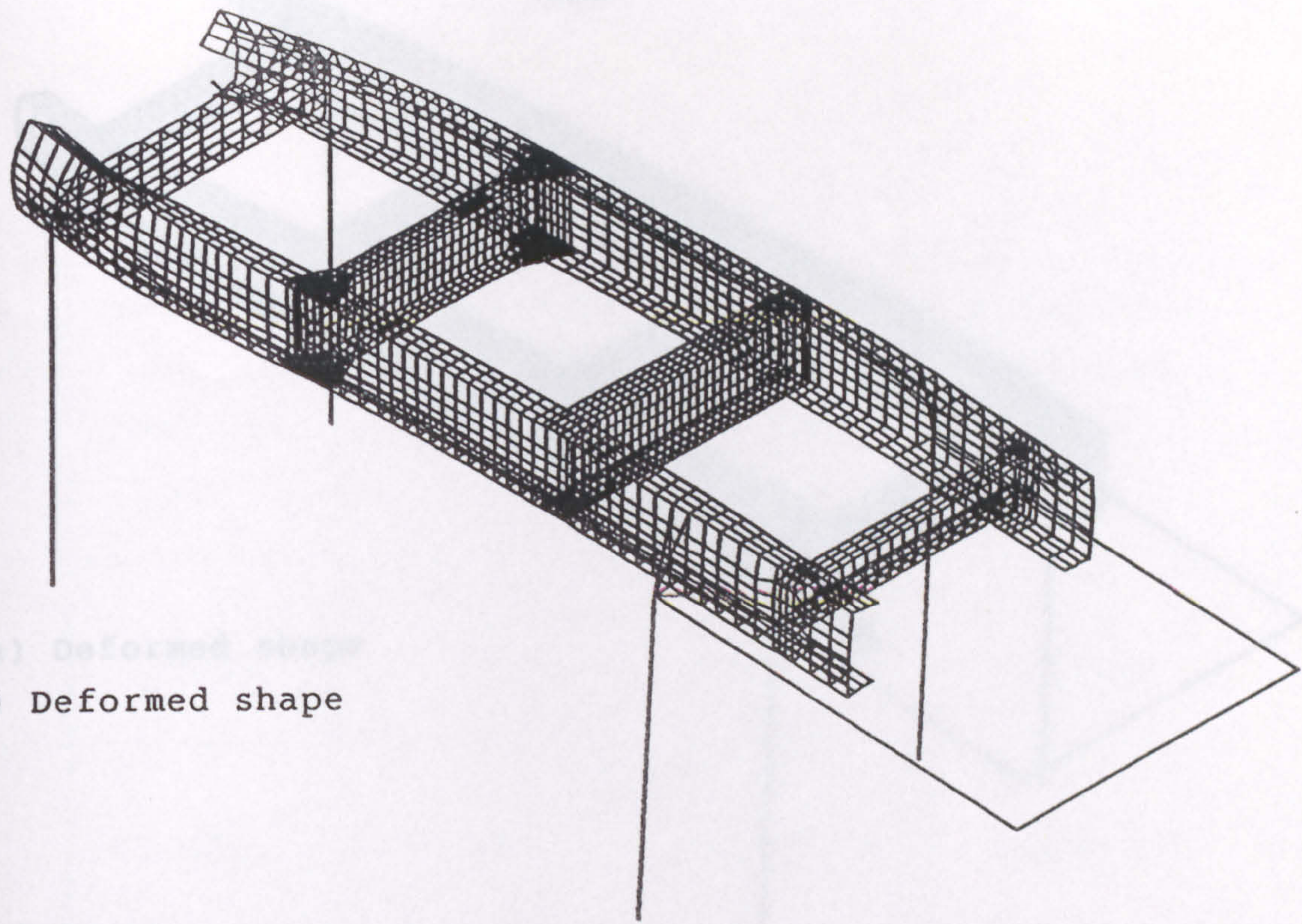
a) Deformed shape



b) Longitudinal stress distribution



Fig.(7.19) Deformation and stress distribution for case (1), when the longitudinal loads are applied at position (2)



a) Deformed shape

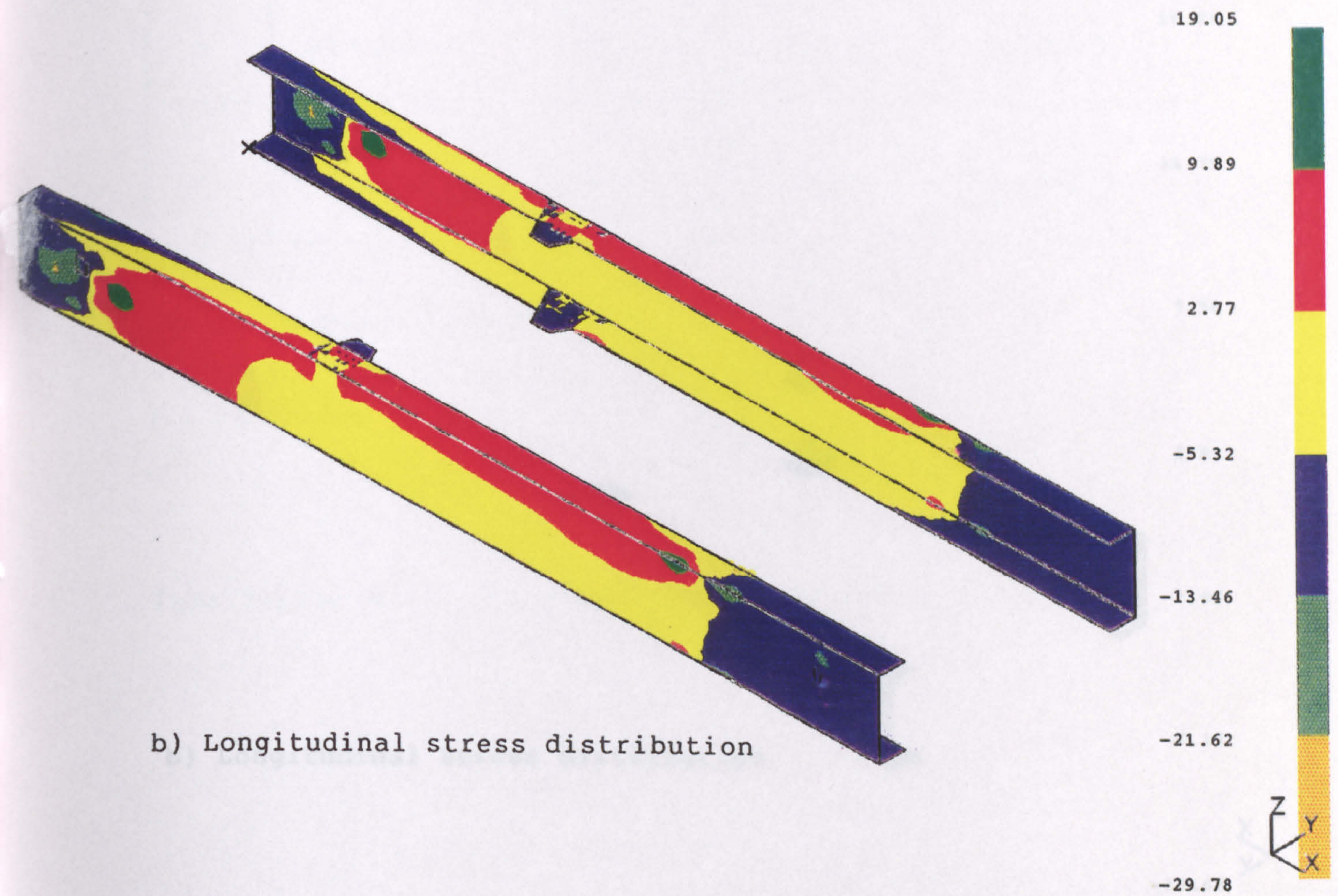


Fig.(7.20) Deformation and stress distribution for case (2), when the longitudinal loads are applied at position (2)

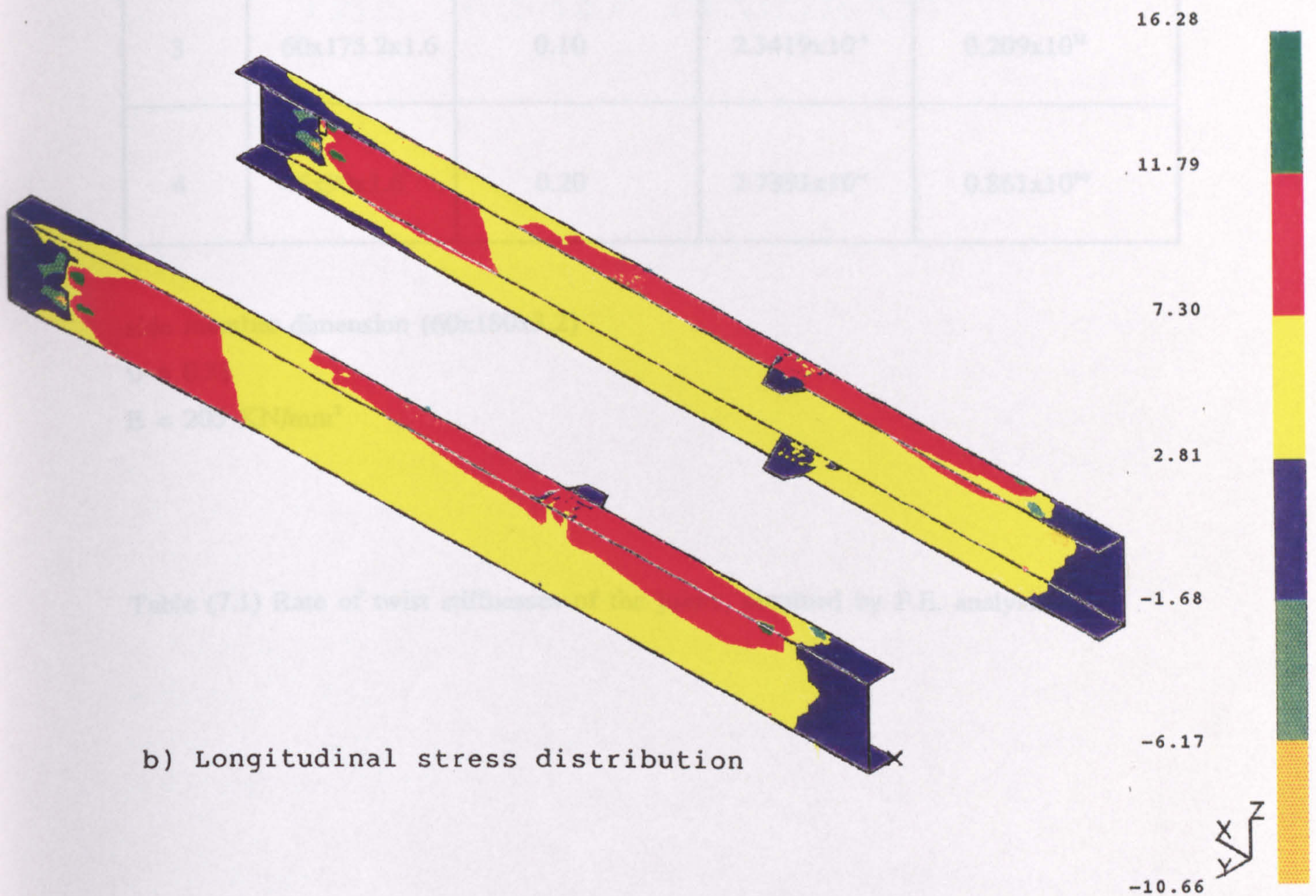
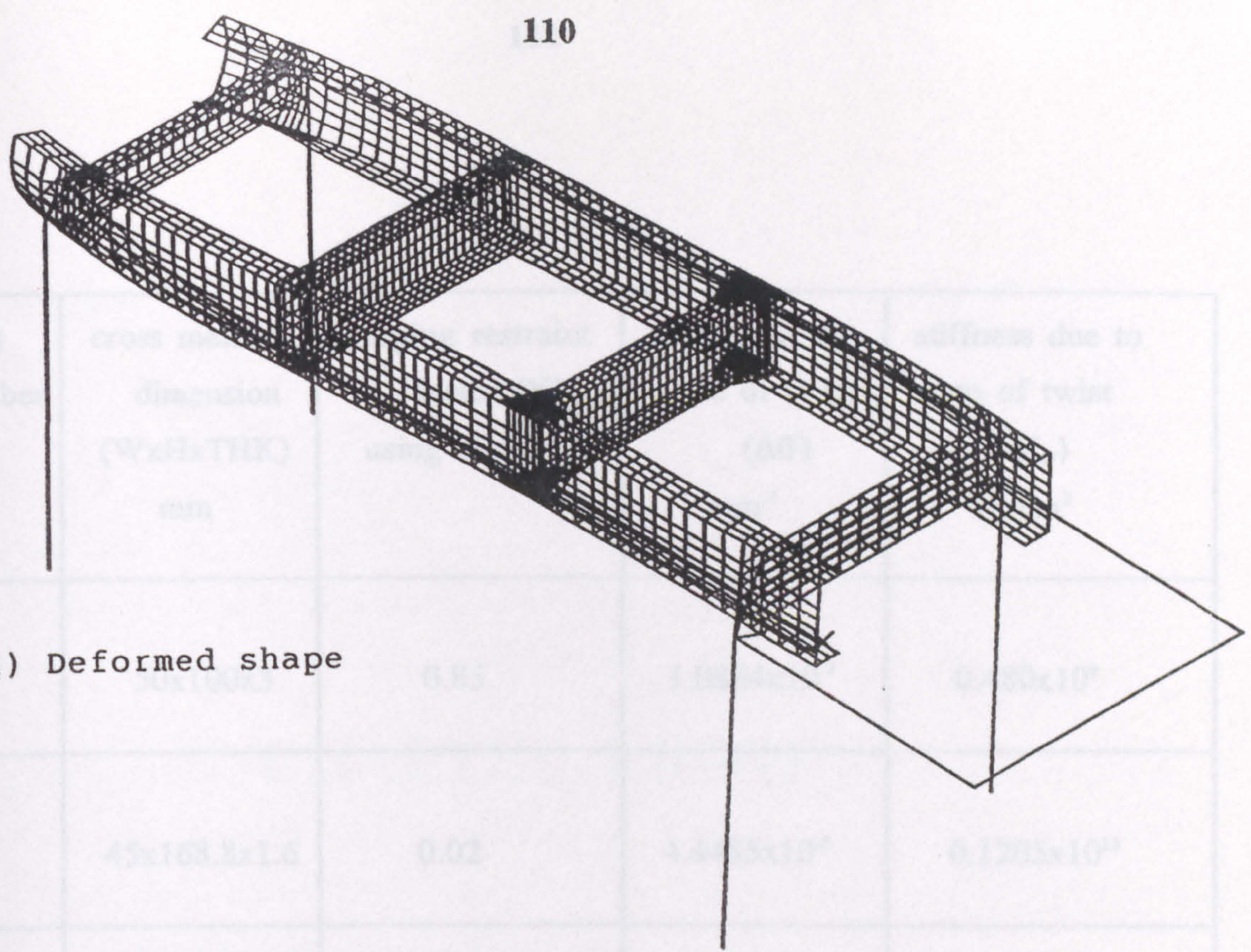


Fig.(7.21) Deformation and stress distribution for case (3), when the longitudinal loads are applied at position (2)

joint number	cross member dimension (WxHxTHK) mm	warping restraint factor (K) using eq.(2-17)	change in the rate of twist ($\Delta\theta'$) mm ⁻¹	stiffness due to rate of twist (K_θ) N.mm ³
1	50x100x3	0.85	1.0864×10^{-7}	0.480×10^9
2	45x168.8x1.6	0.02	4.4485×10^{-5}	0.1205×10^{12}
3	60x175.2x1.6	0.10	2.3419×10^{-4}	0.209×10^{11}
4	45x90x1.6	0.20	2.7391×10^{-4}	0.861×10^{10}

side member dimension (60x180x3.2)

$\nu = 0.31$

$E = 205 \text{ KN/mm}^2$

Table (7.1) Rate of twist stiffnesses of the joints, obtained by F.E. analysis

CHAPTER EIGHT

THE "A.SAFE PROGRAM"

8.1 GENERAL

In this chapter, the developed theory of thin walled beams and joints described in the previous chapters has been incorporated by the author into special purpose finite element program which may be used as a design tool in the preliminary stages of chassis frame design. This program is called the A.SAFE program. The chapter contains the flow chart of the program for analyzing chassis frame structures by the direct stiffness method considering bimoment effects.

The stiffnesses of the joint elements for the joints described in chapter seven are calculated from the finite element output. The bending moments and bimoment distribution due to longitudinal loads applied to the chassis frame in different positions were obtained using the A.SAFE program.

Laboratory tests to validate the theoretical stresses obtained from this program are discussed in chapter (9).

8.2 A.SAFE PROGRAM

Because of the high cost of building and testing prototype truck chassis frames, and the necessity of shortening the time from design to production, finite element analysis is used to predict the effectiveness of design concepts. Finite element calculations may be used early in the process, to provide data for finite element modelling, right through to analysis of the data from vehicle trials.

Finite element shell element offers detailed analysis of the structures, but extremely increases the computing cost and time. At the early stage of structure analysis, it is desirable to have a quick and inexpensive method for the purpose of cost-effective planning and conceptual design. Simple modelling with beam elements is frequently used for this purpose.

Nevertheless, reference (39) claims that finite element analysis of chassis frames should only be used for those areas where normal analytical methods can not be used, such as at the joints. In particular, beam elements where the cross section remains

constant should not be analysed using a finite element method according to this reference.

A computer program called STRU is presently available at Cranfield Institute of Technology, which uses conventional six degree of freedom beams to analyse structures.

A modification has been made to the STRU program to make it capable of calculating displacements, loads, and stresses at chassis frame members considering warping restraint effects.

Therefore, a new computer program is written using direct stiffness method. The new program is called A.SAFE which stands for Al-Hakeem program for Structural Analysis of chassis Frame considering bimoment Effects. The program includes the warping inhibition effects in thin walled beams. The capabilities of A.SAFE program are;-

- i) rigid joints with bimoment, taking the effects of different axes offset.
- ii) flexible joints with bimoments, using joint properties obtained from finite element model.
- iii) analysis of thin walled box section beams considering bimoment effects
- iv) calculates the stresses at the ends of beam element.

Therefore, in case of the analysis of the chassis frame with flexible joint assumptions, the joint element stiffness matrix obtained from finite element analysis can be supplied to the program.

All of the chassis frames to be analyzed by this program are assumed to consist of straight, prismatic members. The material properties for a given structure are taken to be constant throughout the structure.

Only the effects of loads are considered, and no other influence is taken directly into account. The program is designed to handle in a single computer run any number of loading systems for the same structure. Double precision for numerical accuracy is used in the program.

Although the program is only used for the longitudinal load case in this thesis, it is generally applicable for other chassis load cases, including torsion, bending ...etc and combination of these. The program flow chart is shown in figure (8.1), while the subroutines used are shown in figure (8.2). As mentioned before the program can be used as a design tool in the preliminary stages of chassis design, figure (8.3) shows the program incorporation into chassis design programme. Input data to the program consists of:-

- 1- Introductory data-title of the job, elastic constants, ...etc
- 2- Nodal data- number of nodes, bandwidth, nodes sectorial area, nodes coordinates, constraints and forces. Unconstrained structural nodes have seven degrees of freedom.
- 3- Element data- number of elements, element identity number, cross section dimension. Separate subroutines were written and included for channel and rectangular sections to evaluate cross sectional area, second moment of area, torsion constant and warping constant.

Output of the program consists of a listing of all input data as a preliminary check and the displacements for all seven degrees of freedom at all structural nodes. Constrained nodes were stated as such in the displacement list to avoid confusion with zero displacement and the correct list of constraints provided a second check on the data input. Using the calculated displacements and element stiffnesses, the output also contains the forces including bimoments and torques etc, at the ends of each element in the local coordinates.

The stresses at each node at a point on the cross-section with a given sectorial area is provided in the output list.

An example for a simple grillage structure of input and output data decks, annotated to explain each data item, is included in appendix (A).

8.3 THEORETICAL CHASSIS FRAME MODEL UNDER LONGITUDINAL LOAD

A theoretical chassis frame model was constructed using the A.SAFE program with the same dimensions as the finite element model described in the previous chapter. As mentioned before the same load cases and boundary conditions were used with the longitudinal load in different positions. The common value for the longitudinal load applied was (5) KN to each side member of the chassis frame, see figure (8.4). The bimoment input for offset longitudinal loads was calculated in accordance with the methods of chapter (6).

The bimoments, bending moments and stresses along the side members of the theoretical chassis frame model were calculated by A.SAFE at sufficient nodes to account for the gradients of stress to be expected. The computer program A.SAFE calculated the bimoment and bending moments as well as stresses. The bimoment results for the three load cases were plotted in figure (8.5), while the corresponding bending moment results were plotted in figures (8.6/8.7/8.8).

Whilst it is desirable to show the correlation of finite element methods with experimental results, confidence may also be obtained by comparing experimental stress results those obtained from the A.SAFE program. Hence, the A.SAFE model had nodes at equivalent positions to the strain-gauge positions used in the experimental model, see chapter (9).

The stresses along the side members obtained from the A.SAFE program were compared with those obtained from finite element analysis and experimental results as will be shown in chapter (9).

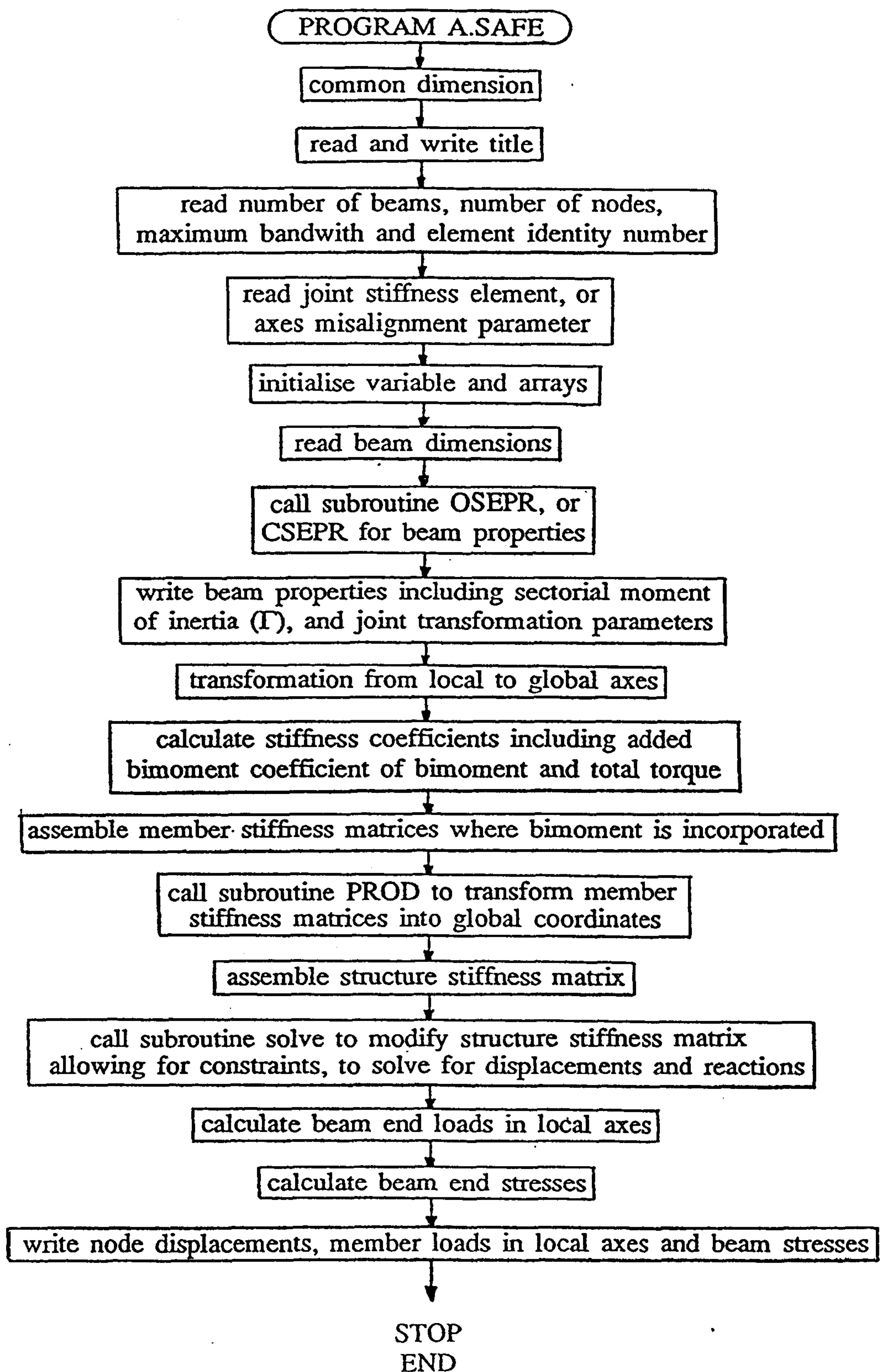


Fig.(8.1) Flow chart of A.SAFE program

SUBROUTINE PROD

dimension

matrix product

RETURN

END

SUBROUTINE OSEPRO

dimension

read open section dimensions

calculation of area, J , I_{yy} , I_{zz} , Γ

RETURN

END

SUBROUTINE CSEPRO

dimension

read closed section dimensions

calculation of area, J , I_{yy} , I_{zz} , Γ

RETURN

END

Fig.(8.2) Flow charts of subroutines used in A.SAFE program

INCORPORATION INTO CHASSIS DESIGN PROGRAMME

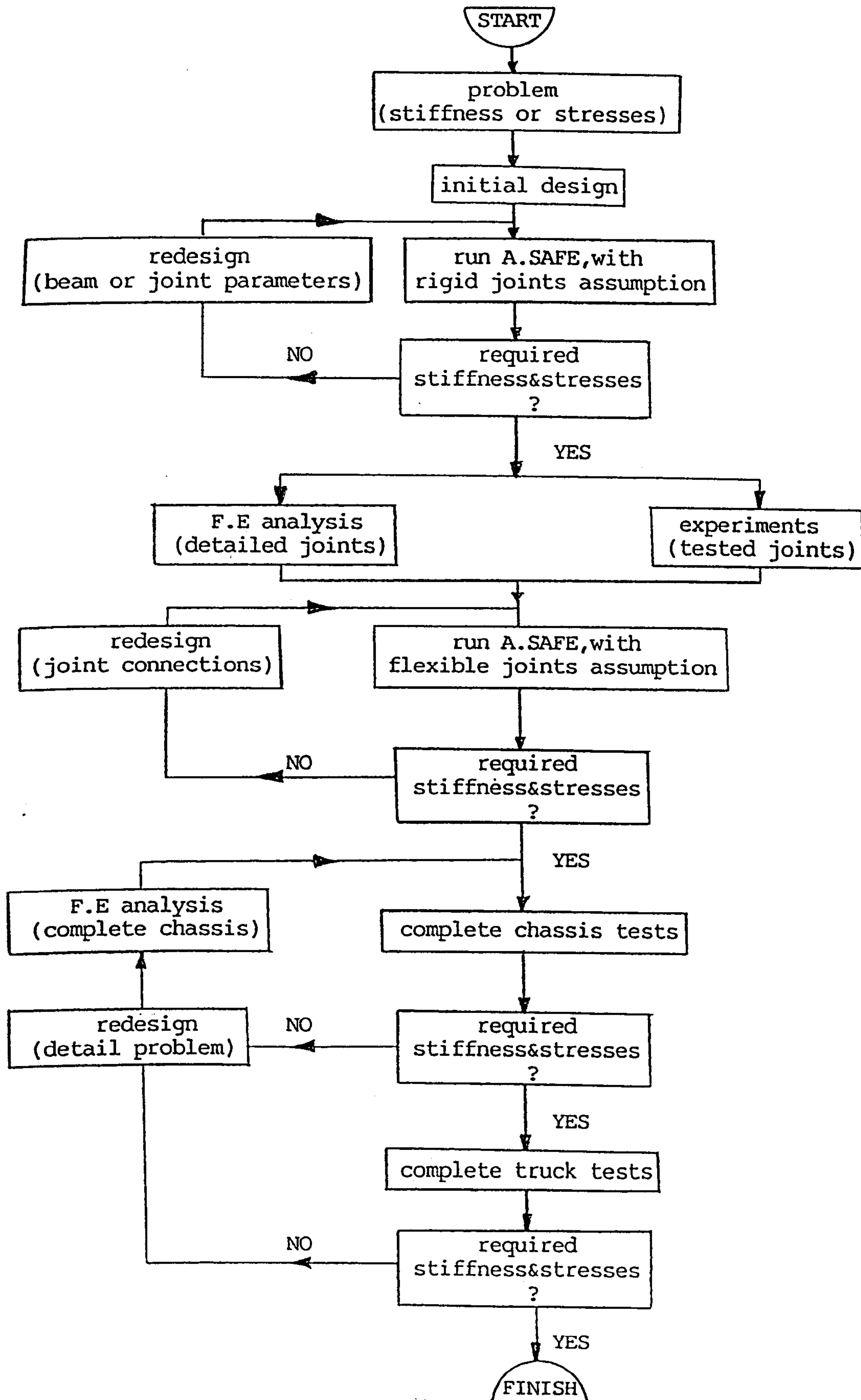


Fig.(8.3) Flow chart shows the incorporation of A.SAFE program into chassis design programme

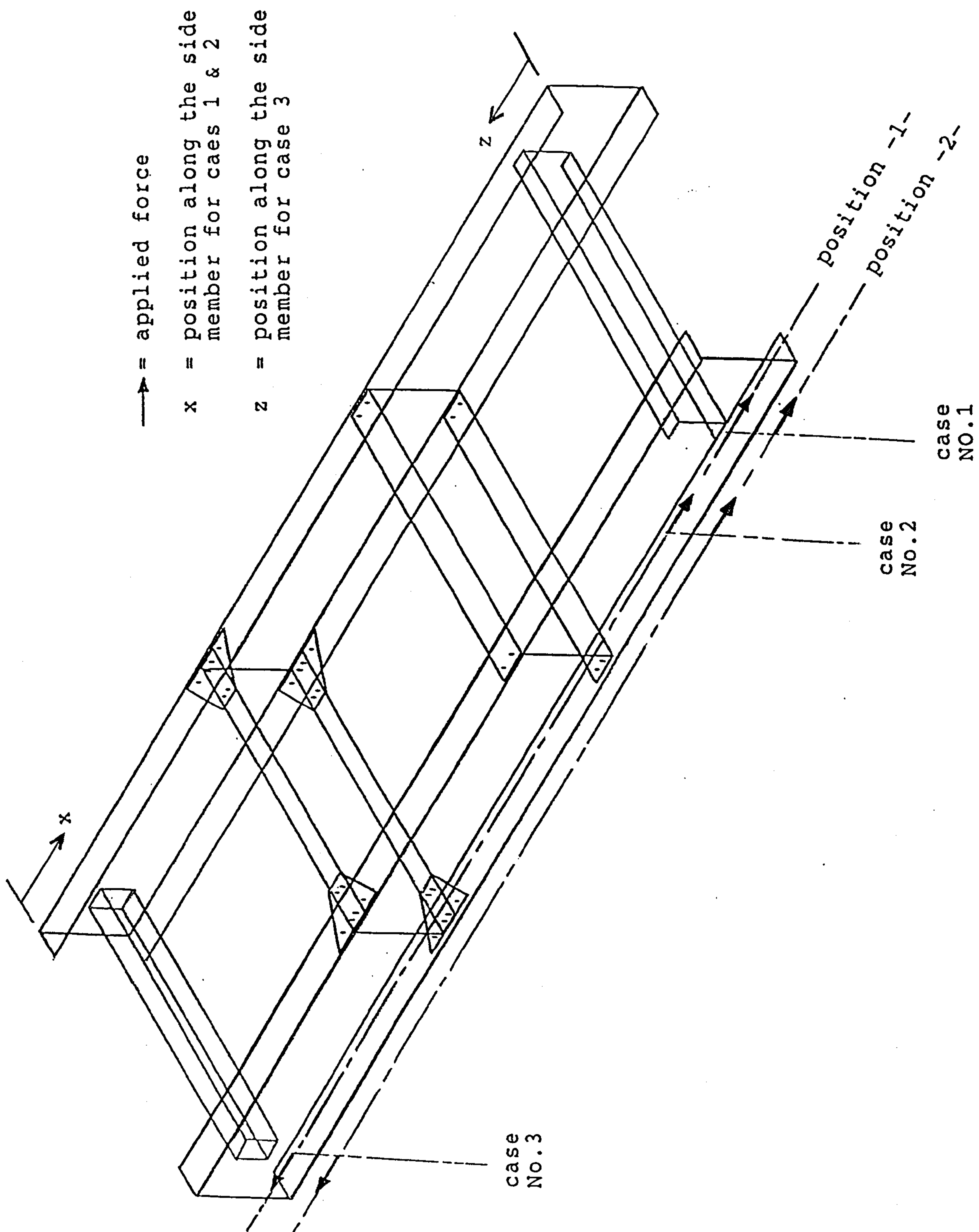


Fig. (8.4) Cases and positions of loading

Fig. (8.5)Bimoment distribution due to longitudinal load,(see fig. 8.4)

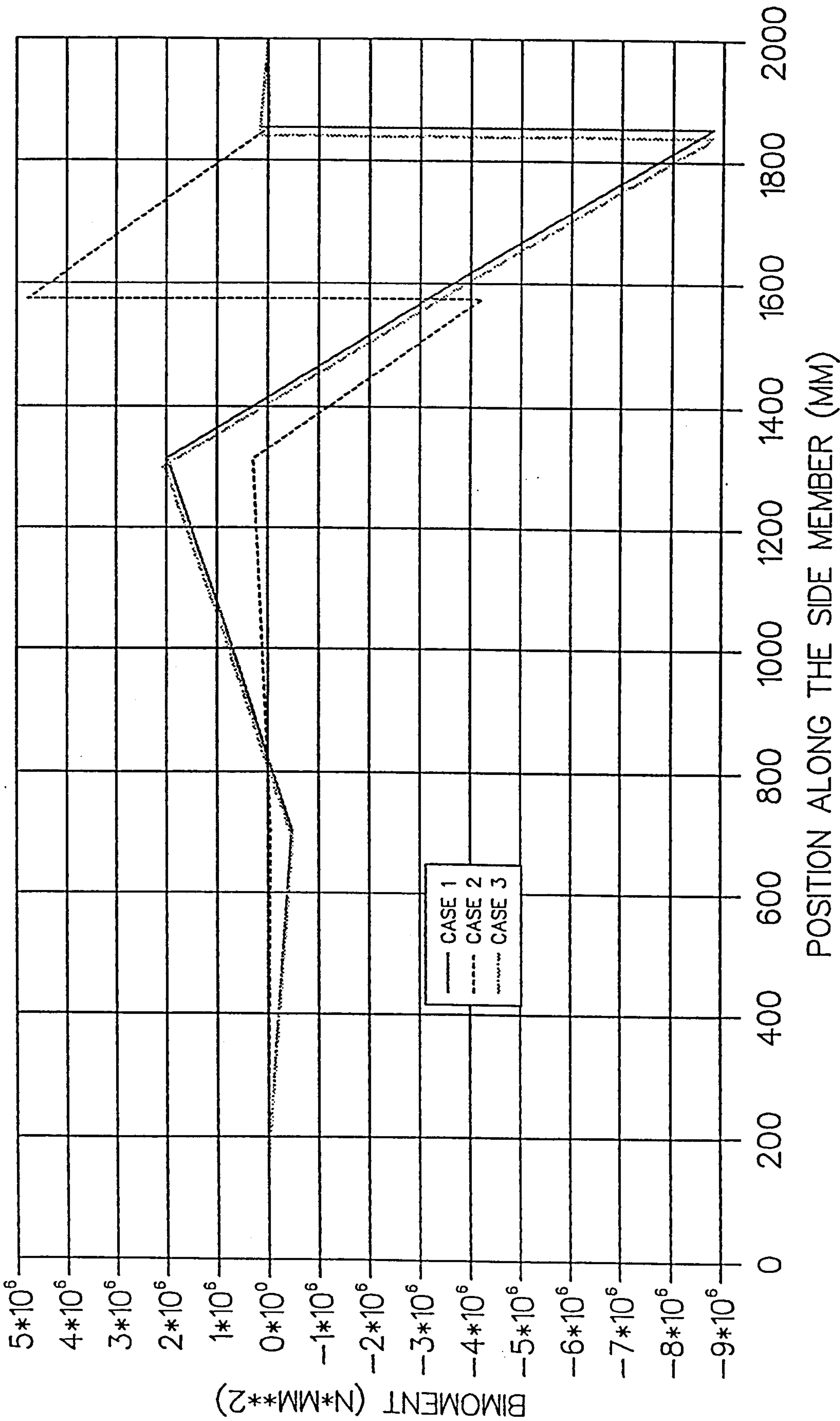


Fig. (8.6) Moment case No.1, Load (p) at position 2, (see fig. 8.4)

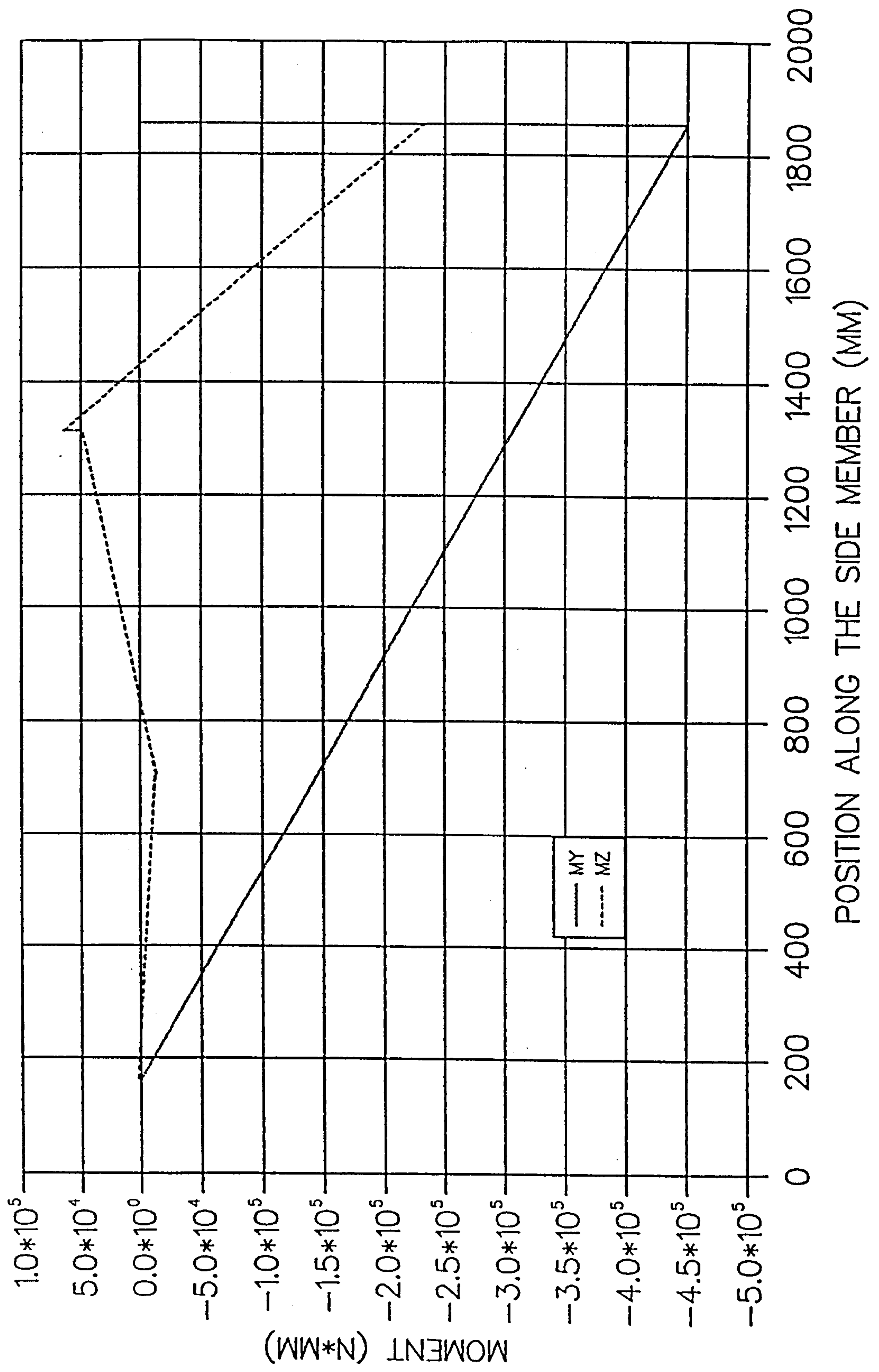


Fig.(8.7) Moment case No.2, Load (p) at position 2, (see fig. 8.4)

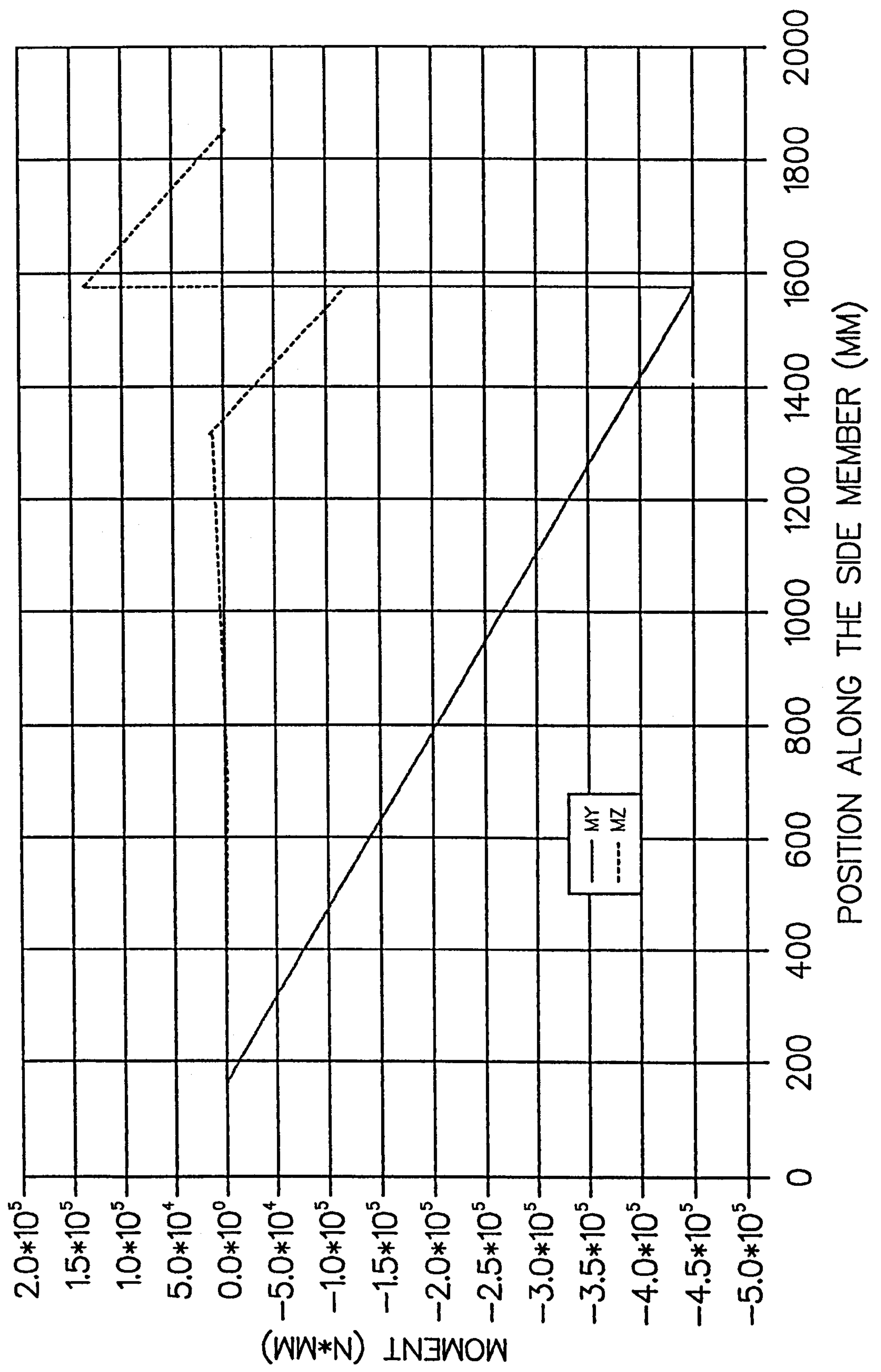
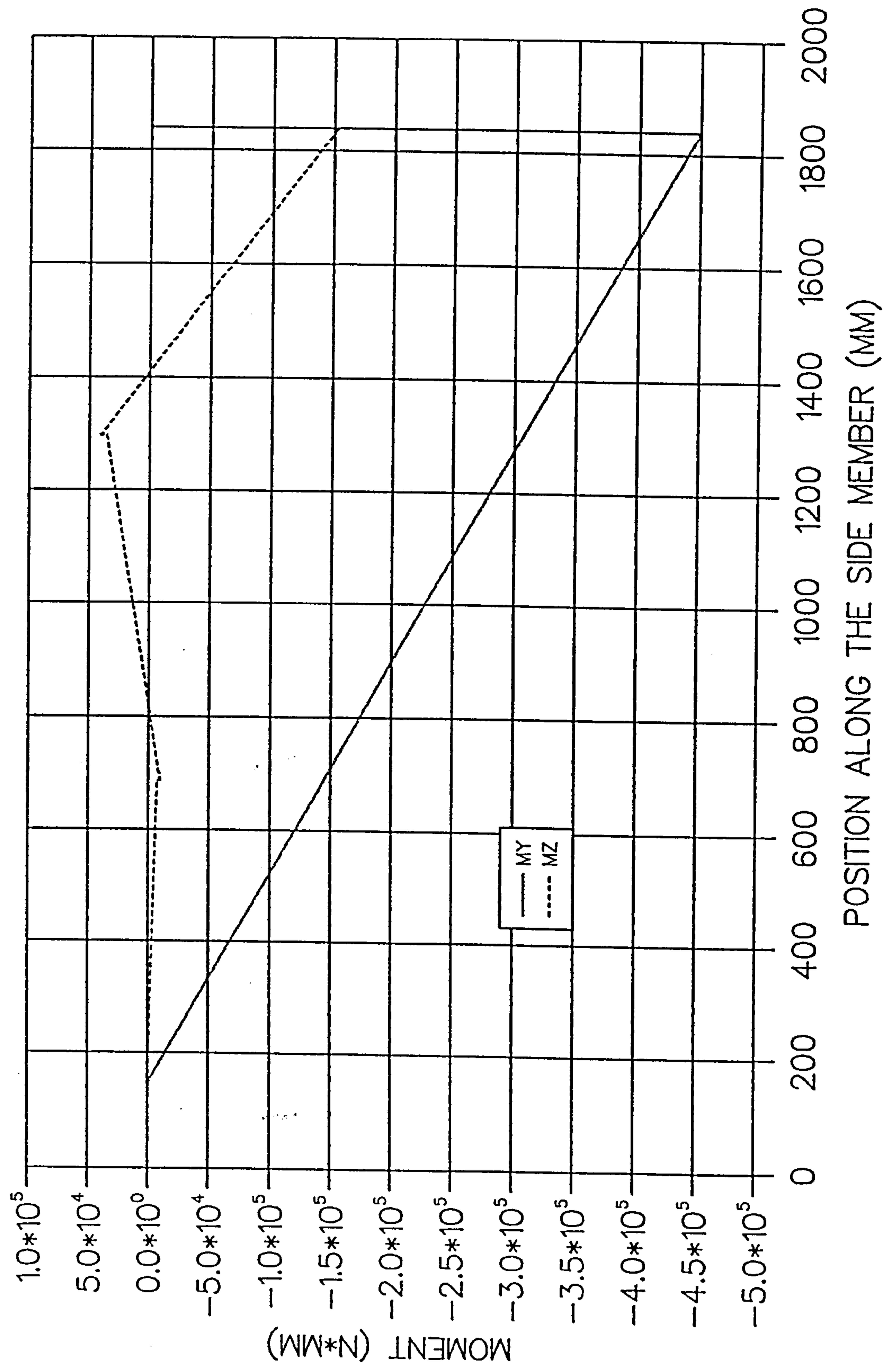


Fig.(8.8) Moment case No.3, Load (p) at position 2, (see fig. 8.4)



CHAPTER NINE

EXPERIMENTAL INVESTIGATION

9.1 GENERAL

This chapter describes the experimental approach used to determine the stress distribution in the side members of an experimental chassis frame under different cases of longitudinal loads applied to the side members. The experimental chassis frame model was constructed with the same dimensions and constructional details as the various cross member to side member joints as the finite element models described in chapter seven.

The purpose of the experimental test lies in the confirmation of the theoretical results obtained by Vlasov's bimoment theory and finite element analysis.

The discussion of the measured and corresponding finite element values with the theoretical results of stresses obtained from A.SAFE program will be given in a later chapter.

9.2 MATERIAL PROPERTIES

Tensile test samples of the mild steel was cut from the same sheets which were used to make the members of the experimental chassis frame model. They were strain gauged by two mutually perpendicular resistance strain gauges placed on each face of the test piece to measure longitudinal and lateral strains.

A tensile test was performed and the stress and longitudinal and lateral strains were recorded for each load increment. The average strains in the longitudinal and lateral directions were determined and the stress-strain curves are shown in figure (9.1). The mean values of poisson's ratio (ν) and the modulus of elasticity (Young's modulus) were found to be (0.31) and (205 KN/mm²) respectively.

9.3 CONSTRUCTION OF THE TEST MODEL

The test chassis was fabricated of mild steel to be representative of typical truck chassis construction. The general nature of the chassis model is shown in figure

(7.15). Channel section side members (size 60x180 mm) were connected by several different types of cross member and cross member to side member joint.

For the same method of a fabrication as actual chassis frames, cold working rivets were replaced by Huck bolts. The flanges of the channel open sections of the cross members for joints No.2 and No.3 were attached to those of the side members by using Huck bolts.

For joints No.1 and No.4, the cross member was MIG welded to the side member web by mild steel electrode. A fillet weld having equal leg length dimensions of (6)mm, was used for welding all round the cross member section. A (6)mm fillet weld was used as it is thought that this is a typical size used for welding of members in ladder chassis frame construction. Care was taken to ensure that the weld size was uniform around the channel section and consistent in both joints. Care also was taken to keep the distortion of the side member web caused by the welding process to a minimum.

The box section cross member consisted of standard cold-formed (ERW) structural steel section while all of the channel sections used for the project were formed from mild steel sheet by a bending machine with a proper radii of bending and consequently showed good forming condition at the free edge of the bent part. The length of the side members was restricted by the maximum length of the available steel sheet as (2000)mm. All of the holes for the mounting of the cross members were designed to be in the line of zero warping along the longitudinal directions of the side member flanges.

9.4 STRAIN MEASUREMENT

Axial constraint direct strains were measured on the surfaces of the side members of the chassis frame by single electrical resistance strain gauges; the gauges were aligned parallel to the longitudinal axis of the side members. The gauges were of U.S.A., Micro-Measurment Division manufacture, with (5)mm gauge: 120 ohm resistance, gauge factor = 2.09 .

The strains were recorded using strain recording unit. Central dummy gauges were used to compensate for surrounding temperature variations during the tests and to complete the full bridge circuit. For each gauge position, the recording unit registered a stable reading.

The gauges had to be attached to the surface of the side member sections after the cross members were welded to avoid damage. The strain gauges were attached to the inside surface of the side members sections to avoid damage during handling and testing.

The gauges were positioned such that each gauge placed at a point on one channel section side member had a corresponding gauge placed symmetrically on the other side member. This was done to check for anti-symmetry in the tension and compression readings. Figure (9.2) shows the positions of the gauges around the channel section for both side members. A gauge position is labelled with an upper case letter and the corresponding anti-symmetrical position labelled using the same lower case letter. The measured strains were converted to stress by multiplying by the pre-determined elastic modulus of the side member material.

9.5 SUPPORT AND LOADING CONDITIONS

Plate (9.1), shows the general arrangement of supports and the loading conditions for the chassis frame under longitudinal loads. Four brackets were attached to the side members of the chassis frame. The chassis frame was horizontally positioned from these brackets by four rigid beam supports. Rose joints were used at both ends of each rigid beam support to idealise pin joints. The system of rigid beams and pin joints was arranged so that it did not contribute to the stiffness of the chassis frame and could easily and accurately be idealised for inclusion in the computer program.

Constraints were introduced, in such a way that these would not distort the measured stresses by influencing internal forces in the chassis frame. The chassis frame was subjected to longitudinal loads. These loads were applied by hydraulic jacks connected by strain-gauged rods to the support brackets on the side members of the chassis frame.

9.6 TESTING PROCEDURE

The horizontal positioning of the chassis frame on the four rigid beam supports with rose joints at the brackets was confirmed using a bubble-in-glass inclinometer.

Initially, in each test, zero strain readings were taken under the self-weight of the frame and the support and loading apparatus. The chassis frame was subjected to longitudinal loads by hydraulic jacks connected to the support brackets on the side members as shown in plate (9.1).

In order to investigate the bimoment effects on the stress distribution in the side members of the chassis frame, different longitudinal load-cases with the longitudinal loads in different positions relative to the shear centre, and hence applying different bimoment, were considered. Three load-cases were used as follows;-

- i) Load-case (No.1). The longitudinal load (p) was applied to the side members at joint (No.4), where the cross member is a channel section. The test was carried out with the load (p) applied in two positions relative to the shear centre.

When the load (p) was applied in position (1), the load would only introduce direct load, and moment about the z-axis. Neither moment about the y-axis nor bimoment would be introduced when the load was applied in this position as shown in plate (9.2a). However, when the load (p) was applied in position (2), direct load, moments about z-axis and y-axis as well as bimoment would be introduced to the side members as shown in plate (9.2b).

- ii) Load-case (No.2). The longitudinal load (p) was applied to the side member between joint (No.3) and joint (No.4), where there is no cross member attachment as shown in plate (9.3). For this case, the test was carried out with both loading positions as used in case (No.1). Hence moments and bimoment would be introduced to the side members.
- iii) Load-case (No.3). The longitudinal load (p) was applied to the side member at joint (No.1), where the cross member is a box section as shown in plate (9.4).

The test was also carried out with both loading positions used in the previous two cases, hence same moments and bimoment would be introduced to the side members due to longitudinal loads.

In all tests with the above load- cases, strain readings were obtained at each load increment of (1) KN at low loads when loading and unloading. The direction of the applied load was then reversed and the measurements repeated. The test results showed that the tension and compression readings were linear and consistent with the load applied in opposite directions. This confirmed the linear elastic behaviour of the structure at low loads. The load was increased until (10) KN, i.e, (5) KN for each side member.

The stress distribution due to longitudinal loads for each station, i.e, the flange and web of the side members, see figure (8.2), were recorded. For each load-case when the longitudinal load was applied at position (1), i.e, when no bimoment is created due to longitudinal load, the stress distributions were plotted in figures (9.3/9.5/9.7). The stress distribution when the longitudinal load is applied at position (2), i.e, when it produces a bimoment, were plotted in figures (9.4/9.6/9.8) for each load-case.

The total axial stress around the cross section of the side members obtained from A.SAFE program with those experimental values are plotted in figures (9.9/9.10/9.11) at selected cross sections, see figure (9.2).

The comparison between the theoretical stresses obtained from finite element analysis and A.SAFE program with those experimental values has been established for the side members of a complete chassis frame. Different load-cases with the longitudinal load in different positions (position 1 and 2) relative to shear centre, and hence applying different bimoment, were considered. The discrepancy between theoretical and measured values of the stress increases towards the bracket attachments. Nevertheless, even in the worst case (case No.1), the discrepancy between A.SAFE program and the measured values is only (19%) at the loading brackets. For the region between the brackets and the joints there is a good

agreement. The reasons for the discrepancy between the theoretical and experimental approach can be regarded as due to:-

- i) Manufacturing inaccuracies in the positioning of bolts, heated structure because of welding process,...etc.
- ii) The friction due to the high tightening forces of the bolts which may have partially inhibited the warping at the position of the loading brackets attachments.
- iii) The stiffness coefficients of the joint element used in A.SAFE program are approximate, because of the assumptions used and the way of obtaining them (i.e from F.E analysis which itself has been built on simplifying assumptions).
- iv) only joint flexibility due to bimoment is considered in A.SAFE program, while flexibilities due to other type of loads, joints regarded to behave in a rigid manner.
- v) approximations used such as ignoring the deformation of the profile of the section, lozenging and the effects of the curvature shape at the web-flange connection of the channel section. Those approximations are used to simplify the mathematical formulae developed to calculate the stiffness sub-matrix due to warping effects.

From figure (8.5), it is clear that the external bimoment applied to the side member due to the longitudinal load (case 2) is shared nearly equally between the two parts of the side member. Therefore, the maximum bimoment near the loading bracket of the side member for this case is lower than the other two cases, that gives a maximum bimoment stress distribution near the loading bracket of the side member for this case lower than the other two cases.

It is also noted that the stresses predicted by the A.SAFE program which uses Vlasov's bimoment theory for beam analysis and finite element analysis for joints are closer to the measured values than those obtained by the finite element analysis of the whole chassis frame. This supports Beermann's claim that finite element analysis should only be used for those areas where normal analytical methods can not be used, i.e, joints. In particular, beam elements where the cross section remains constant, should not be analysed using the finite element method.

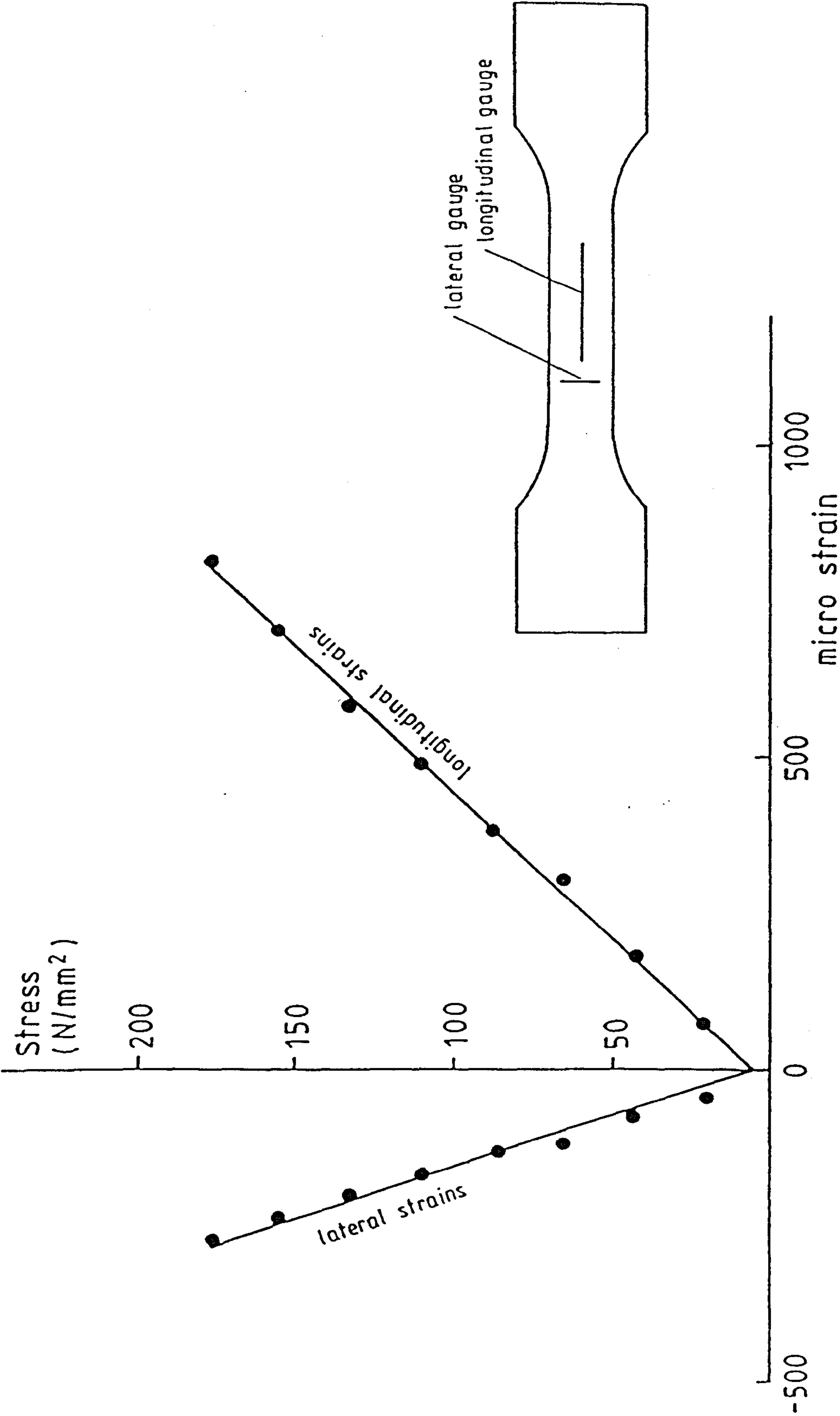


Fig.(9.1) Stress-strain curves for a mild steel tensile test

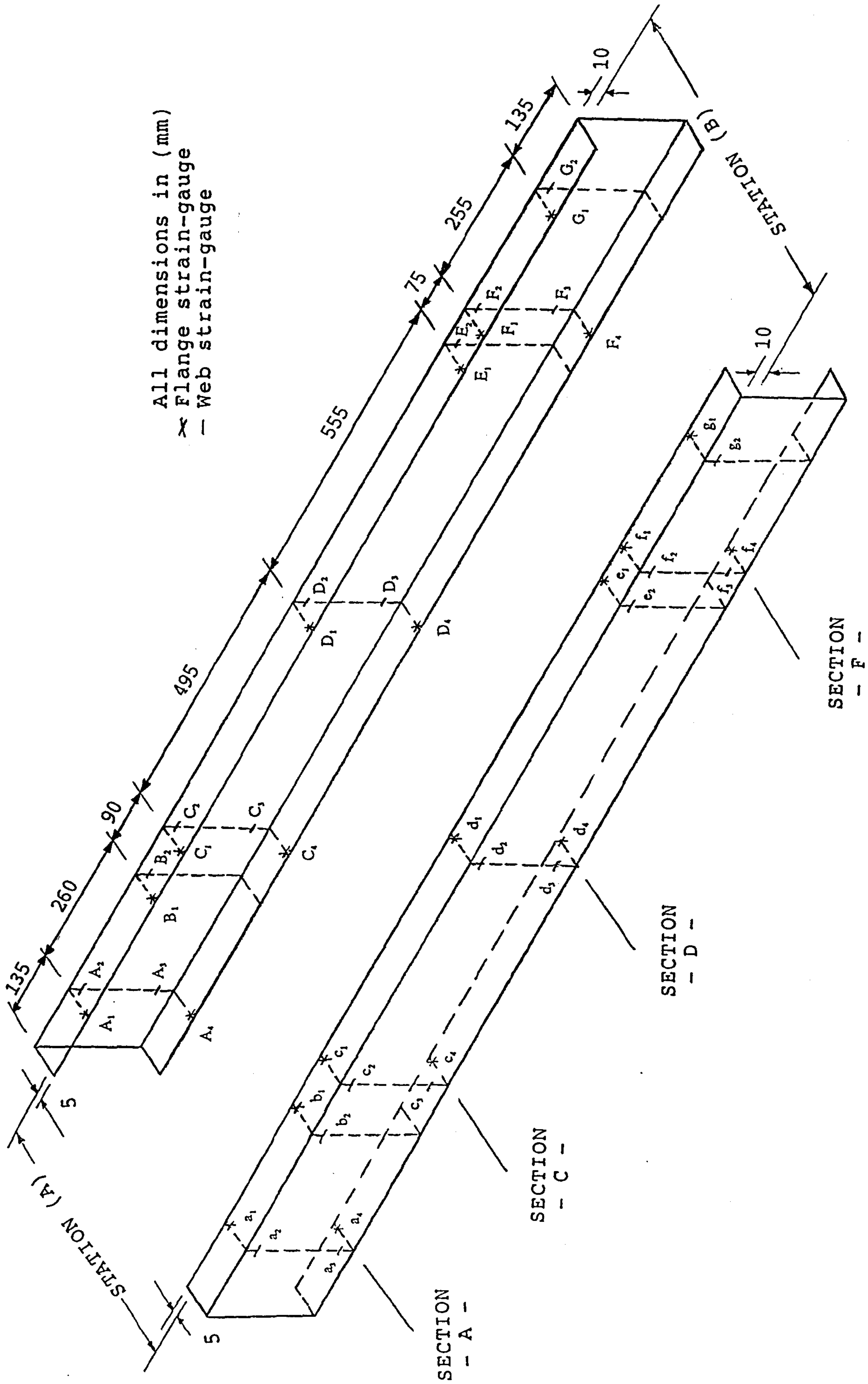
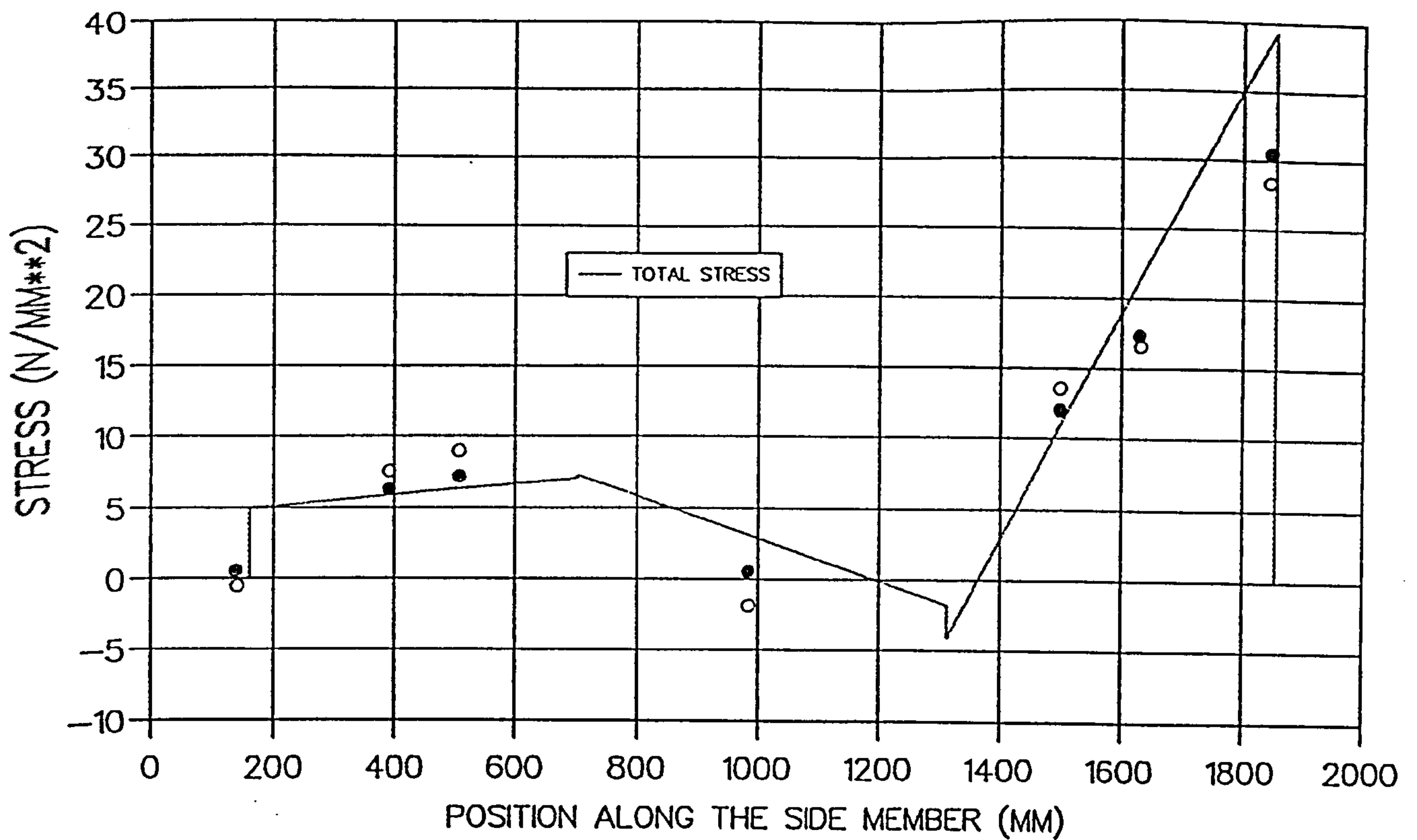


Fig.(9.2) Strain- gauge positions and stations

A) NODES AT THE FLANGE, STATION A (SEE FIG. 9.2)



B) NODES AT THE WEB, STATION B (SEE FIG. 9.2)

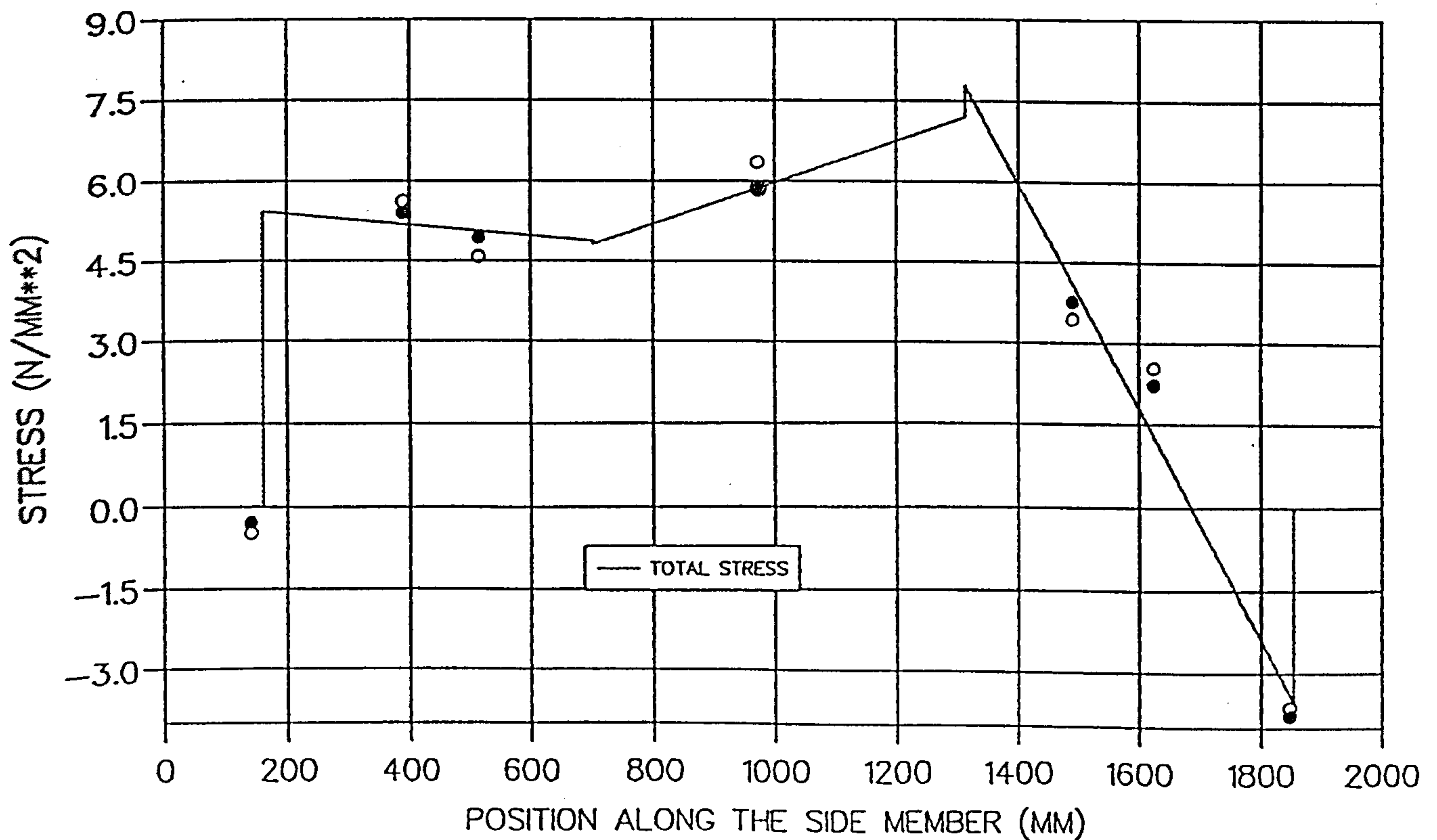
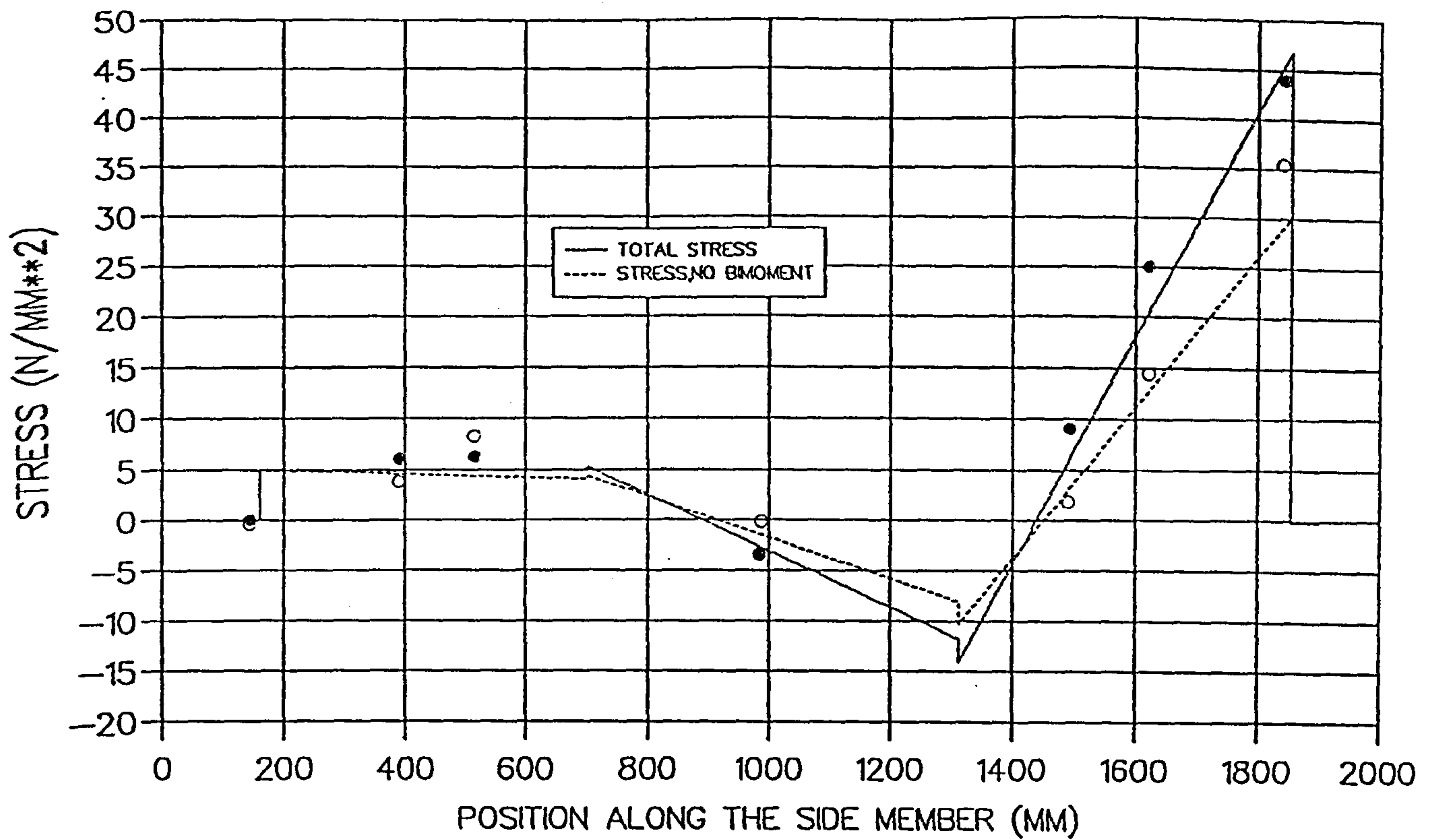


Fig.(9.3) Stress distribution for load-case No.1, when the load (p) is applied at position (1)

A) NODES AT THE FLANGE, STATION A (SEE FIG. 9.2)



• EXP.
○ F.E.
— PROG.

B) NODES AT THE WEB, STATION B (SEE FIG. 9.2)

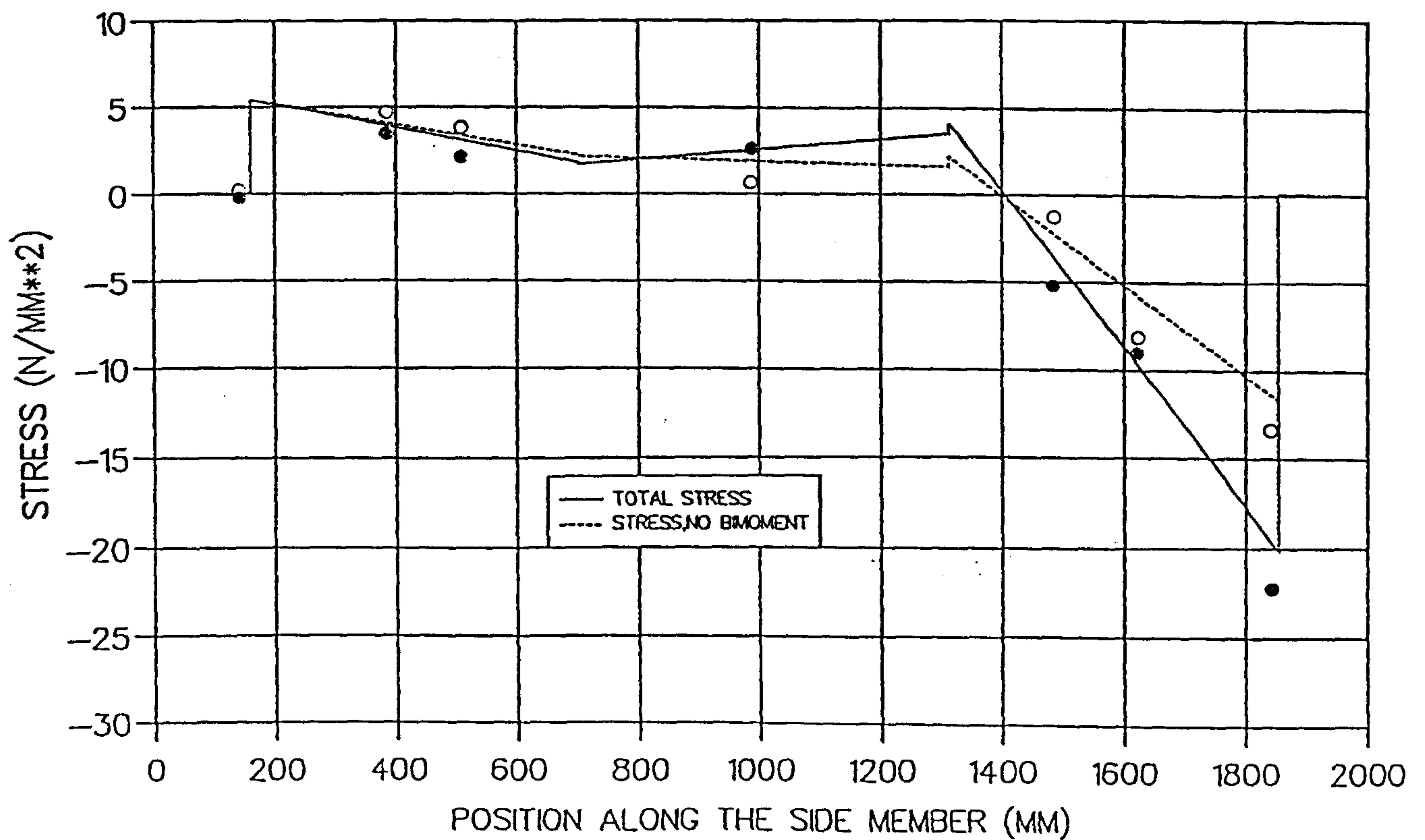
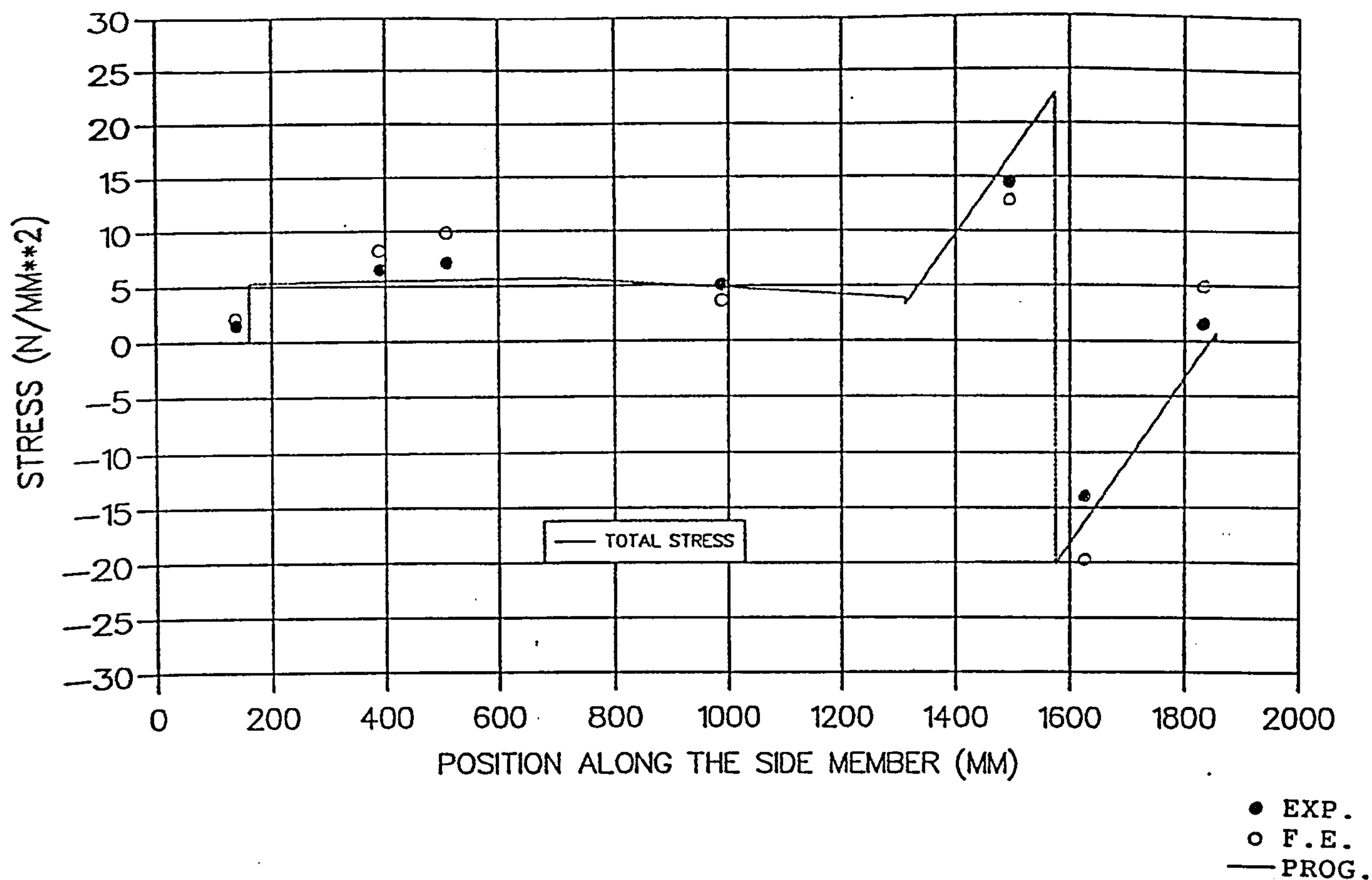


Fig.(9.4) Stress distribution for load-case No.1, when the load (p) is applied at position (2)

A) NODES AT THE FLANGE, STATION A (SEE FIG. 9.2)



B) NODES AT THE WEB, STATION B (SEE FIG. 9.2)

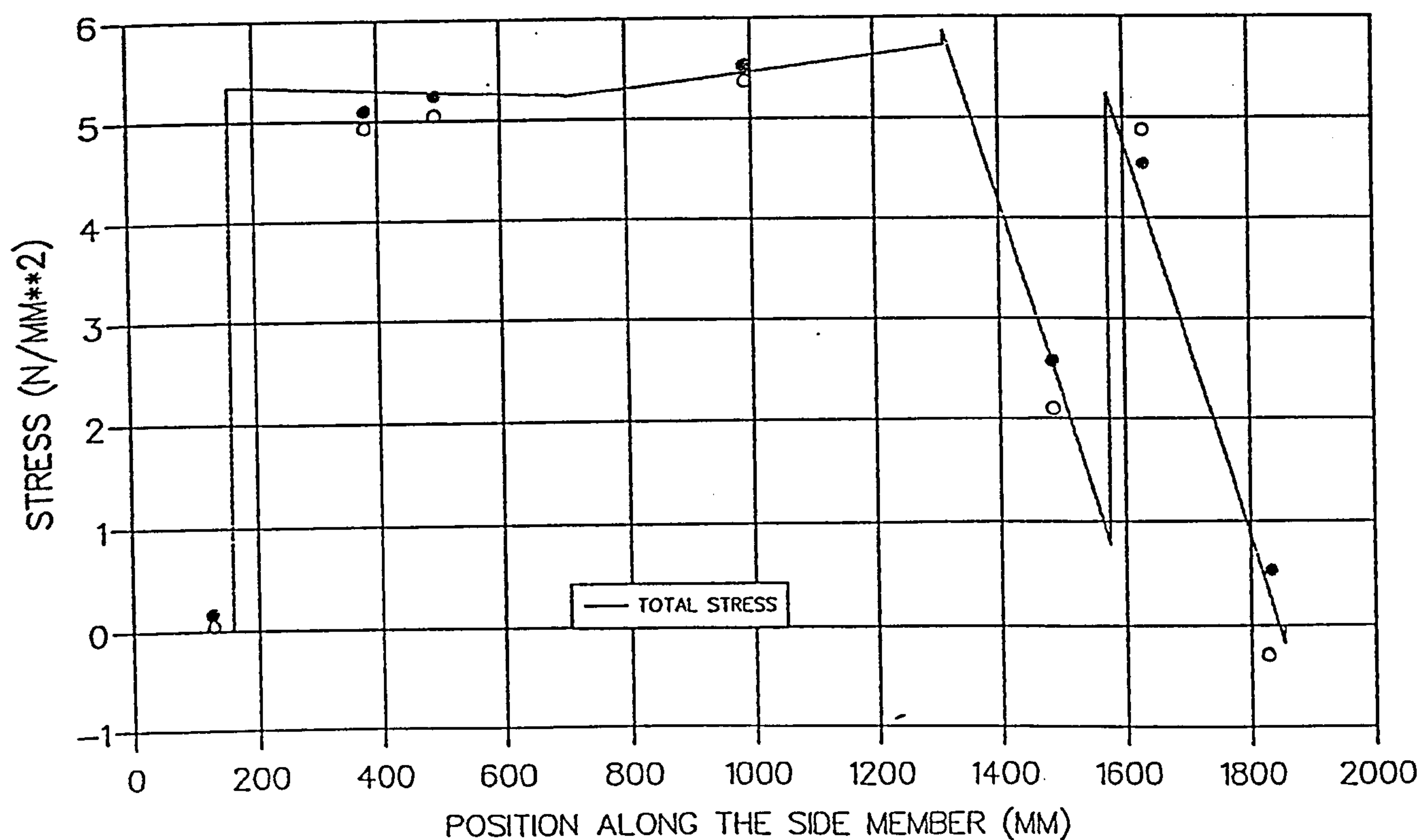
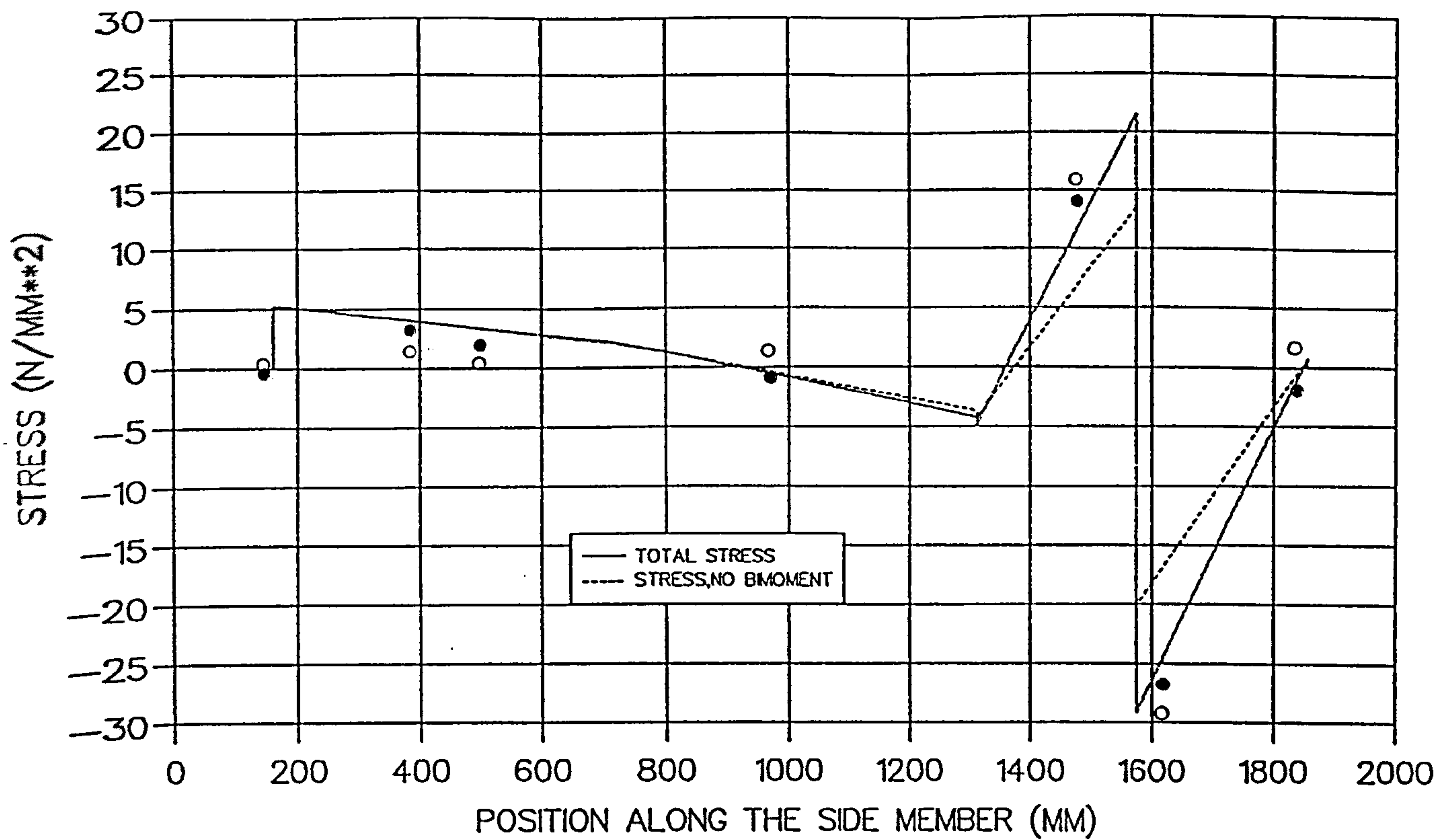


Fig.(9.5) Stress distribution for load-case No.2, when the load (p) is applied at position (1)

A) NODES AT THE FLANGE, STATION A (SEE FIG. 9.2)



B) NODES AT THE WEB, STATION B (SEE FIG. 9.2)

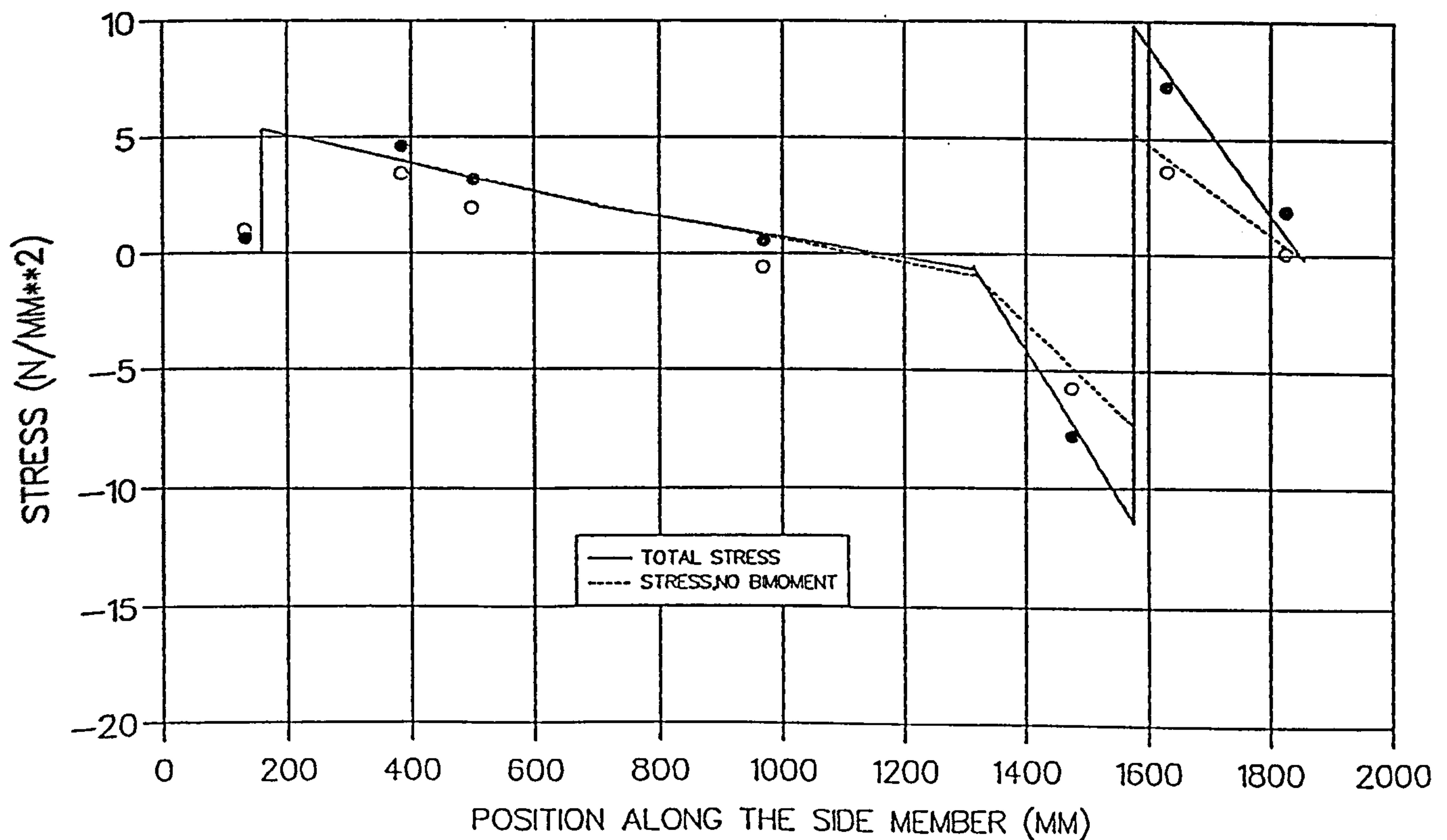
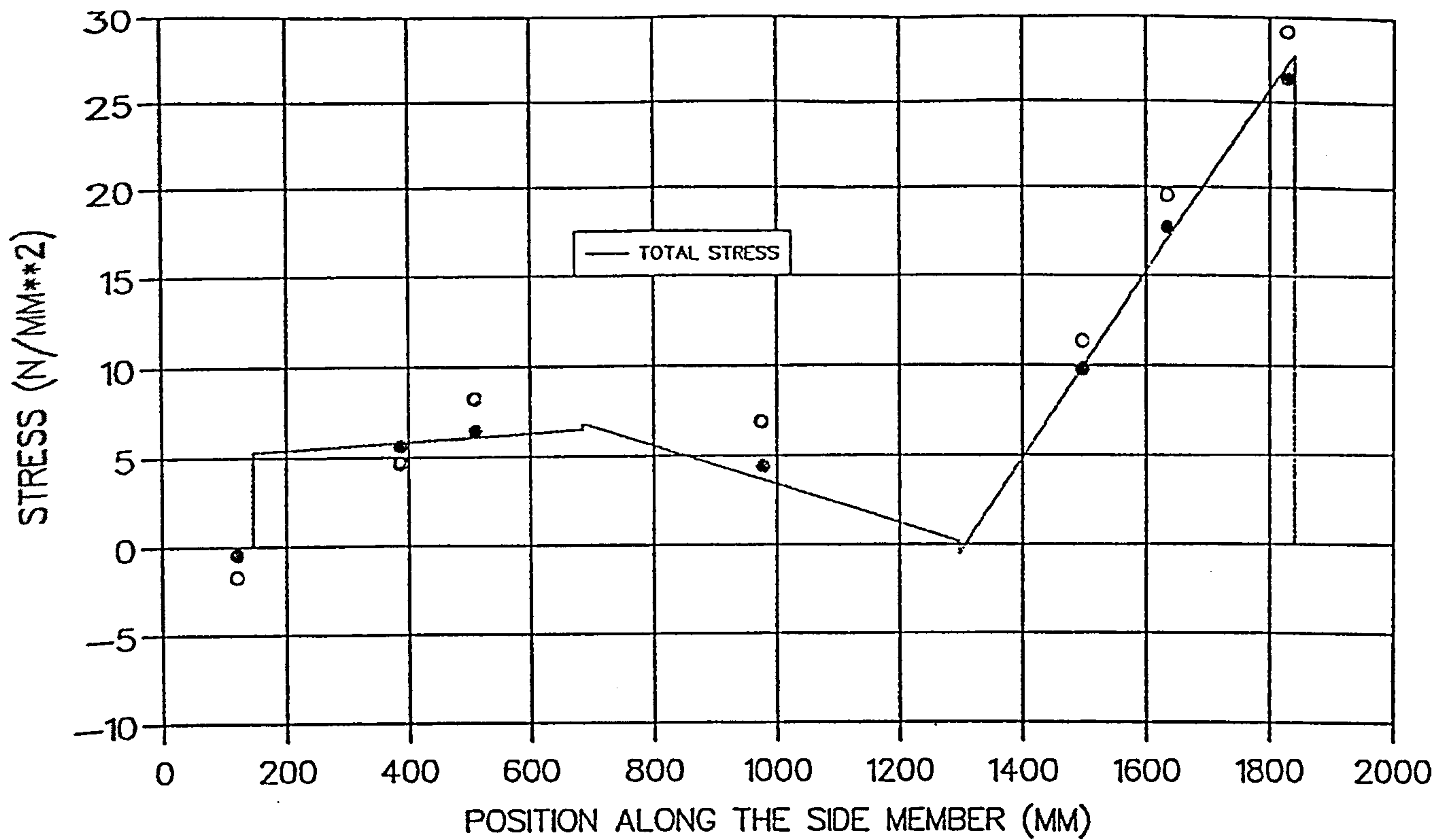


Fig.(9.6) Stress distribution for load-case No.2, when the load (p) is applied at position (2)

A) NODES AT THE FLANGE, STATION A (SEE FIG. 9.2)



B) NODES AT THE WEB, STATION B (SEE FIG. 9.2)

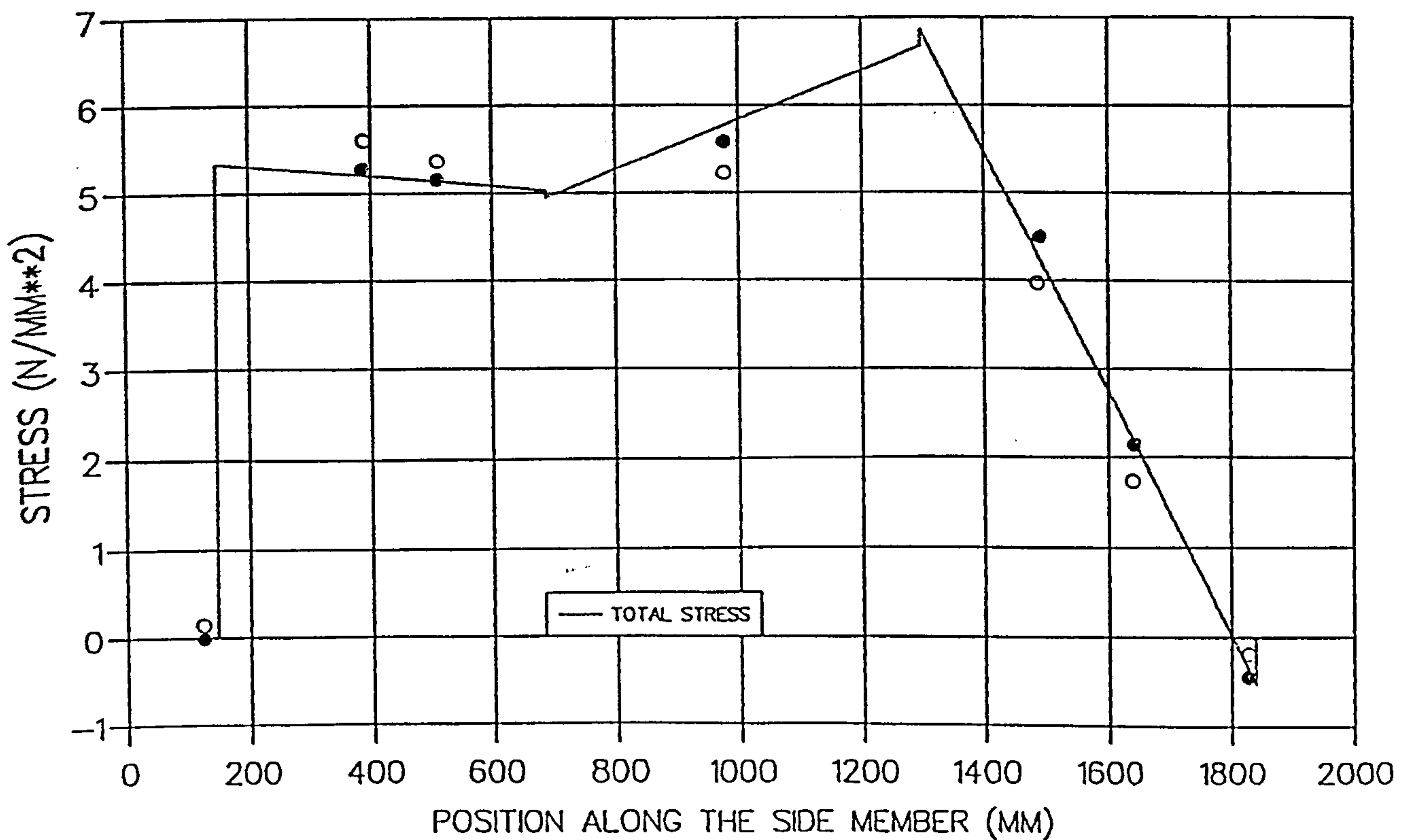
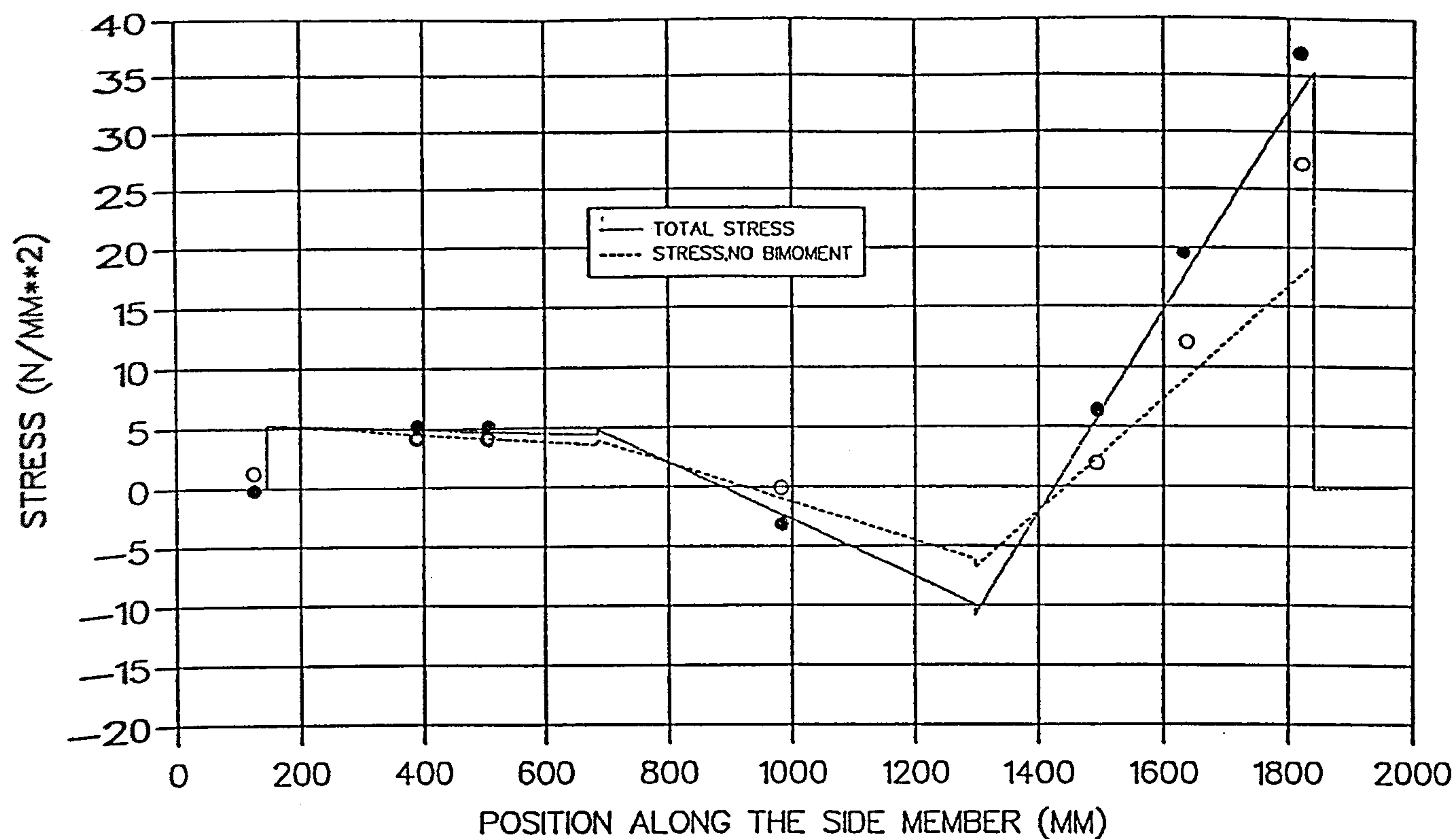


Fig.(9.7) Stress distribution for load-case No.3, when the load (p) is applied at position (1)

A) NODES AT THE FLANGE, STATION A (SEE FIG. 9.2)



B) NODES AT THE WEB, STATION B (SEE FIG. 9.2)

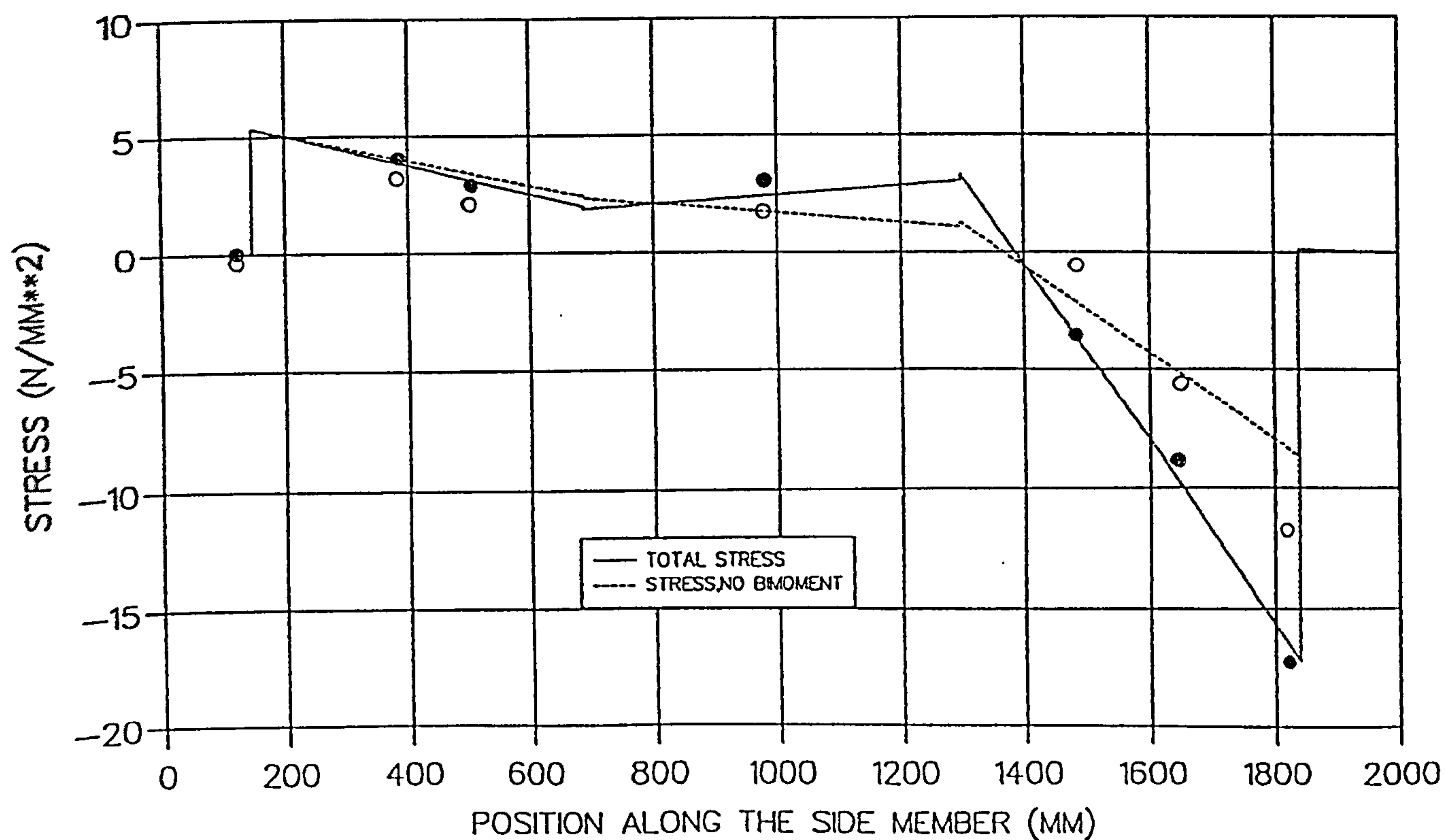
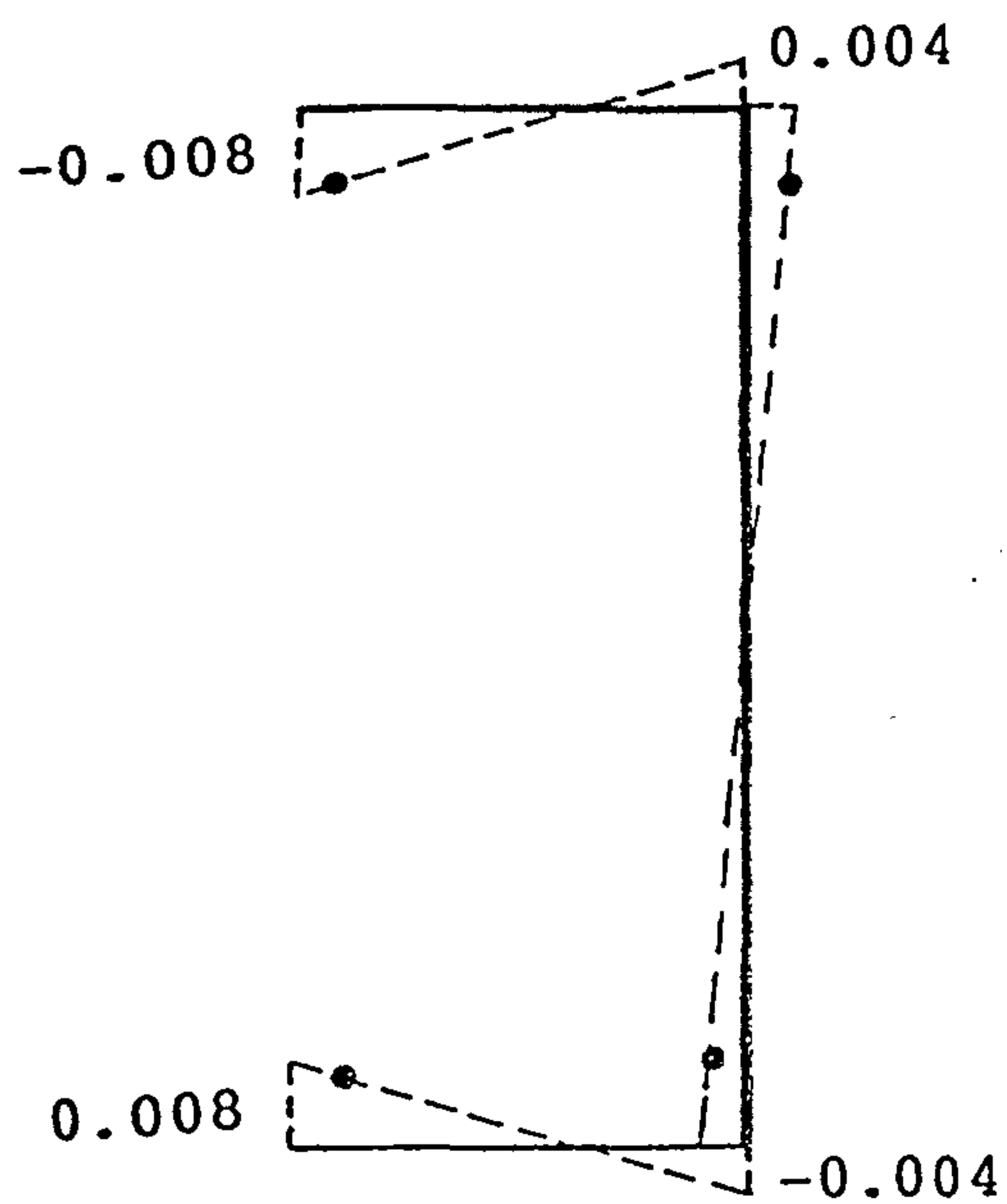
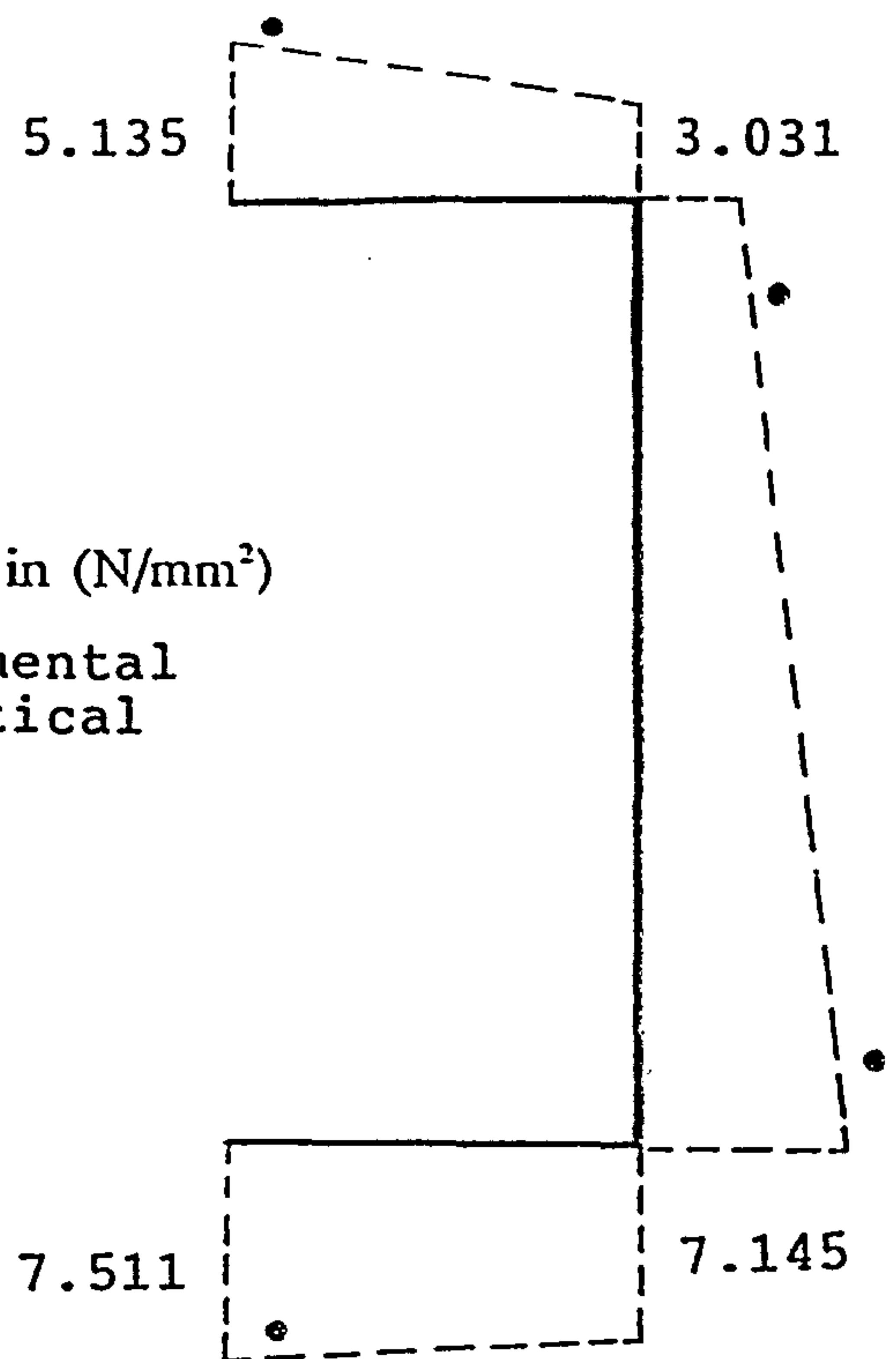


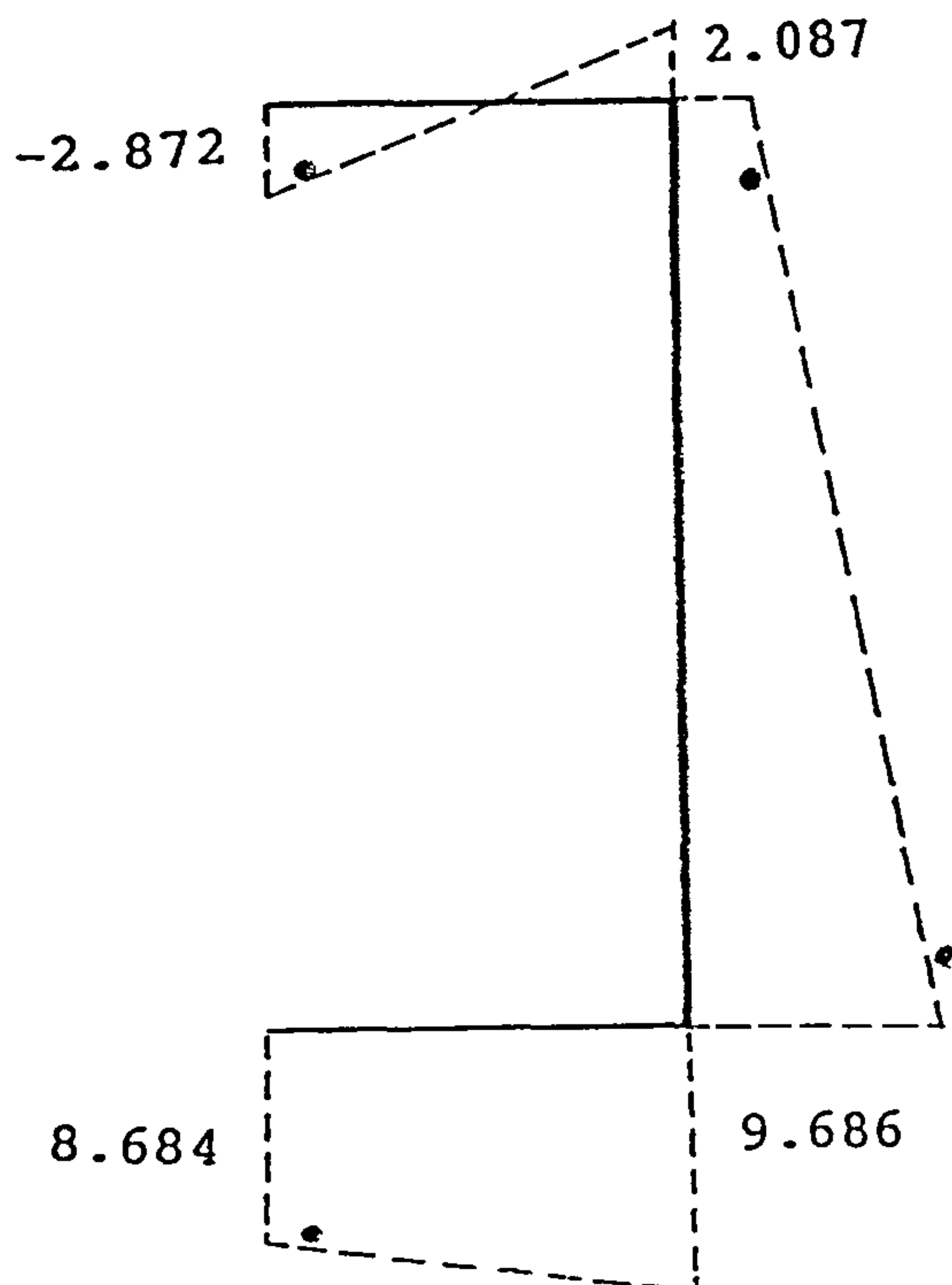
Fig.(9.8) Stress distribution for load-case No.3, when the load (p) is applied at position (2)



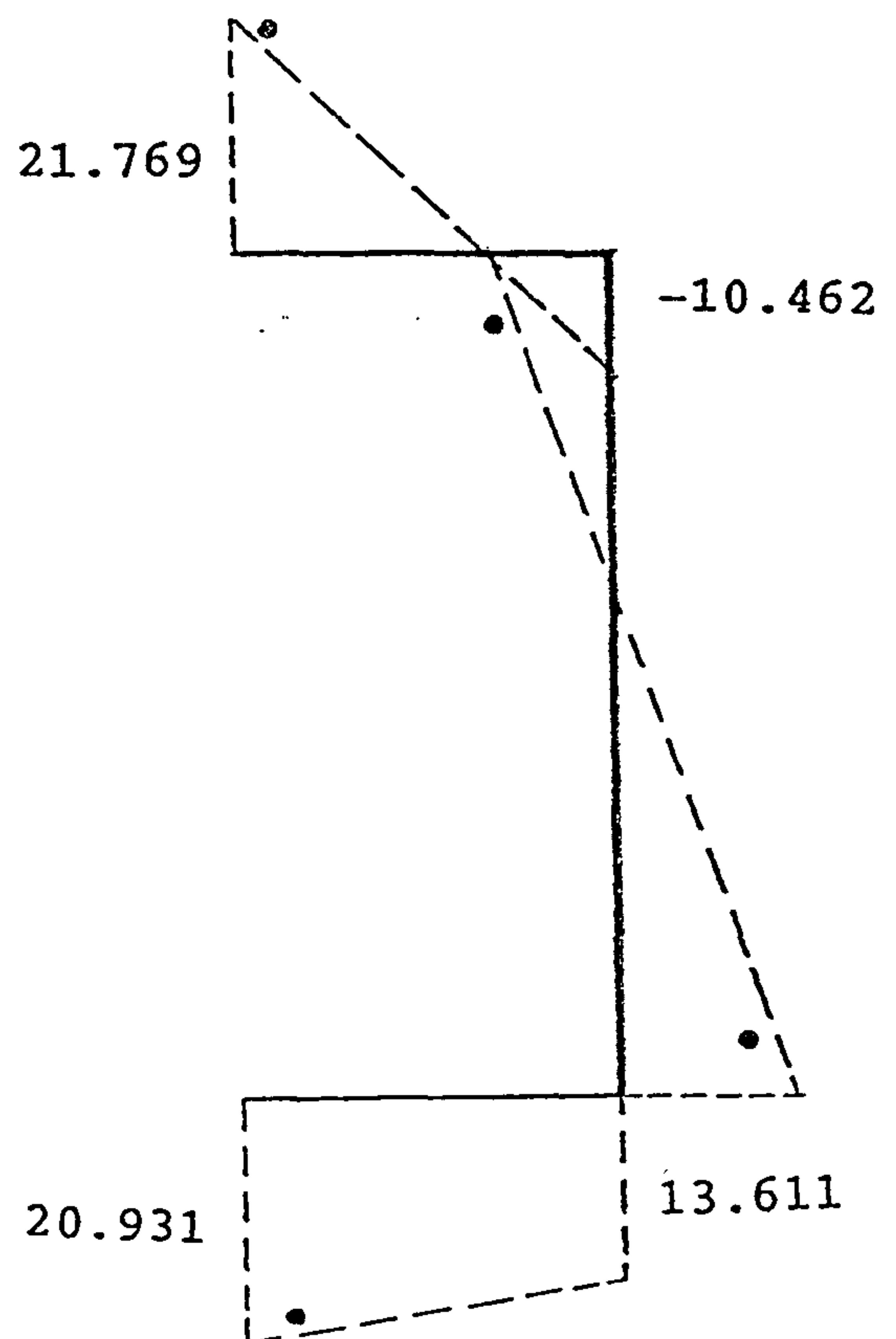
i) section - A -



ii) section - C -

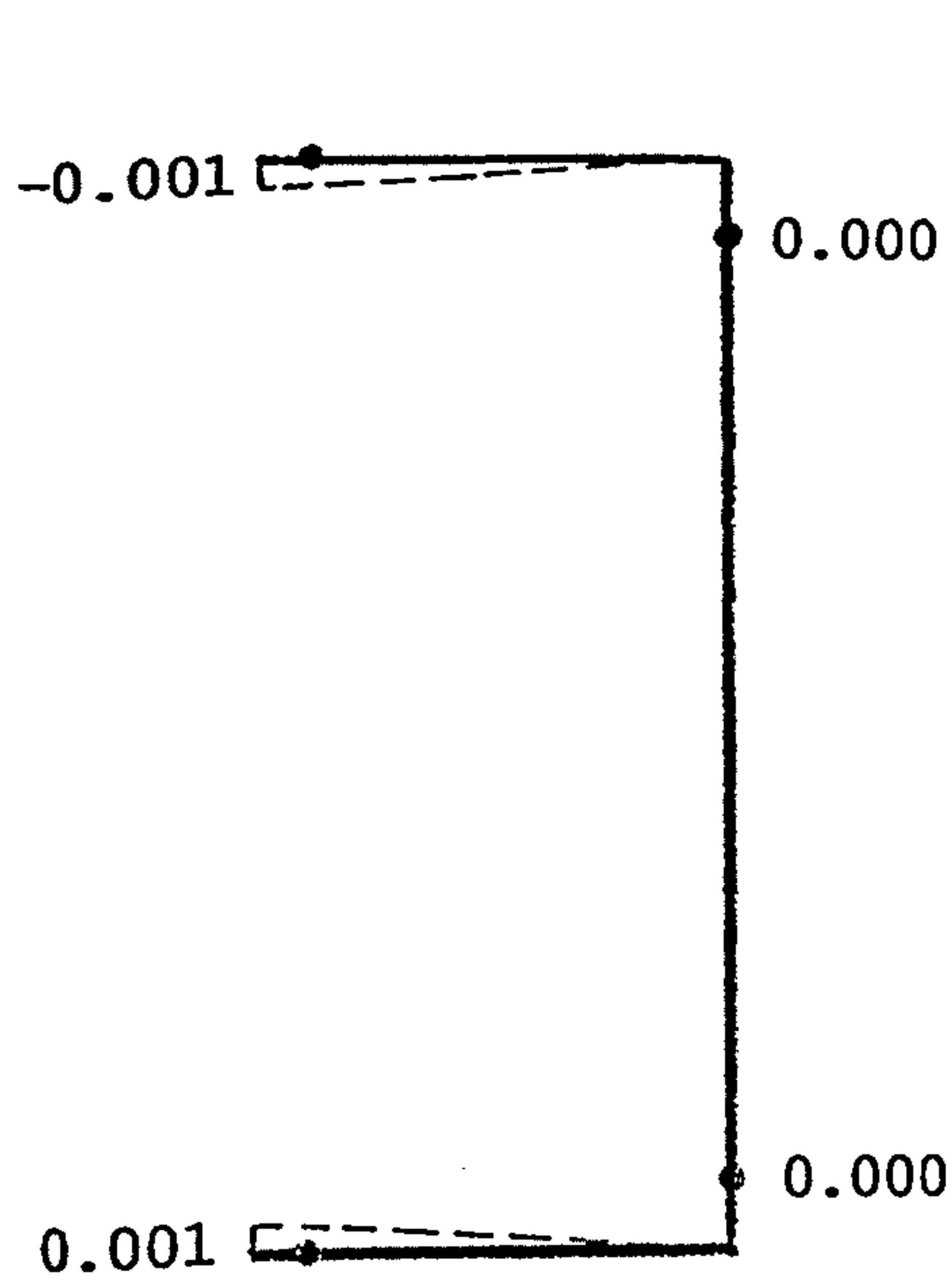


iii) section - D -

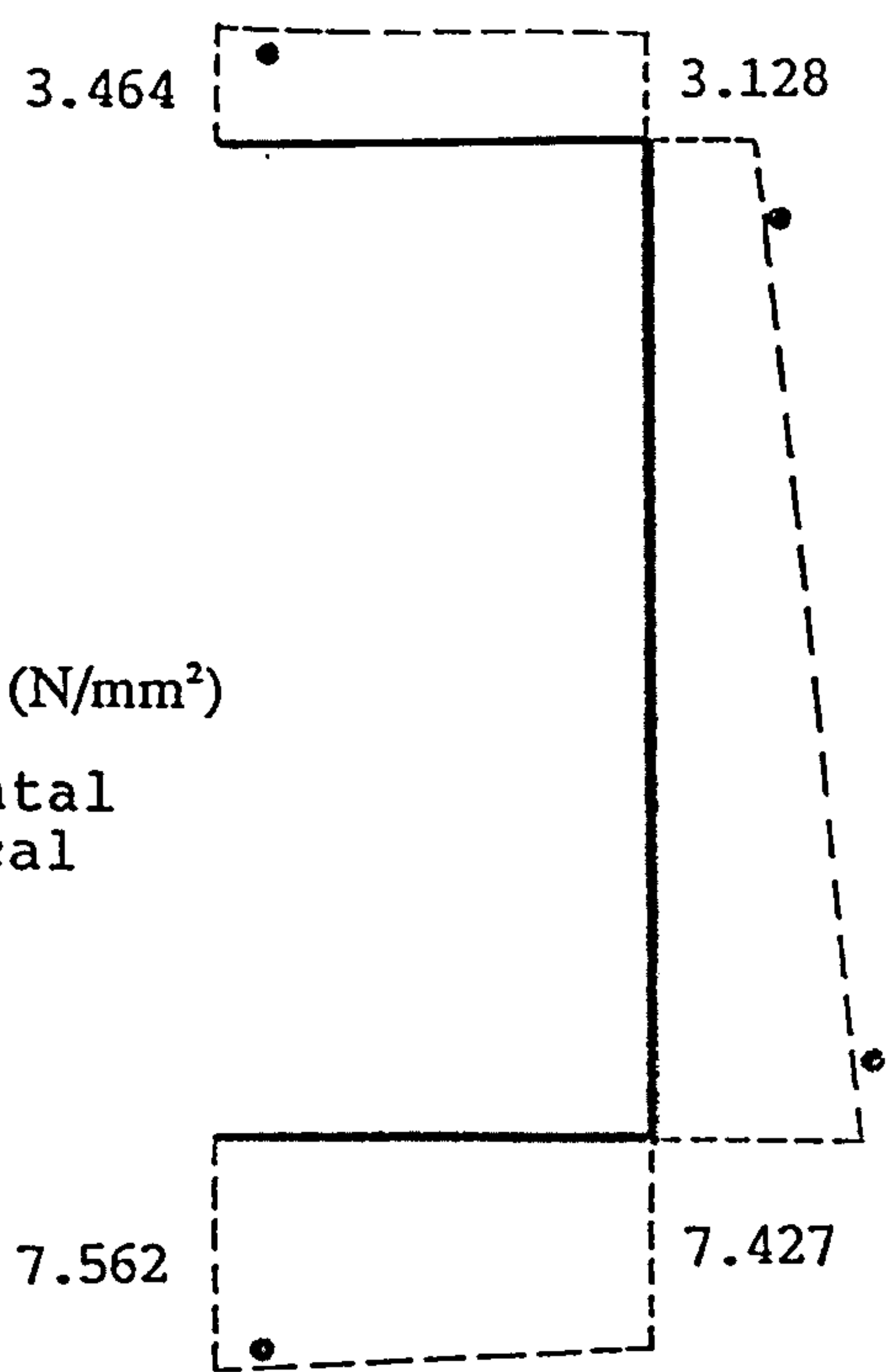


iv) section - F -

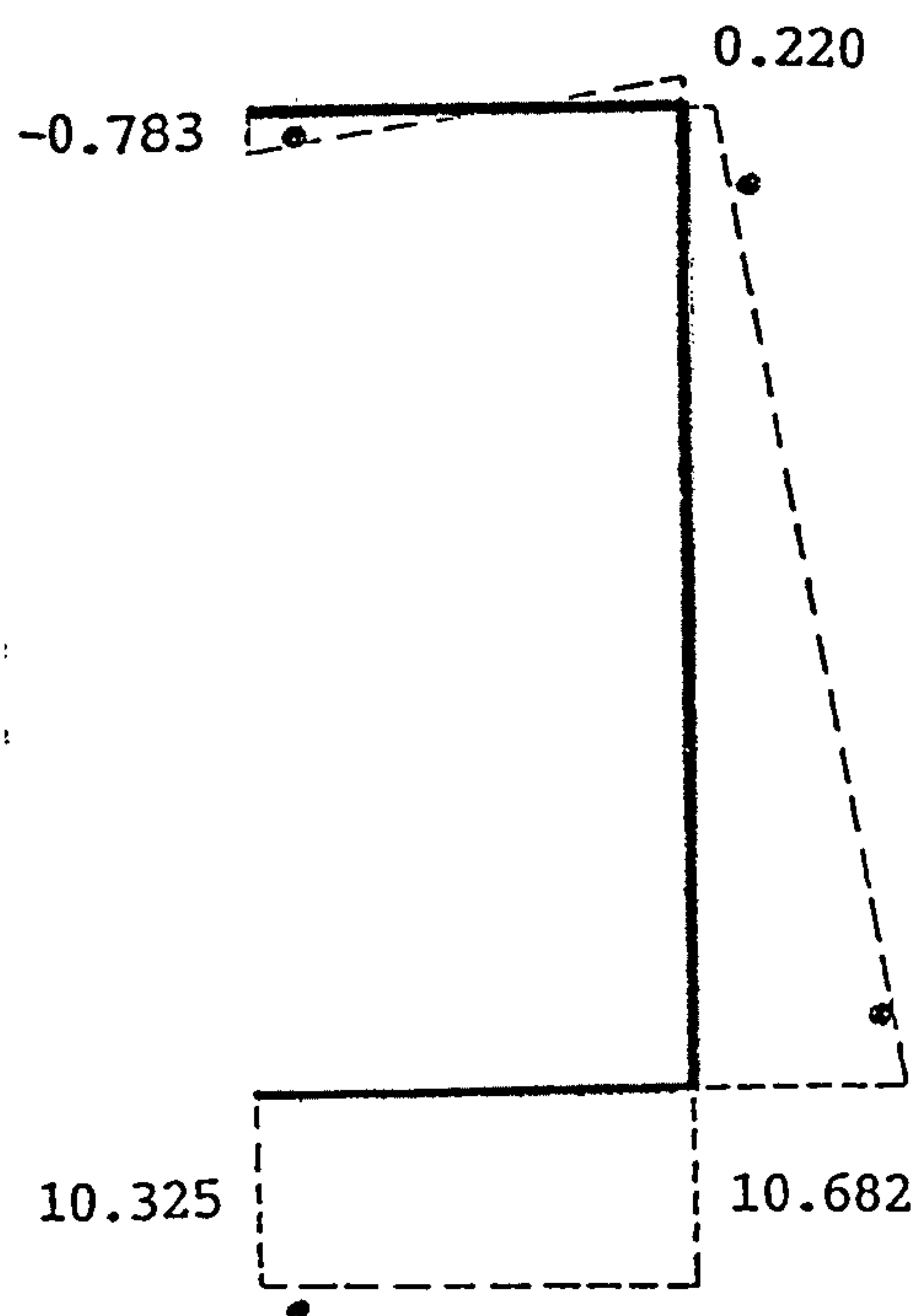
Fig.(9.9) Total stresses around selected cross sections of the side member, see fig.(9.2), for loading-case No.1, when the load (P) is applied at position (2).



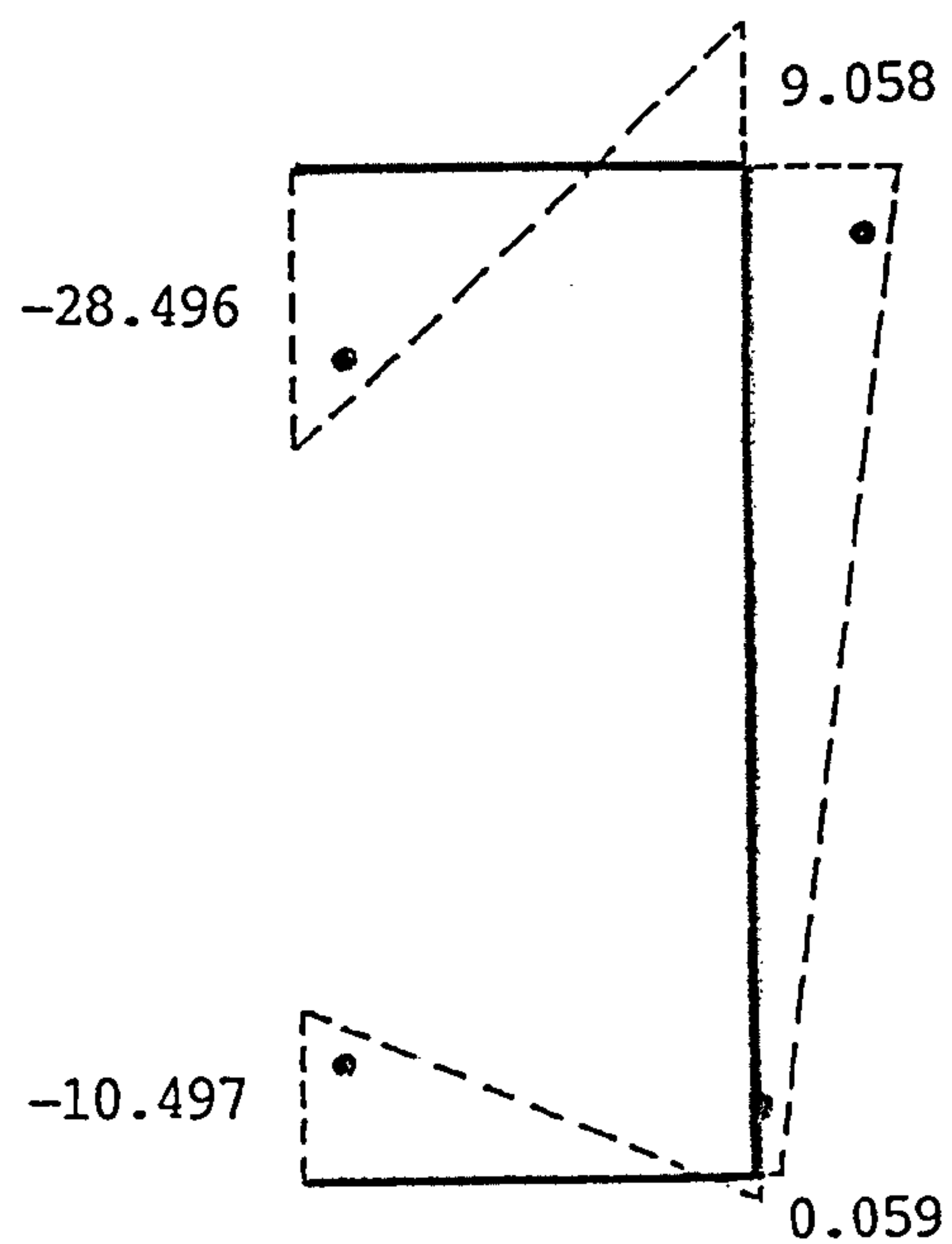
i) Section - A -



ii) Section - C -

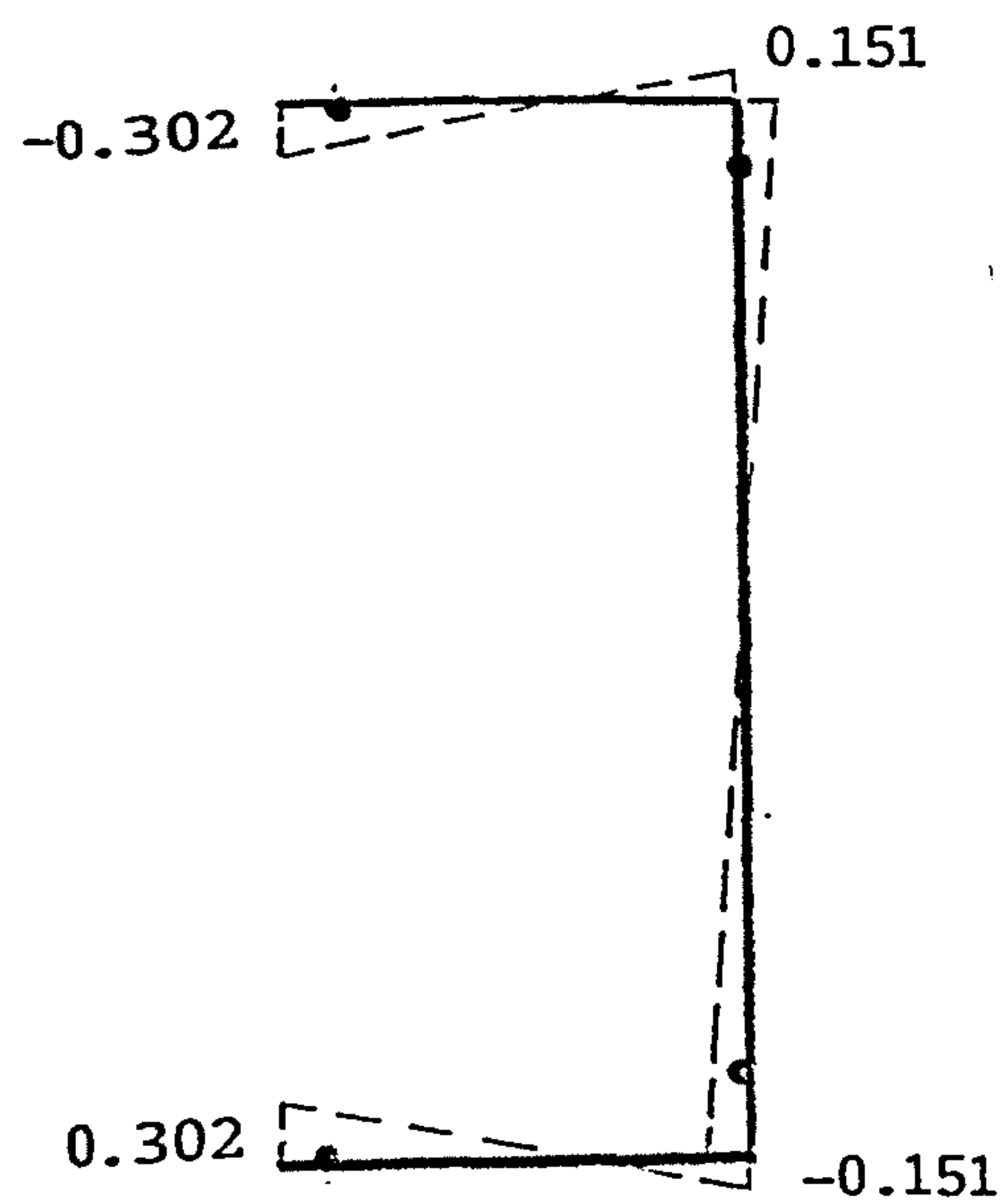


iii) Section - D -

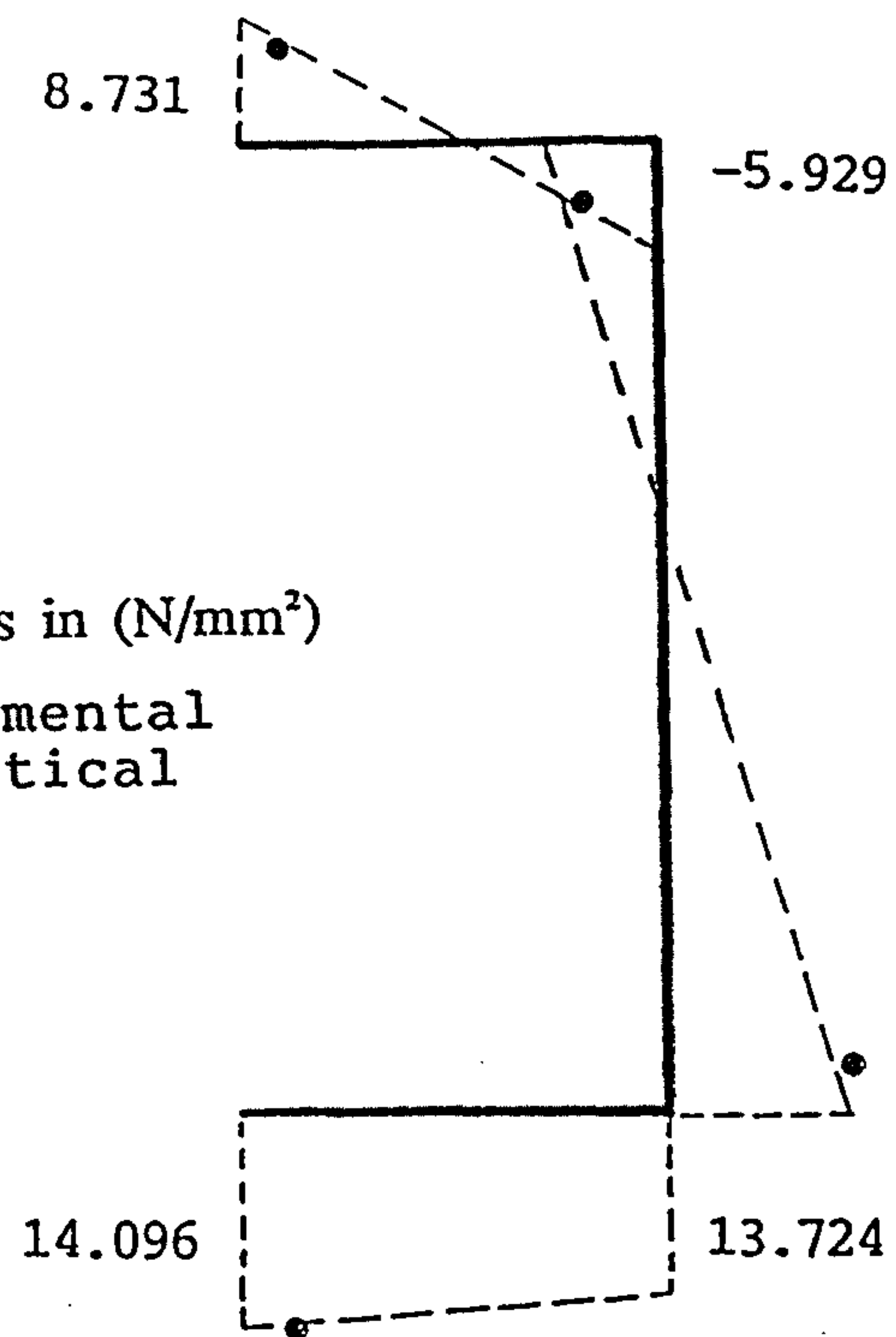


iv) Section - F -

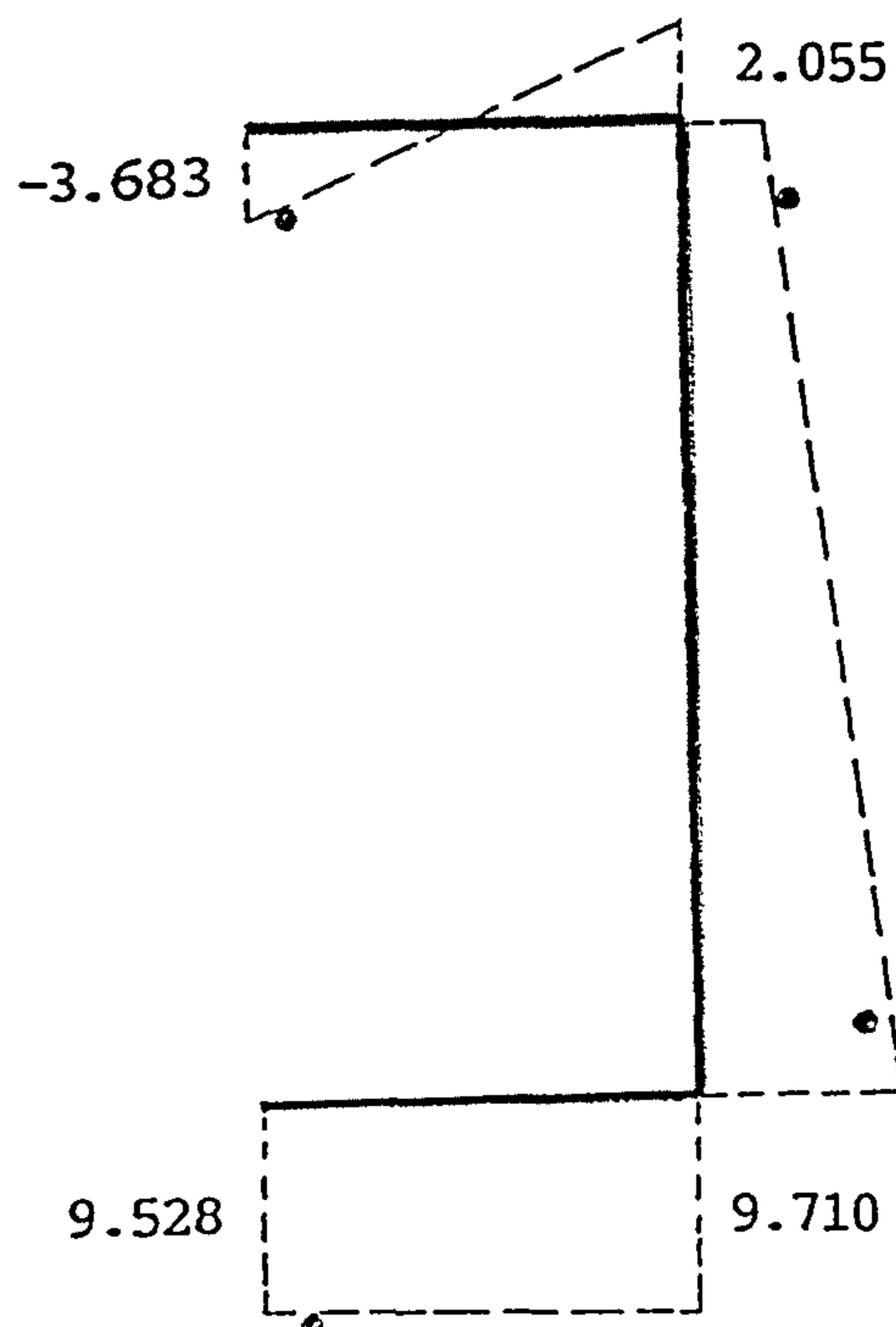
Fig.(9.10) Total stresses around selected cross sections of the side member, see fig.(9.2), for loading-case No.2, when the load (P) is applied at position (2).



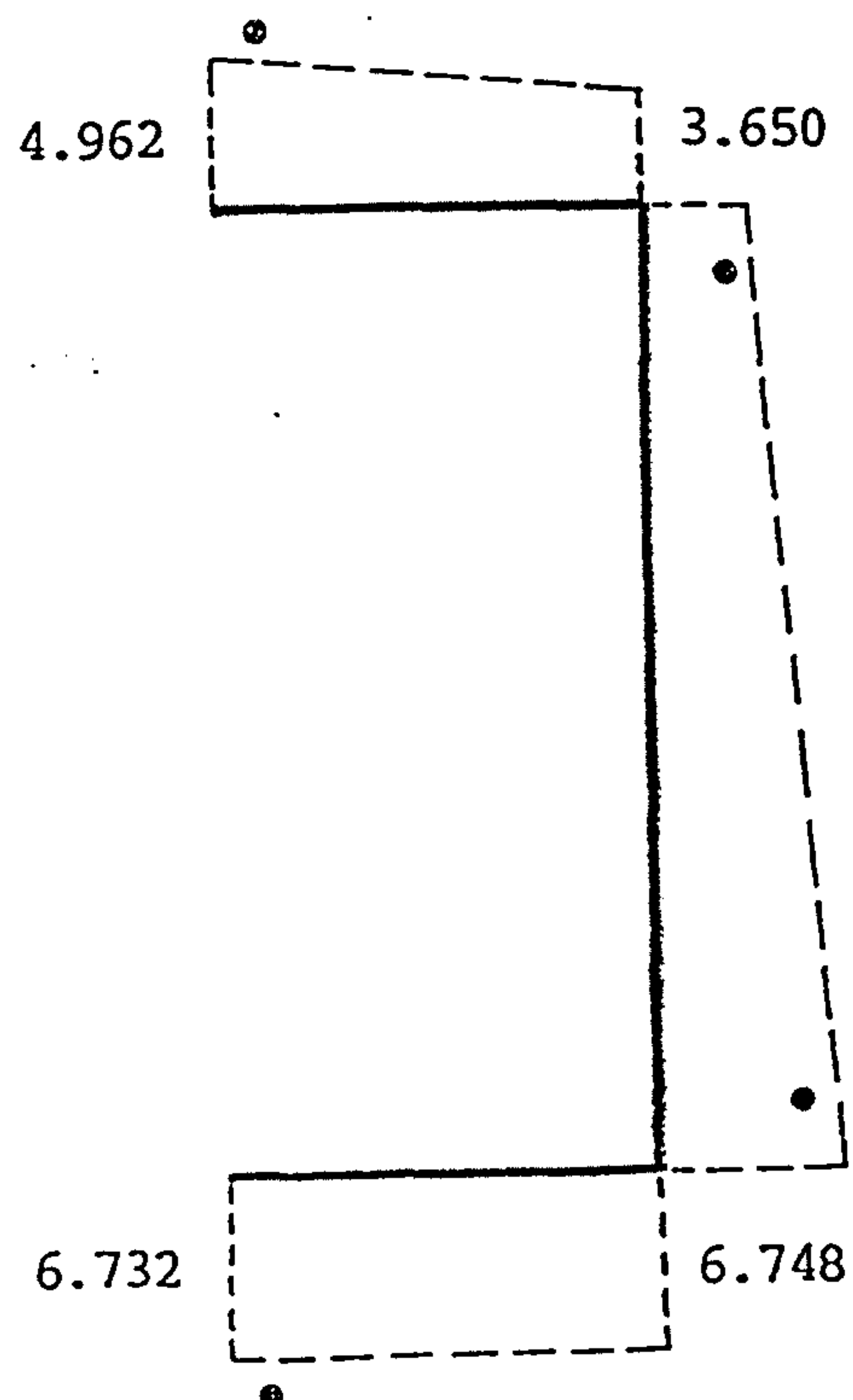
i) Section - A -



ii) Section - C -



iii) Section - D -



iv) Section - F -

Fig.(9.11) Total stresses around selected cross sections of the side member, see fig.(9.2), for loading-case No.3, when the load (P) is applied at position (2).

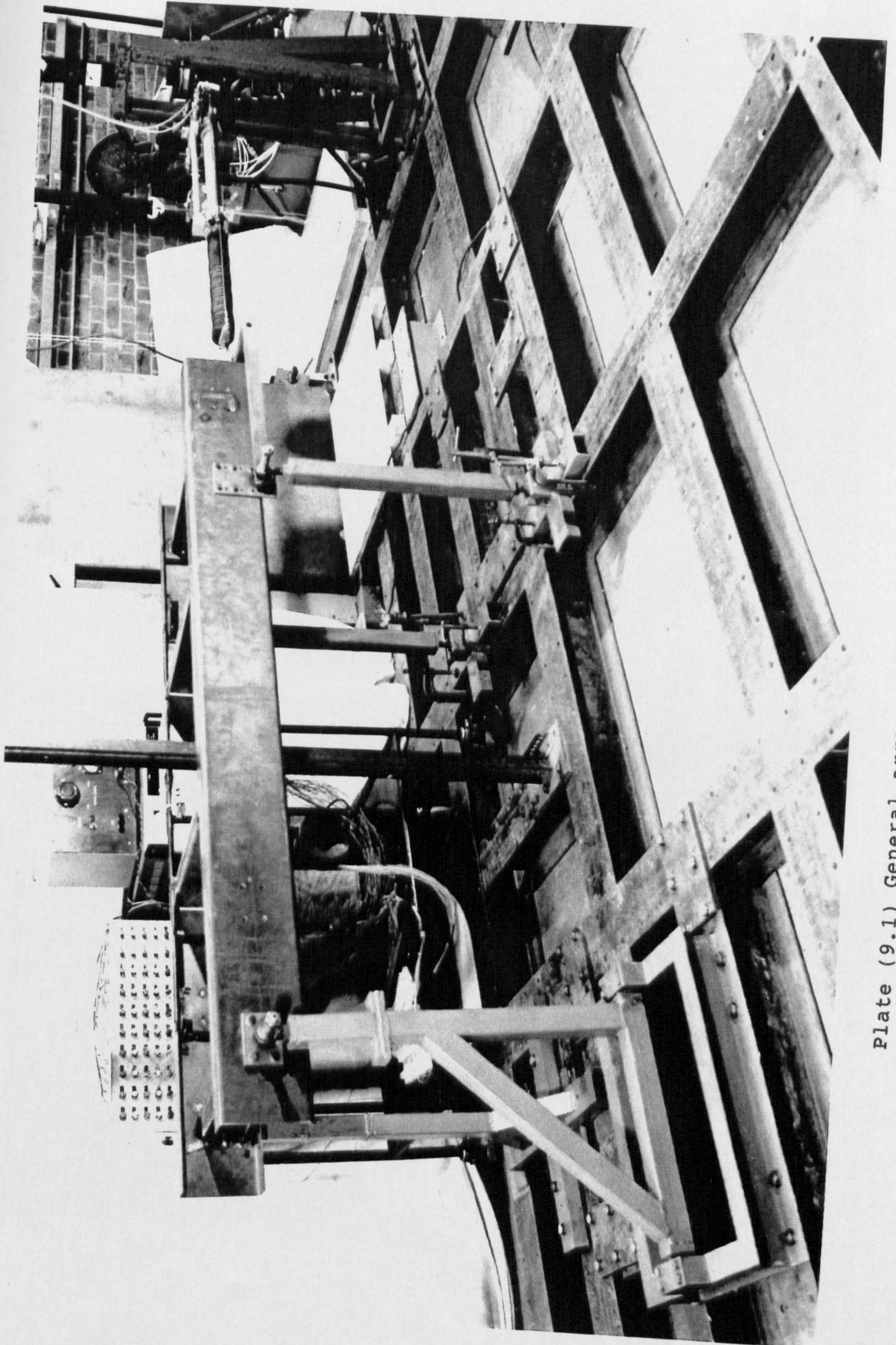
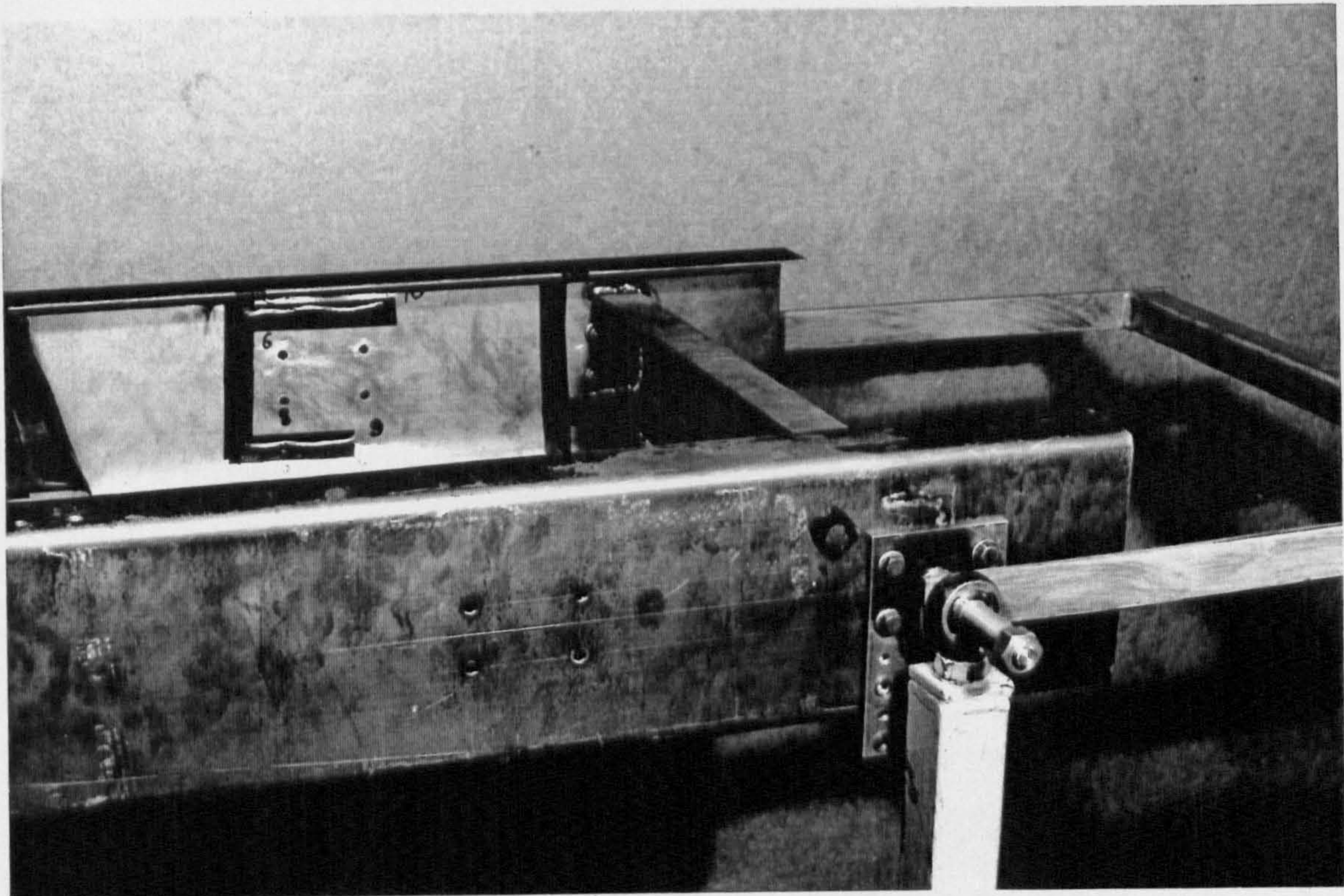
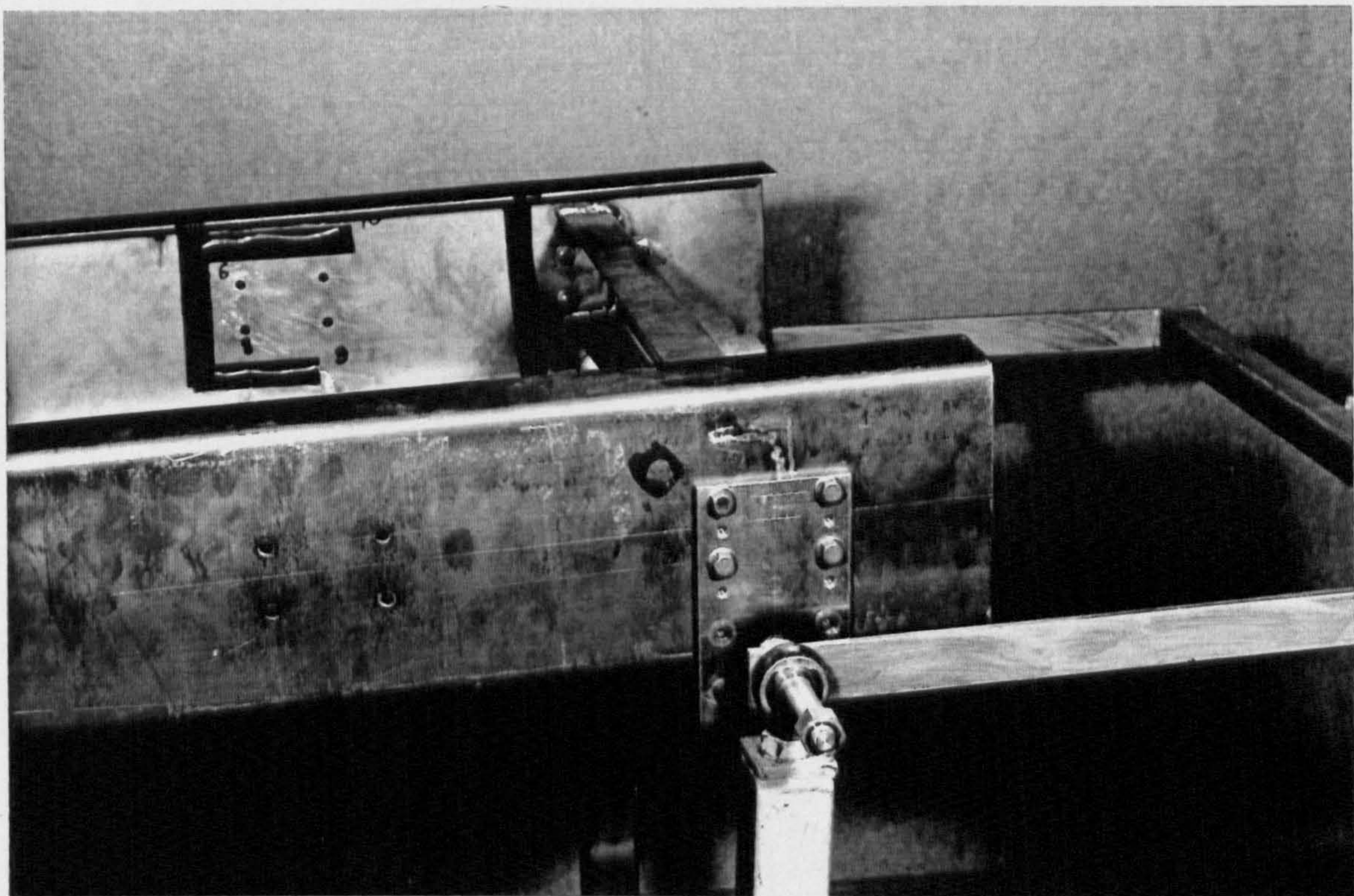


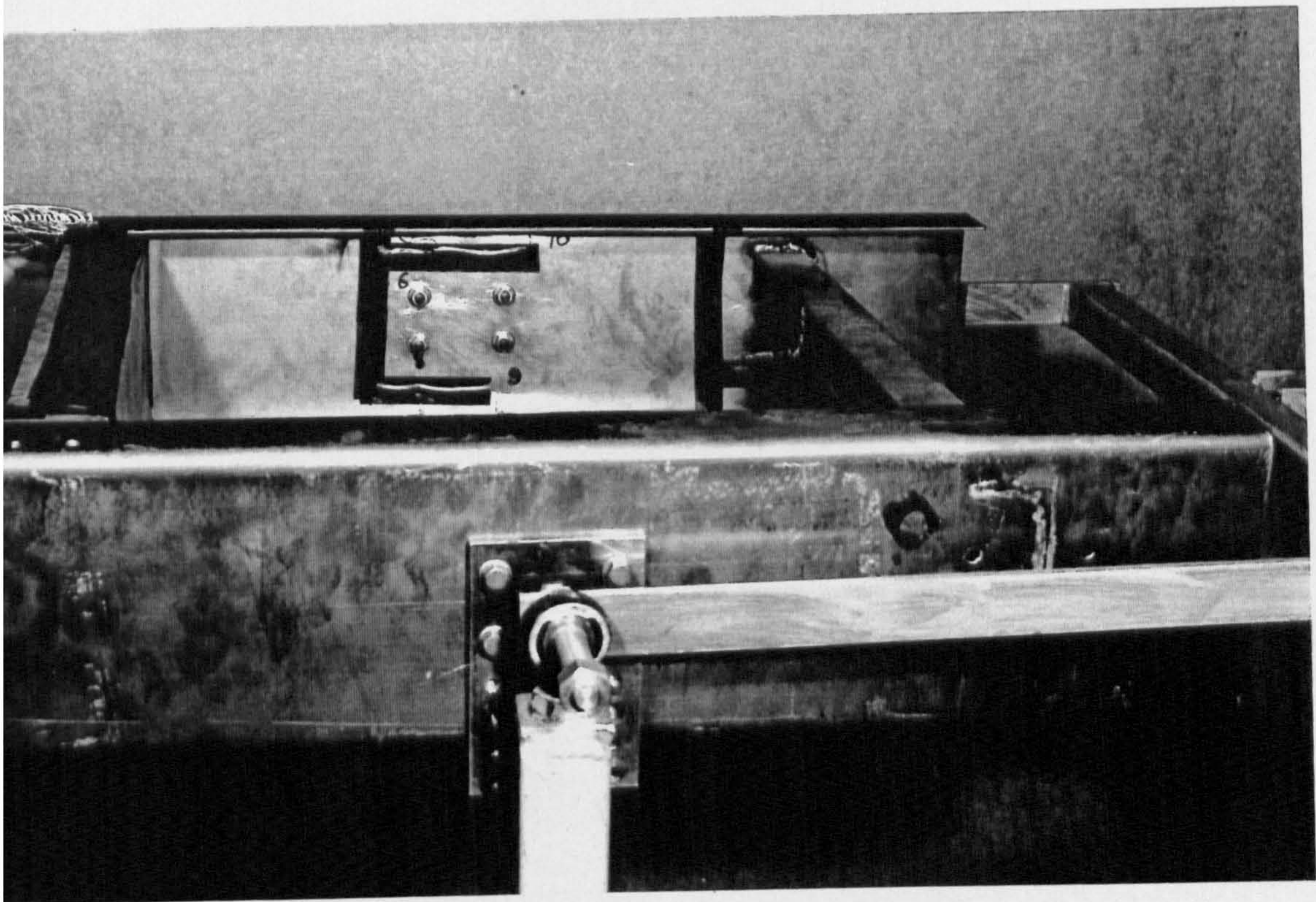
Plate (9.1) General arrangement of chassis test rig



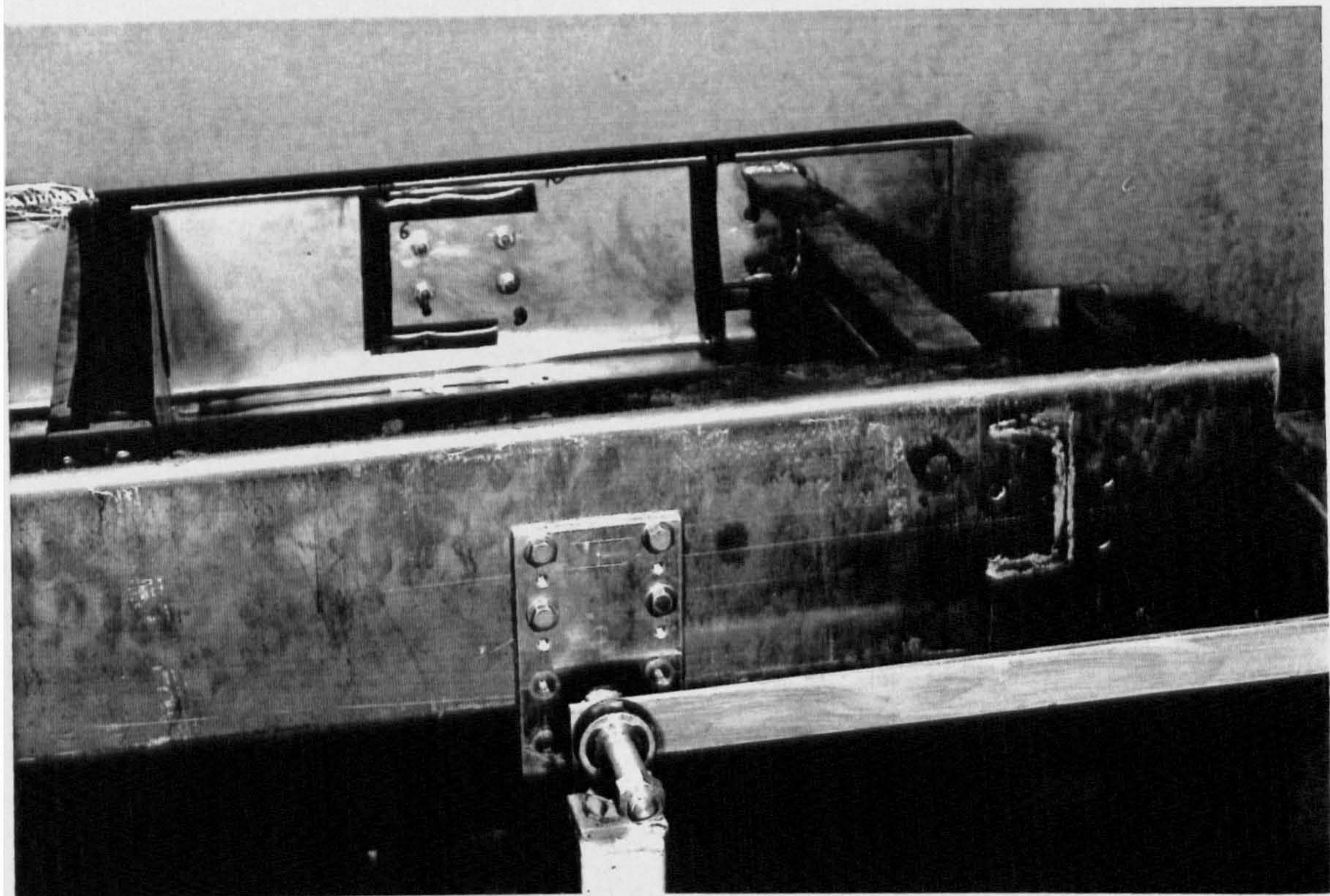
a) position - 1 -



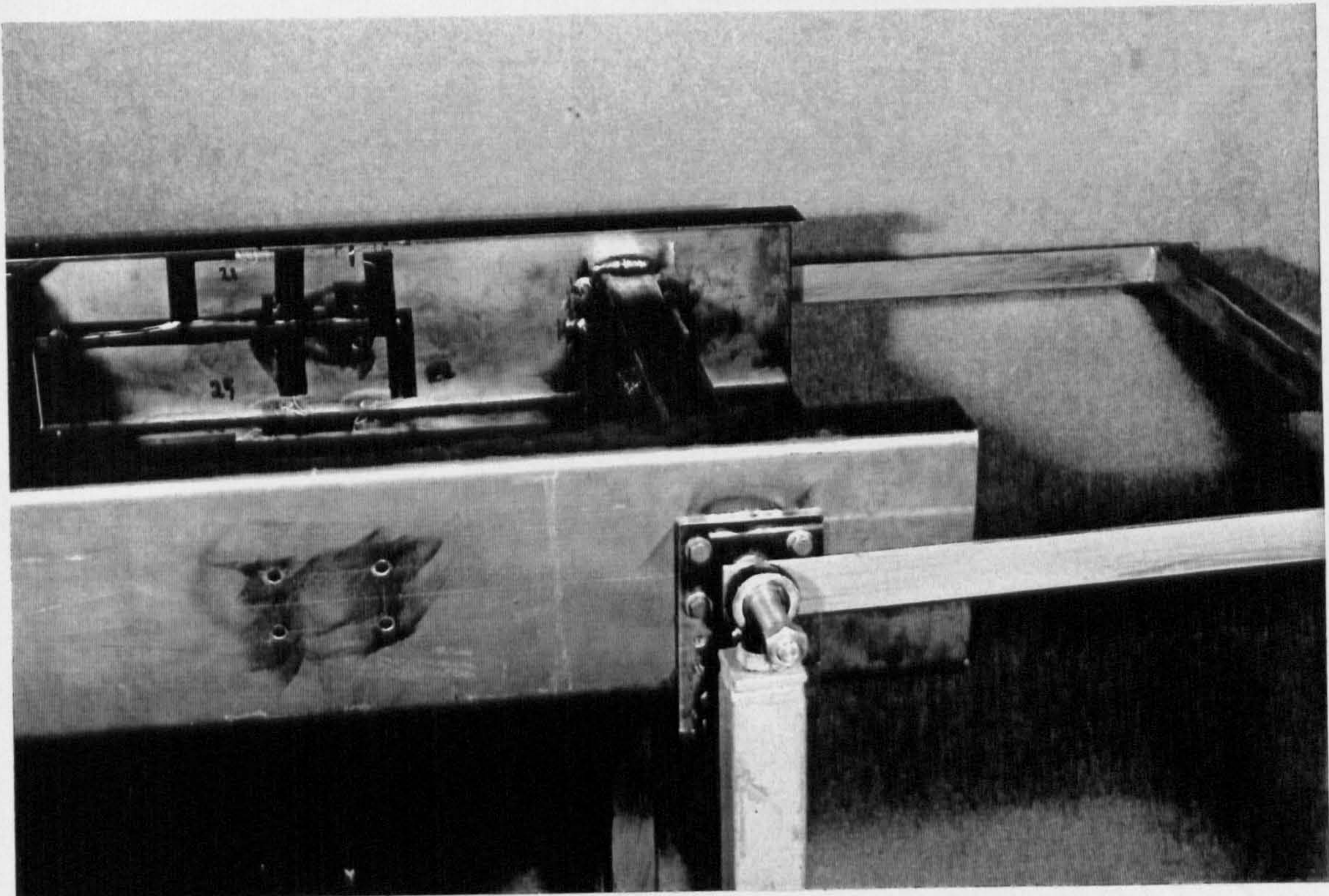
b) position - 2 -



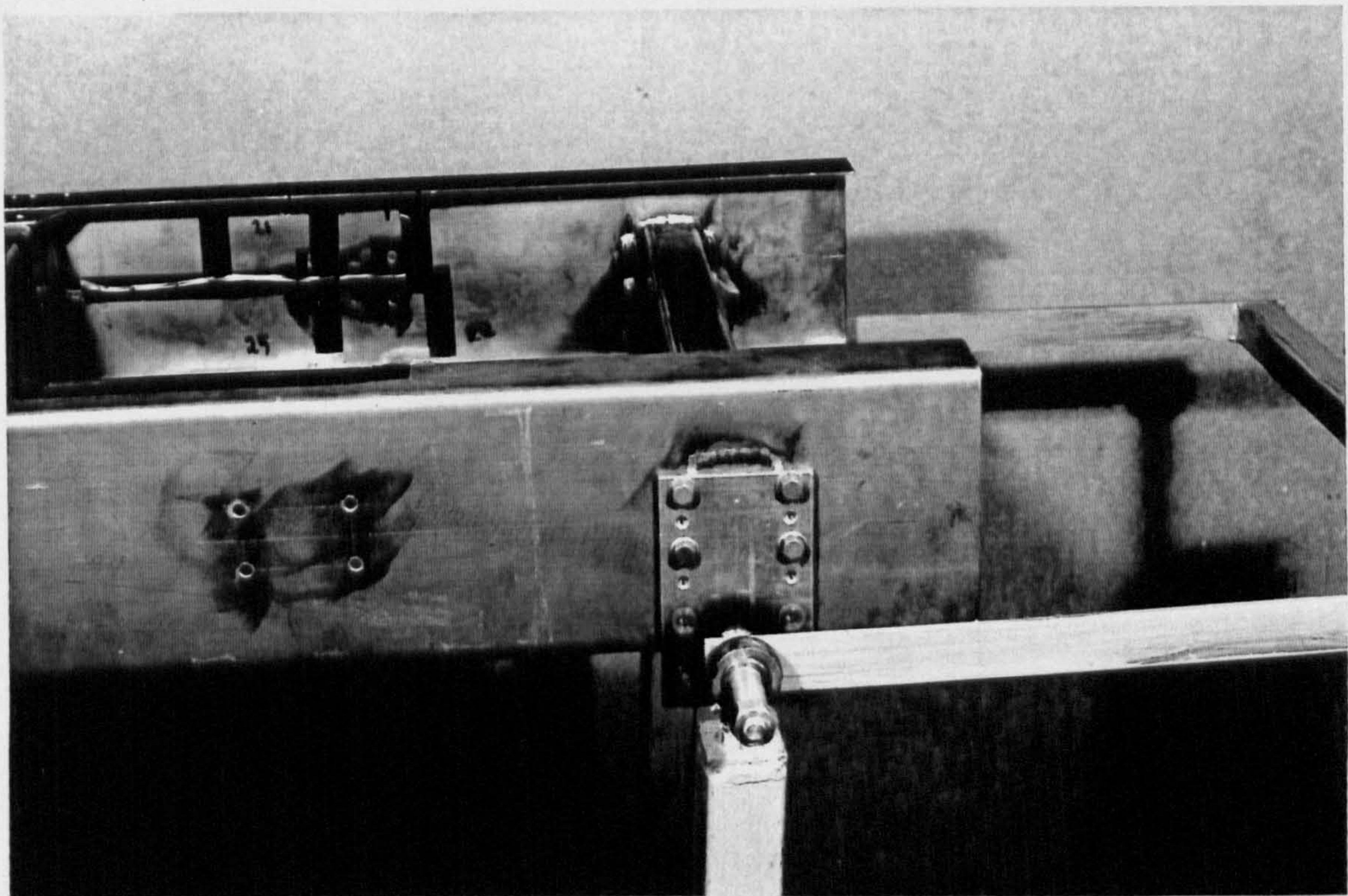
a) position - 1 -



b) position - 2 -



a) position - 1 -



b) position - 2 -

CHAPTER TEN

CONCLUSIONS

10.1 GENERAL

Two load cases for commercial vehicle chassis frames are;-

- a) Torsion due to anti-symmetric vertical loading of the chassis.
- b) The longitudinal load due to braking or acceleration, acting through the spring hanger bracket.

These loadings are relatively independent of each other, and in practical cases may vary considerably in magnitude under different dynamic conditions. The chassis dimensions and material would vary with different designs.

This project dealt with the problems of these loadings. The analysis of the stress distribution in open section side members of commercial vehicle chassis frames under the effects of the previously little studied longitudinal loads which may act on truck chassis has been investigated.

In this chapter the correlation between theoretical and experimental approach is discussed. Suggestions for the optimum design of a spring hanger bracket are discussed from the point of view of longitudinal loading.

10.2 SUMMARY

10.2.1 THEORETICAL INVESTIGATION

The theoretical work undertaken throughout this research is to develop adequate formulae for the analysis of stresses due to longitudinal loads in commercial vehicle chassis frames. In particular, the following theoretical studies were conducted:-

- a) Thin walled beam theory introduced by Vlasov was refined and rederived for appropriate loading and boundary conditions.
- b) Longitudinal stresses were derived accordingly.
- c) The governing differential equations of thin walled beams of open and closed

section were also derived and each term of flexural and torsional loading was identified.

- d) A thin walled beam finite element stiffness matrix was introduced for open and closed sections incorporating bimoments, and detailed discussion was then given.
- e) The equilibrium matrix of rigid joints with the effect of different axes offset was introduced for different cross section profile and orientation of the beams meeting at the joint.
- f) Joints were solved by a finite element program I-DEAS and by the theory adopted in this thesis using flexible joint assumptions.
- g) A complete finite element model of a chassis frame under longitudinal loads was solved for different load positions.
- h) A new computer program which incorporates all the above developed theory of warping inhibition effects in thin walled structures such as chassis frames has been written and tested for a complete chassis frame under longitudinal loads.
- i) The bimoment introduced on the side member of the chassis frame due to longitudinal loading for different bracket connections and different loading positions was studied experimentally and the results were used to validate the theoretical and finite element results.

10.2.2 EXPERIMENTAL INVESTIGATION

The experimental investigation provided several interesting results. It was the experimental evidence reference which first revealed the presence, magnitude and extent of warping stresses in the side members due to the longitudinal loading. This, together with results from the finite element analysis, lead to the conclusion that the side member web allows the distortion in the cross members ends because of the out of plane flexibility of the side member web.

To further assess the effects of loading position along the side member in the experiment, a series of tests were undertaken on the chassis frame model with the longitudinal loads applied at different locations along the side member. For each load-case two different load positions were investigated.

When the longitudinal load (p) was applied in position (1), it was expected that only direct load and moment about the vertical axis would be introduced into the chassis frame side members. But, when the load was applied at position (2), a bimoment as well as direct load and moment about both vertical and lateral axis were expected to apply to the chassis frame side members.

10.3 DISCUSSION

10.3.1 THEORETICAL ANALYSIS

The ladder type normally used for chassis frames of commercial vehicles appear to be simple structures. They are frequently analysed by simple methods. However, accurate analysis of the stress distributions, are actually quite difficult. Rough estimates based on simplified assumptions are justified, when dimensions of the main members are required in early stages of design.

Therefore, beam elements have been developed which include the effect of constrained warping as shown in chapter (3). These elements are principally formulated for thin walled open section beams.

Closed section thin walled beam cross members are only used occasionally in chassis frame designs, but a simplified method of analysis can be used ignoring the deformation of the profile of the section as shown in chapter (4).

The matrix displacement method can be used to analyse a chassis frame with full continuity of bimoment at the joints, i.e, rigid joint assumptions. In this case the cross member stiffness matrix has to be transformed using the equilibrium matrix as shown in chapter (5), in order to maintain compatibility at the joints.

The equilibrium matrix written out in detail in equation (5-10) can be used for one end of the beam element comprising a cross member when only half the frame is analysed because of symmetry. If the symmetry condition can not be used, each

cross member has two equilibrium matrices on the main diagonal. The signs of the coefficients in the equilibrium matrices are found from figure (5.5). The beam elements have been represented by their centroid axes, and the lengths by the distance between the intersections of these axes.

In the case of flexible joints, the displacement transfer across the joint has to be interpreted with respect to the joint flexibility. A joint element has been introduced and the stiffness matrix of the joint element was obtained from detailed finite element analysis of joints.

10.3.2 FINITE ELEMENT ANALYSIS

A finite element method approach was considered in chapter (7), in its favour this method is extremely versatile and can be used to analyse virtually any linear elastic structure under any loading conditions.

From the point of view of a simple model of joints or chassis frames under investigation the method was quite easy to use. The method also had the added advantage that stresses were calculated throughout the whole chassis frame members.

The disadvantages of the finite element method are many but are generally outweighed by its versatility. The main disadvantage is the cost, the finite element method can only practically be used on a large digital computer. Data preparation can also be tedious and time consuming and although this has improved over recent years it can still take a considerable time to be prepared.

The method also requires a high degree of understanding on the part of the engineer; the choice of element types, the application of load, choice of restraints, mesh design and element density are but a few of the factors which need to be considered for any particular analysis.

Stress discontinuities across element boundaries are a problem. Particular care was exercised across folds in the shell structures analysed.

10.3.3 A.SAFE PROGRAM

The simplified finite element program developed in this research (see chapter 8) employed Vlasov's theory, the resulting linear differential equations were solved using the matrix displacement method. This method was easy to program and could be used on a microcomputer without difficulty. The program also executes very quickly and is therefore cheap. As indicated before the program can be used as a design tool in the preliminary stages of chassis design.

10.3.4 GENERAL

The question of whether open or closed section cross members are most efficient is not one that can be easily answered. It is obvious that fewer or smaller closed section cross members are required to achieve a given frame torsional stiffness with acceptable stress distribution in chassis frame members. This is really a question of structural optimisation, with which the present analysis is not concerned. The methods and the program presented however, provide analytical tools which may be used as part of an optimisation technique.

10.3.5 THE SHAPE OF THE GRAPHS

It is seen in chapter (8), that the shape of the graphs in figure (8.5) for the bimoment distribution at points along the side members due to longitudinal loads acting on the side members of the chassis frame test models are straight lines while the theory suggests curves of hyperbolic functions ($\sinh \mu L$ & $\cosh \mu L$). However, because of the chosen cross-sectional dimensions (see table 7.1) the value of the dimension constant (μ) becomes very small ($\mu = 2.708 \times 10^{-4} \text{ mm}^{-1}$), while the range of (μL) is (0 - 0.542). In that range the shape of the hyperbolic sine and cosine is nearly a straight line. So the shape of the bimoment distribution graph at the points along the beam is approximately a straight line. The graphs would be curves if different cross-sectional dimensions are chosen.

Again the graphs of the stress distribution at the points along the side members (station A and station B) are straight lines instead of curves and that difference is for the same reason which is discussed above for the bimoment graphs.

10.4 PRACTICAL SUGGESTIONS

In commercial vehicles, spring hanger brackets are generally attached to the side member chassis frame. These components can apply longitudinal loads on the side members of the chassis frame.

Since it is proved in this project that quite large bimoment stresses as well as bending and direct stresses would be produced due to the longitudinal loading, it is very important to choose an optimum design for these components on the side members of a chassis frame from the point of view of longitudinal loading. Bimoment stresses depend on ;-

- i) Creation of bimoment due to application of longitudinal load at points where (ω_s) is not zero as shown in figure (6.1).
- ii) For the same position of application of longitudinal load, different bimoment effects are caused by different connections to the section profile as shown in figures (6.3/6.4).

Therefore, careful design of the attachment of the spring hanger brackets is recommended in this thesis, which gives a minimum value of principal sectorial area to the points where the longitudinal load is introduced.

Another factor which affects the warping behaviour and has been investigated in this thesis is the position where the longitudinal load is applied, i.e, position (1) or (2), (see figures 7.16, 7.17, and 7.18). This factor is important because it has a significant effect on the bimoment stresses as well as the bending stresses due to the bending moment about the lateral axis of the chassis frame (i.e. axis 'Y', see figure 5.4). The optimum place for applying longitudinal load is position (2), because the side member would be subjected only to stresses due to direct load and moment about the vertical axis of the chassis frame, while the other components of stress due to bimoment and moment about the lateral axis of the chassis frame are zero.

Some typical spring hanger brackets are shown in figure (10.1). An alternative spring hanger bracket which has been designed to minimize the bimoment created due

longitudinal loads taking into consideration the bolt effects mentioned above, is shown in figure (10.2).

10.5 SUGGESTIONS FOR FURTHER RESEARCH

Further research analysis is required into :-

- 1) Vlasov's thin walled beam theory can be used to derive a stiffness matrix for different types of closed section cross members (other than square or rectangular sections which have been investigated in this thesis).
- 2) The determination of the optimum torsional stiffness of a ladder frame taking into account the stress concentrations at the joints.
- 3) The program presented in this thesis would need only slight modification to analyse tapering members or combinations of tapering and constant section members.
- 4) Calculation of the stress distribution for a combined set of torsional and longitudinal loads. The patterns of the stress distribution for a range of ratios of torsional and longitudinal loads and the changes in the stress distribution with changes in the ratio could be calculated. This is likely to be a worse case than when torsional and longitudinal loads are applied separately.
- 5) Calculation of the stress distribution in chassis members for different chassis designs, i.e, different range of ratios of flange width to web width with thickness.
- 6) Measurement of the magnitude of the longitudinal loads transmitted to the side member of actual truck chassis during dynamic tests on the road.
- 7) Measurement of the stresses developed in the side member of an actual truck chassis due to longitudinal (braking) loads during dynamic tests on the road.
- 8) Comparison of the stress distribution in chassis members obtained from theoretical, laboratory experiments, dynamic tests and finite element models for different designs.

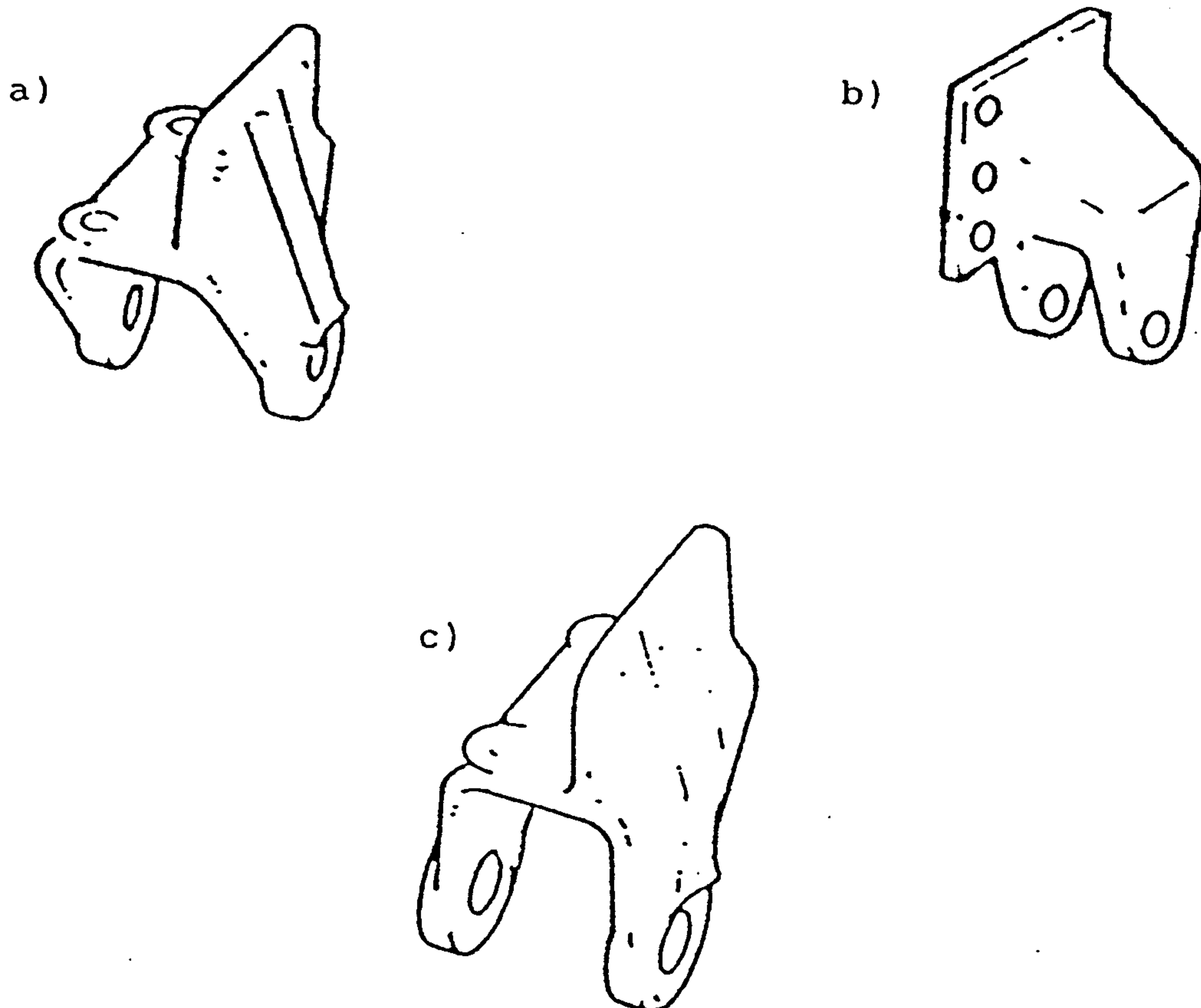


Fig.(10.1) A variety of typical spring hanger brackets

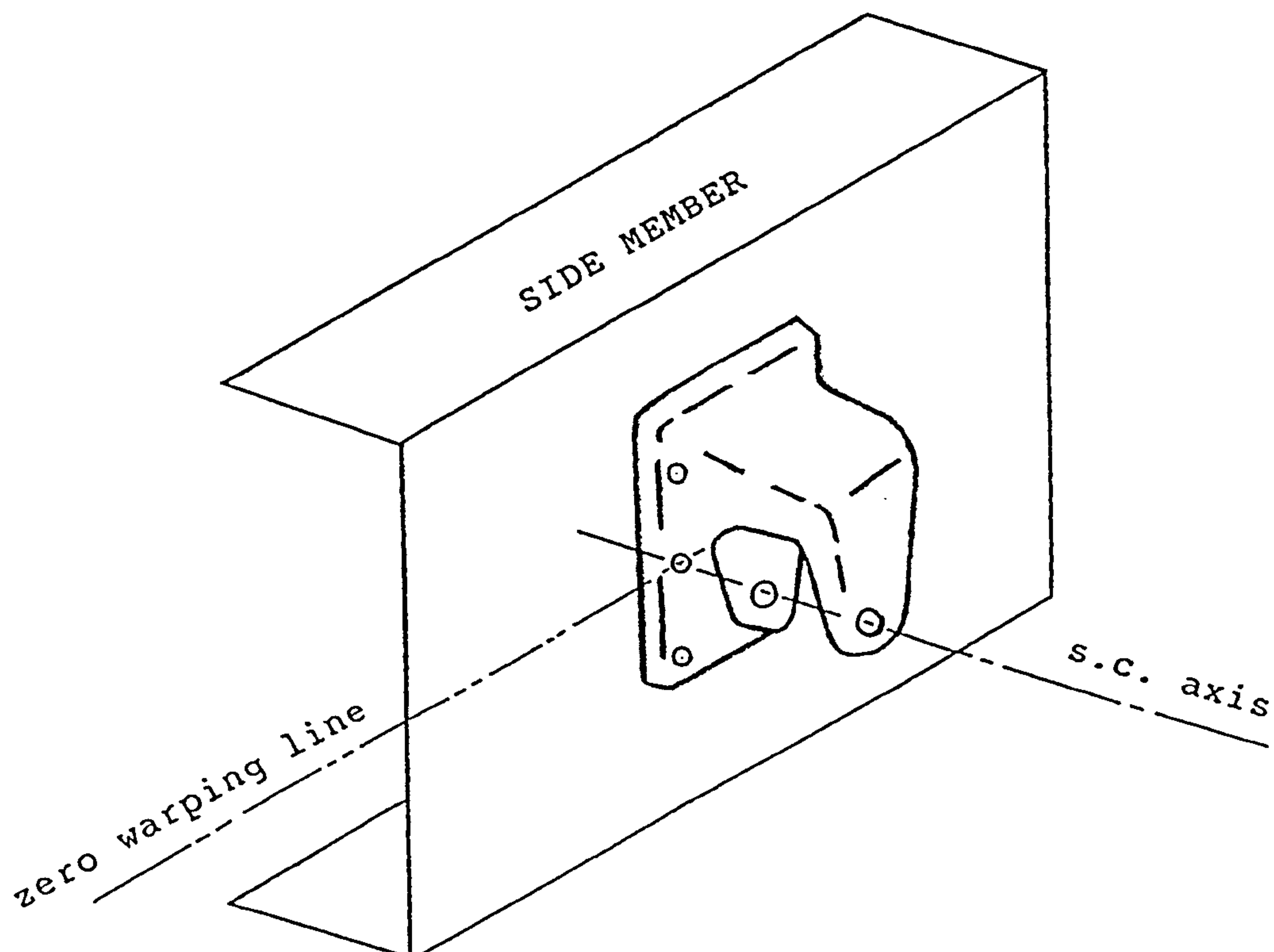


Fig.(10.2) Alternative design and attachment of a spring hanger bracket

REFERENCES

1. VLASOV, V.Z.

"Thin-walled elastic beams"

English translation, National Science foundation,
Washington, D.C., London, oldbourne press, 1961.

2. ZBIROHOWSKI-KOSCIA, K.

"Thin- walled beams from theory to practice"

Crosby Lockwood & Son Ltd., London, 1967.

3. HANKE, M.

"Thin-walled beams in Automobile Engineering"

Part 1: 'Theory of simple frames', Auto.(Prague), NO.1, 1959.

Part 2: 'Theory of plane joints', Auto.(Prague), No.8, 1959.

Part 3: 'Torsion of ladder frame', Auto.(Prague), No.4, 1960.

4. ZAKS, M.N.

"Stress state in joints of a twisted Automobile frame"

NAMI Proceedings, No.61, 1963 (English translation of Russian original)

5. ZAKS, M.N.

"Calculation of the distortion of Motor-Vehicle chassis frame, taking into
consideration the rigidity of the joints"

Automobile Industry, No.4, 1964 (English translation of Russian original)

6. TIMOSHENKO, S. and WOINOWSKY-KRIEGER, S.

"Theory of plates and shells"

Edition 2, McGraw-Hill Book Co. Inc., 1959.

7. KOBRIN, M.N., KILIMNIK, L.SH. and TITOV, A.A.

"Investigation of the stress state and durability of vehicle frame side member walls
at the point of load transfer"

Avtom. Prom No.II, 1969 (English translation of Russian original)

8. SETTLER, W.

"Fundamental reappraisal of the chassis frame"

Automotive Design Engineering, Vol.2, Data sheet 14, 89, October, 1963.

9. COOKE, C.J.

"Strain Energy theory applied to the chassis frame"

Automotive Design Engineering, Vol.2, Data sheet 14, 89, October, 1963.

10. TIDBURY, G.H., MARSHALL, P.H. and ROACH, A.H.

"Torsional stiffness of commercial vehicle chassis frames"

The XII FISITA Congress, Barcelona, 1968.

11. TIDBURY, G.H.

"The torsional stiffness of an open section thin walled beam in terms of bimoment and the generalisation of partial warping inhibition boundary conditions"

Motor & Vech. Conf. Belgrade, 1974.

12. ROACH, A.H.

"Warping inhibition in commercial vehicle frames"

M.Sc thesis, Cranfield Institute of Technology, 1966.

13. ERZ, K.

"Über die durch unebenheiten der fahrban hervorgerufene verdrenung von strassenfahr zeugen"

A.T.Z., No.4 April, No.6 June, No.11 November, No.12 December, 1957.

14. AWUDU, G.

"Warping inhibition in the joints of vehicle chassis frames"

M.Sc thesis, Cranfield Institute of Technology, 1968.

15. MEGSON, T.H.G. and ALADE, G.A.

"Structural analysis of ladder frames under torsion"

Proc. Instn. Mech. Engrs., Auto. Div., Vol.190, 1976.

16. MEGSON, T.H.G., ERGATOUDIS, J. and NUTTALL, J.
"Partially restrained warping of open and closed section thin walled beams"
Proc.International Conf. thin walled structures, Univ. of Strathclyde, April 1979.
17. MEGSON, T.H.G.
"Linear analysis of thin walled elastic structures"
Surrey University Press, 1974.
18. MEGSON, T.H.G.
"Extension of the Wagner torsion bending theory to allow for general systems of loading"
The Aeronautical Quarterly, Vol.XXVI, August 1975.
19. ALADE, G.A.
"Structural analysis of ladder frames under torsion"
Ph.D thesis, University of Leeds, 1974.
20. NUTTALL, J.
"The torsional analysis of ladder frames"
Ph.D thesis, University of Leeds, 1982.
21. DATOO, M.H.
"Stress concentrations in the joints of a ladder frame subjected to torsion"
Ph.D thesis, University of Leeds, 1983.
22. ALVI, M.S.I.
"The stress distribution in the joints of vehicle chassis frames subjected to torsion"
Ph.D thesis, Cranfield Institute of Technology, February 1978.
23. TIDBURY, G.H. and ALVI, M.S.I.
"The theoretical and photoelastic investigation of stresses in chassis frame joints"
Proc. Instn. Mech. Engrs., Vol.198D, No.3, 1984

24. SHARMAN, P.W.
"Optimum stiffness weight design of peripheral and ladder frames"
Proc. Auto. Div. Instn. Mech. Engrs., Vol.182, pt.2A, No.3, 1967-68
25. LASEVICH, L.G., SKOLNIKOV, M.B. and PODLEGAEVA, T.D.
"Selection of optimum sections of commercial vehicles chassis frames"
Avtom. Prom., No.2, 1975.
26. SHARMAN, P.W.
"Torsion of chassis frames"
Automotive Engr., 1, Oct.-Nov., 1976.
27. SHARMAN, P.W.
"Some aspects of the structural analysis and design of commercial vehicles"
Ph.D thesis, Loughborough University, 1974.
28. SHARMAN, P.W.
"The effect of joint flexibility on the torsion of a vehicle body"
Proc. Instn. Mech. Engrs., Vol.196, 1982.
29. SHARMAN, P.W.
"Analysis of structures with thin walled open sections"
Int. J. Mech. Sci., Vol.27, No.10, pp665-677, 1985.
30. TIDBURY, G.H.
"Matrix force analysis applied to chassis frame stiffness"
Automotive Design Engineering, Vol.2, Data sheet 25, 81, September 1964.
31. TIDBURY, G.H.
"Stress analysis of vehicle structures"
Advanced school of Automobile Engineering, Cranfield, Note 1, 1965.

32. MARSHALL, P.H.
"Torsional stiffness of ladder frames"
Advanced school of Automobile Engineering, Cranfield, M.Sc. thesis, 1965.
33. ROBINSON, J.
"Automatic selection of redundancies in the matrix force method"
A.I.A.A./C.A.S.I Joint meeting, Ottawa, Canada, October 1964.
34. ALI, R., HEDGES, J.L. and MILLS, B.
"The application of finite element Techniques to the analysis of an Automobile structure"
Proc. Instr. Mech. Engrs., Vol.185, 1970-71.
35. HEDGES, J.L., NORVILLE, C.C. and GURDOGAN, O.
"Stress analysis of an Automobile chassis frame"
Proc. Instr. Mech. Engrs., Vol.185, 1970-71.
36. TRIMAN, R.S.
"Incorporation of bimoment in matrix structural analysis"
M.Sc. thesis, Cranfield Institute of Technology, 1982.
37. LEE, W.G.
"Bimoment effects in a chassis frame considering joint flexibility"
M.Sc. thesis, Cranfield Institute of Technology, 1987.
38. BEERMANN, H.J.
"Joint deformations and stresses of commercial vehicle frame under torsion"
I. Mech. E. Conference paper, C178/84, 1984.
39. BEERMANN, H.J. (ED. TIDBURY, G.H.)
"The analysis of commercial vehicle structures"
Mechanical Engineering Publications Limited, London, 1989.

40. AL-HAKEEM, A.H.

"The effect of torsional and longitudinal loads on the stress distribution in open section commercial vehicle chassis members"

M.Sc. thesis, Cranfield Institute of Technology, 1988.

41. ARGYIS, J.H.

Appl. Mech. Rev.11, 7, 331, 1958.

42. SDRC

"I-DEAS level 4.0 Supertab-Engineering analysis Pre- and Post- Processing user's Guide"

Structural Dynamics Research Corporation, Milford, Ohio, 1988.

43. SDRC

"I-DEAS level 4.0 Supertab-Engineering analysis Model Solution and Optimization user's Guide"

Structural Dynamics Research Corporation, Milford, Ohio, 1988.

44. PERRY, C.C. and LISSNER, H.R.

"The strain Gauge primer"

McGraw-Hill Book Co., New York, 1962.

45. WILLIAM WEAVER, JR. and JAMES M. GERE

"Matrix analysis of framed structures"

2nd edition, 1980, D.Van Nostrand company, New York.

BIBLIOGRAPHY

1. MEGSON, T.H.G.
"Aircraft structures for engineering students"
Edward Arnold, 1972.
2. AL-SHEIKH, A.M.S.
"Behaviour of thin walled structures under combined load"
Ph.D thesis, Loughborough University, 1985.
3. BEERMANN, H.J.
"Warping torsion in commercial vehicle frames taking into consideration flexible joints"
Int. Journal of vehicle design, Vol.1, No.5, pp397-414, 1980.
4. ROARK & YOUNG
"Formulas for stress and strain"
Fifth edition, McGraw-Hill Book Company, 1975.
5. ROMANOV, F.
"Investigation of stress concentration in thin walled elements of chassis frames"
I. Mech. E. Conference paper, C183/84, 1984.
6. RUSINSKI, E.
"Torsional stiffness of chassis frames with point-welded nodes"
I. Mech. E. Conference paper, C162/84, 1984.
7. TIDBURY, G.H.
"Vehicle structural analysis-a survey"
Int.Journal of vehicle design, Vol.1, No.2, pp165-172, 1980.
8. CARVER, G.C.
"Truck chassis frame considerations in equipment mounting"
S.A.E., No.760291, 1976.

9. BEERMANN, H.J.

"Static analysis of commercial vehicle frames: A hybrid-finite element and analytical method"

Int. Journal of vehicle design, Vol.5, Nos.1&2, pp26-52, 1984.

10. MEGSON, T.H.G., ERGATOUDIS, J. and NUTTALL, J.

"Analysis of closed section thin walled beams subjected to partially restrained warping"

Proceeding of the fifth International specialty Conference on cold- formed steel structures, St. Louis, University of Missouri-Rolla, 1980.

11. ROMANOW, F., PALUCH, Z.

"Experimental studies on the durability of the elements of vehicle frames under complex state of loads"

FISITA Congress, Vienna, May, 1984.

12. RAO, B.V.A., RAMAMURTI, V. and GANESAN, N.

"Torsion of prismatic shells by finite difference approach"

Journal of Aeronautical Society of India, Vol.25, 1973.

13. TAKAHASHI, K.

"A torsional strength analysis of truck frames using open section members"

S.A.E. paper, No.710595, 1971.

14. BAIGENT, A.H. and HANCOCK, G.J.

"Structural analysis of assemblages of thin walled members"

Journal of Eng. struc., Vol.4, pp207-216, July, 1982.

15. BARSOUM, R.S. and GALLAGHER, R.H.

"Finite element analysis of torsional and torsional-flexural stability problems"

Int. Jour. for Num. Meth. in Eng., Vol.2, pp335-352, 1970.

16. MIZUGUCHI, KISHIMOTO.

"Experimental analysis of torsional strength of ladder type truck frame"

MHI Technical Bulletin, Vol.6, No.5, 1959.

17. NAKAMURA

"Stiffness of ladder type frame"

Nissan Diesel Technical Bulletin, No.47, 1985.

18. OKUMOTO, YAMANE, HARADA

"Strength of ladder type truck frame"

ISUZU Technical Bulletin, No.79, 1988.

19. OHNUMA, ET.AL.

"Stiffness of truck frame and its prediction method"

JSAE paper, No.882161, 1988.

20. KAZUO AO., SATORA OHNUMA, TOSHIHARU MATSUI &KUNIO HARA

"Basic study on truck frame torsional stiffness"

MTSIBISHI Motors Technical review, No.2, 1990.

21. MOUNIR M. KAMAL, and JOSEPH A. WOLF, JR.

"Modern Automotive structural analysis"

Van Nostrand Reinhold Co., New York, N.Y, 1982.

22. GURNEY, T.R.

"Fatigue of welded structures"

Cambridge University Press, 1968.

23. MEGSON, T.H.G.

"Analysis of semi-trailer chassis subjected to torsion"

I. Mech. E. Conference paper, C176/84, 1984.

24. TIMOSHENKO, S. and GOODIER, J.N.
"Theory of Elasticity"
McGraw-Hill Co., 1951.
25. BRESLER, B., LIN, T.Y. and SCALZI, J.B.
"Design of steel structures"
John Wiley and Sons, New York, 1968
26. ODEN, J.T.
"Mechanics of elastic structures"
McGraw-Hill Book Co., New York, 1967.
27. DALLY, J.W. and RILEY, W.F.
"Experimental stress analysis"
McGraw-Hill Book Co., 1965.
28. MEGSON, T.H.G.
"Increasing semi-trailer torsional stiffness could enhance operational safety"
Automotive Design Engineering, May, 1970.
29. TIDBURY, G.H.
"Design problems of truck bodies"
Automotive Design Engineering, October, 1962.
30. BOLLAND, G.B.
"Flexibility and stiffness matrices for an open-tube warping constraint finite element"
Department of mechanical Engineering, Lanchester Polytechnic, Sep., 1971.
31. REILLY, R.J.
"Stiffness analysis of Grids including warping"
Journal of the structural Division, ASCE, Vol. 98, July, 1972.

APPENDIX (A)

Example

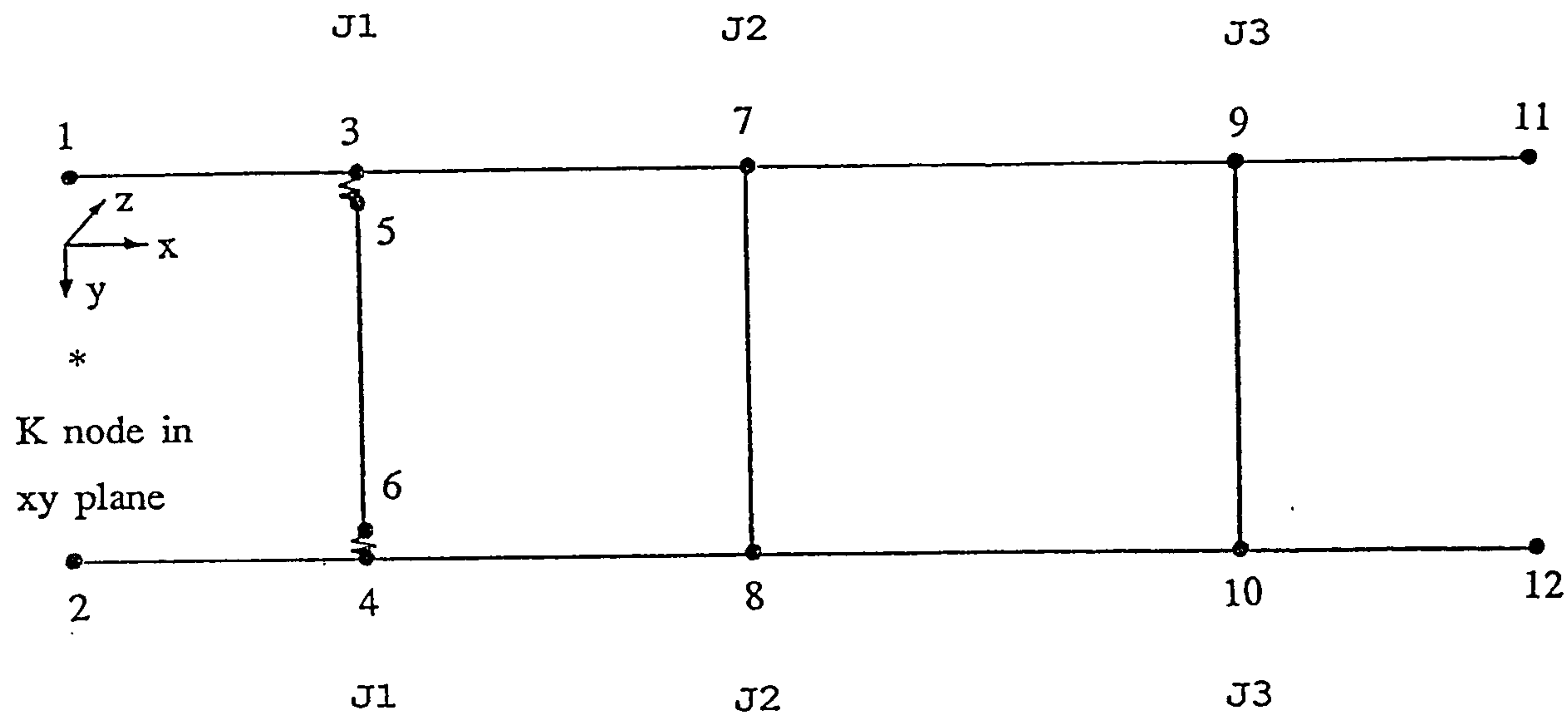


Fig. (A.1) A simple Grillage structure.

El. No.	Node (i)	Node (j)	Element type
E1	1	3	side member
E2	2	4	side member
E3	3	7	side member
E4	4	8	side member
E5	7	9	side member
E6	8	10	side member
E7	9	11	side member
E8	10	12	side member
E9	3	5	joint element
E10	4	6	joint element
E11	5	6	cross member
E12	7	8	cross member
E13	9	10	cross member

Table (A.1) Elements used for the Grillage structure

Joint No.	Joint type
J1	flexibile joint
J2	rigid joint with axes offset
J3	rigid joint without axes offset
Bandwidth=[(N _j - N _i) + 1]*7	
El. Identity No.;- 1= side or cross member without axes offset 2= cross member with axes offset 3= joint element	
Sec. Identity No.;- 1= any section with given properties 2= channel section dimensions 3= box section dimensions	

Table (A.2) Joints used for the grillage structure

Input data	Description
SIMPLE GRILLAGE STRUCTURE 2.05E+05 0.31 13 12 35	* Title * Young's modulus, Poission ratio * No.of El.,No. of Node, Bandwidth
1 1 3 0 0 0 300 0 0 0 200 0 11.37 -90 1800 11.37 -90 1800 2 60 180 3.2	* side member, El.Identity No.=1 * i-Node, j-Node * coord. of i-Node, j-Node, k-Node * (y,z, ω) of i&j Nodes for stress calcul. * channel section, Sec. Identity No.=2 * section dimensions
1 2 4 0 400 0 300 400 0 0 200 0 11.37 90 -1800 11.37 90 -1800 2 60 180 3.2	
1 3 7 300 0 0 700 0 0 0 200 0 11.37 -90 1800 11.37 -90 1800 2 60 180 3.2	
1 4 8 300 400 0 700 400 0 0 200 0 11.37 90 -1800 11.37 90 -1800 2 60 180 3.2	
1 7 9 700 0 0 1200 0 0 0 200 0 11.37 -90 1800 11.37 -90 1800 2 60 180 3.2	
1 8 10 700 400 0 1200 400 0 0 200 0 11.37 90 -1800 11.37 90 -1800 2 60 180 3.2	
1 9 11 1200 0 0 1500 0 0 0 200 0 11.37 -90 1800 11.37 -90 1800 2 60 180 3.2	
1 10 12 1200 400 0 1500 400 0 0 200 0 11.37 90 -1800 11.37 90 -1800 2 60 180 3.2	
3 3 5 300 0 0 300 1 0 0 200 0 0.85E+10	* joint element, El. Identity No.=3 * i-Node, j-Node * coord. of i-Node, j-Node, k-Node * joint stiffness coef. from F.E. analy.
3 4 6 300 400 0 300 399 0 0 200 0 0.85E+10	


```

1
5 6
300 1 0 300 399 0 0 200 0
40 50 1600 40 50 1600
1
250 0.25E+03 0.3E+06 0.5E+05 0.8E+08

```

* any section type, Sec. Identity No.=1
 * Area, J, I_{yy} , I_{zz} , Γ

```

2
7 8
700 0 0 700 400 0 0 200 0
35 45 1500 35 45 1500
20 20 15 15 -5 -5 25 -25 -8 8
2
45 90 1.6

```

* cross m. with axes offset, El. I. No.=2

```

1
9 10
1200 0 0 1200 400 0 0 200 0
25 50 1250 25 50 1250
3
100 3 50 3

```

* offset parameters of i&j Nodes

```

1 1 1 1 1 1 1
1 1 1 1 1 1 1
0 0 0 1 1 1 1
0 1 0 1 1 1 1
1 1 1 1 1 1 1
1 1 1 1 1 1 1
1 1 1 1 1 1 1
1 1 1 1 1 1 1
1 1 1 1 1 1 1
1 1 0 1 1 1 1
1 1 0 1 1 1 1
1 1 1 1 1 1 1
1 1 1 1 1 1 1

```

* box section, Sec. Identity No.=3
 * box section dimensions

* Rest., 7 deg. of fre. for each Node
 1= free
 0= fixed

```

0 0 0 0 0 0 0
0 0 0 0 0 0 0
0 0 0 0 0 0 0
0 0 0 0 0 0 0
0 0 0 0 0 0 0
0 0 0 0 0 0 0
0 0 0 0 0 0 0
0 0 0 0 0 0 0
0 0 0 0 0 0 0
5000 0 0 0 -0.5E6 0.25E6 -0.1E8
5000 0 0 0 -0.5E6 -0.25E6 0.1E8
0 0 0 0 0 0 0
0 0 0 0 0 0 0

```

* Loading

OUTPUT DATA

- ASAPE
- Al-Hakeem program for
- Structural Analysis of
- chassis Frame considering
- bimoment Effects

EXAMPLE FOR A SIMPLE GRILLAGE STRUCTURE

MATERIAL PROPERTIES

YOUNG'S MODULUS = 0.20500E+06 N/MM*2
POISSON'S RATIO= 0.310
SHEAR MODULUS = 0.78244E+05 N/MM*2

PHYSICAL PROPERTIES

EL.	I	J	X1	Y1	Z1	X2	Y2	Z2	AREA	SV*CON.	2ND MOMENT(Y)	2ND MOMENT(Z)	WARPING CONSTANT
1	1	3	0.00	0.00	0.00	300.00	0.00	0.00	939.52	0.32E+04	0.4396259E+07	0.2988049E+06	0.1665948E+10
2	2	4	0.00	400.00	0.00	300.00	400.00	0.00	939.52	0.32E+04	0.4396259E+07	0.2988049E+06	0.1665948E+10
3	3	7	300.00	0.00	0.00	700.00	0.00	0.00	939.52	0.32E+04	0.4396259E+07	0.2988049E+06	0.1665948E+10
4	4	8	300.00	400.00	0.00	700.00	400.00	0.00	939.52	0.32E+04	0.4396259E+07	0.2988049E+06	0.1665948E+10
5	7	9	700.00	0.00	0.00	1200.00	0.00	0.00	939.52	0.32E+04	0.4396259E+07	0.2988049E+06	0.1665948E+10
6	8	10	700.00	400.00	0.00	1200.00	400.00	0.00	939.52	0.32E+04	0.4396259E+07	0.2988049E+06	0.1665948E+10
7	9	11	1200.00	0.00	0.00	1500.00	0.00	0.00	939.52	0.32E+04	0.4396259E+07	0.2988049E+06	0.1665948E+10
8	10	11	1200.00	400.00	0.00	1500.00	400.00	0.00	939.52	0.32E+04	0.4396259E+07	0.2988049E+06	0.1665948E+10
11	5	6	300.00	1.00	0.00	300.00	399.00	0.00	250.00	0.25E+03	0.3000000E+06	0.5000000E+05	0.8000000E+08
12	7	8	700.00	0.00	0.00	700.00	400.00	0.00	282.88	0.24E+03	0.3685512E+06	0.5762006E+05	0.7875915E+08
13	9	10	1200.00	0.00	0.00	1200.00	400.00	0.00	864.00	0.87E+06	0.1121192E+07	0.3743920E+06	0.3741207E+09

JOINT TRANSFORMATION PARAMETRES

EL.	I	J	HS1	RT1	RW1	ST1	SW1	HS2	RT2	RW2	ST2	SW2
1	1	3	0.000	0.000	0.000	0.000	0.000	0.000	0.000	0.000	0.000	0.000
2	2	4	0.000	0.000	0.000	0.000	0.000	0.000	0.000	0.000	0.000	0.000
3	3	7	0.000	0.000	0.000	0.000	0.000	0.000	0.000	0.000	0.000	0.000
4	4	8	0.000	0.000	0.000	0.000	0.000	0.000	0.000	0.000	0.000	0.000
5	7	9	0.000	0.000	0.000	0.000	0.000	0.000	0.000	0.000	0.000	0.000
6	8	10	0.000	0.000	0.000	0.000	0.000	0.000	0.000	0.000	0.000	0.000
7	9	11	0.000	0.000	0.000	0.000	0.000	0.000	0.000	0.000	0.000	0.000
8	10	11	0.000	0.000	0.000	0.000	0.000	0.000	0.000	0.000	0.000	0.000
9	3	5	0.000	0.000	0.000	0.000	0.000	0.000	0.000	0.000	0.000	0.000
10	4	6	0.000	0.000	0.000	0.000	0.000	0.000	0.000	0.000	0.000	0.000
11	5	6	0.000	0.000	0.000	0.000	0.000	0.000	0.000	0.000	0.000	0.000
12	7	8	20.000	15.000	-5.000	25.000	-8.000	20.000	15.000	-5.000	-25.000	8.000
13	9	10	0.000	0.000	0.000	0.000	0.000	0.000	0.000	0.000	0.000	0.000

LOADS AND RESTRAINTS

1	0.00000E+00	1	0.00000E+00	1	0.00000E+00	1	0.00000E+00	1	0.00000E+00	1	0.00000E+00	1	0.00000E+00
1	0.00000E+00	1	0.00000E+00	1	0.00000E+00	1	0.00000E+00	1	0.00000E+00	1	0.00000E+00	1	0.00000E+00
0	0.00000E+00	0	0.00000E+00	0	0.00000E+00	0	0.00000E+00	1	0.00000E+00	1	0.00000E+00	1	0.00000E+00
0	0.00000E+00	1	0.00000E+00	1	0.00000E+00	0	0.00000E+00	1	0.00000E+00	1	0.00000E+00	1	0.00000E+00
1	0.00000E+00	1	0.00000E+00	1	0.00000E+00	1	0.00000E+00	1	0.00000E+00	1	0.00000E+00	1	0.00000E+00
1	0.00000E+00	1	0.00000E+00	1	0.00000E+00	1	0.00000E+00	1	0.00000E+00	1	0.00000E+00	1	0.00000E+00
1	0.00000E+00	1	0.00000E+00	1	0.00000E+00	1	0.00000E+00	1	0.00000E+00	1	0.00000E+00	1	0.00000E+00
1	0.00000E+00	1	0.00000E+00	1	0.00000E+00	1	0.00000E+00	1	0.00000E+00	1	0.00000E+00	1	0.00000E+00
1	0.50000E+04	1	0.00000E+00	1	0.00000E+00	0	0.00000E+00	1	-0.50000E+06	1	0.25000E+06	1	-0.10000E+08
1	0.50000E+04	1	0.00000E+00	1	0.00000E+00	0	0.00000E+00	1	-0.50000E+06	1	-0.25000E+06	1	0.10000E+08
1	0.00000E+00	1	0.00000E+00	1	0.00000E+00	1	0.00000E+00	1	0.00000E+00	1	0.00000E+00	1	0.00000E+00
1	0.00000E+00	1	0.00000E+00	1	0.00000E+00	1	0.00000E+00	1	0.00000E+00	1	0.00000E+00	1	0.00000E+00

SOLUTIONS FOR DISPLACEMENTS

1	0.00000E+00	1	-0.83840E-02	1	0.24966E-01	1	0.31397E-04	1	0.83219E-04	1	0.27947E-04	1	-0.16146E-06
1	0.00000E+00	1	0.77225E-02	1	0.24966E-01	1	-0.31397E-04	1	0.83219E-04	1	-0.27947E-04	1	0.16146E-06
0	0.00000E+00	0	0.00000E+00	0	0.00000E+00	1	-0.17576E-04	1	0.83219E-04	1	0.27947E-04	1	-0.16682E-06
0	0.00000E+00	1	-0.66151E-03	0	0.00000E+00	1	0.17576E-04	1	0.83219E-04	1	-0.27947E-04	1	0.16682E-06
1	-0.71698E-22	1	-0.85180E-08	1	-0.35527E-24	1	-0.17049E-04	1	0.83219E-04	1	0.27803E-04	1	-0.15379E-07
1	0.71410E-22	1	-0.66150E-03	1	-0.71054E-24	1	0.17049E-04	1	0.83219E-04	1	-0.27803E-04	1	0.15379E-07
1	0.10384E-01	1	-0.17838E-02	1	-0.26712E-01	1	0.76698E-04	1	0.33904E-04	1	-0.73948E-04	1	0.10534E-05
1	0.10384E-01	1	0.11223E-02	1	-0.26712E-01	1	-0.76698E-04	1	0.33904E-04	1	0.73948E-04	1	-0.10534E-05
1	0.23364E-01	1	0.48811E-04	0	0.00000E+00	1	-0.20627E-04	1	-0.16644E-03	1	0.30993E-03	1	-0.43319E-05
1	0.23364E-01	1	-0.71032E-03	0	0.00000E+00	1	0.20627E-04	1	-0.16644E-03	1	-0.30993E-03	1	0.43319E-05
1	0.23364E-01	1	0.93027E-01	1	0.49932E-01	1	-0.12923E-02	1	-0.16644E-03	1	0.30993E-03	1	-0.41926E-05
1	0.23364E-01	1	-0.93689E-01	1	0.49932E-01	1	0.12923E-02	1	-0.16644E-03	1	-0.30993E-03	1	0.41926E-05

MEMBER FORCES WITH RESPECT TO LOCAL COORD.

MEMBER (1 3) FORCES ARE:

0.000 0.000
0.000 0.000
0.000 0.000
0.000 0.000
0.000 0.000
0.000 0.000
0.000 0.000
0.000 -12288.309

MEMBER (2 4) FORCES ARE:

0.000 0.000
0.000 0.000
0.000 0.000
0.000 0.000
0.000 0.000
0.000 0.000
0.000 0.000
0.000 12288.309

MEMBER (3 7) FORCES ARE:

-5000.000 5000.000
-85.180 85.180
555.556 -555.556
5268.795 -5268.795
0.000 -222222.222
-1432.082 -32639.739
13575.601 2117597.621

MEMBER (4 8) FORCES ARE:

-5000.000 5000.000
-85.180 85.180
-555.556 555.556
-5268.795 5268.795
0.000 222222.222
-1432.082 -32639.739
-13575.601 -2117597.621

MEMBER (7 9) FORCES ARE:

-5000.000 5000.000
336.143 -336.143
555.556 -555.556
-23705.095 23705.095
222222.222 -500000.000
37007.130 131064.441
-2203958.813 -9673009.524

MEMBER (8 10) FORCES ARE:

-5000.000 5000.000
336.143 -336.143
-555.556 555.556
23705.095 -23705.095
-222222.222 500000.000
37007.130 131064.441
2203958.813 9673009.524

MEMBER (9 11) FORCES ARE:

0.000 0.000
0.000 0.000
0.000 0.000
0.000 0.000
0.000 0.000
0.000 0.000
0.000 0.000
-319090.037 0.000

MEMBER (10 12) FORCES ARE:

0.000 0.000
0.000 0.000
0.000 0.000
0.000 0.000
0.000 0.000
0.000 0.000
0.000 0.000
319090.037 0.000

MEMBER (3 5) FORCES ARE:

85.180 -85.180
0.000 0.000
0.000 0.000
0.000 0.000
5268.795 -5268.795
1432.082 -1432.082
-1287.292 1287.292

MEMBER (4 6) FORCES ARE:

85.180 -85.180
0.000 0.000
0.000 0.000
0.000 0.000
-5268.795 5268.795
1432.082 -1432.082
1287.292 -1287.292

85.180	-85.180
0.000	0.000
0.000	0.000
0.000	0.000
5268.795	-5268.795
1432.082	-1432.082
-1287.292	1287.292

MEMBER (7 8) FORCES ARE:

-421.323	421.323
0.000	0.000
0.000	0.000
0.000	0.000
-20547.436	20547.436
-4367.390	4367.390
-300189.364	300189.364

MEMBER (9 10) FORCES ARE:

336.143	-336.143
0.000	0.000
0.000	0.000
0.000	0.000
23705.095	-23705.095
118935.559	-118935.559
-7900.439	7900.439

BEAM STRESSES (N/MM*2)

(NODE-I)													(NODE-J)			
EL.	I	J	SPX	SMP	SMZ	SBI	TS1	TS2	TS3	SPX	SMP	SMZ	SBI	TS1	TS2	TS3
1	1	3	0.000	0.000	0.000	0.000	0.000	0.000	0.000	0.000	0.000	0.000	-0.013	0.000	-0.013	0.000
2	2	4	0.000	0.000	0.000	0.000	0.000	0.000	0.000	0.000	0.000	0.000	-0.013	0.000	-0.013	0.000
3	3	7	5.322	0.000	0.054	-0.015	5.376	5.362	5.376	5.322	4.549	-1.242	2.288	4.080	10.917	8.629
4	4	8	5.322	0.000	0.054	-0.015	5.376	5.362	5.376	5.322	4.549	-1.242	2.288	4.080	10.917	8.629
5	7	9	5.322	4.549	-1.408	2.381	3.914	10.844	8.463	5.322	10.236	4.987	-10.451	10.309	10.094	20.545
6	8	10	5.322	4.549	-1.408	2.381	3.914	10.844	8.463	5.322	10.236	4.987	-10.451	10.309	10.094	20.545
7	9	11	0.000	0.000	0.000	0.345	0.000	0.345	0.000	0.000	0.000	0.000	0.000	0.000	0.000	0.000
8	10	12	0.000	0.000	0.000	0.345	0.000	0.345	0.000	0.000	0.000	0.000	0.000	0.000	0.000	0.000
11	5	6	-0.341	-0.878	-1.146	0.026	-1.486	-2.339	-2.365	-0.341	-0.878	-1.146	0.026	-1.486	-2.339	-2.365
12	7	8	1.489	2.509	2.653	5.717	4.142	12.368	6.651	1.489	2.509	2.653	5.717	4.142	12.368	6.651
13	9	10	-0.389	-1.057	-7.942	0.026	-8.331	-9.362	-9.388	-0.389	-1.057	-7.942	0.026	-8.331	-9.362	-9.388

- ASAFE
- Al-Hakeem program for
- Structural Analysis of
- chassis Frame considering
- bimoment Effects
